CERAMIDE METABOLISM REGULATES A NEURONAL NADPH OXIDASE

INFLUENCING NEURON SURVIVAL DURING INFLAMMATION

A

THESIS

Presented to the Faculty

of the University of Alaska Fairbanks

in Partial Fulfillment of the Requirements

for the Degree of

DOCTOR OF PHILOSOPHY

By

Brian M. Barth, B.S., M.S.

Fairbanks, Alaska

August 2009

UMI Number: 3386045

UMI®

Dissertation Publishing
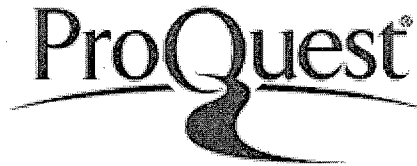
ProQuest®

ProQuest LLC
789 East Eisenhower Parkway
P.O. Box 1346
Ann Arbor, MI 48106-1346
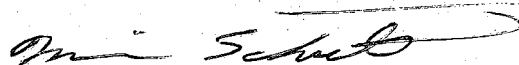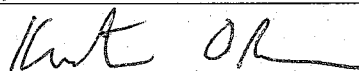
CERAMIDE METABOLISM REGULATES A NEURONAL NADPH OXIDASE

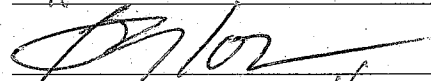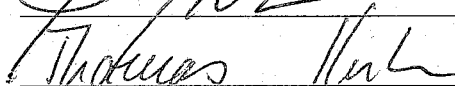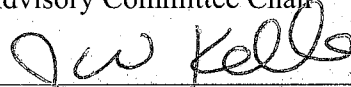INFLUENCING NEURON SURVIVAL DURING INFLAMMATION

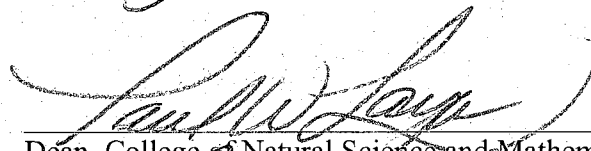By

Brian M. Barth

RECOMMENDED:

Advisory Committee Chair
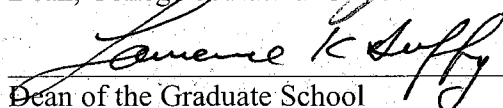
Chair, Department of Chemistry and Biochemistry
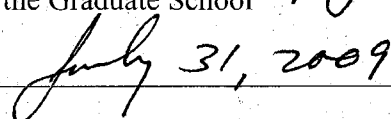
APPROVED:

Dean, College of Natural Science and Mathematics

Dean of the Graduate School

July 31, 2009

Date

Abstract

Inflammation is a major component of acute and chronic pathologies of the central nervous system, including psychiatric disorders. Microglia respond to pathogens, injury, and toxins by secreting inflammatory mediators including pro-inflammatory cytokines in an event known as neuroinflammation. This thesis research investigated a link between neuroinflammation and oxidative stress, and ultimately neurodegeneration. The cytokine tumor necrosis factor alpha was shown to stimulate a neuronal NADPH oxidase (NOX), specifically by stimulating the production of ceramide and ceramide-1-phosphate via Mg^{2+}-neutral sphingomyelinase (Mg^{2+}-nSMase) and ceramide kinase. Intriguingly, glucosylceramide blocked NOX activation, linking ceramide neutralization directly to a decline in oxidative stress. Most importantly, NOX activity interfered with actin and sphingosine kinase-1 via oxidation, demonstrating a positive and detrimental feedback mechanism that impedes neuronal survival pathways. Interestingly, crude extracts from wild Alaskan bog blueberries showed the ability to interfere with Mg^{2+}-nSMase, demonstrating a specific neuroprotective property of the berry. Altogether, this thesis research defined a key neuronal pathway linking inflammation to oxidative stress via ceramide metabolism, potentially allowing for future therapeutic development to improve neuronal function and survival.

TABLE OF CONTENTS

LIST OF FIGURES

LIST OF TABLES

LIST OF ABBREVIATIONS

4HPR .... fenretinide

4OHT .... 4-hydroxy tamoxifen

$A\beta^{1-42}$ .... amyloid beta fragment 1-42

ABC transporter .... ATP-binding cassette transporter

AIR .... auto-inhibitory region

ANOVA ....analysis of variance

ATP ....adenosine triphosphate

BSA ....bovine serum albumin

C1P ceramide-1-phosphate

CAT ....catalase

CER ....ceramide

CerK .... ceramide kinase

CERT .... ceramide transfer protein

CGD ....chronic granulomatous disease

CNS ....central nervous system

CoA ....coenzyme A

COX..cyclooxygenase

$cPLA_2$ .... cytosolic phospholipase A_2

C-terminus ....carboxyl-terminus

Cys..cysteine

DAG .... diacylglycerol

DCF .... dichlorofluorescein

DCFDA..2', 7'-dihydrodichlorofluorescein diacetate

DHCER...dihydroceramide

DHE..dihydroethidium

DPI ....diphenylene iodonium

DOXO.. doxorubicin

DUOX ....dual oxidase

Eth .... ethidium

FAD .... flavin adenine dinucleotide

FAN .... factor associated with neutral sphingomyelinase

FBS .... fetal bovine serum

GAP ....GTPase-activating protein

GCS .... glucosylceramide synthase

GDP .... guanosine diphosphate

GEF .... guanine nucleotide exchange factor

GEM .... gemcitabine

GLUCER .... glucosylceramide

G-protein... guanine nucleotide-binding protein

GTP ....guanosine triphosphate

GTPase... GTP hydrolase

LOX..lipoxygenase

Mg^{2+}-nSMase .... magnesium-dependent neutral sphingomyelinase

mRNA.. messenger ribonucleic acid

MTX .... methotrexate

NAC...N-acetyl L-cysteine

NADPH .... reduced nicotinamide adenine dinucleotide phosphate

NMDA..N-methyl D-aspartic acid

NOX .... NADPH oxidase

NOXA..NOX adapter protein

NOXO... NOX organizer protein

nSMase ....neutral sphingomyelinase

N-terminus ....amino-terminus

PB1 .... phox and bem1 (domain)

PBS...phosphate buffered saline

PCT.. paclitaxel

PDMP D-threo-1-phenyl-2-decanoylamino-3-morpholino-1-propanol

phox..phagocytic oxidase

PKB ....protein kinase B

PKC ζ..protein kinase C zeta

PRR .... proline-rich region

PX..phox homology (domain)

ROS ....reactive oxygen species

RT-PCR..real-time polymerase chain reaction

S1P sphingosine-1-phosphate

SD..standard deviation

SEM.. standard error from the mean

SH3..src-homology 3 (domain)

siRNA..small interfering ribonucleic acid

SMase .... sphingomyelinase

SOD..superoxide dismutase

SphK.. sphingosine kinase

TBS..Tris-buffered saline

TBST .... Tris-buffered saline with Tween-20

TNFα.. tumor necrosis factor alpha

TNFR..TNFα receptor

TPR..tetratricopeptide repeat (motif)

TRAF.. TNFα receptor associated factor

ACKNOWLEDGEMENTS

I would like to take this opportunity to thank several individuals who have made this dissertation possible. My experience at the University of Alaska Fairbanks has been incredibly unique. Prior to my acceptance into the Ph.D. program, I was completing my B.S., and then my M.S. at Colorado State University. Admittedly, it was more difficult than I had imagined, as life presented many challenges during those years. My final year in the B.S. program was my first after a major wrist injury, and I was constantly struggling to bring my grades up and demonstrate my abilities. Thankfully, several individuals at Colorado State University did not give up on me, and continued to push me and advocate on my behalf. I am deeply indebted to each one. Dr. Laurie Stargell, my undergraduate advisor, Dr. Anna Fails, my neuroanatomy instructor, Dr. Michael Fox, and Dr. Scott Summers, my graduate co-advisors. Dr. Summers gave me my first laboratory opportunity, mentored me constantly, and helped to drive my interest in sphingolipids. Since that time, Dr. Summers has kept in contact, and advised me on numerous occasions. In addition, Alexis, Will, Antonio, Kyle, Ping, and Chang, academic colleagues who ultimately became good friends, helped me at various points while at Colorado State University. Without their friendship, I am not sure I would have succeeded.

As mentioned, my experience at the University of Alaska Fairbanks was a unique one. This is mostly in part due to interior Alaska itself. I really had no idea what I was in for, despite having visited the Anchorage area before, and growing up in Colorado. I learned that interior Alaska was unique unto itself, and vastly different from anywhere I had been before. Interior Alaska is one of the more remote places I have been, and is incredibly challenging during the winter months. However, the beauty of interior Alaska is unsurpassed. I will never forget the summer light, the winter darkness, 53 below, ice fog, so much wildlife, and the aurora borealis. Most importantly, I will not forget the education, and opportunity, that I received from the University of Alaska Fairbanks. I am so thankful that my advisor Dr. Tom Kuhn decided to take a chance on me coming out of

xvi

Colorado State University. I soon learned that Dr. Kuhn had also been at Colorado State University, and feel that this helped to make my application stand out. Dr. Kuhn gave me the chance to quickly become involved in a research project that combined his and my interests, and that culminated in the thesis presented here. Dr. Kuhn gave me the laboratory resources and mentorship to succeed, and also provided me with several opportunities to travel to conferences. The conferences that I attended allowed me to learn beyond the classroom, to present my research, and to meet experts within the fields of neuroscience and sphingolipid biology. As with Dr. Summers and sphingolipids, Dr. Kuhn helped to foster my interest in neuroscience, NADPH oxidases, and natural products. I feel that my interests, and hopefully my future successes in research, will be traced back to my mentors and their dedication, support, and inspiration. I also recently began my post-doctoral fellowship in Hershey, PA at the Penn State College of Medicine in the laboratory of Dr. Mark Kester. Dr. Kester has been instrumental to the completion of my dissertation by providing resources and time to finish research begun in Alaska, as well as to address peer review of the research. I am thankful to Dr. Kester for this help, as well as for the post-doctoral fellowship that is the next step in my career.

I am also very thankful for several other individuals at the University of Alaska Fairbanks. My entire committee, Dr. Marvin Schulte, Dr. Kristen O'Brien, and Dr. Barbara Taylor have been instrumental to my success. They have provided important advice and direction at numerous occasions. Dr. Tom Clausen, the former chairman of the Department of Chemistry and Biochemistry, advised as the department leader, and also as a co-investigator on the blueberry project. Dr. John Keller, the new department chairman, was the first person my family and I met when I arrived in 2005, and has always provided advice, friendship, and support. Dr. Tom Green helped to peak my interest in capillary electrophoresis, and always was interested in learning more about sphingolipids. Dr. Larry Duffy, one of the most friendly personalities I have ever encountered, helped as a mentor to the blueberry research, and also as a student advocate in all his leadership positions with the university. Emily, Sheila, and Mist were also all instrumental towards my success in their capacities as office assistants and coordinators

with the department. They truly make everything happen, and never get as much credit as they should.

Beyond faculty, I am also grateful for my relationships with several other students. All the former and current members of Dr. Kuhn's lab helped if not directly, by simply being friends and providing good conversation. In particular, I want to thank Adam Baxter and Sally Gustafson, both undergraduates when I first met them, and both working for Dr. Kuhn. Adam befriended me, and introduced me to several other people who became friends. I always enjoyed poker at his house, and talking to his parents. Sally also was very important, as she helped at several points during my actual research. Helping to mentor her was enjoyable because she was incredibly willing to learn, and help. I will always remember lunch, usually sushi, and our trip to Carmel for the ceramide conference. Additionally, fellow graduate students Colin McGill and Dan Kirschner deserve mention. Colin, Dr. Clausen's student, helped separate blueberry fractions, and I will always remember the unique separations and smells that came from his lab. Dan, Dr. Green's student, became a close friend of mine. We worked together on a side project to separate sphingolipids by capillary electrophoresis. Dan also introduced me to his bible study group, and Friends Church. I am so grateful for my experiences with the Lost and Found study group, the numerous friends I made there, and Friends Church. I became closer to God, and Jesus Christ, and was baptized on a very cold day in January 2008. Fairbanks was a much more pleasurable place, even during the cold, with such love and friendship. Thank you, and god bless.

Finally, I must thank my family and close friends in Colorado. My friends have been close in all regards with support and friendship. Importantly, they have all given me opportunities to have fun and relax when I've needed it most. There are too many friends to name all, but I would especially like to thank Mike Balshi, Scott Edwards, John Betancourt, Bryson Crain, and Marc Lanum. Most importantly, I am forever grateful and thankful to my parents Michael and Teri. If not for their love, guidance, and unwavering support throughout my life, I am not sure where I would be. Family is without a doubt, the most important foundation in life, and I am so grateful to have the loving family that I

do. My mom has also been an incredible inspiration and motivator towards the completion of my Ph.D. Additionally, the rest of my family, including my sister, Amanda, her husband Rudy, my grandparents, and many more that I could mention, have all supported me and given me helpful guidance throughout the years. My entire family has been incredibly supportive, has always been interested in my work, and my success is as much theirs as it is mine. The best advice in my life has always come from my family, and they have been at my side during the best times of my life as well as the difficult times of my life. I hope they all know how thankful I am for them, and how much I love them all.

I am fortunate that I have made it this far in my academic career, and am in much debt to those who helped me along the way. To all I forgot to mention, I apologize. Many other individuals have made a difference in my life and academics. In particular, I would like to extend a special acknowledgement to all of my teachers in grade school. Sometimes it is easy to forget those who educated you initially, but they had a profound impact on my academic future. Again, to all mentioned I extend my sincere thanks. I am always going to remember how you each have helped me. Thank you.

Chapter 1: Introduction

1.1: CNS Health

1.1.1: Neuroinflammation

The cellular make up of the central nervous system (CNS) consists of neurons, oligodendrocytes, astrocytes, and microglia. In particular microglia, which compose up to 12% of cellular CNS mass, respond to extrinsic insults, similar to macrophages, by releasing inflammatory mediators and by phagocytosis in an innate immunological response known as neuroinflammation (Fetler and Amigorena 2005; Nimmerjahn et al. 2005; Town et al. 2005; Block et al. 2007). Microglia and astrocytes play important roles in propagating and regulating neuroinflammation. Following activation by injury, toxins, excitotoxicity, or invading pathogens, microglia and to some degree astrocytes, secrete inflammatory mediators such as eicosanoids, cytokines, complement, and reactive oxygen species (ROS) (Sawada et al. 1989; Town et al. 2005; Block et al. 2007). Both eicosanoids and cytokines act in autocrine and paracrine fashion and exacerbate inflammation and stress responses.

Importantly, neuroinflammation is predominantly detrimental to CNS neurons and can result in loss of function, and ultimately to degeneration. Following extrinsic insults, microglia and astrocytes release proinflammatory cytokines such as tumor necrosis factor alpha (TNFα), which play a key role in the orchestration and spreading of neuroinflammation (Sawada et al. 1989; Lee et al. 1993; Block et al. 2007). TNFα binds two distinct receptors: the high affinity TNFα receptor I with molecular mass 55kD, and the low affinity TNFα receptor type II with molecular mass 75 kD. The type I receptor (TNFR I) is implicated in both global and local cellular stress responses, and apoptosis. TNFR I, in tight association with adaptor protein, is implicated in signaling pathways key in early apoptotic mechanisms as well as subsequent activation of caspases. Other stress-

induced pathways are mediated through TNFR I interactions with a different repertoire of adaptor proteins. More global effects of TNFα include inducing gene expression via the nuclear factor kappa beta pathway, ultimately mediating the transcription of both pro- and anti-inflammatory genes. Additionally, neuroinflammation is linked to the onset of oxidative stress through both releases of reactive oxygen species (ROS) by activated microglia and astrocytes, as well as oxidant-generating pathways induced by TNFα in neurons (Colton and Gilbert 1987; Block et al. 2007).

One important aspect of neuroinflammation is guarding the CNS from toxins, cellular damage, and invading pathogens (Town et al. 2005). However, inflammatory responses accompany almost all chronic CNS diseases, acute CNS injuries, as well as several psychiatric disorders such as schizophrenia and autism (Town et al. 2005; Block et al. 2007). Presently it is unclear whether neuroinflammation actually initiates CNS neurodegenerative disorders or represents a significant component in their progression. One speculation regarding adverse CNS inflammation is that microglia might misinterpret certain extrinsic stimuli, such as the amyloid beta fragment associated with Alzheimer's disease, as "pathogens or toxins".

1.1.2: Nutrition

Diet plays an important role in human health, including the health of the CNS. Much attention has been devoted to diets rich in fruits and vegetables, long known for being beneficial to maintaining good health, as well as for being rich sources for antioxidants (Galli et al. 2002). Recent studies in animal models have revealed the dietary effects of blueberries, showing the ability of these diets to reduce cognitive decline and to reduce ischemia-induced brain damage (Mattson et al. 2002; Sweeney et al. 2002; Joseph et al. 2003). Blueberries, like many fruits, contain numerous polyphenols which can act as antioxidants and slow the progression of neuroinflammation (Ramassamy 2006). However, limited amounts of polyphenols cross into the CNS following dietary

consumption of fruits, suggesting that the efficacy of these foods emerges from other compounds that may act as antagonists of pathways of neuroinflammation (Joseph et al. 2003; Wu et al. 2004; Noyan-Ashraf et al. 2005; Ramassamy 2006). Other foods such as fish have shown importance to maintaining good CNS health, in particular due to the high content of omega-3 polyunsaturated fats (Farooqui et al. 2007). These fats can substitute for arachidonic acid in the synthesis of inflammatory molecules known as eicosanoids; producing a separate class of anti-inflammatory molecules including docosanoids (Eyster 2007; Farooqui et al. 2007).

1.2: NADPH oxidase

1.2.1: NADPH oxidase in phagocytes and other cells

The NADPH oxidase was originally described as an enzyme complex responsible for the cellular respiratory burst in sea urchin eggs, phagocytes, and spermatocytes (Warburg 1908; Baldridge and Gerard 1932; MacLeod 1943). In the 1960s, the phagocyte respiratory burst was shown to result in the generation of hydrogen peroxide through an NADPH oxidase activity, and in 1973 the phagocytic NADPH oxidase product was determined to be superoxide rather than hydrogen peroxide (Iyer et al. 1961; Rossi and Zatti 1964; Babior et al. 1973). Concurrent with these findings, clinical studies showed that a rare disorder resulting in recurrent infections accompanied by granulomatous reaction, defined as chronic granulomatous disease (CGD), resulted from diminished phagocytic antimicrobial capacity (Berendes et al. 1957; Quie et al. 1967; Babior et al. 1975). Furthermore, it was shown in 1967 that CGD resulted from a deficiency in the phagocytic respiratory burst (Baehner and Nathan 1967; Holmes et al. 1967; Quie et al. 1967). In 1978 the cytochrome b558 was identified as missing in patients with CGD, and later in the 1980s the gene encoding gp91[phox] (phox for phagocytic-oxidase like) was cloned (Segal and Jones 1978; Segal et al. 1978; Royer-Pokora et al. 1986; Teahan et al. 1987). Shortly thereafter the other subunits of the NADPH oxidase complex, the

membrane-bound p22^{phox}, cytosolic p67^{phox}, cytosolic p47^{phox}, and cytosolic p40^{phox}, were discovered, the evaluation of the cytosolic subunits aided by the development of a cell-free assay system to monitor phagocytic NADPH oxidase activation (Heyneman and Vercauteren 1984; Bromberg and Pick 1985; Dinauer et al. 1987; Segal 1987; Nunoi et al. 1988; Parkos et al. 1988; Volpp et al. 1988; Wientjes et al. 1993).

Recent findings demonstrated that genetically distinct isoforms of the phagocytic NADPH oxidase existed in many, if not all cell types (Meier et al. 1991; Szatrowski and Nathan 1991; Griendling et al. 1994; Bedard and Krause 2007). The new families of NADPH oxidase (NOX) enzymes are defined by gp91^{phox} now being referred to as NOX2, and includes NOX1, NOX3, NOX4, and NOX5; all identified in various non-phagocytic cells (Suh et al. 1999; Banfi et al. 2000; Geiszt et al. 2000; Kikuchi et al. 2000; Banfi et al. 2001; Cheng et al. 2001; Shiose et al. 2001; Bedard and Krause 2007). Two additional large members of the NADPH oxidase family were identified as DUOX1 and DUOX2 (dual oxidase function enzymes) (Dupuy et al. 1999; De Deken et al. 2000). For many NADPH oxidase isoforms the other subunits are the same in most cellular enzyme systems. However, in the case of NOX1, homologues of p47^{phox} and p67^{phox} subunits were cloned and described as NOXO1 and NOXA1, respectively (Banfi et al. 2003; Geiszt et al. 2003; Takeya et al. 2003). The DUOX group was also shown to express maturation factors DUOXA1 and DUOXA2 (Grasberger and Refetoff 2006).

NADPH oxidase family members have been described in various cell types in addition to phagocytes including cardiomyocytes, skeletal muscle myocytes, hepatocytes, endothelial cells, hematopoietic stem cells, and neurons (Jones et al. 1996; Gorlach et al. 2000; Cheng et al. 2001; Javesghani et al. 2002; Li and Shah 2002; Heymes et al. 2003; Serrano et al. 2003; Piccoli et al. 2005; Reinehr et al. 2005; Bedard and Krause 2007). Recent reports have demonstrated that NADPH oxidase family members and their subunits are also expressed in neurons, both in the central as well as peripheral nervous system (Cheng et al. 2001; Thiels and Klann 2002; Zimmerman et al. 2002; Kamsler and Segal

2004; Vallet et al. 2005; Bedard and Krause 2007). Immunohistochemistry, RT-PCR, and *in situ* hybridization demonstrated the presence of NOX1, NOX2, and NOX4 in neurons (Tammariello et al. 2000; Tejada-Simon et al. 2005; Vallet et al. 2005; Ibi et al. 2006; Bedard and Krause 2007). Regulation of neuronal cell fate, synaptic activity, gene expression, long-term potentiation and learning, and possibly specific modulation of NMDA receptor signaling are potential roles of neuronal NADPH oxidase activity (Tammariello et al. 2000; Thiels et al. 2000; Kim et al. 2002; Knapp and Klann 2002; Thiels and Klann 2002; Zimmerman et al. 2002; Kamsler and Segal 2004; Zimmerman et al. 2004; Kishida et al. 2005; Tejada-Simon et al. 2005; Ibi et al. 2006; Bedard and Krause 2007). Importantly, genetic mouse-models of CGD and human CGD patients have impaired learning and memory demonstrating the neurological role of the NADPH oxidase beyond cell culture work (Pao et al. 2004; Kishida et al. 2006). Additionally, reactive astrocytes have increased expression of NOX2 mRNA, suggesting a role for NOX2 in the oxidative stress induced during neuroinflammation (Abramov et al. 2005; Bedard and Krause 2007).

1.2.2: Structure and function

The NADPH oxidase complex consists of five primary subunits. The complex includes both membrane-bound and cytosolic subunits (Groemping and Rittinger 2005; Bedard and Krause 2007). The two membrane-bound subunits are NOX1-5 (gp91^{phox} and homologues) and p22^{phox}. The large subunit (gp91^{phox}) is heavily glycosylated, composed of six transmembrane α-helices, contains both a NADPH and FAD binding site, contains the cytochrome b_{558}, and engages in multiple interactions with cytosolic subunits (Babior and Kipnes 1977; Harper et al. 1985; Kleinberg et al. 1989; Rotrosen et al. 1992; Sumimoto et al. 1992; Doussiere et al. 1993; Koshkin and Pick 1994; Doussiere et al. 1995; Nisimoto et al. 1995; Wallach and Segal 1997; Groemping and Rittinger 2005). Transmembrane helices III and V each contain two histidine residues that span asymmetrical iron-containing hemes (Yu et al. 1998; Biberstine-Kinkade et al. 2001;

Biberstine-Kinkade et al. 2002). The p22^{phox} subunit contains three transmembrane α-

helices and a C-terminal proline-rich region (PRR) that interacts with the cytosolic

subunit p47^{phox} (Dinauer et al. 1991; Leto et al. 1994; Leusen et al. 1994; Sumimoto et al.

1994; Huang et al. 1995; Yu et al. 1997; Yu et al. 1999; DeLeo et al. 2000; Groemping

and Rittinger 2005).
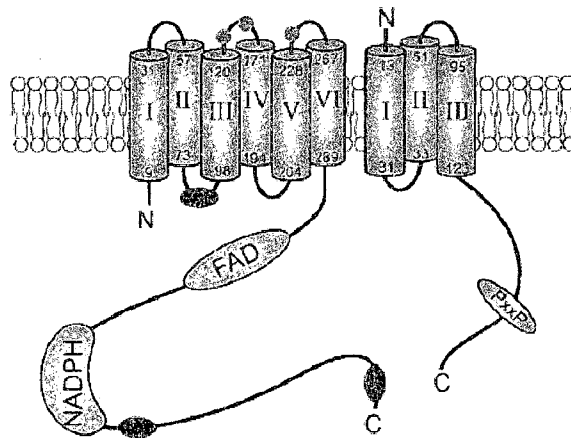
Figure 1.1: Membrane-bound subunits of the NADPH oxidase. Membrane-bound gp91^{phox} and p22^{phox} are shown
spanning the membrane. Transmembrane domains are depicted as dark blue cylinders. The NADPH- and FAD-binding
domains of gp91^{phox} are indicated in pink and light blue, respectively. The proline-rich motif of p22^{phox} is indicated in
gray. Cyan ovals on gp91^{phox} depict regions that interact with cytosolic subunits. Small blue circles indicate sites of
glycosylation on gp91^{phox} (Groemping and Rittinger 2005).

The three cytosolic subunits are p67^{phox}, p47^{phox}, and p40^{phox}. The interactions of all five

subunits together are required for function, and therefore regulation can occur at multiple

points. The cytosolic subunits contain multiple domains that recognize the membrane-

bound subunits as well as specific lipid-binding regions (Groemping and Rittinger 2005).

The p67^{phox} subunit is considered the activator subunit, and contains a TPR

(tetratricopeptide repeat) motif, a PRR, two SH3 (Src homology) domains, and a PB1

domain (Groemping and Rittinger 2005). The TPR domain is implicated in interactions

with the small GTPase Rac1 (Diekmann et al. 1994; Nisimoto et al. 1997; Koga et al.

1999). The second SH3 domain interacts with p47^{phox}, and the PB1 domain interacts with

p40^{phox} (Nakamura et al. 1998; Ito et al. 2001; Kami et al. 2002; Kuribayashi et al. 2002; Ponting et al. 2002; Wilson et al. 2003; Groemping and Rittinger 2005). The p67^{phox} subunit also contains an activation domain that is required for superoxide production, and potentially interfaces with the flavocytochrome on gp91^{phox} (Han et al. 1998; Nisimoto et al. 1999; Han and Lee 2000).

The p47^{phox} subunit, or organizer subunit, contains a PX (Phox homology) domain, two SH3 domains, a polybasic autoinhibitory region (AIR) rich in arginine and lysine residues that covers the SH3 domains, and a PRR that interacts with p67^{phox} (Ponting 1996; Ellson et al. 2001; Kanai et al. 2001; Vignais 2002; Nauseef 2004; Quinn and Gauss 2004). Phosphorylation of numerous sites within the AIR results in its inactivation, revealing the tandem SH3 domains (El Benna et al. 1994; El Benna et al. 1996a; El Benna et al. 1996b; Inanami et al. 1998; Fontayne et al. 2002). The p40^{phox} subunit contains a PX domain, a SH3 domain likely interacting with the PRR of p47^{phox}, and a PB1 domain interacting with p67^{phox} (Someya et al. 1993; Wientjes et al. 1993; Tsunawaki et al. 1994; Fuchs et al. 1995; Grizot et al. 2001). Both the p40^{phox} and p67^{phox} subunits have also been shown to have residues available for phosphorylation (Dusi and Rossi 1993; Benna et al. 1997; Forbes et al. 1999; Someya et al. 1999). NADPH oxidase complexes only produce ROS following assembly of all cytosolic subunits with the two membrane proteins. Phosphorylation is widely viewed as an activating event, ultimately promoting the translocation of the cytosolic subunits to the membrane (Groemping and Rittinger 2005). Interactions between the PRR of p22^{phox} and the two SH3 domains of p47^{phox} initially occur, and promote further interactions between the membrane subunits and both p47^{phox} and p67^{phox} (DeLeo et al. 1995a; DeLeo et al. 1995b; Paclet et al. 2000; Groemping et al. 2003).
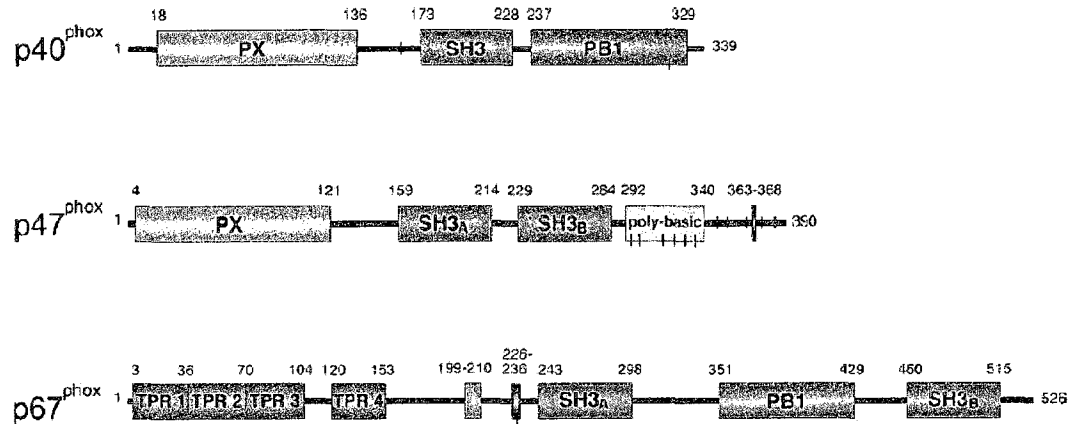
Figure 1.2: Cytosolic subunits of the NADPH oxidase. The predicted domains of the three cytosolic subunits, p40[phox], p47[phox], and p67[phox], are indicated in schematics of primary structure. PX (phox homology) domains are shown in green, SH3 (Src homology) domains are shown in pink, PB1 domains are shown in purple, TPR (tetratricopeptide repeat) motifs are shown in dark blue, the poly basic region of p47[phox] is shown in yellow, PRR (proline-rich region) motifs are shown as thick black bars, and the activation domain of p67[phox] is shown in light blue (Groemping and Rittinger 2005).

Other conflicting studies assign phosphorylation of p40[phox] an inhibitory effect (Sathyamoorthy et al. 1997; Cross 2000; Lopes et al. 2004). Further evaluation has demonstrated that phosphorylation of p47[phox] and p40[phox] induces changes in subunit conformation, unmasking specific lipid-binding domains (Quinn and Gauss 2004; Ueyama et al. 2007). The lipid-binding PX domain recognizes anionic phospholipids such as arachidonic acid phosphatidic acid and phosphoinositides, yet these lipid-binding domains in p47[phox] and p40[phox] may recognize different phosphoinositides (Sato et al. 2001; Xu et al. 2001; Ellson et al. 2002; Wientjes and Segal 2003; Quinn and Gauss 2004; Groemping and Rittinger 2005; Bedard and Krause 2007; Ueyama et al. 2007). Therefore, phosphorylation of p40[phox] could harbor a pivotal targeting signal for the NADPH oxidase complex to different membrane regions. It is important to note that various NADPH oxidase isoforms have been found in different cellular membranes, suggesting that specific membrane targeting of cytosolic subunits may be important for

cellular localization of oxidase activity (Groemping and Rittinger 2005; Bedard and Krause 2007).

Following translocation of the cytosolic subunits to the membrane and interaction with the membrane-bound subunits, the active enzyme complex transfers single electrons from cytosolic NADPH, and to a lesser extent cytosolic NADH, via the cytochrome to oxygen, forming the superoxide anion (Isogai et al. 1995; Doussiere et al. 1996; Koshkin et al. 1997; Cross et al. 1999). The production of superoxide by the NADPH oxidase is extremely rapid, with release of superoxide on the outside of the plasma membrane in the case of the NOX2 isoform. In contrast, ROS production for other NADPH oxidase isoforms in other cell types was shown to release ROS into the cytosol (Groemping and Rittinger 2005; Bedard and Krause 2007). Diphenylene iodonium, an NADPH oxidase inhibitor, targets the single electron transfer reaction of the cytochrome (Bedard and Krause 2007).
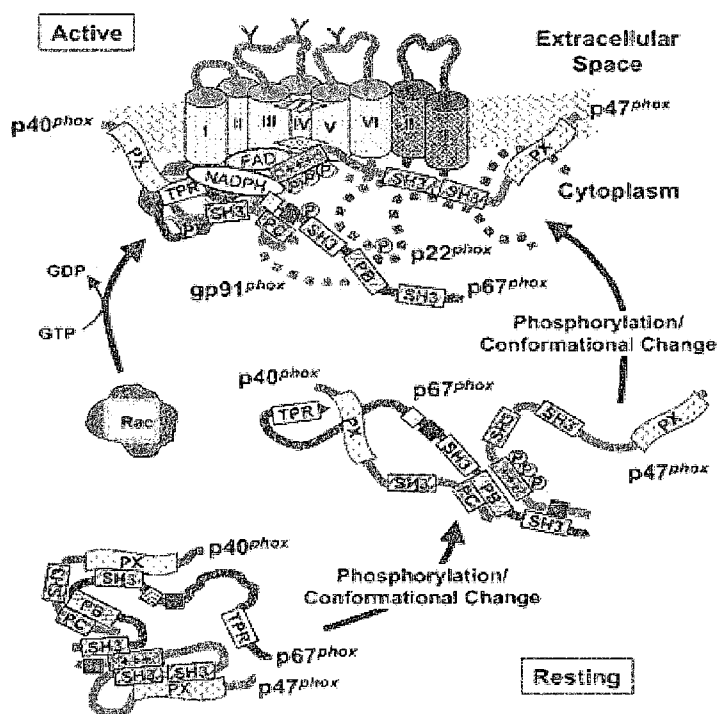
Figure 1.3: Membrane targeting of cytosolic NADPH oxidase subunits. Phosphorylation of p47^{phox} and p40^{phox} induce conformational changes that reveal specific membrane-binding domains. Cytosolic subunits, p47^{phox}, p40^{phox}, and p67^{phox}, translocate to the membrane and interact with the membrane-bound subunits gp91^{phox} and p22^{phox} through specific protein-protein interactions. Interaction of p67^{phox} and Rac with the flavocytochrome allows full oxidase function (Quinn and Gauss 2004).

The small GTPases Rac1 and Rac2 are necessary for NADPH oxidase activation but are not considered true subunits since they play important roles in numerous other cellular processes, such as cytoskeletal dynamics (Van Aelst and D'Souza-Schorey 1997; Bishop and Hall 2000; Etienne-Manneville 2006; Bedard and Krause 2007). Strong evidence suggests that Rac1 regulates NOX1 and NOX2 and potentially also NOX3 and NOX4 in non-phagocytic cells (Gorin et al. 2003; Inoguchi et al. 2003; Groemping and Rittinger 2005; Ueno et al. 2005; Bedard and Krause 2007; Miyano and Sumimoto 2007). Rac1 is active in its GTP-bound state, and inactive in its GDP-bound state. This molecular switching is regulated by GEFs (guanine nucleotide-exchange factors), which promote the release of GDP allowing GTP to bind, and by GAPs (GTPase-activating proteins), which promote GTP hydrolysis (Bourne et al. 1990, 1991). Rac1 is also geranylated at its

C-terminus aiding in membrane association, and Rac1 can translocate to the membrane independent of NADPH oxidase subunits (Regazzi et al. 1992; Hoffman and Cerione 2000; Scheffzek et al. 2000). GTP-bound Rac1 also interacts with the TPR domain of p67^{phox} (Diekmann et al. 1994; Nisimoto et al. 1997; Koga et al. 1999). Both Rac1 and Rac2 appear to regulate NOX2, however Rac2 is inducible and is exclusively expressed in hematopoietic cell types (Roberts et al. 1999; Gu et al. 2001; Groemping and Rittinger 2005; Bedard and Krause 2007).

1.3: Sphingolipids

1.3.1: Sphingolipid metabolism

Sphingolipids are important to cellular structure and function. In addition to being integral components of membranes, several sphingolipids are bioactive and mediate various cellular processes (Futerman and Riezman 2005; Eyster 2007). The nitrogen bound at the 2-carbon of the sphingosine-backbone is a unique characteristic to sphingolipids. The central lipid of sphingolipid metabolism is ceramide, a central point of multiple biosynthetic and catabolic pathways (Futerman and Riezman 2005; Eyster 2007). The biosynthesis of complex sphingolipids involves the addition of various polar head groups to the ceramide-backbone. Various sphingolipids regulate diverse cellular responses, with specific alterations in the general sphingolipid-structure mediating dramatic differences in cellular function (Futerman and Riezman 2005; Eyster 2007). The synthesis of sphingolipids begins in the endoplasmic reticulum and continues in the Golgi apparatus and at the plasma membrane (Futerman and Riezman 2005). The breakdown of sphingolipids occurs at the plasma membrane and even more so in the lysosome (Futerman and Riezman 2005). Cellular localization of sphingolipids is reflective of their synthesis and function. Transport proteins like ABC (ATP-binding cassette) transporters and CERT (ceramide-transfer protein) regulate the localization and movement of certain sphingolipids.

The *de novo* synthesis of ceramide begins with the condensation of serine and palmitoyl-CoA, a reaction catalyzed by the enzyme serine palmitoyltransferase, to give the product 3-ketosphinganine (Futerman and Riezman 2005; Eyster 2007). In the next step, 3-ketoreductase reduces 3-ketosphinganine, also known as 3-ketodihydrosphingosine, to sphinganine or dihydrosphingosine (Futerman and Riezman 2005; Eyster 2007). Sphinganine is then acylated at the amide position by dihydroceramide synthase to give dihydroceramide and desaturation by dihydroceramide desaturase finally results in ceramide formation (Futerman and Riezman 2005; Eyster 2007). It is important to note that palmitate, a saturated fatty acid, is an essential precursor of ceramide biosynthesis, thus linking ceramide synthesis to saturated fat oversupply and obesity (Chavez et al. 2003; Futerman and Riezman 2005; Eyster 2007). Another important point is that acylation can add a variety of fatty acid chains to the amide position, resulting in ceramides with different chain lengths and degrees of unsaturation. In addition to affecting membrane dynamics, research has indicated that different ceramides can have varying effects on cellular function (Hannun 1996; Hannun and Luberto 2000).

Sphingolipid metabolism continues with ceramide as a precursor to complex sphingolipids such as glucosylceramide (Futerman and Riezman 2005; Eyster 2007), lactosylceramide, various gangliosides, and sphingomyelin. Specific synthases add glucose or phosphocholine to form glucosylceramide or sphingomyelin respectively (Futerman and Riezman 2005). Lactosylceramide and the gangliosides are formed by the further addition of sugars, as well as sialic acid in the case of gangliosides, to glucosylceramide. Conversely, the degradation of sphingomyelin by sphingomyelinases, and glucosylceramide by cerebrosidases, liberates ceramide in mechanisms known as the salvage synthetic pathways (Futerman and Riezman 2005; Eyster 2007). Further catabolism of ceramide by ceramidases, enzymes that deacylate ceramide, results in the formation of sphingosine (Futerman and Riezman 2005; Eyster 2007). Importantly, multiple sphingomyelinases and ceramidases have been identified and characterized by their pH optimums. Enzymes with neutral pH optimum exist and breakdown their

substrates at the plasma membrane, while acidic enzymes, including the cerebrosidase, are localized to the lysosome where significant catabolism and turnover occurs (Futerman and Riezman 2005; Eyster 2007). Several deficiencies in the breakdown of complex sphingolipids have been identified, and are characterized as lysosomal storage disorders because they result in specific complex sphingolipid accumulations in the lysosome.

Sphingosine can be acylated to form ceramide again by a variety of ceramide synthases, or it can be phosphorylated by sphingosine kinase (Futerman and Riezman 2005; Eyster 2007). Lipid kinases are a very important feature of sphingolipid metabolism. Two sphingosine kinases, a sphinganine kinase, and a ceramide kinase have been identified, phosphorylating sphingosine, sphinganine, and ceramide respectively (Futerman and Riezman 2005; Eyster 2007). Phosphorylation seems to be an important event in the divergent roles of sphingolipids as phosphosphingolipids are primarily implicated in cellular survival and growth as opposed to their non-phosphorylated counterparts. Specific phosphatases regulate sphingosine-1-phosphate, sphinganine-1-phosphate, and ceramide-1-phosphate by dephosphorylation (Futerman and Riezman 2005; Eyster 2007). Sphingosine-1-phosphate is also a target of irreversible degradation by a specific lyase (Futerman and Riezman 2005; Eyster 2007). The regulation of these kinases, phosphatases, the lyase, and the enzymes described in ceramide metabolism are tightly regulated. Alterations in the regulation of these enzymes can lead to a variety of disorders ranging from degenerative pathologies to cancer.
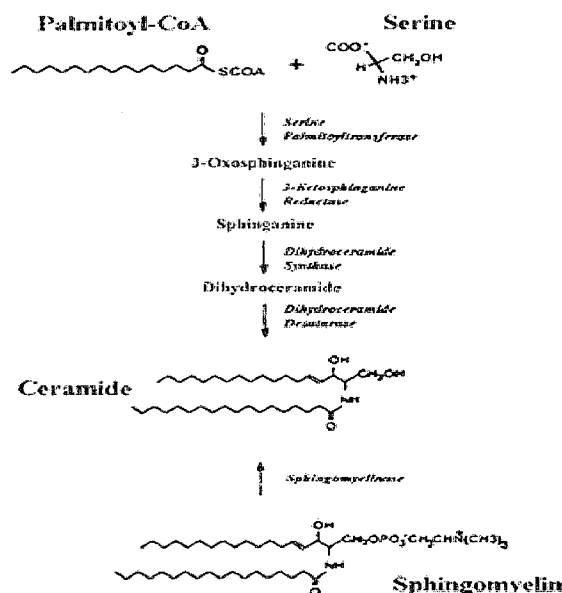
Figure 1.4: Sphingolipid metabolism. *De novo* ceramide synthesis begins with the condensation of palmitoyl-CoA and serine, followed by reduction of 3-ketosphinganine, acylation of sphinganine, and finally introduction of the trans double bond into dihydroceramide. Alternatively, ceramide can be formed from the hydrolysis of complex sphingolipids, like sphingomyelin, through salvage pathways (Summers and Nelson 2005).

1.3.2: Neutral Sphingomyelinase

Sphingomyelinases are enzymes that catalyze the hydrolysis of sphingomyelin, liberating ceramide and phosphocholine (Marchesini and Hannun 2004; Clarke et al. 2006). Sphingomyelinases are identified by their pH optimum and ion dependence (Marchesini and Hannun 2004). Neutral sphingomyelinases, which predominantly localize to the plasma membrane, and acidic sphingomyelinases residing in the lysosome are the most widely studied. Neutral sphingomyelinases were identified as the primary sphingomyelinase induced by cellular stress, including serum deprivation, and growth confluency (Clarke et al. 2006). Mammalian neutral sphingomyelinases share some homology to bacterial sphingomyelinases particularly in the catalytic regions (Clarke et al. 2006). The brain-specific magnesium-dependent neutral sphingomyelinase, neutral sphingomyelinase-2, is specifically inhibited by the pharmacological agent GW4869

(Luberto et al. 2002; Clarke et al. 2006). The activity of this isoform has since been identified in other tissues. In contrast to bacterial sphingomyelinases, mammalian neutral sphingomyelinases are membrane bound proteins and this has made their characterization more difficult (Clarke et al. 2006).

Structures of the catalytic regions of mammalian neutral sphingomyelinases were determined by homology modeling using crystal structures from bacterial sphingomyelinases. Specifically, the acidic residues such as aspartates and histidines were discovered to be important to catalysis (Tomita et al. 1993; Tamura et al. 1995; Matsuo et al. 1996; Hofmann et al. 2000), while other aspartate residues were shown to be important for substrate recognition (Tamura et al. 1995). Some neutral sphingomyelinases have catalytic activity that is dependent on the presence of ions such as magnesium. Two magnesium-binding sites were found, including one requiring a conserved glutamate residue (Fujii et al. 1998; Obama et al. 2003).

Aside from analysis of catalytic sites, additional structural information is more limited. It is known that mammalian neutral sphingomyelinases contain two hydrophobic transmembrane regions (Hofmann et al. 2000; Tani and Hannun 2007), as well as a binding site for anionic phospholipids such as phosphatidylserine (Okamoto et al. 2002; Marchesini et al. 2003; Clarke et al. 2006). The neutral sphingomyelinase also interacts with an adapter protein known as the factor associated with neutral sphingomyelinase (FAN). The TNFα type I receptor couples to FAN, and this interaction mediates TNFα-induced neutral sphingomyelinase activation (Adam-Klages et al. 1996; Segui et al. 2001; Marchesini and Hannun 2004). The enzyme is also redox-sensitive, as the addition of hydrogen peroxide induced its activity (Levy et al. 2006). A recent study evaluated specific S-palmitoylation of cysteine residues of the neutral sphingomyelinase (Tani and Hannun 2007). Two clusters, termed the Cys3 and Cys5 positions, were shown to be S-palmitoylated. The Cys3 modification occurs in the hydrophobic region of the enzyme, suggesting importance in membrane targeting and stability of the enzyme (Tani and

Hannun 2007). The Cys5 modification is localized in the catalytic region, however no specific role was identified (Tani and Hannun 2007). Enzyme activity was determined to be independent of palmitoylation.

1.3.3: Sphingosine Kinase

Sphingosine kinases are novel lipid kinases that phosphorylate sphingosine, producing sphingosine-1-phosphate (Maceyka et al. 2002; Spiegel and Milstien 2003; Hait et al. 2006; Taha et al. 2006b; Wattenberg et al. 2006; Alemany et al. 2007). There are two main homologues of sphingosine kinase. Both sphingosine kinase-1 and -2 phosphorylate D-*erythro*-sphingosine, but sphingosine kinase-2 has the ability to phosphorylate additional isomers of sphingosine that would otherwise inhibit sphingosine kinase-1 (Olivera et al. 1998; Liu et al. 2000; Melendez et al. 2000; Nava et al. 2000; Pitson et al. 2000b; Billich et al. 2003; Alemany et al. 2007). Sphingosine kinase-1 is a cytosolic protein, while sphingosine kinase-2 is a membrane protein and interestingly is involved in the regulation of apoptosis. Sphingosine kinase-1 responds to various stimuli such as growth factors, hormones, and cytokines, and has been shown to translocate to different membranes including the plasma membrane and phagosomal membranes (Olivera and Spiegel 1993; Maceyka et al. 2002; Spiegel and Milstien 2003; Taha et al. 2006b; Wattenberg et al. 2006; Alemany et al. 2007). Recently, research has identified important structural features of sphingosine kinase-1.

The catalytic domain of sphingosine kinase is a DAG kinase catalytic domain (Pitson et al. 2002; Alemany et al. 2007). In sphingosine kinase-1, the nucleotide-binding site has a consensus sequence of SGDGX17-21K, where X is any residue (Pitson et al. 2002). The specific glycine-82 was determined to be absolutely essential for catalytic activity, and its mutation to aspartate resulted in a dominant negative kinase (Pitson et al. 2000a). Similarly, glycine-212 in sphingosine kinase-2 was found to be essential for catalytic activity (Yoshimoto et al. 2003; Maceyka et al. 2005). Glycine-133 is also critical to the

function of sphingosine kinase-1 (Pitson et al. 2001). Mutation to aspartate decreased function while mutation to alanine enhanced catalytic function (Pitson et al. 2001). Sphingosine binding was also evaluated and found to localize to a C4 domain in sphingosine kinase-1, with an essential aspartate residue identified in a mouse isoform of sphingosine kinase-1 (Yokota et al. 2004).

Additional features of sphingosine kinase-1 were identified as its function was evaluated. Research had demonstrated that phosphorylation of sphingosine kinase-1 at serine-225 occurred in response to agonist stimulation (Pitson et al. 2003; Alemany et al. 2007). Mutation analysis later demonstrated that phosphorylation was not required for basal function, but that it was necessary for kinase translocation to the plasma membrane in response to growth factor and cytokine stimuli (Pitson et al. 2005; Alemany et al. 2007). Research has identified TNFα as a stimulating factor for sphingosine kinase-1. Specifically, it was shown that the kinase interacts with TNF receptor associated factor-2 through a consensus PPEE binding site (Xia et al. 2002). Additionally, it was noted that sphingosine kinase-1 bound acid phospholipids via a specific phosphatidylserine-binding site including essential residues threonine-54 and asparagine-89 (Olivera et al. 1996; Stahelin et al. 2005; Alemany et al. 2007). Inhibition of phosphorylation decreased binding to phosphatidylserine, and a model was proposed where phosphorylation causes a conformation change revealing the phosphatidylserine-binding site (Pitson et al. 2003; Stahelin et al. 2005). Sphingosine kinase-1 also interacts with the acidic phospholipid phosphatic acid through a binding site located somewhere in the C-terminal half of the enzyme (Delon et al. 2004). This interaction may be important for targeting to endosomal or phagosomal compartments.

Sphingosine kinase-1 interacts with calcium-dependent calmodulin, an interaction used to measure proper folding of the enzyme (Kohama et al. 1998; Alemany et al. 2007). Some studies suggest that calcium is necessary for kinase activity, but no specific interaction has been noted (Alemany et al. 2007). Other studies imply that the kinase regulates

mobilization of intracellular calcium (Alemany et al. 2007). The calmodulin-binding site has been mapped to residues 191-206 (Sutherland et al. 2006). Without a functional binding site, catalytic activity and phosphorylation remain intact, however phorbol ester-stimulated membrane translocation was impeded (Sutherland et al. 2006). Interestingly in PC12 cells, calcium influx through voltage-gated calcium channels elevated sphingosine-1-phosphate levels, and ultimately enhanced noradrenaline release (Alemany et al. 2001). A more recent study has also implicated sphingosine kinase as a modulator of glutamate release from hippocampal neurons (Kajimoto et al. 2007).

New contradicting studies have suggested that TNFα impedes sphingosine kinase-1-mediated signaling. In one study, MCF-7 breast cancer cells treated with TNFα for a prolonged period entered apoptosis involving lysosomal disruption and release of cathepsin B (Taha et al. 2005; Taha et al. 2006a). Cathepsin B, a cysteine protease, cleaved sphingosine kinase-1 at multiple sites. Another study in SH-SY5Y neuroblastoma cells revealed that the soluble, toxic amyloid beta fragment resulted in a loss of sphingosine kinase-1 activity (Gomez-Brouchet et al. 2007). The researchers were able to overcome loss in kinase activity by using the antioxidant N-acetyl-L-cysteine. These reports suggest that prolonged or excessive exposure to TNFα or amyloid beta actually result in downregulation of sphingosine kinase in certain cell types.

1.3.4: Gangliosides and neuronal membranes

The membranes of neurons contain phospholipids, sphingolipids, cholesterol, and protein. Sphingomyelin and glycosphingolipids, including gangliosides, are particularly prevalent in neuronal membranes (Prioni et al. 2004; Farooqui et al. 2007). These lipids, in addition to cholesterol, play important roles in the organization of lipid microdomains associated with growth factor and cytokine-mediated signaling. Gangliosides regulate cell adhesion, differentiation, neuritogenesis, as well as signaling processes such as those leading to oxidative stress (Prioni et al. 2004; Sonnino et al. 2006). Gangliosides exert

their effects through direct interactions with proteins and enzymes, such as growth factor receptors and protein kinases, found on the outer leaflet of the plasma membrane (Prioni et al. 2004; Sonnino et al. 2006).

An important feature of gangliosides is their strict localization to the outer leaflet of the plasma membrane. Glycosphingolipid synthesis begins with the glycosylation of ceramide by glucosylceramide synthase, an enzyme with activity on the cytosolic-side of the Golgi membrane (Futerman and Riezman 2005; Sonnino et al. 2006). Glucosylceramide is subsequently transported across the membrane, where further glycosylation and sialic acid additions occur on membranes destined to become the outer leaflet of the plasma membrane. The transport of glucosylceramide across the Golgi membrane has been attributed to P-glycoprotein, an ATP-binding cassette (ABC) transporter (Liu et al. 2001; Gouaze-Andersson and Cabot 2006). The position of gangliosides in the outer leaflet of the plasma membrane not only allows for specific interactions with proteins, but also for the space required by the large polar head groups (Futerman and Riezman 2005; Sonnino et al. 2006). Enrichment of gangliosides within microdomains induces positive membrane curvature due to the space required by the head groups with significant consequences for membrane invaginations (Fig. 1.5) (Sonnino et al. 2006).
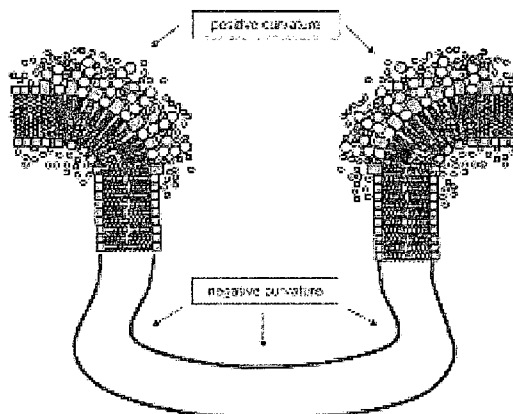
Figure 1.5: Ganglioside-induced membrane alterations. Gangliosides reside on the outer leaflet of the plasma membrane. The large polar head group of gangliosides, when packed together, induces positive membrane curvature due to space constraints. Positive membrane curvature is important to the formation of membrane invaginations (Sonnino et al. 2006).

1.3.5: Interconversion of ceramide and sphingosine-1-phosphate: a potential biostat

Ceramide and sphingosine-1-phosphate are both important bioactive sphingolipids with distinctly opposing functions. Ceramide is implicated in the regulation of cellular stress, oxidative stress regulated by oxidoreductases, ceramide-mediated mitochondrial dysfunction, and apoptosis (Hannun 1996; Hannun and Luberto 2000). Ceramide induces apoptosis through activation of caspases as well as by mediating mitochondrial alterations and release of cytochrome c (Hannun 1996; Hannun and Luberto 2000). Additionally, ceramide can activate various kinases and phosphatases essential for the regulation of cellular stress and apoptosis (Hannun 1996; Hannun and Luberto 2000). A classic example of ceramide-mediated cellular signaling is the case of insulin resistance in which the activity of Akt/PKB is negatively regulated by ceramide (Summers et al. 1998; Chavez et al. 2003; Stratford et al. 2004). Furthermore, ceramide was shown to accumulate in a variety degenerative disorders ranging from diabetes to Alzheimer's disease (Chavez et al. 2003; Grimm et al. 2005; Zheng et al. 2006).

Recent studies suggested that ceramide forms large pores in membranes. Molecular models and experimental data suggest that ceramides pack together, and that the double bond of ceramide was critical to the ability to pack together (Anishkin et al. 2006). In these studies, dihydroceramide was unable to form stable pores. Hydrogen bonding was also proposed as an important structural feature, both between ceramide molecules and between ceramide molecules and with water molecules that fill the pore. Ceramide as a sphingolipid, has several hydrogen bond donors and acceptors within its hydroxyl groups, the carboxyl group, and the amide linkage (Anishkin et al. 2006). The addition of more ceramide molecules was suggested to increase pore size, allowing molecules as large as small proteins to pass through the membrane.
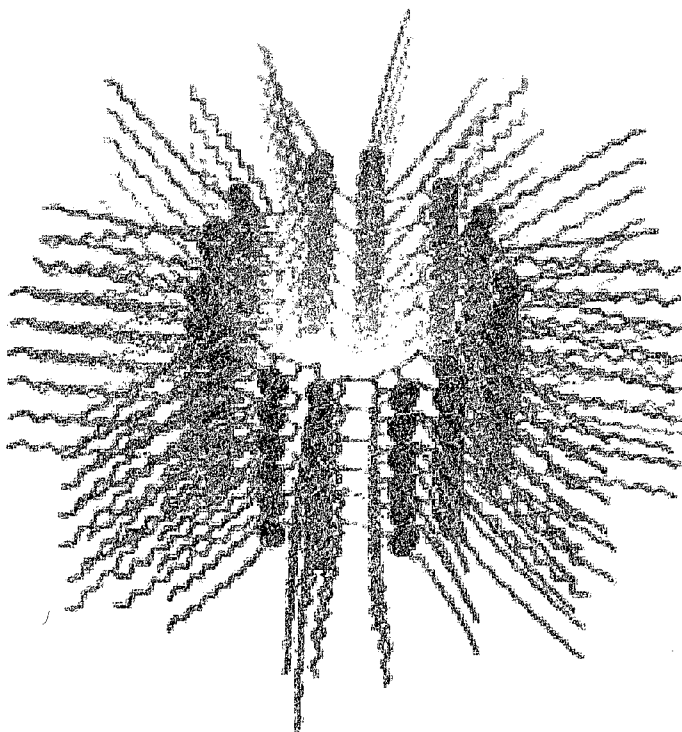

Figure 1.6: Ceramide channel. C16-ceramide channel formed by molecules in 6 layers and 14 columns. Neighboring columns are in antiparallel orientation. Hydrogen bonding stabilizes the channel, and the double bond of ceramide stabilizes the stacking of ceramide molecules (Anishkin et al. 2006).

In contrast to ceramide, sphingosine-1-phosphate regulates cell growth and survival, cytoskeletal dynamics and motility, inflammation, thermotolerance, angiogenesis, tumorgenesis, development, and antagonizes the effects of ceramide (Cuvillier et al. 1996; Pyne and Pyne 2000; Spiegel and Milstien 2002). Sphingosine-1-phosphate regulates these processes by binding to specific G-protein coupled receptors known as sphingosine-1-phosphate receptors (Cuvillier et al. 1996; Pyne and Pyne 2000; Spiegel and Milstien 2002). Additional evidence suggests that intracellular targets may also exist for sphingosine-1-phosphate. However, these targets are currently not defined (Van Brocklyn et al. 1998; Xia et al. 1998; Morita et al. 2000; Rosenfeldt et al. 2001). In summary, these findings suggest that a ceramide-sphingosine-1-phosphate 'biostat' exists where the ratio of ceramide to sphingosine-1-phosphate regulates cellular fate (Pyne and Pyne 2000). In this model, significant accumulation of ceramide would result in degenerative processes while clearance of ceramide and/or accumulation of sphingosine-1-phosphate would promote cell survival and growth. It is noteworthy that certain cancers were identified where the ratio of sphingosine-1-phosphate to ceramide was increased (Ogretmen and Hannun 2004).

1.3.6: Regulation of eicosanoid biosynthesis

Eicosanoids are lipid-derived bioactive molecules with important pro- and anti-inflammatory functions (Needleman et al. 1986; Piomelli 1993; Goetzl et al. 1995; Eyster 2007). Two well-known categories of eicosanoids, prostaglandins and leukotrienes, are products of cyclooxygenases (COX) and lipoxygenases (LOX), respectively (Murakami and Kudo 2006). While eicosanoids are the primary products of these enzymes, ROS represent additional byproducts. COXs include two isoforms that are targeted by several well-known pain medications (Eyster 2007). COX-2 is inducible and its dysregulation has been implicated in a variety of pathological conditions. There are three LOX isoforms, 5-LOX, 12-LOX, and 15-LOX, corresponding to the carbon positions that they oxygenate (Eyster 2007).

COXs and LOXs both utilize arachidonic acid as their primary substrates (Eyster 2007; Farooqui et al. 2007). Arachidonic acid is an omega-6 polyunsaturated fatty acid liberated by phospholipase A_2 activity (Eyster 2007). Arachidonic acid also acts as an important mediator of NADPH oxidase isoforms acting as a membrane anchor (Quinn and Gauss 2004; Groemping and Rittinger 2005; Bedard and Krause 2007). Interestingly, omega-3 polyunsaturated fatty acids such as docosahexaenoic acid reduce the activity of both COXs and LOXs, therefore having an anti-inflammatory effect (Eyster 2007; Farooqui et al. 2007). Additionally, a lipoxygenase-like enzyme utilizes docosahexaenoic acid as a substrate to produce docosatrienes and resolvins (Eyster 2007; Farooqui et al. 2007). These bioactive molecules are known collectively as docosanoids, and act to antagonize eicosanoid effects, as well as down-regulate cytokine production in glial cells (Eyster 2007; Farooqui et al. 2007). Polyunsaturated fatty acids are acquired from dietary sources with omega-6 polyunsaturated fatty acids arising from Western diets, and omega-3 polyunsaturated fatty acids arising from diets rich in certain fish such as salmon and tuna. The importance of arachidonic acid as a substrate for eicosanoid biosynthesis and in the regulation of several other enzymes, suggests that phospholipase A_2 activity is essential for inducible-inflammatory responses. Research has demonstrated that the cytosolic phospholipase A_2 (cPLA$_2$) is a target of ceramide-mediated signaling (Huwiler et al. 2001). In addition to activation through phosphorylation (Kudo and Murakami 2002; Ghosh et al. 2006), which has been proposed to unveil specific lipid-binding domains, it was shown that ceramide could directly interact with cPLA$_2$ (Huwiler et al. 2001). More recent research has shown that cPLA$_2$ interacts with, and is activated by, ceramide-1-phosphate (Pettus et al. 2004; Subramanian et al. 2005; Subramanian et al. 2007). Subsequently, ceramide-1-phosphate has gained considerable attention lately as an important bioactive sphingolipid regulating inflammatory responses. The role of ceramide-1-phosphate appears to be involved in enhancing the association of cPLA$_2$ with target membranes (Pettus et al. 2004; Subramanian et al. 2005; Subramanian et al. 2007). Target membranes of cPLA$_2$ include the nuclear envelope, the endoplasmic reticulum, the Golgi apparatus, and the plasma membrane (Channon and Leslie 1990; Nalefski et al.

1994; Clark et al. 1995; Leslie 1997). Moreover, ceramide kinase, the enzyme responsible for the phosphorylation of ceramide, is regulated in a calcium-dependent manner. Ceramide kinase is localized to the Golgi apparatus as well as the plasma membrane, thus putting the production of ceramide-1-phosphate near the $cPLA_2$ (Lamour et al. 2007). Ceramide-1-phosphate acts as an allosteric activator of $cPLA_2$ enhancing the association of the C2 domain of the enzyme with the target membrane (Pettus et al. 2004; Subramanian et al. 2005; Subramanian et al. 2007). Importantly, several basic amino acids in the C2 domain of $cPLA_2$ were shown to be important to the interaction with and regulation by ceramide-1-phosphate (Pettus et al. 2004; Subramanian et al. 2005; Subramanian et al. 2007).

1.3.7: Regulation of multi-drug resistant and invasive cancer

Chemotherapy and radiation are mainstays of cancer treatment worldwide and resistance to these treatments is often observed in cancers. Advanced cancers also invade secondary tissues and organs (metastasis). Recent research has focused on the role of sphingolipids in cancer drug resistance and invasiveness. Several studies have focused on the proposed ceramide-sphingosine-1-phosphate biostat, and the role these bioactive lipids play in cellular survival (Senchenkov et al. 2001; Ogretmen and Hannun 2004).

Importantly, most chemotherapeutics and radiation treatments induce significant accumulations of ceramide (Senchenkov et al. 2001; Ogretmen and Hannun 2004), which was not the original design of most of these treatments. However, ceramide is an important cellular signal that leads to apoptosis (Hannun 1996; Zheng et al. 2006). Therefore, newer chemotherapeutics aim to increase ceramide levels or deliver ceramide into cancer cells (Senchenkov et al. 2001; Fox et al. 2006; Gouaze-Andersson and Cabot 2006). A recently described feature of drug-resistant cancers is the ability to clear ceramide from the system. Specifically, enzymes that neutralize ceramide or degrade ceramide have been shown to be upregulated in certain drug-resistant cancers

(Senchenkov et al. 2001; Ogretmen and Hannun 2004; Gouaze-Andersson and Cabot 2006). Another important feature of drug resistance is the ability to eliminate chemotherapeutic agents. Positive regulation of drug transporters, including the ABC transporters that also move lipids, was demonstrated in multi-drug resistant cancers (Liu et al. 2001; Gouaze-Andersson and Cabot 2006). Interestingly, glucosylceramide, a sphingolipid generated by neutralizing ceramide through glycosylation, interacts with and positively regulates multi-drug transporters (Liu et al. 2001; Gouaze-Andersson and Cabot 2006).

Additional studies have focused on the roles of acid ceramidase and sphingosine kinase in cancer. Acid ceramidase is upregulated in certain cancers, and this may be important not only in clearing ceramide, but also in allowing sphingosine to accumulate as a substrate for sphingosine kinase (Senchenkov et al. 2001; Ogretmen and Hannun 2004). Sphingosine-1-phosphate, the product of sphingosine kinase, was evaluated due to its role as a pro-survival, pro-growth, and anti-ceramide regulator. Not surprisingly, sphingosine kinase is upregulated in several highly invasive cancers since it also regulates motility (Senchenkov et al. 2001; Ogretmen and Hannun 2004). Additionally, sphingosine-1-phosphate, as a regulator of angiogenesis, allows tumors to form extensive blood vessel networks that maintain high levels of nutrients. In fact, inhibitors of sphingosine kinase or glucosylceramide synthase concurrently with common chemotherapeutics can restore sensitivity of resistant cancers to these treatments (Senchenkov et al. 2001; Ogretmen and Hannun 2004; Gouaze-Andersson and Cabot 2006).

1.4: Rationale and significance of thesis research

Neuroinflammation is a key component in the progression of acute and chronic pathologies of the CNS (Fetler and Amigorena 2005; Block et al. 2007; Farooqui et al. 2007). Induction of oxidative stress during neuroinflammation directly contributes to irreversible damage that affects neuronal function and survival. The primary hypothesis

of this thesis research is that ceramide metabolism plays a crucial role in the regulation of NADPH oxidase-driven oxidative stress in the CNS. This research set forth to elucidate a molecular pathway in neurons linking inflammatory stimuli to the onset of oxidative stress and to neurodegeneration, and evaluated the role of ceramide metabolism and the NADPH oxidase in this process.

In particular, the regulation of the NADPH oxidase by sphingolipids and subsequent oxidative modulation of macromolecules important to neuronal function and survival were evaluated. The sphingolipids ceramide, ceramide-1-phosphate, and sphingosine-1-phosphate, as bioactive molecules regulate a diversity of cellular functions including inflammatory responses, growth, survival, and oxidative stress (Eyster 2007). Therefore, these lipids and their metabolism provided an intriguing potential mechanism for the regulation of the NADPH oxidase, as well as important targets of NADPH oxidase-dependent oxidation. Importantly, ceramide and ceramide-1-phosphate are well established as regulators of Rac GTPase (Yi et al. 2007), protein kinase (Fox et al. 2007), and $cPLA_2$ activity (Huwiler et al. 2001; Subramanian et al. 2005), which are all important regulators of NADPH oxidase (Bedard and Krause 2007).

This research further evaluated NADPH oxidase-dependent oxidation of macromolecules key to neuronal survival and function such as sphingosine kinase-1, a survival kinase, and actin, a component of the neuronal cytoskeleton. Actin plays a prominent role in growth cone motility, axon regeneration, dendritic arborization, and plasticity of synapses (Gungabissoon and Bamburg 2003; Calabrese et al. 2006; Tada and Sheng 2006). Furthermore, disruption of the neuronal actin cytoskeleton is prevalent in both acute CNS injury and chronic CNS pathologies (Fiala et al. 2002; Maloney and Bamburg 2007).

This research also investigated whether a specific ceramide metabolite, glucosylceramide, regulates NADPH oxidase. Since ceramide clearance is linked to cell survival, and generally opposes ceramide exposure, we tested the hypothesis that

glucosylceramide could antagonize the NADPH oxidase. Intriguingly, reports have shown that accumulations of glucosylceramide during type I Gaucher's disease, a lysosomal deficiency in cerebrosidase, are associated with dramatic reductions in superoxide production, similar to that observed in chronic granulomatous disease, which is characterized by a deficiency in NADPH oxidase activity (Liel et al. 1994; Won and Singh 2006).

Detailed knowledge of the pathway between neuroinflammatory mediators and oxidative stress would potentially lead to the development of improved therapeutics to manage acute CNS insults, chronic CNS diseases, and psychiatric disorders. As such, the final portion of this thesis research addressed the possibility that wild Alaskan blueberries contain components that could antagonize pathways of neuroinflammation, particularly sphingolipid-mediated pathways. This study showed the value of blueberries beyond their role as antioxidants and suggested that therapeutics targeting neuroinflammation may already exist in nature.

1.5: Aims, hypotheses, and methods of individual chapters

Chapter 2 - TNFα-Induced Neuronal NADPH Oxidase Activity Mediates Oxidative Damage to the Neuronal Actin Cytoskeleton.

Aim 1: To determine if a neuronal NOX activity is responsive to the pro-inflammatory cytokine TNFα.

Aim 2: To determine the impact of NOX-derived ROS on the neuronal actin cytoskeleton.

Hypothesis: TNFα stimulates a neuronal NOX activity leading to the oxidation of the actin cytoskeleton.

Methods: Immunochemistry was used to detect the presence of NOX subunits in neuronal cells. NOX activity was characterized by analysis of cytosolic subunit phosphorylation, the ability of individual subunits to translocate from the cytosol to the plasma membrane, NADPH-reducing ability, and ROS production. Confocal imaging was used to detect alterations in the actin cytoskeleton in response to TNFα, while actin oxidation in response to TNFα was quantified by immunoprecipitation of actin followed by derivatization of protein carbonyls, and western blotting.

Chapter 3 - TNFα- and Aβ-Induced Neutral Sphingomyelinase Activity Regulates the Neuronal NADPH Oxidase and Subsequent Oxidative Damage to Sphingosine Kinase-1.

Aim 1: To define a role for ceramide, produced by Mg^{2+}-nSMase activation, in the stimulation of neuronal NOX activity in response to either TNFα or $A\beta^{1-42}$, the soluble fragment of the amyloid precursor protein associated with Alzheimer's disease.

Aim 2: To determine the impact of NOX-derived ROS on SphK1, an enzyme responsible for the production of the pro-survival bioactive lipid sphingosine-1-phosphate.

Hypothesis: TNFα and $A\beta^{1-42}$ stimulate Mg^{2+}-nSMase activity, leading to an increase in neuronal NOX activity and the subsequent oxidation of actin and SphK1.

Methods: The activity of Mg^{2+}-nSMase was measured to determine its activation in response to treatment with TNFα or $A\beta^{1-42}$. The serum-stimulated activity of SphK1 was measured to determine if treatment with TNFα or $A\beta^{1-42}$ caused loss of activity. Analysis of cytosolic subunit phosphorylation, cytosol-to-membrane translocation, and ROS production were used to evaluate activity of the neuronal NOX in response to TNFα, $A\beta^{1-42}$, ceramide analogs, or palmitate, the precursor of *de novo* synthesized ceramide. Oxidation of actin and SphK1, in response to treatment with TNFα or $A\beta^{1-42}$, was

evaluated by derivatization of the protein carbonyls from respective immunoprecipitates, followed by western blotting. Lastly, neurite outgrowth was used to evaluate neuronal integrity and functionality in response to treatments.

Chapter 4 - Ceramide Kinase Regulates TNFα-Induced NADPH Oxidase Activity and Eicosanoid Biosynthesis in Neurons.

Aim 1: To explore the role of CerK in TNFα-stimulated neuronal NOX activity.

Aim 2: To evaluate the role of CerK in TNFα-stimulated neuronal eicosanoid biosynthesis.

Hypothesis: CerK mediates TNFα-stimulated neuronal NOX activity and eicosanoid biosynthesis.

Methods: The activity of CerK was evaluated in response to TNFα. Analysis of cytosolic subunit phosphorylation and cytosol-to-membrane translocation, and ROS production were used to evaluate activity of the neuronal NOX in response to TNFα. Pharmacological agents were further used to determine the contribution of 5-LOX and COX-2 to ROS production in response to TNFα exposure. As an enzyme key to prostaglandin biosynthesis, a class of eicosanoids, COX-2 activity was measured in response to TNFα treatment. Phosphorylation of 5-LOX and cPLA$_2$ was used to evaluate activation in response to treatment with TNFα, while ^{3}H-labeled arachidonic acid release was used to evaluate eicosanoid synthesis and release in response to TNFα. Cellular viability assays were also used to evaluate survival in response to TNFα exposure. To evaluate CerK, siRNA was employed using a cationic nanoliposome transfection scheme that was validated by confocal microscopy.

Chapter 5 – Inhibition of NADPH Oxidase by Glucosylceramide Synthase Confers Chemoresistance.

Aim 1: To evaluate the inhibition of NOX by glucosylceramide synthase, either by its depletion of ceramide or via its production of glucosylceramide.

Aim 2: To compare the antioxidant capacity, including glucosylceramide synthase activity, of neuroblastoma and glioblastoma cell lines, and correlate this with differential responses to chemotherapy.

Aim 3: To evaluate the efficacy of interfering with glucosylceramide synthase, or catalase, in combination with chemotherapy.

Hypothesis: Increased glucosylceramide synthase activity, associated with aggressive cancer, impedes TNFα- and chemotherapy-stimulated NOX activity.

Methods: Enzyme activity assays were used to study basal activities of glucosylceramide synthase, superoxide dismutase, and catalase in SH-SY5Y neuroblastoma cells, U-87 MG glioblastoma cells, and LN-18 glioblastoma cells. Analysis of cytosol-to-membrane translocation, and ROS production were used to evaluate NOX activity in response to treatment with TNFα, chemotherapeutics, or nanoliposomes. Viability assays were employed to evaluate cell death in response to treatments with TNFα, chemotherapeutics, or nanoliposomes. Pharmacological agents were evaluated to impede glucosylceramide synthase and catalase activity, while molecular targeting of glucosylceramide synthase was achieved using specific siRNA delivered using a cationic nanoliposome delivery system. Additionally, glucosylceramide synthase was overexpressed in SH-SY5Y neuroblastoma cells to further demonstrate its role in conferring drug-resistance.

Chapter 6 – Wild Alaskan Blueberry Extracts Inhibit a Magnesium-Dependent Neutral Sphingomyelinase Activity in Neurons Exposed to TNFα.

Aim: To determine if wild Alaskan blueberries protect against neuroinflammation, and more specifically block Mg^{2+}-nSMase activity.

Hypothesis: Components of wild Alaskan blueberries block TNFα-stimulated Mg^{2+}-nSMase activity.

Methods: Wild Alaskan blueberries were collected by hand at various locations in the Alaskan interior and aqueous or organic extracts were prepared. Enzyme activity assays were utilized to evaluate impediment of TNFα-stimulated Mg^{2+}-nSMase activity by blueberry extracts. Antioxidant capacity assays were used to justify dosage of extracts as non-antioxidant in the traditional sense, while cellular viability assays were used to evaluate the toxicology of the extracts.

1.6: References

Abramov A. Y., Jacobson J., Wientjes F., Hothersall J., Canevari L. and Duchen M. R. (2005) Expression and modulation of an NADPH oxidase in mammalian astrocytes. *J Neurosci* **25**, 9176-9184.

Adam-Klages S., Adam D., Wiegmann K., Struve S., Kolanus W., Schneider-Mergener J. and Kronke M. (1996) FAN, a novel WD-repeat protein, couples the p55 TNF-receptor to neutral sphingomyelinase. *Cell* **86**, 937-947.

Alemany R., van Koppen C. J., Danneberg K., Ter Braak M. and Meyer Zu Heringdorf D. (2007) Regulation and functional roles of sphingosine kinases. *Naunyn-Schmiedeberg's archives of pharmacology* **374**, 413-428.

Alemany R., Kleuser B., Ruwisch L., Danneberg K., Lass H., Hashemi R., Spiegel S., Jakobs K. H. and Meyer zu Heringdorf D. (2001) Depolarisation induces rapid and transient formation of intracellular sphingosine-1-phosphate. *FEBS letters* **509**, 239-244.

Anishkin A., Sukharev S. and Colombini M. (2006) Searching for the molecular arrangement of transmembrane ceramide channels. *Biophysical journal* **90**, 2414-2426.

Babior B. M. and Kipnes R. S. (1977) Superoxide-forming enzyme from human neutrophils: evidence for a flavin requirement. *Blood* **50**, 517-524.

Babior B. M., Kipnes R. S. and Curnutte J. T. (1973) Biological defense mechanisms. The production by leukocytes of superoxide, a potential bactericidal agent. *The Journal of clinical investigation* **52**, 741-744.

Babior B. M., Curnutte J. T. and Kipnes B. S. (1975) Pyridine nucleotide-dependent superoxide production by a cell-free system from human granulocytes. *The Journal of clinical investigation* **56**, 1035-1042.

Baehner R. L. and Nathan D. G. (1967) Leukocyte oxidase: defective activity in chronic granulomatous disease. *Science (New York, N.Y* **155**, 835-836.

Baldridge C. W. and Gerard R. W. (1932) The extra respiration of phagocytosis. *The American journal of physiology* **103**, 235-236.

Banfi B., Clark R. A., Steger K. and Krause K. H. (2003) Two novel proteins activate superoxide generation by the NADPH oxidase NOX1. *The Journal of biological chemistry* **278**, 3510-3513.

Banfi B., Molnar G., Maturana A., Steger K., Hegedus B., Demaurex N. and Krause K. H. (2001) A Ca(2+)-activated NADPH oxidase in testis, spleen, and lymph nodes. *The Journal of biological chemistry* **276,** 37594-37601.

Banfi B., Maturana A., Jaconi S., Arnaudeau S., Laforge T., Sinha B., Ligeti E., Demaurex N. and Krause K. H. (2000) A mammalian H+ channel generated through alternative splicing of the NADPH oxidase homolog NOH-1. *Science (New York, N.Y* **287,** 138-142.

Bedard K. and Krause K. H. (2007) The NOX family of ROS-generating NADPH oxidases: physiology and pathophysiology. *Physiological reviews* **87,** 245-313.

Benna J. E., Dang P. M., Gaudry M., Fay M., Morel F., Hakim J. and Gougerot-Pocidalo M. A. (1997) Phosphorylation of the respiratory burst oxidase subunit p67(phox) during human neutrophil activation. Regulation by protein kinase C-dependent and independent pathways. *The Journal of biological chemistry* **272,** 17204-17208.

Berendes H., Bridges R. A. and Good R. A. (1957) A fatal granulomatosus of childhood: the clinical study of a new syndrome. *Minnesota medicine* **40,** 309-312.

Biberstine-Kinkade K. J., DeLeo F. R., Epstein R. I., LeRoy B. A., Nauseef W. M. and Dinauer M. C. (2001) Heme-ligating histidines in flavocytochrome b(558): identification of specific histidines in gp91(phox). *The Journal of biological chemistry* **276,** 31105-31112.

Biberstine-Kinkade K. J., Yu L., Stull N., LeRoy B., Bennett S., Cross A. and Dinauer M. C. (2002) Mutagenesis of p22(phox) histidine 94. A histidine in this position is not required for flavocytochrome b558 function. *The Journal of biological chemistry* **277,** 30368-30374.

Billich A., Bornancin F., Devay P., Mechtcheriakova D., Urtz N. and Baumruker T. (2003) Phosphorylation of the immunomodulatory drug FTY720 by sphingosine kinases. *The Journal of biological chemistry* **278**, 47408-47415.

Bishop A. L. and Hall A. (2000) Rho GTPases and their effector proteins. *The Biochemical journal* **348 Pt 2**, 241-255.

Block M. L., Zecca L. and Hong J. S. (2007) Microglia-mediated neurotoxicity: uncovering the molecular mechanisms. *Nat Rev Neurosci* **8**, 57-69.

Bourne H. R., Sanders D. A. and McCormick F. (1990) The GTPase superfamily: a conserved switch for diverse cell functions. *Nature* **348**, 125-132.

Bourne H. R., Sanders D. A. and McCormick F. (1991) The GTPase superfamily: conserved structure and molecular mechanism. *Nature* **349**, 117-127.

Bromberg Y. and Pick E. (1985) Activation of NADPH-dependent superoxide production in a cell-free system by sodium dodecyl sulfate. *The Journal of biological chemistry* **260**, 13539-13545.

Calabrese B., Wilson M. S. and Halpain S. (2006) Development and regulation of dendritic spine synapses. *Physiology (Bethesda, Md* **21**, 38-47.

Channon J. Y. and Leslie C. C. (1990) A calcium-dependent mechanism for associating a soluble arachidonoyl-hydrolyzing phospholipase A2 with membrane in the macrophage cell line RAW 264.7. *The Journal of biological chemistry* **265**, 5409-5413.

Chavez J. A., Knotts T. A., Wang L. P., Li G., Dobrowsky R. T., Florant G. L. and Summers S. A. (2003) A role for ceramide, but not diacylglycerol, in the

antagonism of insulin signal transduction by saturated fatty acids. *The Journal of biological chemistry* **278**, 10297-10303.

Cheng G., Cao Z., Xu X., van Meir E. G. and Lambeth J. D. (2001) Homologs of gp91phox: cloning and tissue expression of Nox3, Nox4, and Nox5. *Gene* **269**, 131-140.

Clark J. D., Schievella A. R., Nalefski E. A. and Lin L. L. (1995) Cytosolic phospholipase A2. *Journal of lipid mediators and cell signalling* **12**, 83-117.

Clarke C. J., Snook C. F., Tani M., Matmati N., Marchesini N. and Hannun Y. A. (2006) The extended family of neutral sphingomyelinases. *Biochemistry* **45**, 11247-11256.

Colton C. A. and Gilbert D. L. (1987) Production of superoxide anions by a CNS macrophage, the microglia. *FEBS letters* **223**, 284-288.

Cross A. R. (2000) p40(phox) Participates in the activation of NADPH oxidase by increasing the affinity of p47(phox) for flavocytochrome b(558). *The Biochemical journal* **349**, 113-117.

Cross A. R., Erickson R. W. and Curnutte J. T. (1999) Simultaneous presence of p47(phox) and flavocytochrome b-245 are required for the activation of NADPH oxidase by anionic amphiphiles. Evidence for an intermediate state of oxidase activation. *The Journal of biological chemistry* **274**, 15519-15525.

Cuvillier O., Pirianov G., Kleuser B., Vanek P. G., Coso O. A., Gutkind S. and Spiegel S. (1996) Suppression of ceramide-mediated programmed cell death by sphingosine-1-phosphate. *Nature* **381**, 800-803.

De Deken X., Wang D., Many M. C., Costagliola S., Libert F., Vassart G., Dumont J. E. and Miot F. (2000) Cloning of two human thyroid cDNAs encoding new members of the NADPH oxidase family. *The Journal of biological chemistry* **275**, 23227-23233.

DeLeo F. R., Nauseef W. M., Jesaitis A. J., Burritt J. B., Clark R. A. and Quinn M. T. (1995a) A domain of p47phox that interacts with human neutrophil flavocytochrome b558. *The Journal of biological chemistry* **270**, 26246-26251.

DeLeo F. R., Burritt J. B., Yu L., Jesaitis A. J., Dinauer M. C. and Nauseef W. M. (2000) Processing and maturation of flavocytochrome b558 include incorporation of heme as a prerequisite for heterodimer assembly. *The Journal of biological chemistry* **275**, 13986-13993.

DeLeo F. R., Yu L., Burritt J. B., Loetterle L. R., Bond C. W., Jesaitis A. J. and Quinn M. T. (1995b) Mapping sites of interaction of p47-phox and flavocytochrome b with random-sequence peptide phage display libraries. *Proceedings of the National Academy of Sciences of the United States of America* **92**, 7110-7114.

Delon C., Manifava M., Wood E., Thompson D., Krugmann S., Pyne S. and Ktistakis N. T. (2004) Sphingosine kinase 1 is an intracellular effector of phosphatidic acid. *The Journal of biological chemistry* **279**, 44763-44774.

Diekmann D., Abo A., Johnston C., Segal A. W. and Hall A. (1994) Interaction of Rac with p67phox and regulation of phagocytic NADPH oxidase activity. *Science (New York, N.Y* **265**, 531-533.

Dinauer M. C., Orkin S. H., Brown R., Jesaitis A. J. and Parkos C. A. (1987) The glycoprotein encoded by the X-linked chronic granulomatous disease locus is a component of the neutrophil cytochrome b complex. *Nature* **327**, 717-720.

Dinauer M. C., Pierce E. A., Erickson R. W., Muhlebach T. J., Messner H., Orkin S. H., Seger R. A. and Curnutte J. T. (1991) Point mutation in the cytoplasmic domain of the neutrophil p22-phox cytochrome b subunit is associated with a nonfunctional NADPH oxidase and chronic granulomatous disease. *Proceedings of the National Academy of Sciences of the United States of America* **88**, 11231-11235.

Doussiere J., Buzenet G. and Vignais P. V. (1995) Photoaffinity labeling and photoinactivation of the O2(-)-generating oxidase of neutrophils by an azido derivative of FAD. *Biochemistry* **34**, 1760-1770.

Doussiere J., Gaillard J. and Vignais P. V. (1996) Electron transfer across the O2-generating flavocytochrome b of neutrophils. Evidence for a transition from a low-spin state to a high-spin state of the heme iron component. *Biochemistry* **35**, 13400-13410.

Doussiere J., Brandolin G., Derrien V. and Vignais P. V. (1993) Critical assessment of the presence of an NADPH binding site on neutrophil cytochrome b558 by photoaffinity and immunochemical labeling. *Biochemistry* **32**, 8880-8887.

Dupuy C., Ohayon R., Valent A., Noel-Hudson M. S., Deme D. and Virion A. (1999) Purification of a novel flavoprotein involved in the thyroid NADPH oxidase. Cloning of the porcine and human cdnas. *The Journal of biological chemistry* **274**, 37265-37269.

Dusi S. and Rossi F. (1993) Activation of NADPH oxidase of human neutrophils involves the phosphorylation and the translocation of cytosolic p67phox. *The Biochemical journal* **296** (Pt 2), 367-371.

El Benna J., Faust L. P. and Babior B. M. (1994) The phosphorylation of the respiratory burst oxidase component p47phox during neutrophil activation. Phosphorylation of sites recognized by protein kinase C and by proline-directed kinases. *The Journal of biological chemistry* **269**, 23431-23436.

El Benna J., Faust R. P., Johnson J. L. and Babior B. M. (1996a) Phosphorylation of the respiratory burst oxidase subunit p47phox as determined by two-dimensional phosphopeptide mapping. Phosphorylation by protein kinase C, protein kinase A, and a mitogen-activated protein kinase. *The Journal of biological chemistry* **271**, 6374-6378.

El Benna J., Han J., Park J. W., Schmid E., Ulevitch R. J. and Babior B. M. (1996b) Activation of p38 in stimulated human neutrophils: phosphorylation of the oxidase component p47phox by p38 and ERK but not by JNK. *Archives of biochemistry and biophysics* **334**, 395-400.

Ellson C. D., Andrews S., Stephens L. R. and Hawkins P. T. (2002) The PX domain: a new phosphoinositide-binding module. *Journal of cell science* **115**, 1099-1105.

Ellson C. D., Gobert-Gosse S., Anderson K. E., Davidson K., Erdjument-Bromage H., Tempst P., Thuring J. W., Cooper M. A., Lim Z. Y., Holmes A. B., Gaffney P. R., Coadwell J., Chilvers E. R., Hawkins P. T. and Stephens L. R. (2001) PtdIns(3)P regulates the neutrophil oxidase complex by binding to the PX domain of p40(phox). *Nature cell biology* **3**, 679-682.

Etienne-Manneville S. (2006) In vitro assay of primary astrocyte migration as a tool to study Rho GTPase function in cell polarization. *Methods in enzymology* **406**, 565-578.

Eyster K. M. (2007) The membrane and lipids as integral participants in signal transduction: lipid signal transduction for the non-lipid biochemist. *Advances in physiology education* **31,** 5-16.

Farooqui A. A., Horrocks L. A. and Farooqui T. (2007) Modulation of inflammation in brain: a matter of fat. *Journal of neurochemistry* **101,** 577-599.

Fetler L. and Amigorena S. (2005) Neuroscience. Brain under surveillance: the microglia patrol. *Science (New York, N.Y* **309,** 392-393.

Fiala J. C., Spacek J. and Harris K. M. (2002) Dendritic spine pathology: cause or consequence of neurological disorders? *Brain Res Brain Res Rev* **39,** 29-54.

Fontayne A., Dang P. M., Gougerot-Pocidalo M. A. and El-Benna J. (2002) Phosphorylation of p47phox sites by PKC alpha, beta II, delta, and zeta: effect on binding to p22phox and on NADPH oxidase activation. *Biochemistry* **41,** 7743-7750.

Forbes L. V., Truong O., Wientjes F. B., Moss S. J. and Segal A. W. (1999) The major phosphorylation site of the NADPH oxidase component p67phox is Thr233. *The Biochemical journal* **338 (Pt 1),** 99-105.

Fox T. E., Finnegan C. M., Blumenthal R. and Kester M. (2006) The clinical potential of sphingolipid-based therapeutics. *Cell Mol Life Sci* **63,** 1017-1023.

Fox T. E., Houck K. L., O'Neill S. M., Nagarajan M., Stover T. C., Pomianowski P. T., Unal O., Yun J. K., Naides S. J. and Kester M. (2007) Ceramide recruits and activates protein kinase C zeta (PKC zeta) within structured membrane microdomains. *The Journal of biological chemistry* **282,** 12450-12457.

Fuchs A., Dagher M. C. and Vignais P. V. (1995) Mapping the domains of interaction of p40phox with both p47phox and p67phox of the neutrophil oxidase complex using the two-hybrid system. *The Journal of biological chemistry* **270**, 5695-5697.

Fujii S., Inoue B., Yamamoto H., Ogata K., Shinki T., Inoue S., Tomita M., Tamura H., Tsukamoto K., Ikezawa H. and Ikeda K. (1998) Mg2+ binding and catalytic function of sphingomyelinase from Bacillus cereus. *Journal of biochemistry* **124**, 1178-1187.

Futerman A. H. and Riezman H. (2005) The ins and outs of sphingolipid synthesis. *Trends in cell biology* **15**, 312-318.

Galli R. L., Shukitt-Hale B., Youdim K. A. and Joseph J. A. (2002) Fruit polyphenolics and brain aging: nutritional interventions targeting age-related neuronal and behavioral deficits. *Annals of the New York Academy of Sciences* **959**, 128-132.

Geiszt M., Kopp J. B., Varnai P. and Leto T. L. (2000) Identification of renox, an NAD(P)H oxidase in kidney. *Proceedings of the National Academy of Sciences of the United States of America* **97**, 8010-8014.

Geiszt M., Lekstrom K., Witta J. and Leto T. L. (2003) Proteins homologous to p47phox and p67phox support superoxide production by NAD(P)H oxidase 1 in colon epithelial cells. *The Journal of biological chemistry* **278**, 20006-20012.

Ghosh M., Tucker D. E., Burchett S. A. and Leslie C. C. (2006) Properties of the Group IV phospholipase A2 family. *Progress in lipid research* **45**, 487-510.

Goetzl E. J., An S. and Smith W. L. (1995) Specificity of expression and effects of eicosanoid mediators in normal physiology and human diseases. *Faseb J* 9, 1051-1058.

Gomez-Brouchet A., Pchejetski D., Brizuela L., Garcia V., Altie M. F., Maddelein M. L., Delisle M. B. and Cuvillier O. (2007) Critical role for sphingosine kinase-1 in regulating survival of neuroblastoma cells exposed to amyloid-beta peptide. *Molecular pharmacology* 72, 341-349.

Gorin Y., Ricono J. M., Kim N. H., Bhandari B., Choudhury G. G. and Abboud H. E. (2003) Nox4 mediates angiotensin II-induced activation of Akt/protein kinase B in mesangial cells. *Am J Physiol Renal Physiol* 285, F219-229.

Gorlach A., Brandes R. P., Nguyen K., Amidi M., Dehghani F. and Busse R. (2000) A gp91phox containing NADPH oxidase selectively expressed in endothelial cells is a major source of oxygen radical generation in the arterial wall. *Circulation research* 87, 26-32.

Gouaze-Andersson V. and Cabot M. C. (2006) Glycosphingolipids and drug resistance. *Biochimica et biophysica acta* 1758, 2096-2103.

Grasberger H. and Refetoff S. (2006) Identification of the maturation factor for dual oxidase. Evolution of an eukaryotic operon equivalent. *The Journal of biological chemistry* 281, 18269-18272.

Griendling K. K., Minieri C. A., Ollerenshaw J. D. and Alexander R. W. (1994) Angiotensin II stimulates NADH and NADPH oxidase activity in cultured vascular smooth muscle cells. *Circulation research* 74, 1141-1148.

Grimm M. O., Grimm H. S., Patzold A. J., Zinser E. G., Halonen R., Duering M., Tschape J. A., De Strooper B., Muller U., Shen J. and Hartmann T. (2005) Regulation of cholesterol and sphingomyelin metabolism by amyloid-beta and presenilin. *Nature cell biology* **7**, 1118-1123.

Grizot S., Fieschi F., Dagher M. C. and Pebay-Peyroula E. (2001) The active N-terminal region of p67phox. Structure at 1.8 A resolution and biochemical characterizations of the A128V mutant implicated in chronic granulomatous disease. *The Journal of biological chemistry* **276**, 21627-21631.

Groemping Y. and Rittinger K. (2005) Activation and assembly of the NADPH oxidase: a structural perspective. *The Biochemical journal* **386**, 401-416.

Groemping Y., Lapouge K., Smerdon S. J. and Rittinger K. (2003) Molecular basis of phosphorylation-induced activation of the NADPH oxidase. *Cell* **113**, 343-355.

Gu Y., Jia B., Yang F. C., D'Souza M., Harris C. E., Derrow C. W., Zheng Y. and Williams D. A. (2001) Biochemical and biological characterization of a human Rac2 GTPase mutant associated with phagocytic immunodeficiency. *The Journal of biological chemistry* **276**, 15929-15938.

Gungabissoon R. A. and Bamburg J. R. (2003) Regulation of growth cone actin dynamics by ADF/cofilin. *J Histochem Cytochem* **51**, 411-420.

Hait N. C., Oskeritzian C. A., Paugh S. W., Milstien S. and Spiegel S. (2006) Sphingosine kinases, sphingosine 1-phosphate, apoptosis and diseases. *Biochimica et biophysica acta* **1758**, 2016-2026.

Han C. H. and Lee M. H. (2000) Activation domain in P67phox regulates the steady state reduction of FAD in gp91phox. *Journal of veterinary science (Suwon-si, Korea)* **1**, 27-31.

Han C. H., Freeman J. L., Lee T., Motalebi S. A. and Lambeth J. D. (1998) Regulation of the neutrophil respiratory burst oxidase. Identification of an activation domain in p67(phox). *The Journal of biological chemistry* **273**, 16663-16668.

Hannun Y. A. (1996) Functions of ceramide in coordinating cellular responses to stress. *Science (New York, N.Y* **274**, 1855-1859.

Hannun Y. A. and Luberto C. (2000) Ceramide in the eukaryotic stress response. *Trends in cell biology* **10**, 73-80.

Harper A. M., Chaplin M. F. and Segal A. W. (1985) Cytochrome b-245 from human neutrophils is a glycoprotein. *The Biochemical journal* **227**, 783-788.

Heymes C., Bendall J. K., Ratajczak P., Cave A. C., Samuel J. L., Hasenfuss G. and Shah A. M. (2003) Increased myocardial NADPH oxidase activity in human heart failure. *Journal of the American College of Cardiology* **41**, 2164-2171.

Heyneman R. A. and Vercauteren R. E. (1984) Activation of a NADPH oxidase from horse polymorphonuclear leukocytes in a cell-free system. *Journal of leukocyte biology* **36**, 751-759.

Hoffman G. R. and Cerione R. A. (2000) Flipping the switch: the structural basis for signaling through the CRIB motif. *Cell* **102**, 403-406.

Hofmann K., Tomiuk S., Wolff G. and Stoffel W. (2000) Cloning and characterization of the mammalian brain-specific, Mg2+-dependent neutral sphingomyelinase.

Proceedings of the National Academy of Sciences of the United States of America **97**, 5895-5900.

Holmes B., Page A. R. and Good R. A. (1967) Studies of the metabolic activity of leukocytes from patients with a genetic abnormality of phagocytic function. *The Journal of clinical investigation* **46**, 1422-1432.

Huang J., Hitt N. D. and Kleinberg M. E. (1995) Stoichiometry of p22-phox and gp91-phox in phagocyte cytochrome b558. *Biochemistry* **34**, 16753-16757.

Huwiler A., Johansen B., Skarstad A. and Pfeilschifter J. (2001) Ceramide binds to the CaLB domain of cytosolic phospholipase A2 and facilitates its membrane docking and arachidonic acid release. *Faseb J* **15**, 7-9.

Ibi M., Katsuyama M., Fan C., Iwata K., Nishinaka T., Yokoyama T. and Yabe-Nishimura C. (2006) NOX1/NADPH oxidase negatively regulates nerve growth factor-induced neurite outgrowth. *Free radical biology & medicine* **40**, 1785-1795.

Inanami O., Johnson J. L., McAdara J. K., Benna J. E., Faust L. R., Newburger P. E. and Babior B. M. (1998) Activation of the leukocyte NADPH oxidase by phorbol ester requires the phosphorylation of p47PHOX on serine 303 or 304. *The Journal of biological chemistry* **273**, 9539-9543.

Inoguchi T., Sonta T., Tsubouchi H., Etoh T., Kakimoto M., Sonoda N., Sato N., Sekiguchi N., Kobayashi K., Sumimoto H., Utsumi H. and Nawata H. (2003) Protein kinase C-dependent increase in reactive oxygen species (ROS) production in vascular tissues of diabetes: role of vascular NAD(P)H oxidase. *J Am Soc Nephrol* **14**, S227-232.

Isogai Y., Iizuka T. and Shiro Y. (1995) The mechanism of electron donation to molecular oxygen by phagocytic cytochrome b558. *The Journal of biological chemistry* **270,** 7853-7857.

Ito T., Matsui Y., Ago T., Ota K. and Sumimoto H. (2001) Novel modular domain PB1 recognizes PC motif to mediate functional protein-protein interactions. *The EMBO journal* **20,** 3938-3946.

Iyer G. Y. N., Islam M. F. and Quastel J. H. (1961) Biochemical aspects of phagocytosis. *Nature* **192,** 535-541.

Javesghani D., Magder S. A., Barreiro E., Quinn M. T. and Hussain S. N. (2002) Molecular characterization of a superoxide-generating NAD(P)H oxidase in the ventilatory muscles. *American journal of respiratory and critical care medicine* **165,** 412-418.

Jones S. A., O'Donnell V. B., Wood J. D., Broughton J. P., Hughes E. J. and Jones O. T. (1996) Expression of phagocyte NADPH oxidase components in human endothelial cells. *The American journal of physiology* **271,** H1626-1634.

Joseph J. A., Denisova N. A., Arendash G., Gordon M., Diamond D., Shukitt-Hale B. and Morgan D. (2003) Blueberry supplementation enhances signaling and prevents behavioral deficits in an Alzheimer disease model. *Nutritional neuroscience* **6,** 153-162.

Kajimoto T., Okada T., Yu H., Goparaju S. K., Jahangeer S. and Nakamura S. (2007) Involvement of sphingosine-1-phosphate in glutamate secretion in hippocampal neurons. *Molecular and cellular biology* **27,** 3429-3440.

Kami K., Takeya R., Sumimoto H. and Kohda D. (2002) Diverse recognition of non-PxxP peptide ligands by the SH3 domains from p67(phox), Grb2 and Pex13p. *The EMBO journal* **21,** 4268-4276.

Kamsler A. and Segal M. (2004) Hydrogen peroxide as a diffusible signal molecule in synaptic plasticity. *Molecular neurobiology* **29,** 167-178.

Kanai F., Liu H., Field S. J., Akbary H., Matsuo T., Brown G. E., Cantley L. C. and Yaffe M. B. (2001) The PX domains of p47phox and p40phox bind to lipid products of PI(3)K. *Nature cell biology* **3,** 675-678.

Kikuchi H., Hikage M., Miyashita H. and Fukumoto M. (2000) NADPH oxidase subunit, gp91(phox) homologue, preferentially expressed in human colon epithelial cells. *Gene* **254,** 237-243.

Kim S. H., Won S. J., Sohn S., Kwon H. J., Lee J. Y., Park J. H. and Gwag B. J. (2002) Brain-derived neurotrophic factor can act as a pronecrotic factor through transcriptional and translational activation of NADPH oxidase. *The Journal of cell biology* **159,** 821-831.

Kishida K. T., Pao M., Holland S. M. and Klann E. (2005) NADPH oxidase is required for NMDA receptor-dependent activation of ERK in hippocampal area CA1. *Journal of neurochemistry* **94,** 299-306.

Kishida K. T., Hoeffer C. A., Hu D., Pao M., Holland S. M. and Klann E. (2006) Synaptic plasticity deficits and mild memory impairments in mouse models of chronic granulomatous disease. *Molecular and cellular biology* **26,** 5908-5920.

Kleinberg M. E., Rotrosen D. and Malech H. L. (1989) Asparagine-linked glycosylation of cytochrome b558 large subunit varies in different human phagocytic cells. *J Immunol* **143**, 4152-4157.

Knapp L. T. and Klann E. (2002) Role of reactive oxygen species in hippocampal long-term potentiation: contributory or inhibitory? *Journal of neuroscience research* **70**, 1-7.

Koga H., Terasawa H., Nunoi H., Takeshige K., Inagaki F. and Sumimoto H. (1999) Tetratricopeptide repeat (TPR) motifs of p67(phox) participate in interaction with the small GTPase Rac and activation of the phagocyte NADPH oxidase. *The Journal of biological chemistry* **274**, 25051-25060.

Kohama T., Olivera A., Edsall L., Nagiec M. M., Dickson R. and Spiegel S. (1998) Molecular cloning and functional characterization of murine sphingosine kinase. *The Journal of biological chemistry* **273**, 23722-23728.

Koshkin V. and Pick E. (1994) Superoxide production by cytochrome b559. Mechanism of cytosol-independent activation. *FEBS letters* **338**, 285-289.

Koshkin V., Lotan O. and Pick E. (1997) Electron transfer in the superoxide-generating NADPH oxidase complex reconstituted in vitro. *Biochimica et biophysica acta* **1319**, 139-146.

Kudo I. and Murakami M. (2002) Phospholipase A2 enzymes. *Prostaglandins & other lipid mediators* **68-69**, 3-58.

Kuribayashi F., Nunoi H., Wakamatsu K., Tsunawaki S., Sato K., Ito T. and Sumimoto H. (2002) The adaptor protein p40(phox) as a positive regulator of the superoxide-producing phagocyte oxidase. *The EMBO journal* **21**, 6312-6320.

Lamour N. F., Stahelin R. V., Wijesinghe D. S., Maceyka M., Wang E., Allegood J. C., Merrill A. H., Jr., Cho W. and Chalfant C. E. (2007) Ceramide kinase uses ceramide provided by ceramide transport protein: localization to organelles of eicosanoid synthesis. *Journal of lipid research* **48,** 1293-1304.

Lee S. C., Liu W., Roth P., Dickson D. W., Berman J. W. and Brosnan C. F. (1993) Macrophage colony-stimulating factor in human fetal astrocytes and microglia. Differential regulation by cytokines and lipopolysaccharide, and modulation of class II MHC on microglia. *J Immunol* **150,** 594-604.

Leslie C. C. (1997) Properties and regulation of cytosolic phospholipase A2. *The Journal of biological chemistry* **272,** 16709-16712.

Leto T. L., Adams A. G. and de Mendez I. (1994) Assembly of the phagocyte NADPH oxidase: binding of Src homology 3 domains to proline-rich targets. *Proceedings of the National Academy of Sciences of the United States of America* **91,** 10650-10654.

Leusen J. H., Bolscher B. G., Hilarius P. M., Weening R. S., Kaulfersch W., Seger R. A., Roos D. and Verhoeven A. J. (1994) 156Pro-->Gln substitution in the light chain of cytochrome b558 of the human NADPH oxidase (p22-phox) leads to defective translocation of the cytosolic proteins p47-phox and p67-phox. *The Journal of experimental medicine* **180,** 2329-2334.

Levy M., Castillo S. S. and Goldkorn T. (2006) nSMase2 activation and trafficking are modulated by oxidative stress to induce apoptosis. *Biochemical and biophysical research communications* **344,** 900-905.

Li J. M. and Shah A. M. (2002) Intracellular localization and preassembly of the NADPH oxidase complex in cultured endothelial cells. *The Journal of biological chemistry* **277**, 19952-19960.

Liel Y., Rudich A., Nagauker-Shriker O., Yermiyahu T. and Levy R. (1994) Monocyte dysfunction in patients with Gaucher disease: evidence for interference of glucocerebroside with superoxide generation. *Blood* **83**, 2646-2653.

Liu H., Sugiura M., Nava V. E., Edsall L. C., Kono K., Poulton S., Milstien S., Kohama T. and Spiegel S. (2000) Molecular cloning and functional characterization of a novel mammalian sphingosine kinase type 2 isoform. *The Journal of biological chemistry* **275**, 19513-19520.

Liu Y. Y., Han T. Y., Giuliano A. E. and Cabot M. C. (2001) Ceramide glycosylation potentiates cellular multidrug resistance. *Faseb J* **15**, 719-730.

Lopes L. R., Dagher M. C., Gutierrez A., Young B., Bouin A. P., Fuchs A. and Babior B. M. (2004) Phosphorylated p40PHOX as a negative regulator of NADPH oxidase. *Biochemistry* **43**, 3723-3730.

Luberto C., Hassler D. F., Signorelli P., Okamoto Y., Sawai H., Boros E., Hazen-Martin D. J., Obeid L. M., Hannun Y. A. and Smith G. K. (2002) Inhibition of tumor necrosis factor-induced cell death in MCF7 by a novel inhibitor of neutral sphingomyelinase. *The Journal of biological chemistry* **277**, 41128-41139.

Maceyka M., Payne S. G., Milstien S. and Spiegel S. (2002) Sphingosine kinase, sphingosine-1-phosphate, and apoptosis. *Biochimica et biophysica acta* **1585**, 193-201.

Maceyka M., Sankala H., Hait N. C., Le Stunff H., Liu H., Toman R., Collier C., Zhang M., Satin L. S., Merrill A. H., Jr., Milstien S. and Spiegel S. (2005) SphK1 and SphK2, sphingosine kinase isoenzymes with opposing functions in sphingolipid metabolism. *The Journal of biological chemistry* **280**, 37118-37129.

MacLeod J. (1943) The role of oxygen in the metabolism and motility of human spermatozoa. *The American journal of physiology* **138**, 512-518.

Maloney M. T. and Bamburg J. R. (2007) Cofilin-mediated neurodegeneration in Alzheimer's disease and other amyloidopathies. *Molecular neurobiology* **35**, 21-44.

Marchesini N. and Hannun Y. A. (2004) Acid and neutral sphingomyelinases: roles and mechanisms of regulation. *Biochemistry and cell biology = Biochimie et biologie cellulaire* **82**, 27-44.

Marchesini N., Luberto C. and Hannun Y. A. (2003) Biochemical properties of mammalian neutral sphingomyelinase 2 and its role in sphingolipid metabolism. *The Journal of biological chemistry* **278**, 13775-13783.

Matsuo Y., Yamada A., Tsukamoto K., Tamura H., Ikezawa H., Nakamura H. and Nishikawa K. (1996) A distant evolutionary relationship between bacterial sphingomyelinase and mammalian DNase I. *Protein Sci* **5**, 2459-2467.

Mattson M. P., Chan S. L. and Duan W. (2002) Modification of brain aging and neurodegenerative disorders by genes, diet, and behavior. *Physiological reviews* **82**, 637-672.

Meier B., Cross A. R., Hancock J. T., Kaup F. J. and Jones O. T. (1991) Identification of a superoxide-generating NADPH oxidase system in human fibroblasts. *The Biochemical journal* **275 (Pt 1),** 241-245.

Melendez A. J., Carlos-Dias E., Gosink M., Allen J. M. and Takacs L. (2000) Human sphingosine kinase: molecular cloning, functional characterization and tissue distribution. *Gene* **251,** 19-26.

Miyano K. and Sumimoto H. (2007) Role of the small GTPase Rac in p22phox-dependent NADPH oxidases. *Biochimie* **89,** 1133-1144.

Morita Y., Perez G. I., Paris F., Miranda S. R., Ehleiter D., Haimovitz-Friedman A., Fuks Z., Xie Z., Reed J. C., Schuchman E. H., Kolesnick R. N. and Tilly J. L. (2000) Oocyte apoptosis is suppressed by disruption of the acid sphingomyelinase gene or by sphingosine-1-phosphate therapy. *Nature medicine* **6,** 1109-1114.

Murakami M. and Kudo I. (2006) Prostaglandin E synthase: a novel drug target for inflammation and cancer. *Current pharmaceutical design* **12,** 943-954.

Nakamura R., Sumimoto H., Mizuki K., Hata K., Ago T., Kitajima S., Takeshige K., Sakaki Y. and Ito T. (1998) The PC motif: a novel and evolutionarily conserved sequence involved in interaction between p40phox and p67phox, SH3 domain-containing cytosolic factors of the phagocyte NADPH oxidase. *European journal of biochemistry / FEBS* **251,** 583-589.

Nalefski E. A., Sultzman L. A., Martin D. M., Kriz R. W., Towler P. S., Knopf J. L. and Clark J. D. (1994) Delineation of two functionally distinct domains of cytosolic phospholipase A2, a regulatory Ca(2+)-dependent lipid-binding domain and a Ca(2+)-independent catalytic domain. *The Journal of biological chemistry* **269,** 18239-18249.

Nauseef W. M. (2004) Assembly of the phagocyte NADPH oxidase. *Histochemistry and cell biology* **122,** 277-291.

Nava V. E., Lacana E., Poulton S., Liu H., Sugiura M., Kono K., Milstien S., Kohama T. and Spiegel S. (2000) Functional characterization of human sphingosine kinase-1. *FEBS letters* **473,** 81-84.

Needleman P., Turk J., Jakschik B. A., Morrison A. R. and Lefkowith J. B. (1986) Arachidonic acid metabolism. *Annual review of biochemistry* **55,** 69-102.

Nimmerjahn A., Kirchhoff F. and Helmchen F. (2005) Resting microglial cells are highly dynamic surveillants of brain parenchyma in vivo. *Science (New York, N.Y* **308,** 1314-1318.

Nisimoto Y., Otsuka-Murakami H. and Lambeth D. J. (1995) Reconstitution of flavin-depleted neutrophil flavocytochrome b558 with 8-mercapto-FAD and characterization of the flavin-reconstituted enzyme. *The Journal of biological chemistry* **270,** 16428-16434.

Nisimoto Y., Motalebi S., Han C. H. and Lambeth J. D. (1999) The p67(phox) activation domain regulates electron flow from NADPH to flavin in flavocytochrome b(558). *The Journal of biological chemistry* **274,** 22999-23005.

Nisimoto Y., Freeman J. L., Motalebi S. A., Hirshberg M. and Lambeth J. D. (1997) Rac binding to p67(phox). Structural basis for interactions of the Rac1 effector region and insert region with components of the respiratory burst oxidase. *The Journal of biological chemistry* **272,** 18834-18841.

Noyan-Ashraf M. H., Sadeghinejad Z. and Juurlink B. H. (2005) Dietary approach to decrease aging-related CNS inflammation. *Nutritional neuroscience* **8,** 101-110.

Nunoi H., Rotrosen D., Gallin J. I. and Malech H. L. (1988) Two forms of autosomal chronic granulomatous disease lack distinct neutrophil cytosol factors. *Science (New York, N.Y* **242,** 1298-1301.

Obama T., Fujii S., Ikezawa H., Ikeda K., Imagawa M. and Tsukamoto K. (2003) His151 and His296 are the acid-base catalytic residues of Bacillus cereus sphingomyelinase in sphingomyelin hydrolysis. *Biological & pharmaceutical bulletin* **26,** 920-926.

Ogretmen B. and Hannun Y. A. (2004) Biologically active sphingolipids in cancer pathogenesis and treatment. *Nature reviews* **4,** 604-616.

Okamoto Y., Obeid L. M. and Hannun Y. A. (2002) Bcl-xL interrupts oxidative activation of neutral sphingomyelinase. *FEBS letters* **530,** 104-108.

Olivera A. and Spiegel S. (1993) Sphingosine-1-phosphate as second messenger in cell proliferation induced by PDGF and FCS mitogens. *Nature* **365,** 557-560.

Olivera A., Rosenthal J. and Spiegel S. (1996) Effect of acidic phospholipids on sphingosine kinase. *Journal of cellular biochemistry* **60,** 529-537.

Olivera A., Kohama T., Tu Z., Milstien S. and Spiegel S. (1998) Purification and characterization of rat kidney sphingosine kinase. *The Journal of biological chemistry* **273,** 12576-12583.

Paclet M. H., Coleman A. W., Vergnaud S. and Morel F. (2000) P67-phox-mediated NADPH oxidase assembly: imaging of cytochrome b558 liposomes by atomic force microscopy. *Biochemistry* **39,** 9302-9310.

Pao M., Wiggs E. A., Anastacio M. M., Hyun J., DeCarlo E. S., Miller J. T., Anderson V. L., Malech H. L., Gallin J. I. and Holland S. M. (2004) Cognitive function in patients with chronic granulomatous disease: a preliminary report. *Psychosomatics* **45,** 230-234.

Parkos C. A., Dinauer M. C., Walker L. E., Allen R. A., Jesaitis A. J. and Orkin S. H. (1988) Primary structure and unique expression of the 22-kilodalton light chain of human neutrophil cytochrome b. *Proceedings of the National Academy of Sciences of the United States of America* **85,** 3319-3323.

Pettus B. J., Bielawska A., Subramanian P., Wijesinghe D. S., Maceyka M., Leslie C. C., Evans J. H., Freiberg J., Roddy P., Hannun Y. A. and Chalfant C. E. (2004) Ceramide 1-phosphate is a direct activator of cytosolic phospholipase A2. *The Journal of biological chemistry* **279,** 11320-11326.

Piccoli C., Ria R., Scrima R., Cela O., D'Aprile A., Boffoli D., Falzetti F., Tabilio A. and Capitanio N. (2005) Characterization of mitochondrial and extra-mitochondrial oxygen consuming reactions in human hematopoietic stem cells. Novel evidence of the occurrence of NAD(P)H oxidase activity. *The Journal of biological chemistry* **280,** 26467-26476.

Piomelli D. (1993) Arachidonic acid in cell signaling. *Current opinion in cell biology* **5,** 274-280.

Pitson S. M., Moretti P. A., Zebol J. R., Vadas M. A., D'Andrea R. J. and Wattenberg B. W. (2001) A point mutant of human sphingosine kinase 1 with increased catalytic activity. *FEBS letters* **509,** 169-173.

Pitson S. M., Moretti P. A., Zebol J. R., Lynn H. E., Xia P., Vadas M. A. and Wattenberg B. W. (2003) Activation of sphingosine kinase 1 by ERK1/2-mediated phosphorylation. *The EMBO journal* **22,** 5491-5500.

Pitson S. M., D'Andrea R J., Vandeleur L., Moretti P. A., Xia P., Gamble J. R., Vadas M. A. and Wattenberg B. W. (2000a) Human sphingosine kinase: purification, molecular cloning and characterization of the native and recombinant enzymes. *The Biochemical journal* **350 Pt 2,** 429-441.

Pitson S. M., Moretti P. A., Zebol J. R., Xia P., Gamble J. R., Vadas M. A., D'Andrea R. J. and Wattenberg B. W. (2000b) Expression of a catalytically inactive sphingosine kinase mutant blocks agonist-induced sphingosine kinase activation. A dominant-negative sphingosine kinase. *The Journal of biological chemistry* **275,** 33945-33950.

Pitson S. M., Xia P., Leclercq T. M., Moretti P. A., Zebol J. R., Lynn H. E., Wattenberg B. W. and Vadas M. A. (2005) Phosphorylation-dependent translocation of sphingosine kinase to the plasma membrane drives its oncogenic signalling. *The Journal of experimental medicine* **201,** 49-54.

Pitson S. M., Moretti P. A., Zebol J. R., Zareie R., Derian C. K., Darrow A. L., Qi J., D'Andrea R. J., Bagley C. J., Vadas M. A. and Wattenberg B. W. (2002) The nucleotide-binding site of human sphingosine kinase 1. *The Journal of biological chemistry* **277,** 49545-49553.

Ponting C. P. (1996) Novel domains in NADPH oxidase subunits, sorting nexins, and PtdIns 3-kinases: binding partners of SH3 domains? *Protein Sci* **5,** 2353-2357.

Ponting C. P., Ito T., Moscat J., Diaz-Meco M. T., Inagaki F. and Sumimoto H. (2002) OPR, PC and AID: all in the PB1 family. *Trends in biochemical sciences* **27,** 10.

Prioni S., Mauri L., Loberto N., Casellato R., Chigorno V., Karagogeos D., Prinetti A. and Sonnino S. (2004) Interactions between gangliosides and proteins in the exoplasmic leaflet of neuronal plasma membranes: a study performed with a tritium-labeled GM1 derivative containing a photoactivable group linked to the oligosaccharide chain. *Glycoconjugate journal* **21,** 461-470.

Pyne S. and Pyne N. (2000) Sphingosine 1-phosphate signalling via the endothelial differentiation gene family of G-protein-coupled receptors. *Pharmacology & therapeutics* **88,** 115-131.

Quie P. G., White J. G., Holmes B. and Good R. A. (1967) In vitro bactericidal capacity of human polymorphonuclear leukocytes: diminished activity in chronic granulomatous disease of childhood. *The Journal of clinical investigation* **46,** 668-679.

Quinn M. T. and Gauss K. A. (2004) Structure and regulation of the neutrophil respiratory burst oxidase: comparison with nonphagocyte oxidases. *Journal of leukocyte biology* **76,** 760-781.

Ramassamy C. (2006) Emerging role of polyphenolic compounds in the treatment of neurodegenerative diseases: a review of their intracellular targets. *European journal of pharmacology* **545,** 51-64.

Regazzi R., Kikuchi A., Takai Y. and Wollheim C. B. (1992) The small GTP-binding proteins in the cytosol of insulin-secreting cells are complexed to GDP dissociation inhibitor proteins. *The Journal of biological chemistry* **267,** 17512-17519.

Reinehr R., Becker S., Eberle A., Grether-Beck S. and Haussinger D. (2005) Involvement of NADPH oxidase isoforms and Src family kinases in CD95-dependent hepatocyte apoptosis. *The Journal of biological chemistry* **280**, 27179-27194.

Roberts A. W., Kim C., Zhen L., Lowe J. B., Kapur R., Petryniak B., Spaetti A., Pollock J. D., Borneo J. B., Bradford G. B., Atkinson S. J., Dinauer M. C. and Williams D. A. (1999) Deficiency of the hematopoietic cell-specific Rho family GTPase Rac2 is characterized by abnormalities in neutrophil function and host defense. *Immunity* **10**, 183-196.

Rosenfeldt H. M., Hobson J. P., Milstien S. and Spiegel S. (2001) The sphingosine-1-phosphate receptor EDG-1 is essential for platelet-derived growth factor-induced cell motility. *Biochemical Society transactions* **29**, 836-839.

Rossi F. and Zatti M. (1964) Biochemical aspects of phagocytosis in polymorphonuclear leucocytes. NADH and NADPH oxidation by the granules of resting and phagocytizing cells. *Experientia* **20**, 21-23.

Rotrosen D., Yeung C. L., Leto T. L., Malech H. L. and Kwong C. H. (1992) Cytochrome b558: the flavin-binding component of the phagocyte NADPH oxidase. *Science (New York, N.Y* **256**, 1459-1462.

Royer-Pokora B., Kunkel L. M., Monaco A. P., Goff S. C., Newburger P. E., Baehner R. L., Cole F. S., Curnutte J. T. and Orkin S. H. (1986) Cloning the gene for an inherited human disorder--chronic granulomatous disease--on the basis of its chromosomal location. *Nature* **322**, 32-38.

Sathyamoorthy M., de Mendez I., Adams A. G. and Leto T. L. (1997) p40(phox) down-regulates NADPH oxidase activity through interactions with its SH3 domain. *The Journal of biological chemistry* **272**, 9141-9146.

Sato T. K., Overduin M. and Emr S. D. (2001) Location, location, location: membrane targeting directed by PX domains. *Science (New York, N.Y* **294,** 1881-1885.

Sawada M., Kondo N., Suzumura A. and Marunouchi T. (1989) Production of tumor necrosis factor-alpha by microglia and astrocytes in culture. *Brain research* **491,** 394-397.

Scheffzek K., Stephan I., Jensen O. N., Illenberger D. and Gierschik P. (2000) The Rac-RhoGDI complex and the structural basis for the regulation of Rho proteins by RhoGDI. *Nature structural biology* **7,** 122-126.

Segal A. W. (1987) Absence of both cytochrome b-245 subunits from neutrophils in X-linked chronic granulomatous disease. *Nature* **326,** 88-91.

Segal A. W. and Jones O. T. (1978) Novel cytochrome b system in phagocytic vacuoles of human granulocytes. *Nature* **276,** 515-517.

Segal A. W., Jones O. T., Webster D. and Allison A. C. (1978) Absence of a newly described cytochrome b from neutrophils of patients with chronic granulomatous disease. *Lancet* **2,** 446-449.

Segui B., Cuvillier O., Adam-Klages S., Garcia V., Malagarie-Cazenave S., Leveque S., Caspar-Bauguil S., Coudert J., Salvayre R., Kronke M. and Levade T. (2001) Involvement of FAN in TNF-induced apoptosis. *The Journal of clinical investigation* **108,** 143-151.

Senchenkov A., Litvak D. A. and Cabot M. C. (2001) Targeting ceramide metabolism--a strategy for overcoming drug resistance. *Journal of the National Cancer Institute* **93,** 347-357.

Serrano F., Kolluri N. S., Wientjes F. B., Card J. P. and Klann E. (2003) NADPH oxidase immunoreactivity in the mouse brain. *Brain research* **988,** 193-198.

Shiose A., Kuroda J., Tsuruya K., Hirai M., Hirakata H., Naito S., Hattori M., Sakaki Y. and Sumimoto H. (2001) A novel superoxide-producing NAD(P)H oxidase in kidney. *The Journal of biological chemistry* **276,** 1417-1423.

Someya A., Nagaoka I. and Yamashita T. (1993) Purification of the 260 kDa cytosolic complex involved in the superoxide production of guinea pig neutrophils. *FEBS letters* **330,** 215-218.

Someya A., Nunoi H., Hasebe T. and Nagaoka I. (1999) Phosphorylation of p40-phox during activation of neutrophil NADPH oxidase. *Journal of leukocyte biology* **66,** 851-857.

Sonnino S., Prinetti A., Mauri L., Chigorno V. and Tettamanti G. (2006) Dynamic and structural properties of sphingolipids as driving forces for the formation of membrane domains. *Chemical reviews* **106,** 2111-2125.

Spiegel S. and Milstien S. (2002) Sphingosine 1-phosphate, a key cell signaling molecule. *The Journal of biological chemistry* **277,** 25851-25854.

Spiegel S. and Milstien S. (2003) Sphingosine-1-phosphate: an enigmatic signalling lipid. *Nat Rev Mol Cell Biol* **4,** 397-407.

Stahelin R. V., Hwang J. H., Kim J. H., Park Z. Y., Johnson K. R., Obeid L. M. and Cho W. (2005) The mechanism of membrane targeting of human sphingosine kinase 1. *The Journal of biological chemistry* **280,** 43030-43038.

Stratford S., Hoehn K. L., Liu F. and Summers S. A. (2004) Regulation of insulin action by ceramide: dual mechanisms linking ceramide accumulation to the inhibition of Akt/protein kinase B. *The Journal of biological chemistry* **279**, 36608-36615.

Subramanian P., Vora M., Gentile L. B., Stahelin R. V. and Chalfant C. E. (2007) Anionic lipids activate group IVA cytosolic phospholipase A2 via distinct and separate mechanisms. *Journal of lipid research* **48**, 2701-2708.

Subramanian P., Stahelin R. V., Szulc Z., Bielawska A., Cho W. and Chalfant C. E. (2005) Ceramide 1-phosphate acts as a positive allosteric activator of group IVA cytosolic phospholipase A2 alpha and enhances the interaction of the enzyme with phosphatidylcholine. *The Journal of biological chemistry* **280**, 17601-17607.

Suh Y. A., Arnold R. S., Lassegue B., Shi J., Xu X., Sorescu D., Chung A. B., Griendling K. K. and Lambeth J. D. (1999) Cell transformation by the superoxide-generating oxidase Mox1. *Nature* **401**, 79-82.

Sumimoto H., Sakamoto N., Nozaki M., Sakaki Y., Takeshige K. and Minakami S. (1992) Cytochrome b558, a component of the phagocyte NADPH oxidase, is a flavoprotein. *Biochemical and biophysical research communications* **186**, 1368-1375.

Sumimoto H., Kage Y., Nunoi H., Sasaki H., Nose T., Fukumaki Y., Ohno M., Minakami S. and Takeshige K. (1994) Role of Src homology 3 domains in assembly and activation of the phagocyte NADPH oxidase. *Proceedings of the National Academy of Sciences of the United States of America* **91**, 5345-5349.

Summers S. A. and Nelson D. H. (2005) A role for sphingolipids in producing the common features of type 2 diabetes, metabolic syndrome X, and Cushing's syndrome. *Diabetes* **54**, 591-602.

Summers S. A., Garza L. A., Zhou H. and Birnbaum M. J. (1998) Regulation of insulin-stimulated glucose transporter GLUT4 translocation and Akt kinase activity by ceramide. *Molecular and cellular biology* **18**, 5457-5464.

Sutherland C. M., Moretti P. A., Hewitt N. M., Bagley C. J., Vadas M. A. and Pitson S. M. (2006) The calmodulin-binding site of sphingosine kinase and its role in agonist-dependent translocation of sphingosine kinase 1 to the plasma membrane. *The Journal of biological chemistry* **281**, 11693-11701.

Sweeney M. I., Kalt W., MacKinnon S. L., Ashby J. and Gottschall-Pass K. T. (2002) Feeding rats diets enriched in lowbush blueberries for six weeks decreases ischemia-induced brain damage. *Nutritional neuroscience* **5**, 427-431.

Szatrowski T. P. and Nathan C. F. (1991) Production of large amounts of hydrogen peroxide by human tumor cells. *Cancer research* **51**, 794-798.

Tada T. and Sheng M. (2006) Molecular mechanisms of dendritic spine morphogenesis. *Current opinion in neurobiology* **16**, 95-101.

Taha T. A., Mullen T. D. and Obeid L. M. (2006a) A house divided: ceramide, sphingosine, and sphingosine-1-phosphate in programmed cell death. *Biochimica et biophysica acta* **1758**, 2027-2036.

Taha T. A., Hannun Y. A. and Obeid L. M. (2006b) Sphingosine kinase: biochemical and cellular regulation and role in disease. *Journal of biochemistry and molecular biology* **39**, 113-131.

Taha T. A., Kitatani K., Bielawski J., Cho W., Hannun Y. A. and Obeid L. M. (2005) Tumor necrosis factor induces the loss of sphingosine kinase-1 by a cathepsin B-dependent mechanism. *The Journal of biological chemistry* **280**, 17196-17202.

Takeya R., Ueno N., Kami K., Taura M., Kohjima M., Izaki T., Nunoi H. and Sumimoto H. (2003) Novel human homologues of p47phox and p67phox participate in activation of superoxide-producing NADPH oxidases. *The Journal of biological chemistry* **278,** 25234-25246.

Tammariello S. P., Quinn M. T. and Estus S. (2000) NADPH oxidase contributes directly to oxidative stress and apoptosis in nerve growth factor-deprived sympathetic neurons. *J Neurosci* **20,** RC53.

Tamura H., Tameishi K., Yamada A., Tomita M., Matsuo Y., Nishikawa K. and Ikezawa H. (1995) Mutation in aspartic acid residues modifies catalytic and haemolytic activities of Bacillus cereus sphingomyelinase. *The Biochemical journal* **309** (**Pt 3**), 757-764.

Tani M. and Hannun Y. A. (2007) Neutral sphingomyelinase 2 is palmitoylated on multiple cysteine residues. Role of palmitoylation in subcellular localization. *The Journal of biological chemistry* **282,** 10047-10056.

Teahan C., Rowe P., Parker P., Totty N. and Segal A. W. (1987) The X-linked chronic granulomatous disease gene codes for the beta-chain of cytochrome b-245. *Nature* **327,** 720-721.

Tejada-Simon M. V., Serrano F., Villasana L. E., Kanterewicz B. I., Wu G. Y., Quinn M. T. and Klann E. (2005) Synaptic localization of a functional NADPH oxidase in the mouse hippocampus. *Molecular and cellular neurosciences* **29,** 97-106.

Thiels E. and Klann E. (2002) Hippocampal memory and plasticity in superoxide dismutase mutant mice. *Physiology & behavior* **77,** 601-605.

Thiels E., Urban N. N., Gonzalez-Burgos G. R., Kanterewicz B. I., Barrionuevo G., Chu C. T., Oury T. D. and Klann E. (2000) Impairment of long-term potentiation and associative memory in mice that overexpress extracellular superoxide dismutase. *J Neurosci* **20,** 7631-7639.

Tomita M., Ueda Y., Tamura H., Taguchi R. and Ikezawa H. (1993) The role of acidic amino-acid residues in catalytic and adsorptive sites of Bacillus cereus sphingomyelinase. *Biochimica et biophysica acta* **1203,** 85-92.

Town T., Nikolic V. and Tan J. (2005) The microglial "activation" continuum: from innate to adaptive responses. *Journal of neuroinflammation* **2,** 24.

Tsunawaki S., Mizunari H., Nagata M., Tatsuzawa O. and Kuratsuji T. (1994) A novel cytosolic component, p40phox, of respiratory burst oxidase associates with p67phox and is absent in patients with chronic granulomatous disease who lack p67phox. *Biochemical and biophysical research communications* **199,** 1378-1387.

Ueno N., Takeya R., Miyano K., Kikuchi H. and Sumimoto H. (2005) The NADPH oxidase Nox3 constitutively produces superoxide in a p22phox-dependent manner: its regulation by oxidase organizers and activators. *The Journal of biological chemistry* **280,** 23328-23339.

Ueyama T., Tatsuno T., Kawasaki T., Tsujibe S., Shirai Y., Sumimoto H., Leto T. L. and Saito N. (2007) A regulated adaptor function of p40phox: distinct p67phox membrane targeting by p40phox and by p47phox. *Molecular biology of the cell* **18,** 441-454.

Vallet P., Charnay Y., Steger K., Ogier-Denis E., Kovari E., Herrmann F., Michel J. P. and Szanto I. (2005) Neuronal expression of the NADPH oxidase NOX4, and its regulation in mouse experimental brain ischemia. *Neuroscience* **132,** 233-238.

Van Aelst L. and D'Souza-Schorey C. (1997) Rho GTPases and signaling networks. *Genes & development* **11,** 2295-2322.

Van Brocklyn J. R., Lee M. J., Menzeleev R., Olivera A., Edsall L., Cuvillier O., Thomas D. M., Coopman P. J., Thangada S., Liu C. H., Hla T. and Spiegel S. (1998) Dual actions of sphingosine-1-phosphate: extracellular through the Gi-coupled receptor Edg-1 and intracellular to regulate proliferation and survival. *The Journal of cell biology* **142,** 229-240.

Vignais P. V. (2002) The superoxide-generating NADPH oxidase: structural aspects and activation mechanism. *Cell Mol Life Sci* **59,** 1428-1459.

Volpp B. D., Nauseef W. M. and Clark R. A. (1988) Two cytosolic neutrophil oxidase components absent in autosomal chronic granulomatous disease. *Science (New York, N.Y* **242,** 1295-1297.

Wallach T. M. and Segal A. W. (1997) Analysis of glycosylation sites on gp91phox, the flavocytochrome of the NADPH oxidase, by site-directed mutagenesis and translation in vitro. *The Biochemical journal* **321 (Pt 3),** 583-585.

Warburg O. (1908) Beobachtungen ueber die Oxydationsprozesse im Seeigelei. *Hoppe-Seyler's Zeitschrift fur physiologische Chemie* **57,** 1-16.

Wattenberg B. W., Pitson S. M. and Raben D. M. (2006) The sphingosine and diacylglycerol kinase superfamily of signaling kinases: localization as a key to signaling function. *Journal of lipid research* **47,** 1128-1139.

Wientjes F. B. and Segal A. W. (2003) PX domain takes shape. *Current opinion in hematology* **10,** 2-7.

Wientjes F. B., Hsuan J. J., Totty N. F. and Segal A. W. (1993) p40phox, a third cytosolic component of the activation complex of the NADPH oxidase to contain src homology 3 domains. *The Biochemical journal* **296** (Pt 3), 557-561.

Wilson M. I., Gill D. J., Perisic O., Quinn M. T. and Williams R. L. (2003) PB1 domain-mediated heterodimerization in NADPH oxidase and signaling complexes of atypical protein kinase C with Par6 and p62. *Molecular cell* **12**, 39-50.

Won J. S. and Singh I. (2006) Sphingolipid signaling and redox regulation. *Free radical biology & medicine* **40**, 1875-1888.

Wu X., Beecher G. R., Holden J. M., Haytowitz D. B., Gebhardt S. E. and Prior R. L. (2004) Lipophilic and hydrophilic antioxidant capacities of common foods in the United States. *Journal of agricultural and food chemistry* **52**, 4026-4037.

Xia P., Wang L., Moretti P. A., Albanese N., Chai F., Pitson S. M., D'Andrea R. J., Gamble J. R. and Vadas M. A. (2002) Sphingosine kinase interacts with TRAF2 and dissects tumor necrosis factor-alpha signaling. *The Journal of biological chemistry* **277**, 7996-8003.

Xia P., Gamble J. R., Rye K. A., Wang L., Hii C. S., Cockerill P., Khew-Goodall Y., Bert A. G., Barter P. J. and Vadas M. A. (1998) Tumor necrosis factor-alpha induces adhesion molecule expression through the sphingosine kinase pathway. *Proceedings of the National Academy of Sciences of the United States of America* **95**, 14196-14201.

Xu Y., Seet L. F., Hanson B. and Hong W. (2001) The Phox homology (PX) domain, a new player in phosphoinositide signalling. *The Biochemical journal* **360**, 513-530.

Yi F., Chen Q. Z., Jin S. and Li P. L. (2007) Mechanism of homocysteine-induced Rac1/NADPH oxidase activation in mesangial cells: role of guanine nucleotide exchange factor Vav2. *Cell Physiol Biochem* **20**, 909-918.

Yokota S., Taniguchi Y., Kihara A., Mitsutake S. and Igarashi Y. (2004) Asp177 in C4 domain of mouse sphingosine kinase 1a is important for the sphingosine recognition. *FEBS letters* **578**, 106-110.

Yoshimoto T., Furuhata M., Kamiya S., Hisada M., Miyaji H., Magami Y., Yamamoto K., Fujiwara H. and Mizuguchi J. (2003) Positive modulation of IL-12 signaling by sphingosine kinase 2 associating with the IL-12 receptor beta 1 cytoplasmic region. *J Immunol* **171**, 1352-1359.

Yu L., Zhen L. and Dinauer M. C. (1997) Biosynthesis of the phagocyte NADPH oxidase cytochrome b558. Role of heme incorporation and heterodimer formation in maturation and stability of gp91phox and p22phox subunits. *The Journal of biological chemistry* **272**, 27288-27294.

Yu L., Quinn M. T., Cross A. R. and Dinauer M. C. (1998) Gp91(phox) is the heme binding subunit of the superoxide-generating NADPH oxidase. *Proceedings of the National Academy of Sciences of the United States of America* **95**, 7993-7998.

Yu L., DeLeo F. R., Biberstine-Kinkade K. J., Renee J., Nauseef W. M. and Dinauer M. C. (1999) Biosynthesis of flavocytochrome b558 . gp91(phox) is synthesized as a 65-kDa precursor (p65) in the endoplasmic reticulum. *The Journal of biological chemistry* **274**, 4364-4369.

Zheng W., Kollmeyer J., Symolon H., Momin A., Munter E., Wang E., Kelly S., Allegood J. C., Liu Y., Peng Q., Ramaraju H., Sullards M. C., Cabot M. and Merrill A. H., Jr. (2006) Ceramides and other bioactive sphingolipid backbones in

health and disease: lipidomic analysis, metabolism and roles in membrane structure, dynamics, signaling and autophagy. *Biochimica et biophysica acta* **1758**, 1864-1884.

Zimmerman M. C., Lazartigues E., Sharma R. V. and Davisson R. L. (2004) Hypertension caused by angiotensin II infusion involves increased superoxide production in the central nervous system. *Circulation research* **95**, 210-216.

Zimmerman M. C., Lazartigues E., Lang J. A., Sinnayah P., Ahmad I. M., Spitz D. R. and Davisson R. L. (2002) Superoxide mediates the actions of angiotensin II in the central nervous system. *Circulation research* **91**, 1038-1045.

Chapter 2: TNFα-induced neuronal NADPH oxidase activity mediates oxidative damage to the neuronal actin cytoskeleton[1]

2.1: Abstract

Inflammation accompanied by oxidative stress substantially contributes to the progression and possibly the initiation of neurodegeneration prevalent in many chronic central nervous system (CNS) disorders and acute CNS injuries. The proinflammatory cytokine tumor necrosis factor alpha (TNFα) plays a key role in the orchestration and progression of CNS inflammatory processes. In several non-neuronal cell types, TNFα stimulates the formation of reactive oxygen species (ROS) and reorganizes actin filaments. Our studies demonstrated that TNFα activates a neuronal NADPH oxidase (NOX) isoform in human neuroblastoma cells and primary chick cortical neurons, which increases the formation of ROS leading to a redox-dependent reorganization of actin filaments into stress fibers. TNFα exposure caused a significant increase in the carbonylation of actin, a marker of irreversible oxidative damage, which was abolished by pharmacological inhibition of NOX activity. Taken together, our findings suggest that TNFα neurotoxicity could be attributed in part to NOX-mediated damage to the neuronal actin cytoskeleton, thus compromising essential cellular processes. Neuronal NOX isoforms might play a key role in inflammation-dependent CNS neurodegeneration.

I, Brian Barth, affirm my contributions to the work outlined in this chapter. I contributed to the conceptualization and experimental design of the study, worked directly on ROS detection, NOX subunit detection, NOX function studies, and actin oxidation studies, and helped in the draft preparation of a manuscript containing most data presented in this chapter all under the supervision, mentorship, and advisement of Dr. Thomas Kuhn. Please see section 2.7 on page 92 for the contributions of the other authors.

2.2: Introduction

Most CNS pathologies, whether associated with acute injuries or chronic disorders, activate microglia and astrocytes and lead to an increase in inflammatory mediators and reactive oxygen species (ROS) (Fetler and Amigorena 2005; Nimmerjahn et al. 2005; Block et al. 2007). The proinflammatory cytokine tumor necrosis factor alpha (TNFα) stimulates apoptosis and elicits the formation ROS in neuronal cells, which cause oxidative stress and irreversibly damage proteins, carbohydrates, membrane lipids, and nucleic acids (Colton and Gilbert 1987; Sawada et al. 1989; Babior 2000; Town et al. 2005; Block et al. 2007).

The classic NADPH oxidase in phagocytic cells represents the prototypic NADPH oxidoreductase activity of the NOX/DUOX family and the large membrane subunit gp91^{phox} (new nomenclature NOX2) defines the NOX/DUOX family (NOX1-5 and DUOX1-2) (Lambeth 2002; Quinn and Gauss 2004; Bedard and Krause 2007). NOX isoforms are multi-subunit protein complexes composed of two membrane-bound subunits (gp91^{phox} and p22^{phox}), and at least three cytosolic subunits (p67^{phox}, p47^{phox}, and p40^{phox}) (Quinn and Gauss 2004; Groemping and Rittinger 2005; Bedard and Krause 2007). Recently, NOX isoforms and their components have been identified in various non-phagocytic cell types including hematopoietic stem cells, endothelial cells, epithelial cells, myocardial cells, muscle cells, hepatocytes, and neurons (Tammariello et al. 2000; Li and Shah 2002; Bedard and Krause 2007). In neuronal cells, functional NADPH oxidase complexes predominately consist either of Nox1, Nox2, or Nox4 (Tejada-Simon et al. 2005; Vallet et al. 2005; Bedard and Krause 2007). NOX activation requires the activation and translocation of all cytosolic subunits to the membrane as well as a series of intricate interactions with the membrane-bound subunits and among cytosolic subunits (Quinn and Gauss 2004; Groemping and Rittinger 2005; Bedard and Krause 2007). Activation of the cytosolic subunits encompasses phosphorylation of specific residues on p40^{phox} and p47^{phox}, enabling protein-lipid interactions, and recruitment of p67^{phox} by the

small GTPase Rac1 or Rac2 (Quinn and Gauss 2004; Groemping and Rittinger 2005; Ueyama et al. 2007).

ROS generated by NOX isoforms are implicated in physiological redox signaling (growth factors, cytokines, hormones) in addition to pathogen defense (Incerpi et al. 2007). Many cellular processes aside from motility are intimately linked to actin filament dynamics including gene expression, mitochondrial homeostasis, and vesicle traffic (Gourlay and Ayscough 2005b; Moldovan et al. 2006; Formigli et al. 2007; Lanzetti 2007). Importantly, disruption of the neuronal actin cytoskeleton is prevalent in both acute CNS injury and chronic CNS pathologies and might represent a major step in neurodegenerative events (Fiala et al. 2002; Maloney and Bamburg 2007). Munch and co-workers recently demonstrated that proinflammatory mediators released from microglia attenuated neurite outgrowth and caused neurite retraction (Munch et al. 2003). Hippocampal neurons responded to TNFα with a reduction in outgrowth and branching of neurites (Neumann et al. 2002). TNFα also induces rearrangements of actin filament organization in non-neuronal cells (Hanna et al. 2001). Actin filament dynamics are highly sensitive to oxidative modification (Lassing et al. 2007). For instance, hydrogen peroxide and nitric oxide reduce the assembly rate of actin filaments and also weaken filament stability, whereas superoxide causes actin oligomerization through conformational changes in monomeric actin (DalleDonne et al. 1995; Milzani et al. 1997; DalleDonne et al. 1998; Milzani et al. 2000). Studies in endothelial cells demonstrated that ROS are involved both in physiological as well as pathological actin filament reorganization (Moldovan et al. 1999; Moldovan et al. 2000; Karnoub et al. 2001).

The primary aim of this study was to determine if a neuronal NOX activity was responsive to TNFα. Secondly, this study sought to evaluate the impact of neuronal NOX-derived ROS on the neuronal actin cytoskeleton. It was hypothesized that TNFα-stimulated neuronal NOX activity would oxidatively damage actin. In this study, we demonstrated that TNFα stimulated NOX activity and the subsequent formation of ROS

in both human SH-SY5Y neuroblastoma cells and primary cortical neurons. Increases in intracellular ROS caused a rapid reorganization of the neuronal actin cytoskeleton concomitant with an increase in actin carbonylation, an irreversible and damaging oxidative modification. Therefore, inflammation-mediated disruption of the neuronal actin cytoskeleton could represent a key step in CNS neurodegeneration.

2.3: Experimental Procedures

Reagents - Recombinant human tumor necrosis factor alpha (TNFα) was purchased from Millipore (Temecula, CA). DMEM and Penicillin/Streptomycin were obtained from Mediatech (Herndon, VA). GlutaMAX-1. Hank's Balanced Salt Solution (HBSS), and trypsin/EDTA solution were from Invitrogen (Carlsbad, CA). Fetal bovine serum was received from Atlanta Biologicals (Atlanta, GA). Streptavidin-agarose beads, protease inhibitor cocktail (PIC), Pico Super Signal chemiluminescent kit, and a BCA protein assay kit were obtained from Pierce (Rockland, IL). Polyclonal rabbit anti-DNP (dinitrophenyl) primary antibodies were from Invitrogen. A polyclonal rabbit anti-human p67^{phox} antibody, and a monoclonal mouse anti-human p40^{phox} antibody were from Millipore. Polyclonal goat antibodies against human gp91^{phox}, human p22^{phox}, and human phospho-p40^{phox} were from Santa Cruz (Santa Cruz, CA) as well as monoclonal mouse antibodies against human p47^{phox} and, human β-actin, normal mouse serum, and horseradish peroxidase-conjugated secondary antibodies. Rhodamine phalloidin was from Cytoskeleton Inc. (Denver, CO), and all other reagents were from Sigma (St. Louis, MO).

Cell Culture - Human SH-SY5Y neuroblastoma cells were grown in 100 mm dishes (Falcon) in medium composed of DMEM, 10% Fetal Bovine Serum (FBS), 1% Glutamax, 100 U/ml Penicillin and 100 U/ml Streptomycin -humidified atmosphere, 5% CO_2 37°C-. For amplification, SH-SY5Y cells were incubated for 5 min with trypsin (0.5 mg/ml)/EDTA (0.2 mg/ml), washed, and immediately re-suspended in medium. Primary cortical neurons were obtained from forebrains of 7 day-old chick embryos (E7), as

detailed by Wright and Kuhn (Wright and Kuhn 2002). Cortical neurons were plated in 6-well plates (5×10^6 cells per well) coated with poly-D-lysine and grown (humidified atmosphere, 5% CO_2 37°C) in DMEM, 1% Glutamax, 10% FBS, and 1% N3 supplement according to Bottenstein and Sato (Bottenstein and Sato 1979).

Growth Cone Particle Preparation - Highly enriched preparations of sealed growth cone particles (GCPs) were obtained as described by Pfenninger and co-workers (Pfenninger et al. 1983), and as modified by Kuhn and co-workers (Kuhn et al. 1999). After homogenizing fresh brains (E11) in 5 mM HEPES, pH 7.3, 1 mM $MgCl_2$, 0.32 M sucrose, nuclei and intact cells were removed by a low spin centrifugation (1,500 x g_{max}, 15 min, 4°C). The supernatant was overlaid onto 5 mM HEPES, pH 7.3, 1 mM $MgCl_2$, 0.75 M sucrose, centrifuged (150,000 x g_{max}, 60 min, 4°C), and the interface material was collected. Following dilution with 5 mM HEPES, pH 7.3, 1 mM $MgCl_2$, 0.32 M sucrose, the solution was overlaid onto Maxidense (Sigma), centrifuged (40,000 x g_{max}, 60 min, 4°C), and sealed GCPs were collected at the interface. GCPs were re-suspended in Kreb's buffer and used immediately.

Confocal Microscopy - Human SH-SY5Y neuroblastoma cells were grown on collagen-coated glass cover slips (0.13 mm thick german glass) in serum-free medium for 24 h. Cultures were supplied with 10 μM DPI or 40 μM MnTBAP (60 min) prior to acute addition of 200 ng/ml TNFα in serum-free medium. Cultures were fixed 15 min or 30 min after TNFα exposure for 30 min (room temperature) in 4% paraformaldehyde, 10 mM MES, pH 6.1, 138 mM KCl, 3 mM $MgCl_2$, 2 mM EGTA, 0.5% Triton X-100. After rinsing with 0.1% Triton X-100 in Tris-buffered saline (TBS-TX), cultures were incubated with rhodamine phalloidin (1:10 dilution, TBS-TX, 20 min, room temperature), followed by several rinses (TBS-TX), and transferred into 60% glycerol/40% PBS. Images were acquired (40X) with a LSM 510 Zeiss confocal microscope equipped with a He/Ne laser and an Argon laser using TRITC fluorescence filter combination.

Quantification of Reactive Oxygen Species Production - Increases in reactive oxygen species (ROS) were detected with the oxidation-sensitive fluorescence indicator 2',7'-dihydrodichlorofluorescein diacetate (H_2DCFDA), or dihydroethidium (DHE). H_2DCFDA is retained in the cytosol after deacetylation to dihydrodichlorofluorescein and increases in fluorescence upon oxidation by H_2O_2 to dichlorofluorescein (DCF). In contrast, DHE is oxidized to ethidium (Eth) preferentially by superoxide. SH-SY5Y cells or E7 cortical neurons were grown (48 h) in 96-well tissue culture dishes (Falcon, 10^5 cells per well) in their respective medium. Cultures were incubated for 1 h either with 50 μM H_2DCFDA, or a combination of both DHE and H_2DCFDA (160 μM DHE and 10 μM H_2DCFDA), in the presence or absence of pharmacological inhibitors or ROS scavenging enzymes. Following a medium exchange, neuronal cells were exposed to 100 ng/ml TNFα (increasing time periods, or 15 min), washed with PBS, and lysed (2 M Tris-Cl pH 8.0, 2% SDS, 10 mM Na_3VO_4). Maximum Eth- or DCF-fluorescence was quantified (100 μl cell lysate) using a Beckman Coulter Multimode DTX 880 microplate reader (Eth: 485 nm excitation filter, 610 emission filter; DCF: 495 nm excitation filter, 525 emission filter). All Eth- or DCF-fluorescence intensity data were normalized to the average maximum Eth- or DCF-fluorescence under control conditions (relative Eth- or DCF-fluorescence values).

Cellular Fractionation - Cells were washed with, and scraped into Buffer A (20 mM HEPES pH 7.4, 250 mM sucrose, 2 mM EDTA, 5 mM $MgCl_2$, 1 mM dithiothreitol, 1 mM AEBSF, and 1% PIC). Following centrifugation (200 x g_{max}, 2 min), the cell pellet was re-suspended in ice cold Buffer A and sonicated. Following centrifugation (1,200 x g_{max}, 5 min), the supernatant was collected (total cellular suspension). Following centrifugation of the total cellular suspension (100,000 x g_{max}, 30 min, 4°C), the supernatant was collected (cytosolic fraction). The pellet was re-suspended in Buffer B (Buffer A containing 1% Triton X-100 and 0.01% saponin), incubated on ice for 15 min, and centrifuged (100,000 x g_{max}, 30 min, 4°C). The supernatant was collected (membrane fraction), and the pellet was re-suspended in Buffer B (cytoskeleton fraction).

Plasma Membrane Translocation of p67^{phox} – An enriched plasma membrane protein fraction was obtained by biotinylation and streptavidin-affinity chromatography as described by Li and Shah with minor modifications (Li and Shah 2002). SH-SY5Y neuroblastoma cells or E7 cortical neurons were grown in 6-well plates (5×10^6 cells per well) for 48 h prior to incubation with arachidonyl trifluoromethylketone (ATK, 10 μM, 60 min) or buffer. Next, cultures were exposed to 100 ng/ml TNFα for 15 min, washed with HBSS-CM (HBSS, 0.1 g/l CaCl$_2$, 0.1 g/l MgCl$_2$, pH 7.5), and incubated with 0.5 mg/ml Sulfo-NHS-Biotin (prepared in 20 mM HEPES, HBSS-CM, pH 8.0) for 40 min on ice. Excess Sulfo-NHS-Biotin was neutralized (on ice, 15 min) with 50 mM glycine (prepared in HBSS-CM), and cells were scraped into HBSS-CM. After centrifugation (200 x g$_{max}$, 2 min), cells were resuspended in 500 μL loading buffer (20 mM HEPES pH 7.5, HBSS, 1% Triton X-100, 0.2 mg/ml saponin, 1% PIC), and sonicated. Cell lysates were incubated with streptavidin-agarose beads (25 μl, 2 h, 4°C), beads collected (2,500 x g$_{max}$, 2 min), and resuspended in 150 μL of loading buffer. After heating beads (5 min, boiling water bath), and centrifugation (2,500 x g$_{max}$, 2 min), membrane proteins were enriched in the supernatant and total protein content was determined using a BCA protein assay.

Derivatization of Carbonylated Actin - SH-SY5Y cells were treated with 10 μM DPI or 10 μM ATK for 60 min, prior to acute addition of TNFα (100 ng/ml) for 60 min. Cells were lysed in 2 M Tris-Cl pH 8.0, 2% SDS, 1 mM Na$_3$VO$_4$ and centrifuged (3,000 x g$_{max}$, 4°C, 20 min), supernatants (100 μl) incubated with 1 μg normal mouse serum (45 min, 25°C, agitated), and normal IgG removed with protein A/G agarose beads (20 μl). Cleared lysates (100 μl) were mixed with 1 μg monoclonal mouse anti-human β-actin primary antibody (agitation 2 h, 4°C) followed by overnight incubation with protein A/G agarose beads (20 μl, 4°C, agitation). Protein A/G beads were collected by centrifugation (200 x g$_{max}$, 2 min), washed three times in lysis buffer, and bound proteins were released by boiling for 5 min. Actin carbonyl residues were derivatized with 2,4-dinitrophenylhydrazine (DNPH) according to Levine and co-workers (Levine et al.

1994). Briefly, immunoprecipitated actin samples in lysis buffer were mixed with an equal volume of 12% SDS, and further incubated with two sample volumes of 20 mM DNPH in 2M HCl (45 minutes, 25°C). Actin was recovered by chloroform/methanol precipitation according to Wessel and Flugge (Wessel and Flugge 1984), and protein concentration was determined (BCA protein assay).

Polyacrylamide Gel Electrophoresis and Western blotting - Equal amounts of total protein (30-50 µg total cellular protein, or 5 µg immunoprecipitated protein) were separated by SDS-polyacrylamide (15%) gel electrophoresis (125 volts, 50 watts, 75 mA). For native gel electrophoresis, stacking gel (3% acrylamide) and separation gel (3% to 12% acrylamide-gradient) were prepared in 200 mM Tris, 162.5 mM glycine, and 0.2% Triton X-100 and chilled (4°C). Protein samples (20 µg per well in 1.25% Triton X-100, 20 mM Tris-Cl pH 7.5, 1 mM EDTA, 15% glycerol, 0.01% bromphenol blue) were subjected to gel electrophoresis (10 mA, 4°C, 90 min). For in-gel NADPH oxidoreductase activity staining, gels were incubated in 100 mM potassium phosphate pH 7.0, 1 mg/ml NBT, 0.3 mg/ml NADPH at room temperature. The staining reaction was stopped with 5% acetic acid. For western blotting, proteins were transferred from SDS or native polyacrylamide gels onto PVDF membranes (2.5 hours, 50 volts, 50 watts, 250 mA) according to Towbin and co-workers (Towbin et al. 1992). Following transfer, membranes were blocked with TBST-BSA (50 mM Tris-Cl pH 7.4, 150 mM NaCl, 0.1% Tween-20 mg/ml, bovine serum albumin), and probed overnight with the respective primary antibody (1 µg/µl in TBST). After several washes in TBST, membranes were incubated with the corresponding secondary antibody (0.2 µg/µl in TBST, 45 min). Immunoreactivity was detected by chemiluminescence and quantified using a GE Healthcare Typhoon Imager with ImageQuant software (United Kingdom).

Statistical Analysis - Analysis of variance (ANOVA) was used to determine statistically significant differences between treatments ($p < 0.05$). At least three independent experiments were performed for each condition. *Post hoc* comparisons of specific

treatments were performed using Scheffe's test to determine statistical significance based on the calculated ANOVA data. A Dunette's test was used for multiple comparisons between treatments and a single control. All error bars represent standard deviations.

2.4: Results

TNFα stimulates ROS production in SH-SY5Y neuroblastoma cells and primary cortical neurons. Studies in endothelial cells, hepatocytes, cardiomyocytes, and other non-neuronal cells revealed that TNFα stimulates the formation of ROS (Vilcek and Lee 1991; Babior 2000). We expanded these findings into neuronal cells, since many neuronal cell types contain TNFα receptors and are vulnerable to TNFα exposure both *in vitro* and *in vivo* (Sawada et al. 1989; Fetler and Amigorena 2005; Block et al. 2007).

Human SH-SY5Y neuroblastoma cells or cortical neurons obtained from forebrain of 7-day old chick embryos (E7) were loaded with the oxidation-sensitive fluorescence indicator H_2DCFDA. Upon exposure to 100 ng/ml TNFα, ROS formation was quantified in cell lysates every 7.5 min time over a 60 min time period (Fig. 2.1). Indicative of ROS formation, TNFα elicited a rapid increase in relative DCF-fluorescence intensity (1.34 ± 0.17, $*p<0.05$, n=5) in lysates of SH-SY5Y cells within 7.5 minutes after addition compared to control (0.95 ± 0.08, n=3), which persisted for up to 60 min (Fig. 2.1A). A presence of 5 mM N-acetyl-L-cysteine (NAC; 0.86 ± 0.04, n=3), or 5000 U/ml exogenous catalase (CAT; 1.14 ± 0.10, n=3) negated TNFα-induced ROS formation (Fig. 2.1A). In sharp contrast, ROS formation was not compromised by the presence of 200 U/ml exogenous superoxide dismutase (SOD; 1.20 ± 0.08, n=3) (Fig. 2.1A). TNFα-mediated ROS formation was further inhibited by the 1e⁻ transport inhibitor diphenylene iodonium (10 μM DPI; 0.97 ± 0.06, n=4) as well as the $cPLA_2$ inhibitor arachidonyl trifluoromethylketone (10 μM ATK; 0.92 ± 0.03, n=3), (Fig. 2.1B). In lysates of E7 cortical neurons, TNFα (15 min) stimulated a significant ROS formation (2.22 ± 0.18, $*p<0.05$, n=13) as opposed to control (0.99 ± 0.10, n=25), which was sensitive to 5 mM NAC (0.79 ± 0.13, n=7), 5000 U/ml CAT (1.54 ± 0.27, n=7), 10 μM

DPI (1.16 ± 0.32, n=7), and 10 μM ATK (1.31 ± 0.20, n=7), but not 200 U/ml SOD (2.98 ± 0.40, **p<0.05, n=7) (Fig. 2.1C). To more closely evaluate superoxide, SH-SY5Y cells were pre-incubated simultaneously with both H_2DCFDA (10 μM) and DHE (160 μM). The ROS species preference of DCF is mostly for peroxide, while Eth is for superoxide. In the presence of both indicators, TNFα (15 min) only stimulated a significant increase in relative Eth-fluorescence (Eth-control: 1.00 ± 0.13, n=6; Eth-TNFα: 1.47 ± 0.07, *p<0.01, n=3) (DCF-control: 1.00 ± 0.09, n=6; DCF-TNFα: 1.06 ± 0.21, n=3), indicative of superoxide formation (Fig. 2.1D). TNFα-stimulated superoxide formation was still abrogated by 5 mM NAC (Eth: 1.00 ± 0.08, n=3; DCF: 0.63 ± 0.09, n=3), 10 μM DPI (Eth: 0.92 ± 0.03, n=3; DCF: 0.95 ± 0.27, n=3), and 10 μM ATK (Eth: 1.03 ± 0.20, n=3; DCF: 0.95 ± 0.07, n=3). Taken together, these findings demonstrate that TNFα stimulates the formation of ROS in human SH-SY5Y neuroblastoma cells and E7 cortical neurons. The apparent ineffectiveness of SOD to quench DCF-detected ROS, combined with the ability of Eth to detect ROS and quench DCF-detected ROS, together with the sensitivity of ROS formation to DPI (NOX inhibitor) and ATK ($cPLA_2$ inhibitor) implied a superoxide-generating mechanism; presumably a neuronal NADPH oxidase activity.
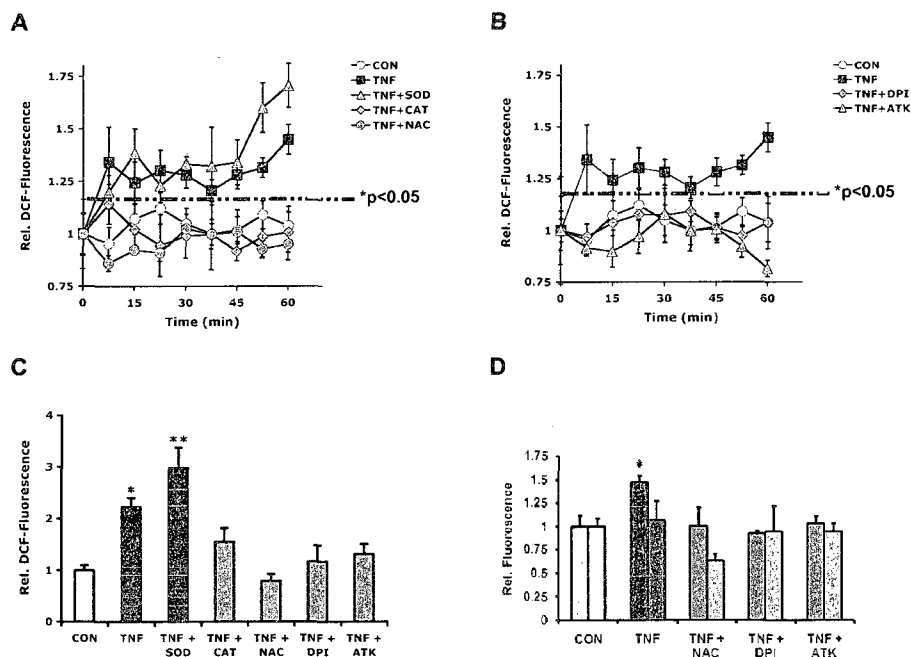
Figure 2.1. TNFα stimulates ROS production in neuronal cells via a NOX activity. Human SH-SY5Y neuroblastoma cells and E7 cortical neurons were pre-loaded (1 h) with 50 μM 2',7'-dihydrodichlorofluorescein diacetate (H_2DCFDA), or a combination of dihydroethidium (DHE, 160 μM) and H_2DCFDA (10 μM), in the presence or absence of pharmacological inhibitors or antioxidant enzymes. H_2DCFDA is oxidized preferentially by peroxide, while DHE is oxidized primarily by superoxide. Cultures were exposed to 100 ng/ml TNFα, and maximum ethidium (Eth)- or DCF-fluorescence was quantified in whole cell lysates. Eth- or DCF measurements were normalized to the average maximum Eth- or DCF-fluorescence under control conditions (relative fluorescence values). (A) In SH-SY5Y cells, TNFα stimulated ROS formation within 7.5 min upon exposure and lasting up to 60 min (TNF, filled squares) indicated by significant increases in relative DCF-fluorescence (*p<0.05) compared to control (CON, filled circles). TNFα-stimulated ROS formation was blocked by 5 mM NAC (TNF+NAC, open triangles) or 5,000 U/ml catalase (TNF+CAT, filled diamonds), but not 200 U/ml superoxide dismutase (TNF+SOD, filled triangles), which was ineffective. (B) Pre-treatment of SH-SY5Y cells with 10 μM DPI (TNF+DPI, filled diamonds), a NOX inhibitor, or 10 μM ATK (TNF+ATK, filled triangles), a $cPLA_2$ inhibitor, also abolished TNFα-stimulated ROS formation. (C) E7 cortical neurons also responded with a significant formation of ROS (TNF, black bar) within 15 min of TNFα exposure compared to controls (CON, white bar) (*p<0.05). ROS formation was suppressed by a presence of 5 mM NAC (TNF+NAC, grey bar), 5,000 U/ml catalase (TNF+CAT, grey bar), 10 μM DPI (TNF+DPI, grey bar), or 10 μM ATK (TNF+ATK, grey bar), but not by 200 U/ml superoxide dismutase (TNF+SOD, black bar, **p<0.05 compared to TNFα-alone). (D) SH-SY5Y cells exposed to 15 min of TNFα exhibited a significant increase in relative Eth-fluorescence (red bars) (sensitive to 5 mM NAC, 10 μM DPI, or 10 μM ATK) (*p<0.01), even in the presence of H_2DCFDA, indicative of a superoxide-generating mechanism (DCF-fluorescence: green bars). All data represent the mean of at least three independent experiments ± standard deviations.

SH-SY5Y neuroblastoma cells and E7 cortical neurons express a functional NOX activity.
The classic NADPH oxidase (NOX) in phagocytes is a multi-subunit complex composed of two membrane-bound subunits (gp91^{phox} or NOX2, and p22^{phox}), and at least three cytosolic subunits (p67^{phox}, p47^{phox}, and p40^{phox}). Only recently, NOX2 homologues were identified in many different cell types including sensory and cortical neurons (Bedard and Krause 2007).

Using human subunit-specific antibodies, we found immunoreactivity against all subunits of the NOX2 complex in whole cell lysates of human SH-SY5Y neuroblastoma cells with apparent molecular weights of 65 kDa for NOX2, 20 kDa for p22^{phox}, 65 kDa for p67^{phox}, 45 kDa for p47^{phox}, and 40 kDa for p40^{phox} (Fig. 2.2A). In phagocytes, phorbol 12-myristate 10-acetate (PMA) and arachidonic acid potently stimulate NOX2 activity reflected by a translocation of cytosolic subunits such as p67^{phox} to the plasma membrane. Treatment of SH-SY5Y cells with 200 nM PMA and 50 μM arachidonic acid caused a time-dependent translocation of the cytosolic subunit p67^{phox} to the plasma membrane (Fig. 2.2B). More importantly, TNFα (100 ng/ml, 15 min) induced a significant translocation of p67^{phox} to the plasma membrane (1.48 ± 0.09, *p<0.05, n=3) in SH-SY5Y cells compared to control (1.01 ± 0.02, n=3), which was completely negated by the cPLA$_2$ inhibitor ATK (10 μM; 1.13 ± 0.03, n=3) (Fig. 2.2C). Similarly, phosphorylation of the cytosolic subunit p40^{phox} (1.65 ± 0.21, *p<0.05, n=3) significantly increased compared to control (1.02 ± 0.08, n=3) upon TNFα stimulation (100 ng/ml, 15 min) (Fig. 2.2D).

A

gp91phox   p22phox   p67phox   p47phox   p40phox   actin

B

    p67phox

(min)   0   3   10   30   60
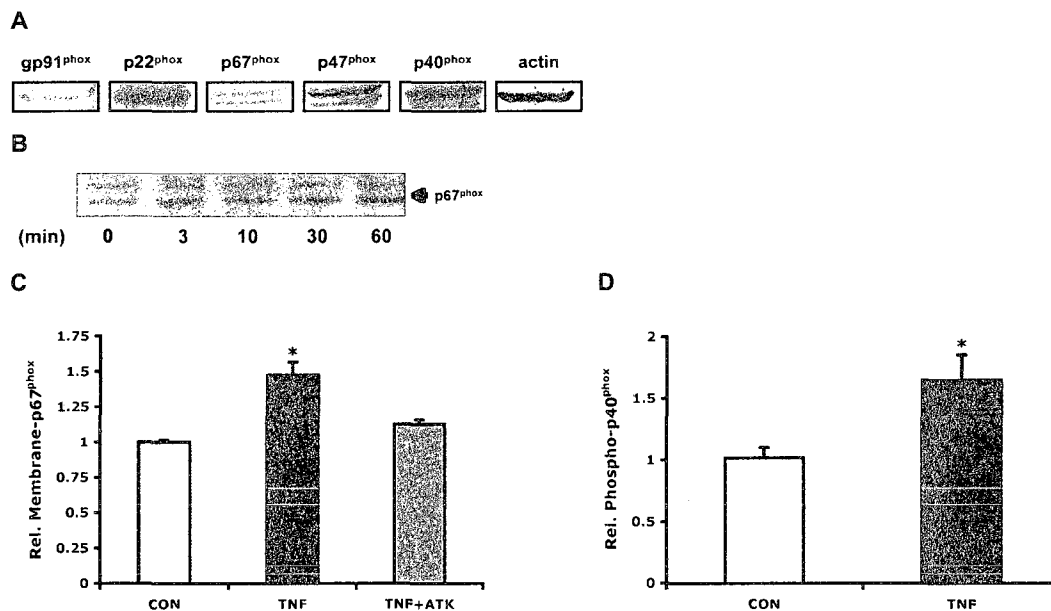
C   D

Figure 2.2. SH-SY5Y neuroblastoma cells express a functional NOX2. (A) Whole cell lysates of human SH-SY5Y neuroblastoma cells revealed immunoreactivity against both membrane-bound subunits (gp91^{phox}, p22^{phox}) and the cytosolic subunits (p67^{phox}, p47^{phox}, and p40^{phox}) of the NOX2 complex using anti-human subunit specific antibodies (loading-control: actin). (B) Treatment of SH-SY5Y cells over a 60 min time course with 200 nM phorbol 12-myristate 10-acetate (PMA) and 50 µM arachidonic acid stimulated a time-dependent translocation of p67^{phox} into plasma membrane. Equal amounts of total plasma membrane protein were separated by SDS-gel electrophoresis followed by western blotting against p67^{phox} and quantification of p67^{phox} immunoreactivity. (C) SH-SY5Y cells were incubated with 100 ng/ml TNFα for 15 min and plasma membrane proteins biotinylated with Sulfo-NHS-biotin. Membrane proteins were affinity-purified on streptavidin-agarose, and equal amounts of membrane protein were separated by SDS-gel electrophoresis, followed by western blotting. Immunoreactivity against p67^{phox} was quantified (chemiluminescence). TNFα elicited a significant translocation of p67^{phox} to plasma membranes (1.48 ± 0.09, *p<0.05, n=3, black bar), which was blocked by the cPLA$_2$ inhibitor ATK, (10 µM, TNF+ATK, grey bar). (D) SH-SY5Y cells were incubated with TNFα (100 ng/ml, 15 min) and whole cell lysates subjected to gel electrophoresis followed by western blotting. Phospho-p40^{phox} immunoreactivity (chemiluminescence) was quantified using a Typhoon Imager with ImageQuant software. Clearly, TNFα increased levels of phospho-p40^{phox} (1.65 ± 0.21, *p<0.05, n=3, black bar) in SH-SY5Y cells compared to control (CON, white bars). All data represent the mean of three independent experiments ± standard deviations.

Cortical neurons also expressed a TNFα-sensitive NOX2-like activity. We found immunoreactivity against all NOX subunits in E7, E9, and E11 whole brain homogenates using human NOX subunit-specific antibodies (Fig. 2.3A). The apparent molecular

weight of the subunits were nearly identical to those detected in SH-SY5Y cells. Utilizing native polyacrylamide gel electrophoresis followed by NBT staining, NADPH oxidoreductase activities were detected in E7 whole brain homogenates (Fig. 2.3B, lane 1), in growth cone particles freshly prepared from E11 whole brains (Fig. 2.3B, lane 2), as well as in a plasma membrane preparations obtained from E7 cortical neurons (Fig. 2.3B, lane 3) with one activity corresponding to NOX2 (Fig. 2.3B, lane 4). Quantitative analysis revealed a significant translocation of $p67^{phox}$ to plasma membranes of E7 cortical neurons stimulated with 100 ng/ml TNFα (1.36 $\pm$ 0.03, *$p<0.05$, n=3) compared to control (1.04 $\pm$ 0.04, n=3). As in the case of human SH-SY5Y neuroblastoma cells, $p67^{phox}$ membrane translocation was abolished by 10 μM ATK (1.13 $\pm$ 0.01, n=3) (Fig. 2.3C). Taken together, these findings provided evidence that human SH-SY5Y neuroblastoma cells and E7 cortical neurons both express a functional NOX2 complex.
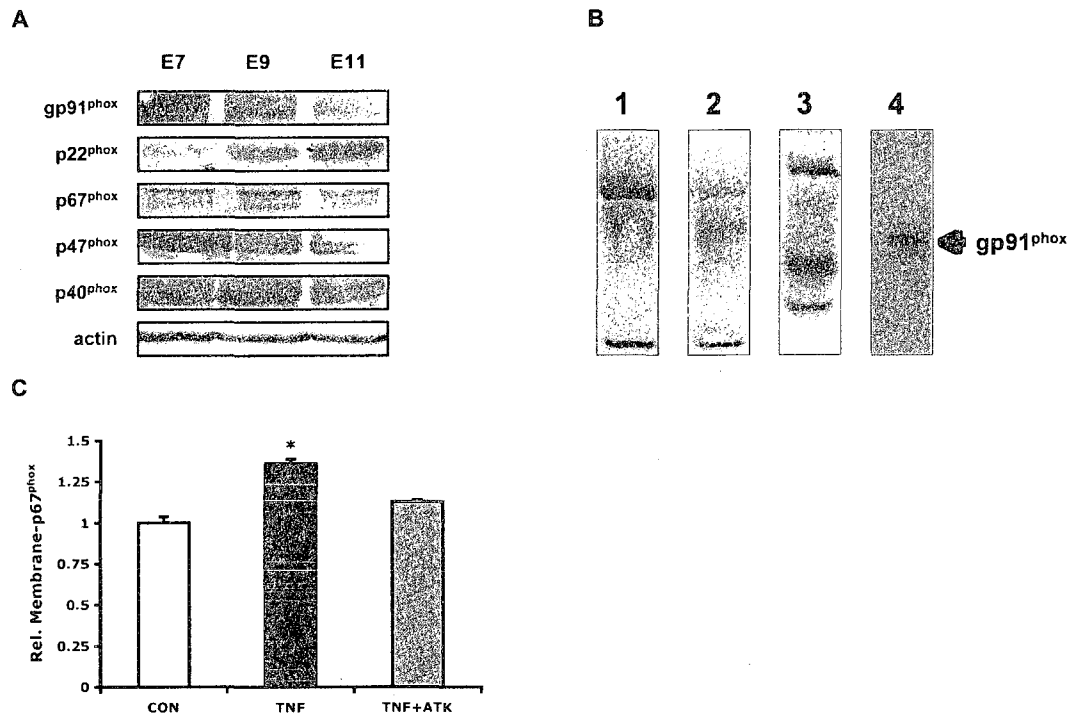
A

B

C

Figure 2.3. Primary cortical neurons express a functional NOX2. (A) Membrane-bound subunits (gp91^{phox}, p22^{phox}) and cytosolic subunits (p67^{phox}, p47^{phox}, and p40^{phox}) of the NOX2 complex were detected in chick E7, E9, and E11 whole brain homogenates using anti-human subunit specific antibodies (loading-control: actin). (B) NADPH oxidoreductase activities were detected in E7 whole brain homogenates (lane 1) and growth cone particles freshly prepared from chick E11 brains (lane 2) by native-gel electrophoresis and subsequent in-gel NBT staining. Similar activities were found in plasma membranes of E7 cortical neurons (lane 3), with one activity corresponding to Nox2 (lane 4, western blot against gp91^{phox}). (C) TNFα stimulated a significant translocation of p67^{phox} to plasma membranes (1.36 ± 0.03, *p<0.05, n=3, black bar) of E7 cortical neurons, which was blocked by 10 μM ATK (TNF+ATK, grey bar). Following stimulation of E7 cortical neurons with 100 ng/ml TNFα (15 min), plasma membrane proteins were biotinylated (Sulfo-NHS-biotin), affinity-purified on streptavidin-agarose, analyzed by SDS-gel electrophoresis followed by western blotting, and p67^{phox} immunoreactivity was quantified (Typhoon Imager). All values were normalized to control (CON, white bar). All data represent the mean of three independent experiments ± standard deviations.

TNFα stimulates a redox-dependent reorganization of the neuronal actin cytoskeleton.
The proinflammatory cytokine TNFα induces a rearrangement of the cellular actin cytoskeleton in many cell types reflecting changes in actin filament dynamics (Hanna et al. 2001). Moldovan and coworkers recently demonstrated in endothelial cells a causal

link between intracellular formation of ROS and reorganization of actin filaments (Moldovan et al. 2006). Thus, we explored in human SH-SY5Y neuroblastoma cells whether TNFα mediated a ROS-dependent rearrangement of the neuronal actin cytoskeleton.

Serum-starved SH-SY5Y neuroblastoma cells grown on collagen displayed a highly condensed morphology with little or no lamellipodia but responded with a dramatic, yet transient increase in lamellipodial formation within 15 min upon exposure to 200 ng/ml TNFα (Fig. 2.4, upper panel). In sharp contrast, incubation of serum-starved SH-SY5Y neuroblastoma cells with 10 μM DPI negated lamellipodial activity in response to TNFα, and cells retained their condensed morphology (Fig. 2.4, middle panel). Similarly, scavenging ROS with the catalytic antioxidant Manganese (III) tetrakis (4-benzoic acid) porphyrin chloride (MnTBAP, 40 μM), a superoxide dismutase mimetic, largely suppressed a rearrangement of the neuronal actin cytoskeleton in the presence of TNFα. The sensitivity of actin filament dynamics to DPI and the catalytic antioxidant MnTBAP suggested a direct role of ROS in TNFα-mediated reorganization of the neuronal actin cytoskeleton.
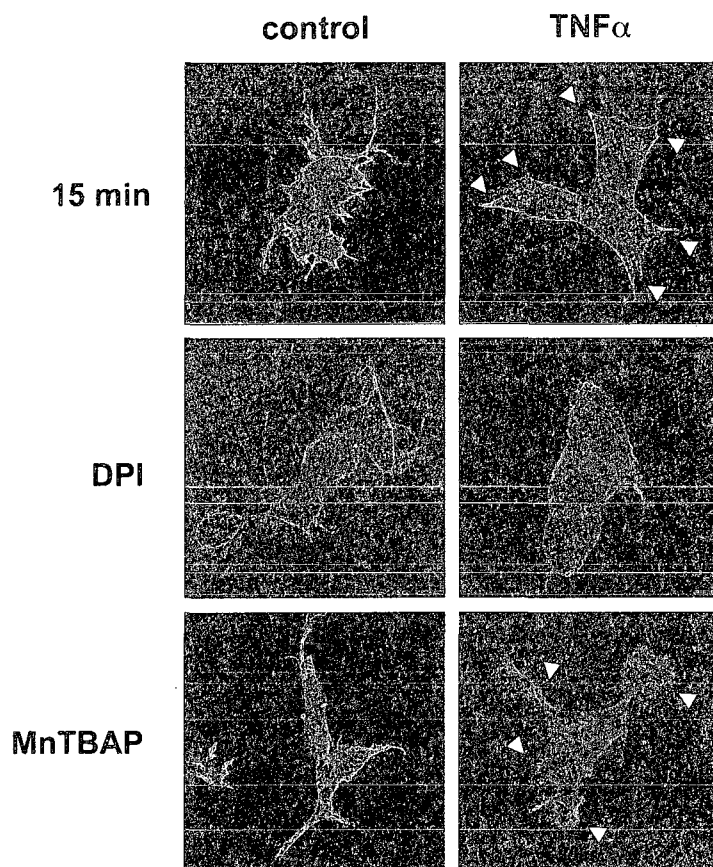
control   TNFα

15 min

DPI

MnTBAP

Figure 2.4. TNFα stimulates a redox-dependent, transient rearrangement of actin filaments in neuronal cells.
Human SH-SY5Y neuroblastoma cells were grown on collagen in serum-free medium and incubated either with 10 μM
DPI, 40 μM MnTBAP, or buffer for 1 h. Next, cultures were exposed to 200 ng/ml TNFα and then processed for
rhodamine phalloidin staining. Serum-starved SH-SY5Y cells exhibited a condensed morphology with little or no
lamellipodia (control). In contrast, acute exposure of serum-starved SH-SY5Y cells to TNFα elicited the formation of
lamellipodia -arrow heads- within 15 min. However, lamellipodia formation ceased and 30 min after TNFα-exposure,
SH-SY5Y cells reverted to their condensed morphology. The NOX inhibitor DPI blocked lamellipodia formation upon
addition of TNFα (200 ng/ml, 15 min), and SH-SY5Y cells retained a condensed morphology typical of serum-starved
cells. Preincubation of SH-SY5Y cells with MnTBAP also interfered with a transient formation of lamellipodia in the
presence of TNFα (200 ng/ml, 15 min).

TNFα elicits oxidative damage to the neuronal actin cytoskeleton. Actin is highly

susceptible to oxidative modification, which compromises polymerization,

depolymerization, and the stability of actin filaments (Lassing et al. 2007). Thus

oxidative damage of actin adversely affects many critical cellular processes that depend

on proper actin dynamics such as cellular motility (Moldovan et al. 2006), gene expression (Formigli et al. 2007), mitochondrial viability (Gourlay and Ayscough 2005a), vesicle trafficking (Lanzetti 2007), and synaptic plasticity (Gungabissoon and Bamburg 2003; Calabrese et al. 2006; Tada and Sheng 2006). In fact, actin oxidation is prevalent in many neurodegenerative disorders (Fiala et al. 2002; Maloney and Bamburg 2007). Therefore, we examined whether the neurotoxicity of TNFα, at least partially, could be attributed to oxidative damage to the neuronal actin cytoskeleton using carbonylation as a marker of oxidative stress.

As shown in Figure 2.5, SH-SY5Y neuroblastoma cells exhibited significant actin carbonylation upon treatment with TNFα (100 ng/ml, 60 min) (1.24 $\pm$ 0.02, *p<0.05, n=3) compared to control (0.99 $\pm$ 0.02, n=3). As expected, preincubation of SH-SY5Y neuroblastoma cells with 10 μM DPI completely negated actin carbonylation in the presence of TNFα to levels comparable to control conditions (1.09 $\pm$ 0.01, n=3). Inhibition of cPLA$_2$ using 10 μM ATK also reduced actin carbonylation (0.98 $\pm$ 0.01, n=3). Neither pharmacological treatment altered actin carbonylation in the absence of TNFα and residual carbonylation was indistinguishable from control conditions -data not shown-. These findings provide evidence that TNFα exposure results in irreversible oxidative damage (carbonylation) to the neuronal actin cytoskeleton by stimulating a NOX2-like activity.
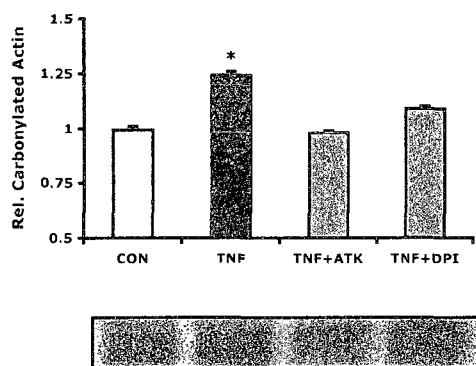
Figure 2.5. TNFα mediates carbonylation of actin in neuronal cells via NOX2 activation. Total actin was immunoprecipitated from whole cell lysates of SH-SY5Y neuroblastoma cells treated with TNFα (100 ng/ml, 60 min) following a 1h pretreatment with the NOX inhibitor DPI (10 μM), or the cPLA$_2$ inhibitor ATK (10 μM). Protein carbonyls of the precipitated actin were derivatized with 2,4-dinitrophenylhydrazine (DNP). Following SDS-gel electrophoresis and western blotting, DNP immunoreactivity (chemiluminescence) was quantified using a Typhoon Imager with ImageQuant software. TNFα induced a significant increase in carbonylation of total actin (1.24 ± 0.02, *p<0.05, n=3, black bar) compared to control (CON, white bar). Note, either DPI or ATK diminished carbonylation of actin (grey bars) to control levels despite a presence of TNFα. All values were normalized to controls and represent the mean of three independent experiments ± standard deviations.

2.5: Discussion

Our studies in human SH-SY5Y neuroblastoma cells and E7 chick cortical neurons demonstrated that TNFα stimulated the formation of ROS via a neuronal NOX2 activity resulting in increased carbonylation concomitant with a dramatic rearrangement of actin filaments into stress fibers. Carbonylation of actin, an irreversible and likely debilitating oxidative modification, could severely compromise fundamental cellular processes such as motility, gene expression, vesicle traffic, and mitochondrial homeostasis, which all require proper actin filament dynamics. These findings imply a key role for neuronal NOX activities in CNS inflammation ultimately contributing to neuronal cell death.

The pro-inflammatory cytokine TNFα exerts pleiotropic effects in the developing, adult, and injured CNS. Yet persistent, high expression levels of TNFα are neurotoxic

due to the generation of ROS and production of adverse lipid second messengers. We measured a significant increase in maximum DCF-fluorescence intensity, indicative of ROS formation, in both human SH-SY5Y neuroblastoma cells and E7 cortical neurons exposed to TNFα (Fig. 2.1). Passive ROS scavenging with the antioxidant NAC or enzymatic ROS scavenging by exogenous catalase both completely abolished TNFα-mediated ROS formation whereas exogenous superoxide dismutase (SOD) was ineffective. Since addition of exogenous SOD did not quench ROS formation, it could be implied that the TNFα-stimulated ROS source may either produce peroxide directly, or generate superoxide, which would rapidly be converted by the additional SOD to peroxide (detected preferentially by DCF). To further evaluate this discrepancy, we utilized two ROS indicators simultaneously (Eth and DCF) (Figure 2.1D). The preference of Eth is almost entirely for superoxide; therefore its use in excess would deplete superoxide and only allow remaining peroxide to react with DCF. Indeed, Eth detected a significant increase in ROS in response to TNFα, however the excess of Eth negated any DCF-detectable ROS. This demonstrated that TNFα-stimulated intracellular ROS production was from a superoxide-generating source. The fact that both the 1e$^-$ transport inhibitor DPI and the cPLA$_2$ inhibitor ATK, respectively, abolished ROS formation in response to TNFα provided indirect evidence for a superoxide-generating source such as neuronal NOX isoform. Also, activity of many NOX isoforms depends on the transfer of electrons from NADPH onto oxygen and the lipid second messenger arachidonic acid, the product of cPLA$_2$ activity (Bedard and Krause 2007). Indeed, recent studies describe the expression of the multi subunit proteins Nox1, Nox2, and Nox4 in neuronal cells (Tejada-Simon et al. 2005; Vallet et al. 2005; Bedard and Krause 2007). Using human-specific antibodies, we found immunoreactivity against all subunits of Nox2 in human SH-SY5Y neuroblastoma cells (Fig. 2.2). Our finding was in agreement with Nikolova and co-workers who recently found mRNA for all subunits of Nox2 in SH-SY5Y cells (Nikolova et al. 2005). We further corroborated this finding in homogenates prepared from whole brains of 7 day-, 9 day-, and 11 day-old chick embryos (Fig. 2.3).

In addition to increases in ROS formation, stimulus-dependent translocation of the cytosolic subunit p67^{phox} to plasma membranes or phosphorylation of p40^{phox} are strong indicators of a functional NOX assembly. PMA and arachidonic acid are well-documented activators of NOX enzymes due to PMA stimulating kinase activities and arachidonic acid serving as a membrane-anchor upon interaction with Phox homology domains present in the p40^{phox} and p47^{phox} subunits (Groemping and Rittinger 2005; Bedard and Krause 2007; Ueyama et al. 2007). SH-SY5Y cells exposed to PMA and arachidonic acid revealed qualitative increases in p67^{phox} in a plasma membrane protein fraction suggesting the translocation of p67^{phox} from the cytosol to the plasma membrane. Native gel electrophoresis in conjunction with NBT staining demonstrated a presence of NADPH oxidoreductase activities in whole E7 chick brain homogenates, growth cone particles freshly prepared from E11 chick brains, as well as in plasma membrane preparations of E7 chick cortical neurons (Fig. 2.3). Relevant to our studies, TNFα stimulated both phosphorylation of p40^{phox} (SH-SY5Y neuroblastoma cells) and plasma membrane translocation of p67^{phox} (SH-SY5Y cells and E7 cortical neurons). Together these findings provide evidence that human SH-SY5Y neuroblastoma cells and primary cortical neurons express a NOX2 isoform generating ROS upon stimulation by TNFα. Whether other NOX isoforms are expressed in neuronal cells, and contribute to ROS formation, remains to be determined. If TNFα neurotoxicity could be attributed to increased ROS formation, oxidation-sensitive cellular targets should be detectable. We focused our investigations on the neuronal actin cytoskeleton due to 1) a strong vulnerability to oxidative damage, 2) the presence of oxidized actin in many chronic CNS disorders, 3) the ability of TNFα to alter actin filament organization, and 4) the essential role of actin in fundamental cellular processes.

Due to the complex morphology of primary neurons, we focused our studies on SH-SY5Y neuroblastoma cells and their actin cytoskeleton response to TNFα exposure. Serum-starved SH-SY5Y neuroblastoma cells grown on a collagen substrate exhibited an atrophic, condensed morphology with some actin stress fibers but virtually no lamellipodia or filopodia (Fig. 2.4). Upon bath application of TNFα, SH-SY5Y

neuroblastoma cells displayed a transient phase of cell spreading associated with the formation of lamellipodia and filopodia followed by stress fiber formation. Notably, this rearrangement of actin filaments was not reversible by washing out TNFα and exhibited a prolonged recovery phase, suggesting an irreversible process (data not shown). Conversely, preincubation of SH-SY5Y neuroblastoma cells with DPI or the catalytic SOD mimetic MnTBAP, preserved a predominant atrophic condensed morphology of SH-SY5Y neuroblastoma cells despite TNFα exposure. These findings implied that TNFα elicited a permanent reorganization of the neuronal actin cytoskeleton via NOX-derived ROS. Carbonylation of amino acid residues (lysines, prolines, and arginines) and the protein backbone reflect an irreversible oxidative modification known to cause dramatic conformational changes, oligomerization, as well as loss of protein function (Nystrom 2005). Indeed, we found a profound increase in carbonyl residues in total actin of SH-SY5Y neuroblastoma cells exposed to TNFα, which was completely abolished by inhibiting NOX activity via a preincubation of cells with either DPI or ATK (Fig. 2.5).

In conclusion, our studies revealed that SH-SY5Y neuroblastoma cells and chick E7 cortical neurons, and likely other neuronal cell types, express a functional NOX 2 activity responding to the proinflammatory cytokine TNFα. Furthermore, TNFα-induced neuronal NOX activity resulted in an irreversible oxidation of actin concomitant with a severe rearrangement of actin filaments into stress fibers. Organization and dynamics of actin filaments are essential for fundamental neuronal processes ranging from changes in the motility and morphology of subcellular structures (spines, synapses, axons, dendrites), to gene expression, mitochondrial homeostasis, and vesicle trafficking. Therefore irreversible oxidative modification of actin could dramatically compromise the functionality and survivability of CNS neurons.

There is a substantial presence of activated microglia and astrocytes in the CNS associated with acute injuries, chronic neurodegenerative diseases, and psychiatric disorders. Activated microglia and astrocytes play a key role in the orchestration and progression of CNS inflammation by releasing numerous inflammatory mediators such as cytokines and eicosanoids as well as ROS (Fetler and Amigorena 2005; Nimmerjahn et

al. 2005; Block et al. 2007). Therefore, persistent inflammation accompanied by oxidative stress contributes, to a large extent, to neuronal death. Our findings provided evidence that inflammatory mediators (TNFα) prevalent in many CNS pathologies could compromise neurons through a direct and irreversible oxidative modification of actin, thus disrupting key cellular processes. The fact that neuronal NOX isoforms play a vital role in this neurotoxicity-mechanism could potentially open new therapeutic strategies to alleviate neurodegeneration and improve neuronal survival and connectivity.

2.6: Acknowledgements

2.7: Contributions

Several individuals contributed to this research study. Shelli Smeets performed the confocal microscopy showing that TNFα caused transient changes in the SH-SY5Y actin cytoskeleton. Mark Wright conducted the native-gel electrophoresis that revealed the presence of an NADPH oxidoreductase activity in cortical neurons and growth cone particles. Sally Gustafson and Danielle LaVictorie assisted in the identification of NOX subunits and functional characterization of the neuronal NOX.

2.8: References

Babior B. M. (2000) Phagocytes and oxidative stress. *The American journal of medicine* **109**, 33-44.

Bedard K. and Krause K. H. (2007) The NOX family of ROS-generating NADPH oxidases: physiology and pathophysiology. *Physiological reviews* **87**, 245-313.

Block M. L., Zecca L. and Hong J. S. (2007) Microglia-mediated neurotoxicity: uncovering the molecular mechanisms. *Nat Rev Neurosci* **8**, 57-69.

Bottenstein J. E. and Sato G. H. (1979) Growth of a rat neuroblastoma cell line in serum-free supplemented medium. *Proceedings of the National Academy of Sciences of the United States of America* **76**, 514-517.

Calabrese B., Wilson M. S. and Halpain S. (2006) Development and regulation of dendritic spine synapses. *Physiology (Bethesda, Md* **21**, 38-47.

Colton C. A. and Gilbert D. L. (1987) Production of superoxide anions by a CNS macrophage, the microglia. *FEBS letters* **223**, 284-288.

DalleDonne I., Milzani A. and Colombo R. (1995) H2O2-treated actin: assembly and polymer interactions with cross-linking proteins. *Biophysical journal* **69**, 2710-2719.

DalleDonne I., Milzani A. and Colombo R. (1998) G-actin conformational change and polymerization induced by paraquat. *Biochemistry and cell biology = Biochimie et biologie cellulaire* **76**, 583-591.

Fetler L. and Amigorena S. (2005) Neuroscience. Brain under surveillance: the microglia patrol. *Science (New York, N.Y* **309**, 392-393.

Fiala J. C., Spacek J. and Harris K. M. (2002) Dendritic spine pathology: cause or consequence of neurological disorders? *Brain Res Brain Res Rev* **39**, 29-54.

Formigli L., Meacci E., Zecchi-Orlandini S. and Orlandini G. E. (2007) Cytoskeletal reorganization in skeletal muscle differentiation: from cell morphology to gene expression. *Eur J Histochem* **51 Suppl 1,** 21-28.

Gourlay C. W. and Ayscough K. R. (2005a) The actin cytoskeleton in ageing and apoptosis. *FEMS yeast research* **5,** 1193-1198.

Gourlay C. W. and Ayscough K. R. (2005b) The actin cytoskeleton: a key regulator of apoptosis and ageing? *Nat Rev Mol Cell Biol* **6,** 583-589.

Groemping Y. and Rittinger K. (2005) Activation and assembly of the NADPH oxidase: a structural perspective. *The Biochemical journal* **386,** 401-416.

Gungabissoon R. A. and Bamburg J. R. (2003) Regulation of growth cone actin dynamics by ADF/cofilin. *J Histochem Cytochem* **51,** 411-420.

Hanna A. N., Berthiaume L. G., Kikuchi Y., Begg D., Bourgoin S. and Brindley D. N. (2001) Tumor necrosis factor-alpha induces stress fiber formation through ceramide production: role of sphingosine kinase. *Molecular biology of the cell* **12,** 3618-3630.

Incerpi S., Fiore A. M., De Vito P. and Pedersen J. Z. (2007) Involvement of plasma membrane redox systems in hormone action. *The Journal of pharmacy and pharmacology* **59,** 1711-1720.

Karnoub A. E., Der C. J. and Campbell S. L. (2001) The insert region of Rac1 is essential for membrane ruffling but not cellular transformation. *Molecular and cellular biology* **21,** 2847-2857.

Kuhn T. B., Brown M. D., Wilcox C. L., Raper J. A. and Bamburg J. R. (1999) Myelin and collapsin-1 induce motor neuron growth cone collapse through different pathways: inhibition of collapse by opposing mutants of rac1. *J Neurosci* **19,** 1965-1975.

Lambeth J. D. (2002) Nox/Duox family of nicotinamide adenine dinucleotide (phosphate) oxidases. *Current opinion in hematology* **9,** 11-17.

Lanzetti L. (2007) Actin in membrane trafficking. *Current opinion in cell biology* **19,** 453-458.

Lassing I., Schmitzberger F., Bjornstedt M., Holmgren A., Nordlund P., Schutt C. E. and Lindberg U. (2007) Molecular and structural basis for redox regulation of beta-actin. *Journal of molecular biology* **370,** 331-348.

Levine R. L., Williams J. A., Stadtman E. R. and Shacter E. (1994) Carbonyl assays for determination of oxidatively modified proteins. *Methods in enzymology* **233,** 346-357.

Li J. M. and Shah A. M. (2002) Intracellular localization and preassembly of the NADPH oxidase complex in cultured endothelial cells. *The Journal of biological chemistry* **277,** 19952-19960.

Maloney M. T. and Bamburg J. R. (2007) Cofilin-mediated neurodegeneration in Alzheimer's disease and other amyloidopathies. *Molecular neurobiology* **35,** 21-44.

Milzani A., Dalledonne I., Vailati G. and Colombo R. (1997) Paraquat induces actin assembly in depolymerizing conditions. *Faseb J* **11,** 261-270.

Milzani A., Rossi R., Di Simplicio P., Giustarini D., Colombo R. and DalleDonne I. (2000) The oxidation produced by hydrogen peroxide on Ca-ATP-G-actin. *Protein Sci* 9, 1774-1782.

Moldovan L., Mythreye K., Goldschmidt-Clermont P. J. and Satterwhite L. L. (2006) Reactive oxygen species in vascular endothelial cell motility. Roles of NAD(P)H oxidase and Rac1. *Cardiovascular research* 71, 236-246.

Moldovan L., Irani K., Moldovan N. I., Finkel T. and Goldschmidt-Clermont P. J. (1999) The actin cytoskeleton reorganization induced by Rac1 requires the production of superoxide. *Antioxidants & redox signaling* 1, 29-43.

Moldovan L., Moldovan N. I., Sohn R. H., Parikh S. A. and Goldschmidt-Clermont P. J. (2000) Redox changes of cultured endothelial cells and actin dynamics. *Circulation research* 86, 549-557.

Munch G., Gasic-Milenkovic J., Dukic-Stefanovic S., Kuhla B., Heinrich K., Riederer P., Huttunen H. J., Founds H. and Sajithlal G. (2003) Microglial activation induces cell death, inhibits neurite outgrowth and causes neurite retraction of differentiated neuroblastoma cells. *Experimental brain research. Experimentelle Hirnforschung* 150, 1-8.

Neumann H., Schweigreiter R., Yamashita T., Rosenkranz K., Wekerle H. and Barde Y. A. (2002) Tumor necrosis factor inhibits neurite outgrowth and branching of hippocampal neurons by a rho-dependent mechanism. *J Neurosci* 22, 854-862.

Nikolova S., Lee Y. S., Lee Y. S. and Kim J. A. (2005) Rac1-NADPH oxidase-regulated generation of reactive oxygen species mediates glutamate-induced apoptosis in SH-SY5Y human neuroblastoma cells. *Free radical research* **39**, 1295-1304.

Nimmerjahn A., Kirchhoff F. and Helmchen F. (2005) Resting microglial cells are highly dynamic surveillants of brain parenchyma in vivo. *Science (New York, N.Y* **308**, 1314-1318.

Nystrom T. (2005) Role of oxidative carbonylation in protein quality control and senescence. *The EMBO journal* **24**, 1311-1317.

Pfenninger K. H., Ellis L., Johnson M. P., Friedman L. B. and Somlo S. (1983) Nerve growth cones isolated from fetal rat brain: subcellular fractionation and characterization. *Cell* **35**, 573-584.

Quinn M. T. and Gauss K. A. (2004) Structure and regulation of the neutrophil respiratory burst oxidase: comparison with nonphagocyte oxidases. *Journal of leukocyte biology* **76**, 760-781.

Sawada M., Kondo N., Suzumura A. and Marunouchi T. (1989) Production of tumor necrosis factor-alpha by microglia and astrocytes in culture. *Brain research* **491**, 394-397.

Tada T. and Sheng M. (2006) Molecular mechanisms of dendritic spine morphogenesis. *Current opinion in neurobiology* **16**, 95-101.

Tammariello S. P., Quinn M. T. and Estus S. (2000) NADPH oxidase contributes directly to oxidative stress and apoptosis in nerve growth factor-deprived sympathetic neurons. *J Neurosci* **20**, RC53.

Tejada-Simon M. V., Serrano F., Villasana L. E., Kanterewicz B. I., Wu G. Y., Quinn M. T. and Klann E. (2005) Synaptic localization of a functional NADPH oxidase in the mouse hippocampus. *Molecular and cellular neurosciences* **29**, 97-106.

Towbin H., Staehelin T. and Gordon J. (1992) Electrophoretic transfer of proteins from polyacrylamide gels to nitrocellulose sheets: procedure and some applications. 1979. *Biotechnology (Reading, Mass* **24**, 145-149.

Town T., Nikolic V. and Tan J. (2005) The microglial "activation" continuum: from innate to adaptive responses. *Journal of neuroinflammation* **2**, 24.

Ueyama T., Tatsuno T., Kawasaki T., Tsujibe S., Shirai Y., Sumimoto H., Leto T. L. and Saito N. (2007) A regulated adaptor function of p40phox: distinct p67phox membrane targeting by p40phox and by p47phox. *Molecular biology of the cell* **18**, 441-454.

Vallet P., Charnay Y., Steger K., Ogier-Denis E., Kovari E., Herrmann F., Michel J. P. and Szanto I. (2005) Neuronal expression of the NADPH oxidase NOX4, and its regulation in mouse experimental brain ischemia. *Neuroscience* **132**, 233-238.

Vilcek J. and Lee T. H. (1991) Tumor necrosis factor. New insights into the molecular mechanisms of its multiple actions. *The Journal of biological chemistry* **266**, 7313-7316.

Wessel D. and Flugge U. I. (1984) A method for the quantitative recovery of protein in dilute solution in the presence of detergents and lipids. *Analytical biochemistry* **138**, 141-143.

Wright M. V. and Kuhn T. B. (2002) CNS neurons express two distinct plasma membrane electron transport systems implicated in neuronal viability. *Journal of neurochemistry* **83,** 655-664.

Chapter 3: TNFα- and Aβ-induced neutral sphingomyelinase activity regulates the neuronal NADPH oxidase and subsequent oxidative damage to sphingosine kinase-1[2]

3.1: Abstract

Inflammation and its mediators are implicated in the orchestration and progression of chronic degenerative CNS pathologies commonly accompanied by signs of severe oxidative stress. The bioactive sphingolipid ceramide is generated by the hydrolysis of sphingomyelin through the action of neutral sphingomyelinase (nSMase), which is found associated with type I receptors of the pro-inflammatory cytokine tumor necrosis factor alpha (TNFα). Ceramide and its metabolites play a key role in mediating oxidative stress and stimulating apoptosis in neurons and non-neuronal cells. In human SH-SY5Y neuroblastoma cells or primary cortical neurons, both TNFα and the amyloid beta fragment ($A\beta^{1-42}$) stimulated nSMase activity, subsequent ceramide generation, and the formation of ROS via a neuronal NADPH oxidase (NOX) activity. Neuronal degeneration was further provoked by NOX-dependent oxidative damage to sphingosine kinase-1, an enzyme responsible for the generation of the pro-survival messenger sphingosine-1-phosphate. Our studies suggest that ceramide-mediated activation of a neuronal NOX activity in combination with a loss of sphingosine-1-phosphate formation greatly contributes to CNS neurodegeneration.

I, Brian Barth, affirm my contributions to the work outlined in this chapter. I contributed to the conceptualization and experimental design of the study, worked directly on all aspects of the study, and prepared the manuscript, all under the supervision, mentorship, and advisement of Dr. Thomas Kuhn. Please see section 3.7 on page 128 for the contributions of the other authors.

3.2: Introduction

Central nervous system (CNS) neurodegeneration associated with acute injuries, chronic diseases, or psychiatric disorders, exhibits widespread inflammation [1]. Microglia and astrocytes respond to injury, toxins, and invading pathogens by secreting inflammatory mediators such as cytokines, eicosanoids, and reactive oxygen species (ROS) [1-4]. The pro-inflammatory cytokine tumor necrosis factor alpha (TNFα) elicits ceramide accumulation and formation of ROS upon binding to a high affinity (type I) receptor expressed on the surface of many neuronal cell types [1, 5-7]. The TNFα type I receptor is coupled to Mg^{2+}-dependent neutral sphingomyelinase (Mg^{2+}-nSMase) through the adaptor protein FAN (factor associated with nSMase) [8-10]. SMases are enzymes identified by their pH optimum and ion dependence that catalyze the hydrolysis of sphingomyelin, liberating ceramide and phosphocholine [9, 11]. Mg^{2+}-nSMase is localized at the plasma membrane, and was identified as the primary SMase induced by cellular stress signaling [11]. The brain-specific SMase, Mg^{2+}-nSMase2, is specifically inhibited by the pharmacological agent GW4869 [11, 12].

Ceramide, the product of SMase activity, is implicated in stress kinase activation, oxidative stress, and apoptosis [9, 10, 13-15]. Oxidative stress results from aberrant stimulation of a variety of oxidoreductases, as well as through ceramide-mediated mitochondrial dysfunction that results in the uncoupling of electron transport [1, 14, 16, 17]. One particular family of oxidoreductases, the NADPH oxidase (NOX) family, was originally discovered in phagocytic cells, yet has recently been identified in various non-phagocytic cell types, including neurons [18-21]. NOX enzymes are highly regulated multi-subunit complexes. Assembly of NOX requires phosphorylation of cytosolic subunits followed by interactions between lipid-binding PX (Phox-homology) domains and anionic phospholipids [19, 22-24].

Activation of NOX results in the rapid production of superoxide anion, a highly reactive oxygen radical [18]. Numerous cellular processes are sensitive to oxidative modification, including those associated with cellular function and survival. Sphingosine kinases (SphK) are novel lipid kinases that phosphorylate the ceramide metabolite

sphingosine to produce sphingosine-1-phosphate (S1P), a pro-growth and pro-survival mediator [25-28]. Importantly, S1P opposes the detrimental effects of ceramide. In addition to regulating survival, recent studies have also implicated S1P as a modulator of neurodevelopment. Toman and co-workers demonstrated that S1P induced neurite outgrowth in both PC12 cells and dorsal root ganglia (DRG) neurons [29], while another study by Mizugishi and co-workers showed that mice with both isoforms of SphK knocked out did not develop to term due to neurodevelopment complications [30]. Additionally, a more recent study by Strochlic and co-workers suggested that S1P was involved in axon guidance of the developing *Xenopus* visual system by acting as a repulsive factor, directing retinal growth cones toward the optic tectum and away from other regions of the brain [31].

The aim of our study was to determine the pathway by which TNFα and the amyloid beta fragment (Aβ^{1-42}) stimulated NOX in neurons. We demonstrated that both TNFα and Aβ^{1-42} stimulated Mg^{2+}-nSMase activity, and that the subsequent generation of ceramide stimulated a neuronal NOX activity. We further showed that SphK1 was a novel target for NOX-derived ROS; identifying a mechanism where ceramide-signaling interfered directly with S1P formation and neuron survival.

3.3: Materials and Methods

Reagents

Recombinant human TNFα was purchased from Millipore (Temecula, CA). Aβ^{1-42} was from AnaSpec (San Jose, CA). Sphingolipids were from Avanti Polar Lipids (Alabaster, AL). GW4869 and naphthalene dicarboxylaldehyde (NDA) were purchased from EMD Biosciences (San Diego, CA). Polyclonal rabbit anti-DNP (dinitrophenyl) primary antibodies were from Invitrogen (Carlsbad, CA). Polyclonal rabbit anti-human p67^{phox} primary antibodies were from Millipore. Polyclonal goat anti-mouse SphK1 primary antibodies, polyclonal goat anti-human phospho-p40^{phox} primary antibodies, monoclonal mouse anti-human β-actin primary antibodies, normal goat serum, and

horseradish peroxidase-conjugated secondary antibodies were from Santa Cruz (Santa Cruz, CA). DMEM and Penicillin/Streptomycin were obtained from Mediatech (Herndon, VA). GlutaMAX-1, Hank's Balanced Salt Solution (HBSS), trypsin/EDTA solution, and an Amplex Red Sphingomyelinase assay kit were purchased from Invitrogen. Fetal bovine serum was received from Atlanta Biologicals (Atlanta, GA). Streptavidin-agarose beads, protease inhibitor cocktail (PIC), Pico Super Signal chemoluminescent kit, and a BCA protein assay kit were obtained from Pierce (Rockland, IL). All other reagents were purchased from Sigma (St. Louis, MO).

Cell Culture

Human SH-SY5Y neuroblastoma cells were grown in 100 mm dishes (Falcon) in medium composed of DMEM, 10% fetal bovine serum (FBS), 1% Glutamax, 100 U/ml Penicillin and 100 U/ml Streptomycin (humidified atmosphere, 5% CO_2, 37°C). For amplification, SH-SY5Y cells were incubated for 5 min with trypsin (0.5 mg/ml)/EDTA (0.2mg/ml), washed, and immediately re-suspended in medium. Primary cortical neurons were obtained from forebrains of 7 day-old chicken embryos (E7), as detailed by Wright and Kuhn [32]. Cortical neurons were plated and grown on poly-D-lysine-coated 6-well plates (5 million cells per well) in DMEM, 1% Glutamax, 10% FBS, and 1% N3 supplement (humidified atmosphere, 5% CO_2, 37°C) according to Bottenstein and Sato [33].

Dorsal Root Ganglia Neurite Outgrowth Assay

Dorsal root ganglia (DRG) were harvested from 9 day-old chick embryos and plated in 24-well falcon dishes pre-coated with poly-D-lysine (50 µg per cm^2) and laminin (2 µg per cm^2). Ganglia were maintained for 36 hours in DMEM, 1% Glutamax, 10% FBS, and 1% N3 supplement (humidified atmosphere, 5% CO_2, 37°C) according to Bottenstein and Sato [33]. After a pre-incubation of ganglia for 60 min with 10 µM GW4869, 10 µM diphenylene iodonium (DPI), 10 µM dimethylsphingosine (DMS), or 5 mM N-acetyl-L-cysteine (NAC), 100 ng/ml TNFα was acutely added to the medium for

15 min, and ganglia were fixed in 10% glutaraldehyde solution. Six neurites, from four separately treated ganglia, were counted for each condition using Metamorph imaging software.

Sphingomyelinase Assay

Subconfluent cultures of SH-SY5Y cells or cortical neurons (5 million cells per well) were treated, harvested in cold PBS, and sonicated. Quantitative measurement of Mg^{2+}-neutral sphingomyelinase (nSMase) activity was performed in cell lysates containing equal amounts of total protein (BCA assay) and using an enzyme coupled Amplex Red fluorescence assay kit. Briefly, Mg^{2+}-nSMase activity in samples generates ceramide and phosphocholine. Next, choline is liberated by alkaline phosphatase and then converted to betaine and peroxide by choline oxidase. In the last step, horseradish peroxidase reacts with Amplex Red and peroxide to form the highly fluorescent product resorufin measured at 590 nm using a Beckman Coulter Multimode DTX 880 microplate reader.

Sphingosine Kinase-1 Assay

Cortical neurons (5 million cells per well) were pre-incubated for 60 min with 10 µM DMS, 100 ng/ml TNFα, or vehicle, and 20% serum was acutely added to the medium for 60 min, and cortical neurons were scraped into PBS and sonicated. Samples containing equal amounts of total protein (BCA assay) were incubated for 60 min with 50 µM D-*erythro*-sphingosine, 1 mM $CaCl_2$, 4 mg/ml BSA, 2% Triton X-100, 1% PIC, and 1 mM Na_3VO_4 (150 µL total reaction volume). Reactions were terminated with an equal volume of chloroform, and sphingosine-1-phosphate was extracted by basic-pH chloroform:methanol extraction. Sphingosine-1-phosphate was derivatized with NDA (one volume sample, one volume 1 mM NDA in methanol, one volume 1 mM NaCN in sodium tetraborate buffer pH 10.3), and separated by silica thin layer chromatography (chloroform/acetone/methanol/acetic acid/water) (10/4/3/2/1). NDA-labeled sphingosine-

1-phosphate was observed and quantified using a GE Healthcare Typhoon Imager with ImageQuant software (United Kingdom).

Quantification of Reactive Oxygen Species Production

Increases in ROS were detected with dihydro-dichlorofluorescein diacetate (H_2DCFDA), an oxidation-sensitive fluorescence indicator. Upon uptake by cells, H_2DCFDA is de-acetylated to dihydro-dichlorofluorescein and increases in fluorescence upon oxidation by H_2O_2 to dichlorofluorescein (DCF). SH-SY5Y cells or E7 cortical neurons were grown in 96-well tissue culture dishes (Falcon, poly-D-lysine coated for cortical neurons, 100,000 cells per well, 48 h) in their respective medium. Cultures were incubated for 1 h with 50 µM H_2DCFDA in the presence or absence of pharmacological inhibitors or oxygen radical scavenging enzymes. Following a medium exchange, neuronal cells were exposed to TNFα (100 ng/ml, 15 min), C2-ceramide (10 µM, 30 min), N-oleoylethanolamine (NOE, 10 µM, 2 h), or palmitic acid (250 µM, 4 h), washed with 1X PBS, and lysed in 2 M Tris-HCl pH 8.0, 2% SDS, 10 mM Na_3VO_4. DCF-fluorescence was quantified (100 µl cell lysate) using a Beckman Coulter Multimode DTX 880 microplate reader (495 nm excitation filter, 525 emission filter). All DCF-fluorescence data were normalized to the average DCF-fluorescence under control conditions (relative DCF-fluorescence values).

Plasma Membrane Translocation of p67^{phox}

Plasma membrane proteins were prepared by biotinylation and streptavidin-affinity chromatography as described by Li and Shah with minor modifications [34]. SH-SY5Y neuroblastoma cells were grown in 6-well plates (5 million cells per well) for 48 h. Following incubation with GW4869 (10 µM, 60 min), L-cycloserine (5 mM, 60 min), or vehicle, cultures were treated with TNFα (100 ng/ml, 15 min), or palmitic acid (250 µM, 4 h). After washing with HBSS-CM (1X HBSS, 0.1 g/l $CaCl_2$, 0.1 g/l $MgCl_2$, pH 7.5), cultures were incubated with 0.5 mg/ml Sulfo-NHS-Biotin (prepared in 20 mM HEPES, HBSS-CM, pH 8.0) for 40 min on ice, and excess Sulfo-NHS-Biotin was neutralized with

50 mM glycine (prepared in HBSS-CM) on ice for 15 min. Cells were scraped into HBSS-CM, centrifuged (200 x g_{max}, 2 min), re-suspended in 500 μL loading buffer (20 mM HEPES pH 7.5, HBSS, 1% Triton X-100, 0.2 mg/ml saponin, 1% PIC), and sonicated. Streptavidin-agarose beads (25 μL) were added to the cell lysates (2 h, 4°C). Beads were collected (2,500 x g_{max}, 2 min), re-suspended in 150 μL of loading buffer, and heated (5 min, boiling water bath). Supernatants were obtained by centrifugation (2,500 x g_{max}, 2 min), and total cellular protein content was determined (BCA protein assay).

Derivatization of Carbonylated Sphingosine Kinase-1

SH-SY5Y cells were treated for 60 min with TNFα (100 ng/ml) or Aβ$^{1-42}$ (5 μM) ± 60 min pre-treatment with GW4869 (10 μM), DPI (10 μM), or NAC (5 mM), and lysed (2 M Tris-Cl pH 8.0, 2% SDS, 1 mM Na$_3$VO$_4$), and centrifuged (3,000 x g_{max}, 4°C, 20 min). Lysate supernatants (100 μl) were incubated with 1 μg normal goat serum (45 min, 25°C, agitated). After removing normal IgG with protein A/G agarose beads (20 μl), cleared lysates (100 μl) were first incubated with polyclonal goat anti-mouse SphK1 primary antibodies (1 μg, 4°C, agitated) for 2 h and then overnight with protein A/G agarose beads (20 μl, 4°C, agitated). Protein A/G beads were collected by centrifugation (200 x g_{max}, 2 min), washed three times in lysis buffer, and bound proteins were released by boiling for 5 min. SphK1 carbonylation was revealed by 2,4-dinitrophenylhydrazine (DNPH) modification according to Levine and co-workers [35]. Briefly, immunoprecipitated SphK1 samples in lysis buffer were mixed with an equal volume of 12% SDS, and further incubated with two sample volumes of 20 mM DNPH in 2M HCl (45 minutes, 25°C). SphK1 was recovered by chloroform/methanol precipitation according to Wessel and Flugge [36], and protein concentration was determined (BCA protein assay).

Western Blotting

Equal amounts of total protein (30 µg total cellular protein, or 5 µg immunoprecipitated protein, BCA protein assay) were separated by SDS-polyacrylamide (15%) gel electrophoresis (125 volts, 50 watts, 75 mA). Proteins were transferred from SDS-polyacrylamide gels onto PVDF membranes (2.5 hours, 50 volts, 50 watts, 250 mA) according to Towbin and co-workers [37]. Following transfer, membranes were blocked with 1X TBST-BSA (5 mg/ml bovine serum albumin, 50 mM Tris-HCl pH 7.4, 150 mM NaCl, 0.1% Tween-20), and probed overnight with polyclonal rabbit anti-human p67^{phox} primary antibodies (1 µg/µl in 1X TBST), polyclonal goat anti-human phospho-p40^{phox} primary antibodies (1 µg/µl in 1X TBST), polyclonal goat anti-mouse SphK1 primary antibodies (1 µg/µl in 1X TBST), monoclonal mouse anti-human β-actin primary antibodies (1 µg/µl in 1X TBST), or polyclonal rabbit anti-DNP primary antibodies (1 µg/µl in 1X TBST. Following incubation with horseradish peroxidase-conjugated secondary antibodies (0.2 µg/µl in 1X TBST, 45 min), immunoreactivity was detected by chemoluminescence and quantified using a GE Healthcare Typhoon Imager with ImageQuant software (United Kingdom).

Statistical Analysis

Analysis of variance (ANOVA) was used to determine statistically significant differences between treatments ($p<0.05$). At least three independent experiments were performed for each condition. *Post hoc* comparisons of specific treatments were performed using a Bonferroni test or a Dunette's test. All error bars represent standard error of the mean (SEM).

3.4: Results

TNFα stimulated Mg^{2+}-nSMase activity in neurons.

Recent studies in non-neuronal cells have demonstrated that the inflammatory stimulus TNFα mediates nSMase-dependent accumulation of the bioactive lipid ceramide

[15]. In our study, TNFα elicited significant Mg^{2+}-nSMase activity in human SH-SY5Y neuroblastoma cells (Fig. 3.1A). Compared to controls (1.00 ± 0.10, n=4), addition of TNFα stimulated significant Mg^{2+}-nSMase activity within 15 min (100 ng/ml TNFα, 1.71 ± 0.15, *$p<0.05$, n=4, and 200 ng/ml TNFα, 1.52 ± 0.04, *$p<0.05$, n=4, respectively), a response completely blocked by 60 min pretreatment with 10 μM of the Mg^{2+}-nSMase-specific inhibitor GW4869 (100 ng/ml TNFα, 0.48 ± 0.03, n=4, and 200 ng/ml TNFα, 0.45 ± 0.03, n=4, respectively). Notably, the presence of GW4869 also significantly reduced basal Mg^{2+}-nSMase activity in SH-SY5Y cells (0.45 ± 0.02, **$p<0.05$, n=4) compared to control (1.00 ± 0.10, n=4), suggesting a role for Mg^{2+}-nSMase in neuronal homeostasis.

TNFα-stimulated Mg^{2+}-nSMase activity was corroborated in primary cortical neurons isolated from 7 day-old (E7) chick embryos (Fig. 3.1B). 100 ng/ml TNFα significantly increased Mg^{2+}-nSMase activity (1.26 ± 0.05, *$p<0.05$, n=3) measured 15 min after exposure compared to control (1.00 ± 0.06, n=3). Pre-treatment of E7 cortical neurons with 10 μM GW4869 (60 min) completely blocked Mg^{2+}-nSMase activity (0.91 ± 0.03, n=3). These findings demonstrated that Mg^{2+}-nSMase activity increased in both human SH-SY5Y neuroblastoma cells as well as primary E7 cortical neurons in response to the pro-inflammatory cytokine TNFα.
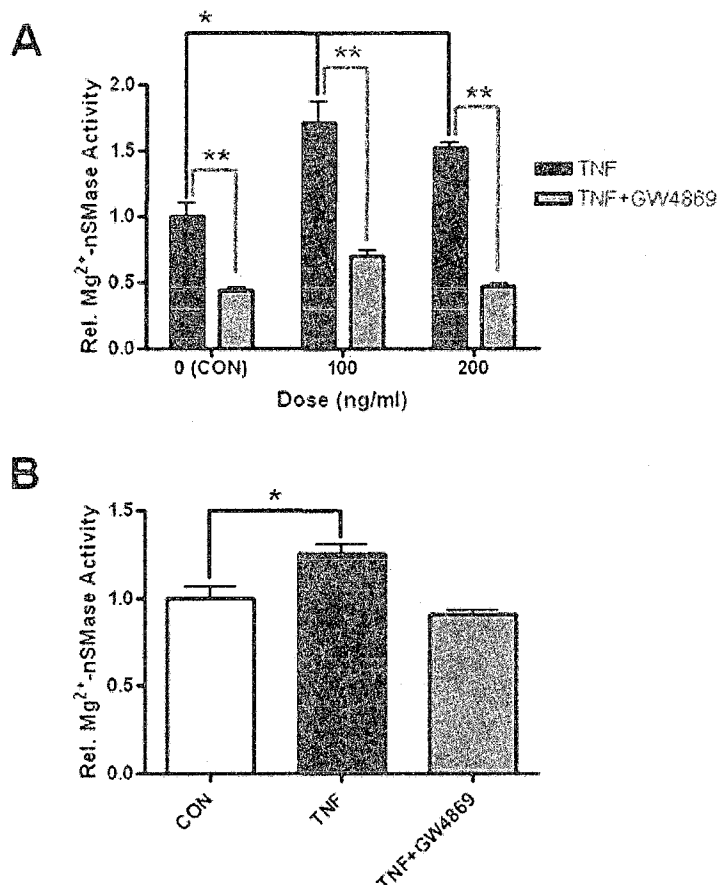
Fig. 3.1. TNFα stimulates Mg^{2+}neutral sphingomyelinase activity in neuronal cells. Cultures of SH-SY5Y neuroblastoma cells or E7 cortical neurons were exposed to TNFα in the presence or absence of 10 μM GW4869. Mg^{2+}neutral sphingomyelinase (Mg^{2+}nSMase) activity was quantified in whole cell lysates using an enzyme-coupled Amplex Red fluorescence assay. (A) Incubation of SH-SY5Y neuroblastoma cells with 100 or 200 ng/ml TNFα for 15 min resulted in an increase in Mg^{2+}nSMase activity (*$p<0.05$) compared to untreated cells, which was significantly abolished by pre-treated with the Mg^{2+}nSMase inhibitor GW4869 (**$p<0.05$). (B) In E7 cortical neurons, 100 ng/ml TNFα stimulated Mg^{2+}nSMase activity (*$p<0.05$) compared to control or cultures treated with GW4869. Data represent SEM of at least three independent experiments.

$A\beta^{1-42}$ stimulated Mg^{2+}-nSMase activity in neurons.

Reports have indicated a pathological role for SMases in the progression of Alzheimer's disease, and a recent study by Grimm and co-workers demonstrated that $A\beta^{1-42}$ could interact directly with a recombinant nSMase in a cell-free system [38]. In line with these data, we found that exposure of human SH-SY5Y neuroblastoma cells for

10 min to 5 μM $A\beta^{1-42}$ dramatically stimulated Mg^{2+}-nSMase activity (1.81 ± 0.25,

*p<0.05, n=3) compared to control (1.00 ± 0.03, n=3), which was suppressed by 60 min

pre-treatment with 10 μM GW4869 (0.51 ± 0.03, n=3) (Fig. 3.2). Taken together, both

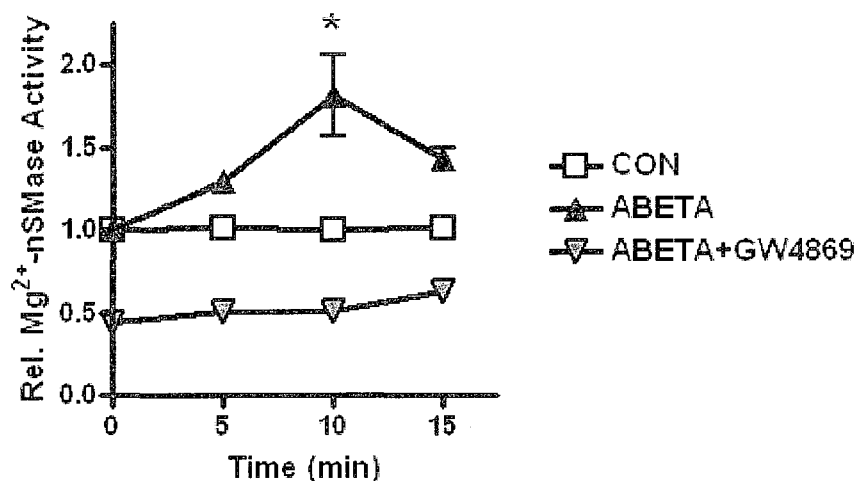$TNF\alpha$ and $A\beta^{1-42}$ are able stimulate Mg^{2+}-nSMase activity in neuronal cells.

Fig. 3.2. $A\beta^{1-42}$ stimulates Mg^{2+}neutral sphingomyelinase activity in SH-SY5Y cells. SH-SY5Y neuroblastoma cells were exposed to 5 μM $A\beta^{1-42}$ and Mg^{2+}nSMase activity was quantified as a function of time using an enzyme-coupled Amplex Red fluorescence assay. $A\beta^{1-42}$ elicited a significant increase in Mg^{2+}nSMase activity within 10 min after acute addition (*p<0.05) compared to control that was blocked by 10 μM GW4869 (Mg^{2+}nSMase inhibitor). Data represent SEM of at least three independent experiments.

Neuronal NOX activity mediates TNFα-stimulated ROS accumulation.

Activation of NOX results in the generation of superoxide anions, which are

rapidly dismutated to hydrogen peroxide by superoxide dismutase (SOD), or converted to

other reactants such as hydroxyl radicals, or peroxynitrite. We measured intracellular

ROS accumulation utilizing the redox-sensitive indicator DCF. In cultures of human SH-

SY5Y neuroblastoma cells (Fig. 3.3A) or primary E7 cortical neurons (Fig. 3.3B), 100

ng/ml $TNF\alpha$ elicited, within 15 min, a significant increase in maximum DCF-

fluorescence intensity (SH-SY5Y cells: 1.24 ± 0.05, *p<0.05, n=5; cortical neurons: 2.23

± 0.05, *p<0.05, n=14) compared to control (SH-SY5Y cells: 1.00 ± 0.03, n=12, cortical

neurons: 0.99 ± 0.02, n=21) indicative of an accumulation of intracellular ROS. Addition

of 200 units/ml of SOD to SH-SY5Y neuroblastoma cells or E7 cortical neurons concurrent with TNFα-exposure augmented ROS production measured as maximum DCF-fluorescence (SH-SY5Y cells: 1.39 ± 0.07, *p<0.05, n=3; cortical neurons: 2.98 ± 0.15, **p<0.05, n=7). This effect suggested that a superoxide-generating mechanism was stimulated by TNFα because the indicator DCF primarily measures H_2O_2, and SOD converts superoxide to H_2O_2. In stark contrast, incubation of neuronal cultures with 5000 units/ml of catalase concurrently with TNFα-exposure, negated increases in DCF-fluorescence intensity (SH-SY5Y cells: 1.02 ± 0.04, n=3; cortical neurons: 1.54 ± 0.10, n=7). TNFα-dependent ROS formation was also completely blocked by a presence of 5 mM of the antioxidant NAC (SH-SY5Y cells: 0.92 ± 0.01, n=3; cortical neurons: 0.79 ± 0.05, n=7). Lastly, 60 min pre-treatment of neuronal cultures with 10 μM of the NOX inhibitor diphenylene iodonium negated TNFα-stimulated intracellular ROS formation (SH-SY5Y cells: 1.02 ± 0.04, n=8; cortical neurons: 1.16 ± 0.12, n=7), indicating the involvement of a neuronal NOX activity.
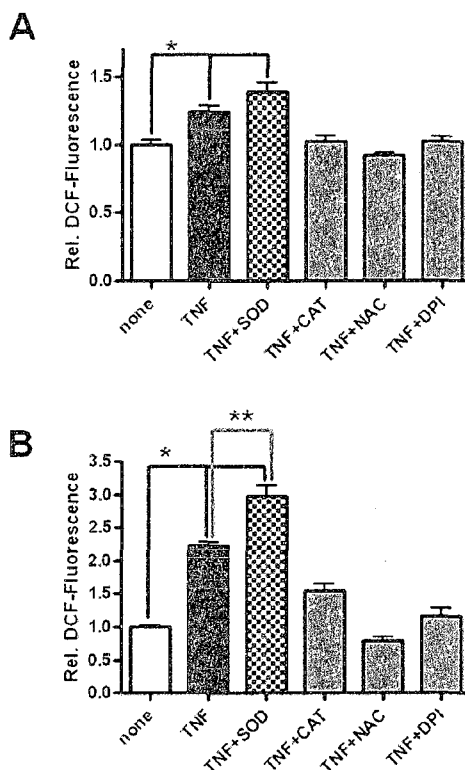
Fig. 3.3. TNFα stimulates a neuronal NOX activity increasing intracellular ROS formation. ROS formation in neuronal cells was quantified employing the H_2O_2-sensitive fluorescence indicator dihydrodichlorofluorescein. Cultures of SH-SY5Y neuroblastoma cells (A) or E7 cortical neurons (B) were exposed to 100 ng/ml TNFα for 15 min, maximum DCF fluorescence was quantified in whole cell lysates and normalized to control. TNFα stimulated a robust formation of ROS (*p<0.05) compared to control SH-SY5Y cultures or E7 cortical cultures. ROS formation in response to TNFα was negated by a pre-incubation of cultures with 10 μM diphenylene iodonium (DPI, a NOX inhibitor), 5 mM N-acetyl-L-cysteine (NAC, an antioxidant), or 5000 U/ml exogenous catalase (CAT). Addition of exogenous superoxide dismutase (SOD, 200 U/ml) was ineffective, or even significantly augmented TNFα–stimulated ROS formation (**p<0.05). This effect suggested a superoxide-generating mechanism as DCF responds primarily to H_2O_2. Data represent SEM of at least three independent experiments.

Ceramide mediates TNFα-stimulated neuronal ROS accumulation.

Since TNFα stimulated ceramide accumulation via Mg^{2+}-nSMase activity (Fig. 3.1), as well as ROS accumulation (Fig. 3.3), we tested whether ceramide is directly involved in the generation of ROS. In cultures of human SH-SY5Y neuroblastoma cells (Fig. 3.4A) or primary E7 cortical neurons (Fig. 3.4B), 100 ng/ml TNFα elicited, within 15 min, significant increases in DCF-fluorescence intensity (SH-SY5Y cells: 1.24 ± 0.05,

*p<0.05, n=5; cortical neurons: 2.23 ± 0.05, *p<0.05, n=14) compared to control cells (SH-SY5Y cells: 1.00 ± 0.03, n=12; cortical neurons: 0.99 ± 0.02, n=21), which was negated by 60 min pre-treatment of neuronal cultures with 10 μM of the Mg^{2+}-nSMase inhibitor GW4869 (SH-SY5Y cells: 1.07 ± 0.01, n=4; cortical neurons: 1.21 ± 0.07, n=7). This finding suggested that Mg^{2+}-nSMase-generated ceramide is involved in the formation of ROS.

Incubation of neuronal cells for 30 min with 10 μM C2-ceramide, a short-chain ceramide analog, resulted in significant increases in DCF-fluorescence intensity (SH-SY5Y cells: 1.23 ± 0.03, *p<0.05, n=4; cortical neurons: 1.54 ± 0.04, *p<0.05, n=7). Additionally, stimulation of *de novo* ceramide synthesis in human SH-SY5Y neuroblastoma cells (250 μM palmitate, 4 h) indeed caused a significant increase in DCF-fluorescence intensity suggesting an increase in ROS (1.26 ± 0.06, *p<0.05, n=6) as opposed to control (1.00 ± 0.03, n=12). Inhibition of *de novo* ceramide synthesis in SH-SY5Y cells by a pre-treatment (60 min) with 5 mM L-cycloserine (a serine palmitoyltransferase inhibitor), or 10 μM fumonisin B_1, (a dihydroceramide synthase inhibitor) both completely blocked palmitate-stimulated increases in DCF-fluorescence (1.03 ± 0.03, n=6, or 0.98 ± 0.03, n=6, respectively).

In E7 cortical neurons, ceramide metabolism was further evaluated by treating neurons for 2 h with 10 μM of *N*-oleoylethanolamine (NOE), an acid ceramidase inhibitor, thus blocking ceramide-degradation. Monitoring *de* novo ceramide synthesis was impractical in E7 cortical neurons due to their extremely high sensitivity. A presence of NOE significantly increased DCF-fluorescence intensity in cortical neurons indicative of an increase in intracellular ROS production (1.64 ± 0.04, *p<0.05, n=7). Taken together, these results provided evidence that ceramide is actively involved in the regulation of intracellular ROS production. Combined, these results further demonstrated that TNFα-stimulated ROS production was due in part to TNFα-stimulation of a neuronal NOX activity.
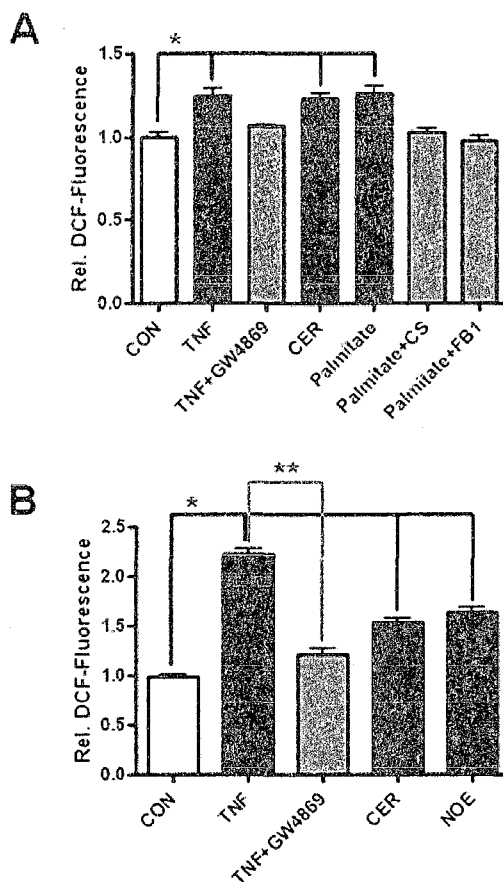
Fig. 3.4. Ceramide stimulates intracellular ROS formation. ROS formation in neuronal cells was quantified employing the H_2O_2-sensitive fluorescence indicator dihydrodichlorofluorescein. Maximum DCF fluorescence was quantified in whole cell lysates and normalized to controls. (A) In SH-SY5Y cells, TNFα (100 ng/ml, 15 min) stimulated a robust formation of ROS (*p<0.05) compared to control cultures. Inhibiting ceramide production through sphingomyelin hydrolysis with 10 µM GW4869 (Mg^{2+}-nSMase inhibitor) negated TNFα-mediated ROS formation. In contrast, 30 min treatment with 10 µM C2-ceramide (CER) significantly increased ROS formation (*p<0.05) in the absence of TNFα. Alternatively, stimulation of *de novo* ceramide synthesis with palmitate (250 µM, 4 h) also significantly increased ROS formation (*p<0.05). Palmitate effects were mitigated with 5 mM L-cycloserine (CS; serine palmitoyltransferase inhibitor), or 10 µM fumonisin B_1 (FB1; dihydroceramide synthase inhibitor). (B) In E7 cortical neurons, TNFα (100 ng/ml, 15 min) stimulated a robust formation of ROS (*p<0.05) compared to controls. Inhibiting ceramide production through sphingomyelin hydrolysis with 10 µM GW4869 significantly negated TNFα-mediated ROS formation (**p<0.05). In the absence of TNFα, 10 µM CER (30 min) exposure to E7 cortical cultures significantly increased ROS formation (*p<0.05). Additionally, inducing ceramide accumulation by inhibition of acid ceramidase with 10 µM *N*-oleoylethanolamine (NOE) resulted in significantly increased ROS formation (*p<0.05). Data represent SEM of at least three independent experiments.

Ceramide mediates TNFα-stimulated neuronal NOX assembly.

NOX is a multi-subunit NADPH oxidoreductase responsible for the rapid production of superoxide, requiring proper assembly of both membrane and cytosolic subunits [18, 19]. Release of auto-inhibitory conformations of cytosolic subunits such as p40^{phox} by phosphorylation is key for NOX activation [18, 19]. In this study, we evaluated membrane assembly of the neuronal NOX subunits p40^{phox} and p67^{phox} in response to either TNFα or ceramide. Treatment of SH-SY5Y cells with 100 ng/ml TNFα for 15 min significantly increased phosphorylation of p40^{phox} (1.65 ± 0.12, *p<0.05, n=3) compared to control (1.02 ± 0.05, n=3) (Fig. 3.5A). TNFα-stimulated p40^{phox} phosphorylation was completely blocked by incubating SH-SY5Y cultures with 10 μM of the Mg^{2+}-nSMase inhibitor GW4869 (1.19 ± 0.04, n=3) prior to TNFα exposure. Likewise, we quantified the translocation of the p67^{phox} subunit to plasma membranes of SH-SY5Y neuroblastoma cells (Fig. 3.5B). We measured a significant translocation of p67^{phox} to plasma membranes (1.48 ± 0.05, *p<0.05, n=3) within 15 min after application of 100 ng/ml TNFα compared to control (1.01 ± 0.01, n=3). Similarly, p67^{phox} membrane translocation was significantly negated following a 60 min pre-treatment of SH-SY5Y neuroblastoma cells with 10 μM of GW4869 (1.20 ± 0.02, **p<0.05, n=3). These findings demonstrated that both p40^{phox} phosphorylation and p67^{phox} membrane translocation critically depended on the generation of ceramide through Mg^{2+}-nSMase activity.

To further corroborate that ceramide is implicated in the proper assembly of NOX, we stimulated *de novo* ceramide synthesis by treating SH-SY5Y cells with palmitate (250 μM, 4 h), a precursor of endogenous ceramide synthesis. As opposed to controls (1.01 ± 0.01, n=3), palmitate did elicit a significant translocation of p67^{phox} to plasma membranes (1.34 ± 0.02, *p<0.05, n=3) that was significantly prevented by a 60 min pre-treatment with 5 mM L-cycloserine (1.07 ± 0.01, ***p<0.05, n=3), a serine palmitoyltransferase inhibitor. Taken together, these data strongly suggested that ceramide acts as a pivotal lipid-activator of NOX in response to the pro-inflammatory cytokines TNFα.
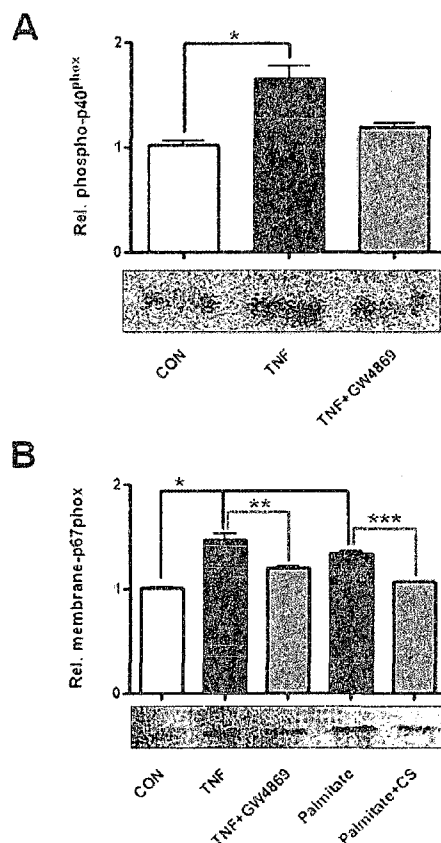
Fig. 3.5. Ceramide mediates TNFα-dependent neuronal NOX assembly. SH-SY5Y neuroblastoma cells were exposed to 100 ng/ml TNFα for 15 min following a one-hour pre-incubation with either 10 μM GW4869, which blocks ceramide generation through Mg^{2+}nSMase activity, or buffer only (control). Increases in the phosphorylation of p40^{phox} and translocation of p67^{phox} to plasma membranes were evaluated as an indication of NOX activation. (A) TNFα substantially increased phosphorylation of p40^{phox} (*p<0.05) compared to control or a presence of GW4869. (B) TNFα stimulated the translocation of p67^{phox} to plasma membranes (*p<0.05) as opposed to control (CON), or a presence of GW4869 (**p<0.05). Stimulation of *de novo* ceramide synthesis palmitate (250 μM, 4 hours) also increased p67^{phox} levels in SH-SY5Y plasma membranes (*p<0.05), which was completely negated with 5 mM L-cycloserine (***p<0.05), a serine palmitoyltransferase inhibitor. Data represent SEM of at least three independent experiments.

SphK1 activity is impeded by TNFα-stimulated ROS.

SphKs are responsible for the formation of sphingosine-1-phosphate, a pro-survival and pro-growth lipid messenger [25]. Since several studies have suggested that SphK1 is activated by TNFα in non-neuronal cells, we tested the responses of neuronal cells [25]. Important to our study, it was shown that SphK1 is stimulated by a variety of

mitogens as well as serum [25, 39]. In human SH-SY5Y neuroblastoma cells we found that addition of 20% FBS for 30 min stimulated a significant increase in SphK1 activity (1.81 $\pm$ 0.17, *p<0.05, n=3) compared to basal activity (1.00 $\pm$ 0.06, n=3) (Fig. 3.6A). Likewise, in E7 cortical neuron cultures, we found a significant increase in SphK1 activity in response to 30 min of 20% FBS (1.89 $\pm$ 0.19, *p<0.05, n=3) compared to basal activity (1.00 $\pm$ 0.03, n=3) (Fig. 3.6B). Expectedly, FBS-stimulated SphK1 activity was blocked by 60 min pre-treatment with 10 μM of the SphK1 inhibitor N',N'-dimethylsphingosine (DMS) (SH-SY5Y cells: 1.07 $\pm$ 0.06, n=3; cortical neurons: 0.80 $\pm$ 0.06, n=3). In contrast to other studies done in non-neuronal cells, 60 min exposure to 100 ng/ml TNFα alone had no measurable effects on basal SphK1 activity (SH-SY5Y cells: 1.07 $\pm$ 0.08, n=3; cortical neurons: 0.81 $\pm$ 0.01, n=3), showing that TNFα alone did not stimulate SphK1 activity in neuronal cells. However, 60 min pre-treatment with 100 ng/ml TNFα prior to 20% FBS stimulation (30 min) completely blunted increases in SphK1 activity (SH-SY5Y cells: 1.08 $\pm$ 0.02, n=3; cortical neurons: 0.95 $\pm$ 0.07, n=3) above basal levels. FBS-stimulated SphK1 activity impeded by TNFα was restored by 60 min pre-treatment with 10 μM of the Mg^{2+}nSMase inhibitor GW4869 (SH-SY5Y cells: 1.60 $\pm$ 0.07, *p<0.05, n=3; cortical neurons: 1.44 $\pm$ 0.02, *p<0.05, n=3), 10 μM of the NOX inhibitor DPI (SH-SY5Y cells: 1.93 $\pm$ 0.13, *p<0.05, n=3; cortical neurons: 1.45 $\pm$ 0.03, *p<0.05, n=3), or 5 mM of the antioxidant NAC (SH-SY5Y cells: 1.72 $\pm$ 0.10, *p<0.05, n=3; cortical neurons: 1.48 $\pm$ 0.04, *p<0.05, n=3). These data showed that TNFα-mediated loss of serum-stimulated SphK1 activity was due to Mg^{2+}nSMase- and NOX-regulated mechanisms in neuronal cells.
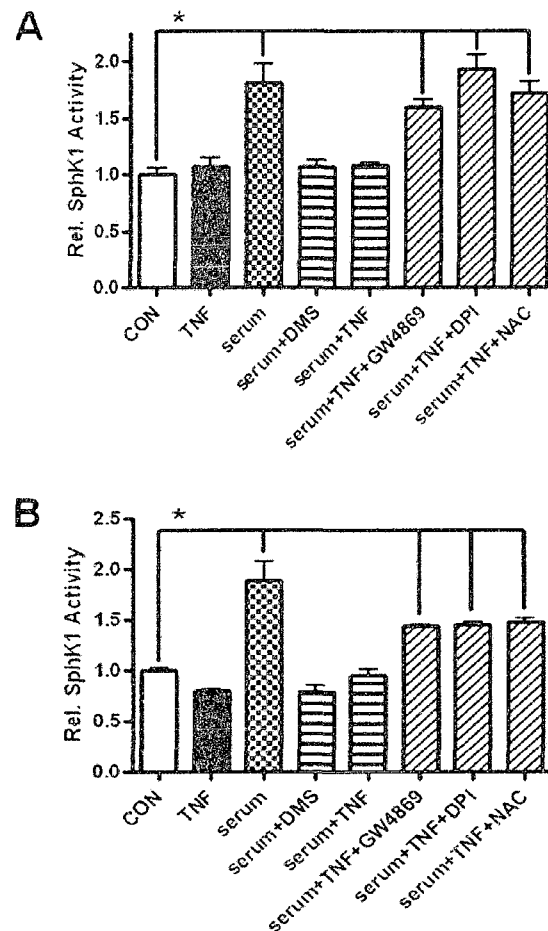
Fig. 3.6. TNFα-stimulated ROS inhibit neuronal sphingosine kinase-1 activity. Sphingosine kinase-1 (SphK1) activity was greatly stimulated in SH-SY5Y cells (A) or E7 cortical neuron cultures (B) by an addition of 20% fetal bovine serum for 60 min (*p<0.05), but not by TNFα alone (100 ng/ml). In both SH-SY5Y cells and E7 cortical neurons, serum-stimulated SphK1 activity was blocked with a 60 min pre-treatment with 10 μM of the SphK1 inhibitor N',N'-dimethylsphingosine (DMS), as well as by TNFα exposure (100 ng/ml). TNFα-abolished serum-stimulated SphK1 activity was restored by 60 min pre-treatment with 10 μM GW4869 (Mg^{2+}nSMase inhibitor), 10 μM DPI (NOX inhibitor), or 5 mM NAC (antioxidant). Data represent SEM of at least three independent experiments.

Inhibition of SphK1 by oxidation in neurons exposed to TNFα or Aβ$^{1-42}$.

A recent study in human SH-SY5Y neuroblastoma cells revealed that Aβ$^{1-42}$ also inhibited SphK1 activity, and that this inhibition was negated by a presence of the antioxidant NAC [40]. Thus, we assayed SphK1 for TNFα-dependent and Aβ$^{1-42}$-

dependent carbonylation, an irreversible oxidative modification detrimental to protein stability and function (Fig. 3.7). Treatment of human SH-SY5Y neuroblastoma cells with 100 ng/ml TNFα (60 min) resulted in a substantial increase in carbonylation of SphK1 (27.91 $\pm$ 1.79, *p<0.05, n=5) compared to control (1.00 $\pm$ 0.13, n=5). Likewise, treatment of SH-SY5Y cells with 5 µM Aβ$^{1-42}$ (60 min) resulted in a dramatic increase in carbonylation of SphK1 (75.49 $\pm$ 13.23, *p<0.05, n=5) compared to control. TNFα- and Aβ$^{1-42}$-stimulated SphK1 carbonylation was completely abolished by 60 min pre-treatment with 10 µM of the Mg^{2+}nSMase inhibitor GW4869 (TNFα+GW4869: 0.83 $\pm$ 0.22, n=5; Aβ$^{1-42}$+GW4869: 3.06 $\pm$ 0.99, n=5), 10 µM of the NOX inhibitor DPI (TNFα+DPI: 1.00 $\pm$ 0.25, n=5; Aβ$^{1-42}$+DPI: 10.91 $\pm$ 5.70, n=5), or 5 mM of the antioxidant NAC (TNFα+NAC: 2.00 $\pm$ 1.06, n=5; Aβ$^{1-42}$+NAC: 3.75 $\pm$ 1.57, n=5). Taken together, TNFα- and Aβ$^{1-42}$-mediated loss of SphK1 activity, and therefore loss of a critical survival signal in neuronal cells, was due to irreversible Mg^{2+}nSMase- and NOX-dependent oxidative modification of SphK1.
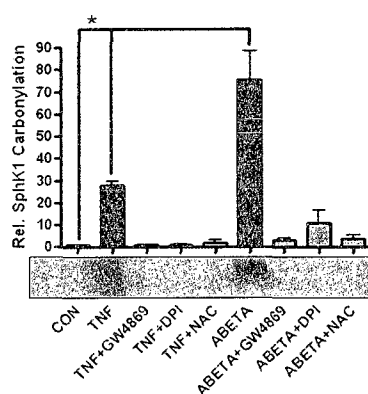

Fig. 3.7. TNFα- and Aβ$^{1-42}$-stimulated ROS oxidize neuronal sphingosine kinase-1. (A) Sphingosine kinase-1 (SphK1) was immunoprecipitated from lysates of SH-SY5Y cultures treated with TNFα (100 ng/ml, 1 h) or Aβ$^{1-42}$ (5 µM) with or without a pre-incubation with 10 µM GW4869 (Mg^{2+}nSMase inhibitor), 10 µM DPI (NOX inhibitor), or 5 mM NAC (antioxidant). SphK1 carbonyls were derivatized with 2,4-dinitrophenylhydrazine (DNPH), subjected to SDS gel electrophoresis followed by western blotting, and DNP immunoreactivity quantified. TNFα or Aβ$^{1-42}$ exposure caused a significant increase in SphK1 carbonylation (*p<0.05). In contrast, inhibiting Mg^{2+}nSMase , NOX, or simply using an antioxidant substantially blocked oxidative damage to SphK1. Data represent SEM of at least three independent experiments.

TNFα inhibited neurite outgrowth.

Neurite outgrowth is a functional process important to development of the CNS, and to neuronal connectivity. Neurite outgrowth is dependent on pro-growth signaling and a dynamic actin cytoskeleton [41, 42]. Importantly, a recent study in phagocytic cells revealed that actin co-localized with functional SphK1 suggesting a causal link between the production of S1P and the actin cytoskeleton [43]. In this study we evaluated the impact of TNFα-induced oxidative stress, inhibitory to SphK1, on neurite outgrowth (Fig. 3.8). DRG from 9 day-old chick embryos were plated on laminin and maintained for 36 hours to allow vigorous neurite outgrowth in a radial fashion away from the ganglia body. DRG cultures were incubated with inhibitors for 1 h prior to acute addition of 100 ng/ml TNFα for 15 min. TNFα caused a rapid retraction of outgrown neurites (67% $\pm$ 3%, *$p < 0.05$, n=24) compared to neurites of control DRG (100% $\pm$ 4%, n=24). Preventing ceramide accumulation by inhibition of Mg^{2+}-nSMase (10 μM GW4869) prior to TNFα-exposure protected neurite outgrowth (95% $\pm$ 3%, n=24). Likewise, inhibition of NOX activity (10 μM DPI) or scavenging of ROS with 5 mM NAC rescued neurite outgrowth in the presence of TNFα (DPI: 107% $\pm$ 3%, n=24; NAC: 109% $\pm$ 2%, n=24). In contrast inhibition of SphK1 activity (10 μM DMS) had no effect on TNFα-stimulated neurite retraction, yielding neurites of significantly reduced neurite length (64% $\pm$ 3%, *$p < 0.05$, n=24) as compared to control. This nearly identical response to what was measured in the presence of TNFα-alone indicates again that in neurons SphK1 is not a downstream effector of TNFα. Altogether these findings suggest that SphK1 plays an important role in neurite outgrowth, a process important to neurodevelopment and synaptic plasticity, and that TNFα impedes this process via oxidation of SphK1.
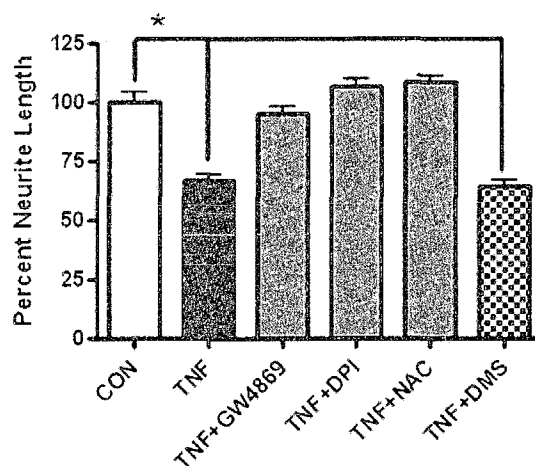
Fig. 3.8. TNFα-dependent inhibition of neurite outgrowth is mediated by ceramide and ROS. E9 dorsal root ganglia (DRG) were plated on laminin (2 μg/cm^2) and maintained for 36 hours to allow radial neurite outgrowth. After pre-incubation with pharmacological inhibitors, DRG cultures were treated with TNFα (100 ng/ml, 15 min), fixed with 10% glutaraldehyde, and neurite length measured using Metamorph Imaging software. TNFα significantly impeded neurite outgrowth (*p<0.05) compared to control. Neurite outgrowth in the presence of TNFα was protected when blocking ceramide generation by sphingomyelin hydrolysis through Mg^{2+}nSMase (10 μM GW4869), preventing NOX activity (10 μM DPI), or by scavenging ROS formation (10 μM NAC). Inhibiting SphK1 activity with 10 μM DMS did not protect neurite outgrowth from TNFα. Data represent SEM of at least three independent experiments.

3.5: Discussion

The pro-inflammatory cytokine TNFα, and soluble amyloid fragment Aβ$^{1-42}$, are severely detrimental to the viability of neuronal cells, due in part to their roles as a mediators of the production of damaging ROS. Prolonged inflammation, and therefore prolonged oxidative stress, is strongly linked to neurodegeneration associated with acute CNS injuries, chronic CNS disorders, and psychiatric conditions [1]. In particular, the oxidation of cellular targets including lipids, DNA, and protein ultimately drives these pathologies to a point where survival and regeneration of the CNS becomes impossible. In our study we demonstrated that TNFα or Aβ$^{1-42}$ stimulated Mg^{2+}nSMase activity in neuronal cells. We further demonstrated that ceramide, the product of Mg^{2+}nSMase

activity, induced production of ROS via a neuronal NOX activity. It is very intriguing that ceramide and S1P, metabolically linked sphingolipids, are diametrically opposed regulators of cell survival [15, 17, 25]. On this notion we investigated and determined that in neurons, SphK1 was a target of ceramide-mediated NOX-dependent oxidation; an event shifting sphingolipid metabolism towards ceramide production, and subsequently impeding neuron survival and regeneration.

In response to injury, pathogens, and a variety of toxins including chemical compounds, heavy metals, prions, and others peptides, the microglia of the CNS elicit a dramatic response characterized by the release of ROS and a variety inflammatory mediators including TNFα [1, 2, 7]. While TNFα exerts pleiotropic effects in the CNS, persistent high levels are highly neurotoxic. TNFα, as an inflammatory cytokine, elicits numerous cellular stress responses itself, including oxidative stress [1, 2, 7]. TNFα type I receptors are bound to the adaptor protein FAN, allowing rapid activation of Mg^{2+}-nSMase in response to stimuli. In our study, we evaluated the effects of TNFα on human SH-SY5Y neuroblastoma cells and primary chick (E7) cortical neurons. We determined that the Mg^{2+}-nSMase was significantly stimulated in SH-SY5Y cells and cortical neurons in response to treatment with TNFα (Fig. 3.1). Mg^{2+}-nSMase activity generates the bioactive lipid ceramide; a mediator of cellular stress, and in our study, a second messenger transducing TNFα-signaling to more detrimental responses in neuronal cells.

In Alzheimer's disease, $A\beta^{1-42}$ is generated by improper proteolytic cleavage of the amyloid precursor protein [38]. $A\beta^{1-42}$ is highly neurotoxic and acts in much the same way as a cytokine, by eliciting cellular stress responses associated with neuroinflammation such as oxidative stress. Additionally $A\beta^{1-42}$ has been shown to induce the expression, production, and release of pro-inflammatory cytokines from microglia and astrocytes, which previously was thought to be the primary mechanism that $A\beta^{1-42}$ induces neuroinflammatory responses [1, 2, 4, 7]. In our study, we determined that the Mg^{2+}-nSMase was significantly stimulated in SH-SY5Y cells in response to treatment with $A\beta^{1-42}$ (Fig. 3.2). The rapid activation of the Mg^{2+}-nSMase by $A\beta^{1-42}$ may indicate that a direct interaction between $A\beta^{1-42}$ and the Mg^{2+}-nSMase occurs as suggested by cell-

free studies done by Grimm and coworkers [38]. Furthermore, these results demonstrated that $A\beta^{1-42}$ alone can stimulate a neuroinflammatory pathway in neuronal cells.

Neuroinflammation is characterized by responses of microglia and astrocytes in the CNS during acute injuries, chronic disorders, and psychiatric conditions [1, 2, 7]. A key part of the inflammatory response is the release of damaging ROS, however the characterization of ROS release by neurons is not well established. In our study we utilized the H_2O_2-sensitive dye DCF to study intracellular ROS in neuronal cells. We found that human SH-SY5Y neuroblastoma cells and primary chick (E7) cortical neurons responded to TNFα with significant increases in DCF-fluorescence indicative of ROS production (Fig. 3.3). We further characterized this ROS production utilizing SOD, which dismutates superoxide to H_2O_2, and catalase, which neutralizes H_2O_2 to water. By adding exogenous SOD to accelerate the conversion of superoxide to the DCF-detectable H_2O_2, we demonstrated that TNFα-stimulated ROS were derived from a superoxide-generating source. Further investigation with the NOX inhibitor DPI allowed us to attribute this TNFα-stimulated superoxide generation to a neuronal NOX activity.

Previous work by other labs has linked ceramide to the onset of oxidative stress in non-neuronal cells [14, 15]. Since we linked TNFα responses in neuronal cells to the stimulation of the Mg^{2+}-nSMase, it became important to evaluate the role of ceramide in the regulation of ROS generation in neurons (Fig. 3.4). In both SH-SY5Y cells and cortical neurons, we employed the Mg^{2+}-nSMase-specific inhibitor GW4869 to block TNFα-stimulated ROS production indicating a role for ceramide as a mediator of ROS generation in neuronal cells. To further evaluate ceramide, we manipulated its levels in a variety of ways. In both SH-SY5Y cells and cortical neurons, exogenous addition of the short-chain C2 analog of ceramide stimulated ROS production. Alternatively we induced *de novo* ceramide synthesis in SH-SY5Y cells with the saturated fat palmitate, and noted a dramatic increase in ROS production. Palmitate-stimulated ROS production was completely blocked by inhibitors of serine palmitoyltransferase and (dihydro)ceramide synthase, two enzymes critical to *de novo* ceramide synthesis. In primary cortical neurons, palmitate-based studies were impractical due to the high sensitivity of the

primary cultures. Consequentially we evaluated ceramide in primary cortical neurons by preventing acid ceramidase activity, which degrades ceramide to sphingosine. Prevention of ceramide degradation also resulted in dramatic ROS production. Altogether these results clearly showed that ceramide is a mediator of ROS production in neuronal cells.

Since we demonstrated that TNFα and $A\beta^{1-42}$ stimulated ceramide-generating Mg^{2+}nSMase activity, and that TNFα-stimulated ROS were derived from a neuronal NOX, we speculated that the oxidase itself may be regulated by ceramide. NOX is a highly regulated multi-subunit complex that generates superoxide anion [18]. NOX2 (the phagocytic oxidase-like isoform) requires at least two membrane-bound subunits, gp91^{phox} and p22^{phox} (phox for phagocytic-oxidase-like), and at least three cytosolic subunits p67^{phox}, p47^{phox}, and p40^{phox} [18, 22]. NOX2 activity relies on phosphorylation of cytosolic subunits followed by their translocation to and assembly with the membrane-bound subunits. The role of ceramide or ceramide metabolites may be to stimulate NOX2 directly, stimulate known regulators of NOX2 (protein kinases; Rac GTPase), or to stimulate the production of the lipid arachidonic acid. The ceramide/ceramide-1-phosphate-binding protein cPLA$_2$ produces arachidonic acid [44, 45], while ceramide has been shown to interact with and activate PKCζ [46]: a kinase capable of regulating the multiple targets including the stress activated protein kinase JNK (c-jun N-terminal kinase) [47]. In our study we evaluated the role of ceramide in the assembly of NOX2 in human SH-SY5Y neuroblastoma cells (Fig. 3.5). We demonstrated that the Mg^{2+}nSMase inhibitor GW4869 blocked TNFα-stimulated phosphorylation of p40^{phox}. Further evaluation of membrane translocation of p67^{phox} revealed a similar Mg^{2+}nSMase-dependent response to TNFα. We expanded our study of ceramide-mediated NOX2 assembly by showing that palmitate-stimulated p67^{phox} membrane translocation was blocked by preventing *de novo* ceramide synthesis. Combined these results showed that TNFα stimulated ROS generation through activation of Mg^{2+}nSMase-dependent ceramide production, and that ceramide mediated the activation of a neuronal NOX2. Likewise other mechanisms that stimulate ceramide accumulation, through SMase activity or *de novo* synthesis, potentially could stimulate NOX2 activity.

Lastly, our research investigated a recent report that SphK1 was inhibited through a redox-mechanism. Gomez-Brouchet and co-workers reported that $A\beta^{1-42}$ inhibited SphK1 activity in SH-SY5Y neuroblastoma cells, and that inhibition could be prevented by the antioxidant NAC [40]. Likewise, we were able to show that TNFα prevented serum-stimulated SphK1 activity in both SH-SY5Y neuroblastoma cells and primary E7 cortical neurons (Fig. 3.6). We showed that this inhibition of SphK1 activity was directly attributed to Mg^{2+}nSMase and NOX activity. We further demonstrated for the first time, by monitoring protein carbonylation, that SphK1 is a target of oxidative modification (Fig. 3.7). Carbonylation is a specific, prevalent, and irreversible oxidative modification that can result in dramatic protein conformational changes, protein oligomerization, as well as protein loss of function [48]. We showed that both TNFα and $A\beta^{1-42}$ caused specific oxidation of SphK1. By utilizing pharmacological inhibitors, we further showed that Mg^{2+}nSMase and NOX activity in SH-SY5Y neuroblastoma cells was responsible for TNFα- and $A\beta^{1-42}$-induced oxidation of SphK1. Lastly, we showed that TNFα caused retraction of outgrown neurites from DRGs (Fig. 3.8). Neurite outgrowth is an important neurodevelopment mechanism, as well as a mechanism important to dendritic spine formation and synaptic plasticity. Therefore neurite outgrowth from DRGs can be used as a measure of neuronal development and function. We found that TNFα-stimulated neurite retraction was prevented by an antioxidant, inhibition of NOX, or inhibition of the Mg^{2+}nSMase. This demonstrated the role of TNFα-mediated, Mg^{2+}nSMase-dependent stimulation of a neuronal NOX2 that subsequently caused oxidative damage to critical neuronal components, including SphK1.

SphK1 is an important component of neurons not only due to its role in regulating survival, but also in roles important to synaptic plasticity, development, and potentially to regeneration. S1P has been shown to stimulate neurite outgrowth, a process important to both the developing and adult CNS [29]. Actin, another important effector of neurite outgrowth, has been recently reported to interact with functional SphK1, suggesting a link between actin cytoskeletal dynamics and S1P production [43]. Interestingly we have also found that actin is a target of NOX2-mediated oxidation in neurons (data to be

published elsewhere). Additionally, other recent studies have implicated S1P as a modulator of neuronal function. Alemany and co-workers showed that calcium influx through voltage-gated calcium channels elevated S1P levels, and ultimately enhanced noradrenaline release from PC12 cells [49]. Additionally, Kajimoto and co-workers provided evidence that SphK is a modulator of glutamate release from hippocampal neurons [50]. Combined these studies suggest that SphKs may play a more profound role in the functionality of neurons, further demonstrating that disruption of S1P-signaling could have profound and highly detrimental effects on the CNS.

Altogether, our research identified Mg^{2+}-nSMase-dependent NOX2 activity as a specific neuroinflammatory pathway that resulted in oxidation of SphK1, an important neuronal survival, developmental, and functional component. We showed that both TNFα and Aβ^{1-42} stimulated Mg^{2+}-nSMase activity, indicating a diversity of molecules that stimulated this particular neuroinflammatory pathway. The ceramide-driven NOX2-dependent oxidative down-regulation of SphK1 revealed by our study further showed how ceramide-signaling directly promoted neurodegeneration (Fig. 3.9). NOX enzymes are important players in normal redox-signaling; hence their expression and abundance in non-phagocytic cells. However chronic activation of NOXs can contribute to a massive and excessive oxidative response. Oxidative regulation of specific neuronal survival mechanisms, as well as functional and regenerative mechanisms allows for CNS pathologies to become degenerative in nature. Specific therapeutic targeting of the Mg^{2+}-nSMase or the neuronal NOX2 could offer improved treatments for acute injuries of the CNS, chronic neurodegenerative disorders of the CNS, and psychiatric disorders, and ultimately strategies to improve neuronal survival, connectivity and functionality, and perhaps promote regeneration.
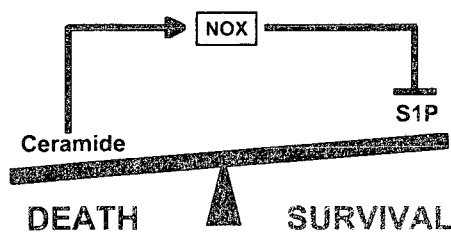
Fig. 3.9. Ceramide elicits oxidative damage via NOX-derived ROS to SphK1. Ceramide and sphingosine-1-phosphate (S1P) are metabolically linked through the intermediate sphingosine. These two lipid messengers regulate fundamental yet opposing cellular processes. Whereas ceramide is implicated in apoptosis and other mechanisms detrimental for cellular homeostasis, S1P plays a key role in cell survival pathways. Our study defined a specific neuroinflammatory pathway that directly influences ceramide/S1P metabolism, therefore influencing neuronal fate. Specifically we showed that Mg^{2+}nSMase-generated ceramide stimulated a neuronal NOX, which subsequently inhibited SphK1 via irreversible oxidation.

3.6: Acknowledgements

3.7: Contributions

Two students contributed directly to this research study. Danielle LaVictorie spent a semester helping to optimize the $p67^{phox}$ translocation studies. Later, Sally Gustafson joined the lab and assisted in Mg^{2+}nSMase assays, as well as ROS detection and neurite outgrowth studies.

3.8: References

[1] Block, M. L.; Zecca, L.; Hong, J. S. Microglia-mediated neurotoxicity: Uncovering the molecular mechanisms. *Nat. Rev. Neurosci.* **8**:57-69; 2007.

[2] Fetler, L.; Amigorena, S. Neuroscience. brain under surveillance: The microglia patrol. *Science*309:392-393; 2005.

[3] Nimmerjahn, A.; Kirchhoff, F.; Helmchen, F. Resting microglial cells are highly dynamic surveillants of brain parenchyma in vivo. *Science*308:1314-1318; 2005.

[4] Polazzi, E.; Contestabile, A. Reciprocal interactions between microglia and neurons: From survival to neuropathology. *Rev. Neurosci.*13:221-242; 2002.

[5] Colton, C. A.; Gilbert, D. L. Production of superoxide anions by a CNS macrophage, the microglia. *FEBS Lett.*223:284-288; 1987.

[6] Sawada, M.; Kondo, N.; Suzumura, A.; Marunouchi, T. Production of tumor necrosis factor-alpha by microglia and astrocytes in culture. *Brain Res.*491:394-397; 1989.

[7] Town, T.; Nikolic, V.; Tan, J. The microglial "activation" continuum: From innate to adaptive responses. *J. Neuroinflammation*2:24; 2005.

[8] Adam-Klages, S.; Adam, D.; Wiegmann, K.; Struve, S.; Kolanus, W.; Schneider-Mergener, J.; Kronke, M. FAN, a novel WD-repeat protein, couples the p55 TNF-receptor to neutral sphingomyelinase. *Cell*86:937-947; 1996.

[9] Marchesini, N.; Hannun, Y. A. Acid and neutral sphingomyelinases: Roles and mechanisms of regulation. *Biochem. Cell Biol.*82:27-44; 2004.

[10] Segui, B.; Cuvillier, O.; Adam-Klages, S.; Garcia, V.; Malagarie-Cazenave, S.; Leveque, S.; Caspar-Bauguil, S.; Coudert, J.; Salvayre, R.; Kronke, M.; Levade, T. Involvement of FAN in TNF-induced apoptosis. *J. Clin. Invest.*108:143-151; 2001.

[11] Clarke, C. J.; Snook, C. F.; Tani, M.; Matmati, N.; Marchesini, N.; Hannun, Y. A. The extended family of neutral sphingomyelinases. *Biochemistry*45:11247-11256; 2006.

[12] Luberto, C.; Hassler, D. F.; Signorelli, P.; Okamoto, Y.; Sawai, H.; Boros, E.; Hazen-Martin, D. J.; Obeid, L. M.; Hannun, Y. A.; Smith, G. K. Inhibition of tumor necrosis factor-induced cell death in MCF7 by a novel inhibitor of neutral sphingomyelinase. *J. Biol. Chem.***277**:41128-41139; 2002.

[13] Andrieu-Abadie, N.; Gouaze, V.; Salvayre, R.; Levade, T. Ceramide in apoptosis signaling: Relationship with oxidative stress. *Free Radic. Biol. Med.***31**:717-728; 2001.

[14] Hannun, Y. A. Functions of ceramide in coordinating cellular responses to stress. *Science***274**:1855-1859; 1996.

[15] Hannun, Y. A.; Luberto, C. Ceramide in the eukaryotic stress response. *Trends Cell Biol.***10**:73-80; 2000.

[16] Babior, B. M. Phagocytes and oxidative stress. *Am. J. Med.***109**:33-44; 2000.

[17] Eyster, K. M. The membrane and lipids as integral participants in signal transduction: Lipid signal transduction for the non-lipid biochemist. *Adv. Physiol. Educ.***31**:5-16; 2007.

[18] Bedard, K.; Krause, K. H. The NOX family of ROS-generating NADPH oxidases: Physiology and pathophysiology. *Physiol. Rev.***87**:245-313; 2007.

[19] Quinn, M. T.; Gauss, K. A. Structure and regulation of the neutrophil respiratory burst oxidase: Comparison with nonphagocyte oxidases. *J. Leukoc. Biol.***76**:760-781; 2004.

[20] Cheng, G.; Cao, Z.; Xu, X.; van Meir, E. G.; Lambeth, J. D. Homologs of gp91phox: Cloning and tissue expression of Nox3, Nox4, and Nox5. *Gene***269**:131-140; 2001.

[21] Serrano, F.; Kolluri, N. S.; Wientjes, F. B.; Card, J. P.; Klann, E. NADPH oxidase immunoreactivity in the mouse brain. *Brain Res.***988:**193-198; 2003.

[22] Groemping, Y.; Rittinger, K. Activation and assembly of the NADPH oxidase: A structural perspective. *Biochem. J.***386:**401-416; 2005.

[23] Cross, A. R.; Erickson, R. W.; Curnutte, J. T. Simultaneous presence of p47(phox) and flavocytochrome b-245 are required for the activation of NADPH oxidase by anionic amphiphiles. evidence for an intermediate state of oxidase activation. *J. Biol. Chem.***274:**15519-15525; 1999.

[24] Ueyama, T.; Tatsuno, T.; Kawasaki, T.; Tsujibe, S.; Shirai, Y.; Sumimoto, H.; Leto, T. L.; Saito, N. A regulated adaptor function of p40phox: Distinct p67phox membrane targeting by p40phox and by p47phox. *Mol. Biol. Cell***18:**441-454; 2007.

[25] Alemany, R.; van Koppen, C. J.; Danneberg, K.; Ter Braak, M.; Meyer Zu Heringdorf, D. Regulation and functional roles of sphingosine kinases. *Naunyn Schmiedebergs Arch. Pharmacol.***374:**413-428; 2007.

[26] Maceyka, M.; Payne, S. G.; Milstien, S.; Spiegel, S. Sphingosine kinase, sphingosine-1-phosphate, and apoptosis. *Biochim. Biophys. Acta***1585:**193-201; 2002.

[27] Taha, T. A.; Hannun, Y. A.; Obeid, L. M. Sphingosine kinase: Biochemical and cellular regulation and role in disease. *J. Biochem. Mol. Biol.***39:**113-131; 2006.

[28] Wattenberg, B. W.; Pitson, S. M.; Raben, D. M. The sphingosine and diacylglycerol kinase superfamily of signaling kinases: Localization as a key to signaling function. *J. Lipid Res.***47:**1128-1139; 2006.

[29] Toman, R. E.; Payne, S. G.; Watterson, K. R.; Maceyka, M.; Lee, N. H.; Milstien, S.; Bigbee, J. W.; Spiegel, S. Differential transactivation of sphingosine-1-phosphate receptors modulates NGF-induced neurite extension. *J. Cell Biol.* **166**:381-392; 2004.

[30] Mizugishi, K.; Yamashita, T.; Olivera, A.; Miller, G. F.; Spiegel, S.; Proia, R. L. Essential role for sphingosine kinases in neural and vascular development. *Mol. Cell. Biol.***25**:11113-11121; 2005.

[31] Strochlic, L.; Dwivedy, A.; van Horck, F. P.; Falk, J.; Holt, C. E. A role for S1P signalling in axon guidance in the xenopus visual system. *Development***135**:333-342; 2008.

[32] Wright, M. V.; Kuhn, T. B. CNS neurons express two distinct plasma membrane electron transport systems implicated in neuronal viability. *J. Neurochem.***83**:655-664; 2002.

[33] Bottenstein, J. E.; Sato, G. H. Growth of a rat neuroblastoma cell line in serum-free supplemented medium. *Proc. Natl. Acad. Sci. U. S. A.***76**:514-517; 1979.

[34] Li, J. M.; Shah, A. M. Intracellular localization and preassembly of the NADPH oxidase complex in cultured endothelial cells. *J. Biol. Chem.***277**:19952-19960; 2002.

[35] Levine, R. L.; Williams, J. A.; Stadtman, E. R.; Shacter, E. Carbonyl assays for determination of oxidatively modified proteins. *Methods Enzymol.***233**:346-357; 1994.

[36] Wessel, D.; Flugge, U. I. A method for the quantitative recovery of protein in dilute solution in the presence of detergents and lipids. *Anal. Biochem.***138**:141-143; 1984.

[37] Towbin, H.; Staehelin, T.; Gordon, J. Electrophoretic transfer of proteins from polyacrylamide gels to nitrocellulose sheets: Procedure and some applications. 1979. *Biotechnology***24**:145-149; 1992.

[38] Grimm, M. O.; Grimm, H. S.; Patzold, A. J.; Zinser, E. G.; Halonen, R.; Duering, M.; Tschape, J. A.; De Strooper, B.; Muller, U.; Shen, J.; Hartmann, T. Regulation of cholesterol and sphingomyelin metabolism by amyloid-beta and presenilin. *Nat. Cell Biol.***7**:1118-1123; 2005.

[39] Olivera, A.; Spiegel, S. Sphingosine-1-phosphate as second messenger in cell proliferation induced by PDGF and FCS mitogens. *Nature***365**:557-560; 1993.

[40] Gomez-Brouchet, A.; Pchejetski, D.; Brizuela, L.; Garcia, V.; Altie, M. F.; Maddelein, M. L.; Delisle, M. B.; Cuvillier, O. Critical role for sphingosine kinase-1 in regulating survival of neuroblastoma cells exposed to amyloid-beta peptide. *Mol. Pharmacol.***72**:341-349; 2007.

[41] Gourlay, C. W.; Ayscough, K. R. The actin cytoskeleton: A key regulator of apoptosis and ageing? *Nat. Rev. Mol. Cell Biol.***6**:583-589; 2005.

[42] Gungabissoon, R. A.; Bamburg, J. R. Regulation of growth cone actin dynamics by ADF/cofilin. *J. Histochem. Cytochem.***51**:411-420; 2003.

[43] Kusner, D. J.; Thompson, C. R.; Melrose, N. A.; Pitson, S. M.; Obeid, L. M.; Iyer, S. S. The localization and activity of sphingosine kinase 1 are coordinately regulated with actin cytoskeletal dynamics in macrophages. *J. Biol. Chem.***282**:23147-23162; 2007.

[44] Huwiler, A.; Johansen, B.; Skarstad, A.; Pfeilschifter, J. Ceramide binds to the CaLB domain of cytosolic phospholipase A2 and facilitates its membrane docking and arachidonic acid release. *FASEB J.***15**:7-9; 2001.

[45] Pettus, B. J.; Bielawska, A.; Subramanian, P.; Wijesinghe, D. S.; Maceyka, M.; Leslie, C. C.; Evans, J. H.; Freiberg, J.; Roddy, P.; Hannun, Y. A.; Chalfant, C. E. Ceramide 1-phosphate is a direct activator of cytosolic phospholipase A2. *J. Biol. Chem.***279**:11320-11326; 2004.

[46] Fox, T. E.; Houck, K. L.; O'Neill, S. M.; Nagarajan, M.; Stover, T. C.; Pomianowski, P. T.; Unal, O.; Yun, J. K.; Naides, S. J.; Kester, M. Ceramide recruits and activates protein kinase C zeta (PKC zeta) within structured membrane microdomains. *J. Biol. Chem.***282**:12450-12457; 2007.

[47] Bourbon, N. A.; Yun, J.; Kester, M. Ceramide directly activates protein kinase C zeta to regulate a stress-activated protein kinase signaling complex. *J. Biol. Chem.***275**:35617-35623; 2000.

[48] Nystrom, T. Role of oxidative carbonylation in protein quality control and senescence. *EMBO J.***24**:1311-1317; 2005.

[49] Alemany, R.; Kleuser, B.; Ruwisch, L.; Danneberg, K.; Lass, H.; Hashemi, R.; Spiegel, S.; Jakobs, K. H.; Meyer zu Heringdorf, D. Depolarisation induces rapid and transient formation of intracellular sphingosine-1-phosphate. *FEBS Lett.***509**:239-244; 2001.

[50] Kajimoto, T.; Okada, T.; Yu, H.; Goparaju, S. K.; Jahangeer, S.; Nakamura, S. Involvement of sphingosine-1-phosphate in glutamate secretion in hippocampal neurons. *Mol. Cell. Biol.***27**:3429-3440; 2007.

Chapter 4: Ceramide kinase regulates TNFα-induced NADPH oxidase activity and eicosanoid biosynthesis in neuronal cells[3]

4.1: Abstract

Inflammation plays a key role in the exacerbation of neurodegeneration in acute, chronic, and psychiatric pathologies of the central nervous system (CNS). Activated microglia and astrocytes secrete inflammatory mediators, such as tumor necrosis factor alpha (TNFα), which stimulate ceramide metabolism. Bioactive lipids are implicated in oxidative stress and eicosanoid biosynthesis, respectively affecting cellular survival. In our study, we demonstrated that TNFα-stimulated oxidative stress was due in part to the stimulation of NADPH oxidase (NOX) activity, as well as oxidoreductases responsible for eicosanoid production. We further demonstrated that TNFα increases ceramide kinase activity in human SH-SY5Y neuroblastoma cells, and that this activity stimulated neuronal NOX, as well as neuronal eicosanoid biosynthesis. We further found that blockade of TNFα-stimulated ceramide kinase activity, and therefore neuronal NOX activity, prevented loss of neuronal viability. Therefore, ceramide kinase could represent a promising therapeutic target for intervention of CNS degeneration.

I, Brian Barth, affirm my contributions to the work outlined in this chapter. I contributed to the conceptualization and experimental design of the study, worked directly on all aspects of the study, coordinated collaborations, and prepared the manuscript, all under the supervision, mentorship, and advisement of Dr. Thomas Kuhn. Please see section 4.7 on page 160 for the contributions of the other authors.

4.2: Introduction

Many pathologies of the central nervous system (CNS) exhibit a strong inflammatory component that substantially contributes to neurodegeneration (Block et al. 2007). Microglia and astrocytes respond to acute injury, toxins, or invading pathogens by secreting inflammatory mediators such as eicosanoids, cytokines, and reactive oxygen species (ROS) (Block et al. 2007; Fetler and Amigorena 2005; Nimmerjahn et al. 2005; Polazzi and Contestabile 2002). Tumor necrosis factor alpha (TNFα), a pro-inflammatory cytokine, binds to two receptors. The type I receptor is coupled to the Mg^{2+}-dependent neutral sphingomyelinase (Mg^{2+}-nSMase) through an adaptor protein known as the factor associated with nSMase (FAN) (Adam-Klages et al. 1996; Marchesini and Hannun 2004; Segui et al. 2001). SMases hydrolyze sphingomyelin to produce the bioactive lipid ceramide, which is implicated in mediating oxidative stress and apoptosis (Andrieu-Abadie et al. 2001; Chalfant and Spiegel 2005; Hannun 1996; Hannun and Luberto 2000; Marchesini and Hannun 2004).

Ceramide, and its metabolites, have been shown to regulate numerous enzymes key to inflammatory pathways. Cytosolic phospholipase A_2 (cPLA$_2$), which liberates arachidonic acid, is targeted to specific lipid microdomains by ceramide and its metabolites (Huwiler et al. 2001). In response to distinct extrinsic stimuli, cPLA$_2$ translocates to target membranes such as the endoplasmic reticulum, the Golgi apparatus, and the plasma membrane (Channon and Leslie 1990; Clark et al. 1995; Leslie 1997; Nalefski et al. 1994). Ceramide kinase (CerK), the enzyme responsible for the phosphorylation of ceramide, is localized in the Golgi apparatus as well as at the plasma membrane, thus establishing a connection between the production of ceramide-1-phosphate and cPLA$_2$ (Lamour et al. 2007). More recently, it was shown that cPLA$_2$ interacts with and is activated by ceramide-1-phosphate (Balsinde et al. 2000; Pettus et al. 2004; Subramanian et al. 2005; Subramanian et al. 2007).

The principal product of cPLA$_2$ activity, arachidonic acid, is a pivotal precursor of eicosanoid biosynthesis. Eicosanoids are lipid-derived bioactive molecules with pleiotropic effects regulating pro- and anti-inflammatory functions (Eyster 2007; Goetzl et al. 1995; Needleman et al. 1986; Piomelli 1993). The cyclooxygenases (COXs) and lipoxygenases (LOXs), specific oxidoreductases, produce eicosanoids known as prostaglandins, and leukotrienes, respectively (Murakami and Kudo 2006; Poff and Balazy 2004). While COXs and LOXs both convert arachidonic acid to eicosanoids, they also generate significant amounts of ROS as byproducts (Eyster 2007; Farooqui et al. 2007). In addition, arachidonic acid acts as a key component of membrane microdomains containing various enzymes, including members of the NADPH oxidase (NOX) family. Arachidonic acid has been linked as both a membrane anchor for NOX components, and as a cofactor to the NOX-proton channel (Bedard and Krause 2007; Groemping and Rittinger 2005; Lowenthal and Levy 1999; Mankelow et al. 2003; Quinn and Gauss 2004).

In this study, we investigated the role of CerK as a key mediator of NOX activity and eicosanoid biosynthesis in neuronal cells. We utilized both pharmacological and molecular approaches to demonstrate that TNFα-stimulated NOX activity and eicosanoid biosynthesis were dependent on CerK. Altogether, this study demonstrated, for the first time, that CerK was necessary for inflammatory-stimulated neuronal NOX activity, in addition to enhanced neuronal activities of cPLA$_2$, COX-2, and 5-LOX.

4.3: Materials and Methods

Reagents

Recombinant human tumor necrosis factor alpha (TNFα) was purchased from Millipore (Temecula, CA). DMEM and Penicillin/Streptomycin solution were obtained from Mediatech (Herndon, VA). Solutions of GlutaMAX-1 and trypsin/EDTA, as well as fluorescent siRNA, were from Invitrogen (Carlsbad, CA). The siRNA directed against

CerK, and non-targeting siRNA was from Dharmacon (Lafayette, CO). The Mg^{2+}-nSMase inhibitor GW4869, and the CerK inhibitor K1, were from EMD Biosciences (San Diego, CA). VECTASHIELD hard set mounting medium with 4,6-diamidino-2-phenylindole (DAPI) was purchased from Vector Laboratories (Burlingame, CA). Fetal bovine serum was received from Atlanta Biologicals (Atlanta, GA). The COX assay kit was from Cayman (Ann Arbor, MI). The XTT cell proliferation kit was from Trevigen (Gaithersburg, MD). ^{3}H-arachidonic acid was from American Radiolabeled Chemicals (St. Louis, MO). All other lipids were from Avanti Polar Lipids (Alabaster, AL). A polyclonal rabbit anti-human CerK antibody was from Exalpha (Shirley, MA). A polyclonal goat anti-human phospho-cPLA$_2$ antibody, a polyclonal goat anti-human phospho-p40^{phox} antibody, a polyclonal rabbit anti-human GAPDH antibody, a polyclonal rabbit anti-human p67^{phox} antibody, a monoclonal mouse anti-human β-actin antibody, and corresponding horseradish peroxidase-conjugated secondary antibodies were from Santa Cruz (Santa Cruz, CA). Streptavidin-agarose beads, sulfo-NHS-biotin, protease inhibitor cocktail (PIC), a Pico Super Signal chemoluminescent kit, and a BCA protein assay kit were obtained from Pierce (Rockland, IL). A polyclonal rabbit anti-human phospho-5-LOX antibody and all other reagents were purchased from Sigma (St. Louis, MO).

Cell Culture

Human SH-SY5Y neuroblastoma cells were grown in 100 mm dishes (Falcon) in medium composed of DMEM, 10% fetal bovine serum (FBS), 1% Glutamax, 100 U/ml Penicillin and 100 U/ml Streptomycin (humidified atmosphere, 5% CO_2, 37°C). For re-plating, cells were treated with trypsin (0.5 mg/ml)/EDTA (0.2mg/ml) (5 min), washed with PBS, centrifuged (200 x g_{max}, 2 min), and seeded onto 100 mm tissue culture dishes ($2x10^7$ cells per dish), 6-well tissue culture plates ($5x10^6$ cells per well), or 96-well tissue culture plates ($5x10^3$ to $5x10^4$ cells per well).

Cationic Nanoliposome Formation and siRNA Loading

Aliquots of 1,2-dioleoyl-2-trimethylammonium-propane (DOTAP), 1,2-distearoyl-*sn*-glycero-3-phosphoethanolamine-N-[methoxy(polyethylene glycol)-2000] (PEG2000-DSPE), and 1,2-dioleoyl-*sn*-glycero-3-phosphoethanolamine (DOPE), suspended in chloroform, were made in a 4.75:0.5:4.75 molar ratio, or alternatively, aliquots of DOTAP, PEG2000-DSPE, DOPE, and lissamine rhodamine B-labeled DOPE were made in a 4.75:0.5:4.7025:0.0475 molar ratio. Lipids were dried to a film under a stream of nitrogen, then hydrated by addition of 0.9% NaCl to a final lipid concentration of 25 mg/ml. Solutions were wrapped in parafilm, heated at 60°C (60 min), and subjected to vortex mixing and sonicated until light no longer diffracted through the suspension. The lipid vesicle-containing solution was quickly extruded at 60°C by passing the solution 10 times through 100 nm polycarbonate filters in an Avanti Mini-Extruder (Avanti Polar Lipids, Alabaster, AL). Nanoliposome solutions were stored at 4°C until use, protected from light when necessary. To prepare siRNA-loaded cationic nanoliposomes, siRNA was aliquoted into 0.9% NaCl, and nanoliposomes were added in a 10:1 weight ratio to siRNA. The solution was allowed to incubate overnight at room temperature prior to use. The RNA interference sequence was previously published by the Chalfant group (UGCCUGCUCUGUGCCUGUAdTdT and UACAGGCACAGAGCAGGCAdTdT) (Lamour et al. 2007).

Confocal Microscopy

Two-day old SH-SY5Y cultures (6-well plates, 5×10^6 cells per well) were maintained in regular growth media, and transfected with 200 nM FITC-labeled, non-targeted, siRNA loaded into Rhodamine-labeled cationic nanoliposomes. After 24 h, the cells were detached with trypsin (0.5 mg/ml)/EDTA (0.2mg/ml), and re-plated onto poly-D-lysine (50 µg per cm^2) coated glass cover slips. Following an additional 24 h growth period in regular media, the cells were washed three times in PBS, and fixed for 15 min at room temperature in 2% paraformaldehyde in PBS, pH 7.0. The cover slips were mounted onto glass slides with DAPI-containing mounting medium. Images were acquired using a

Leica (TCS SP2 AOBS) scanning confocal microscope (Bannockburn, IL), and filter combinations for FITC, rhodamine, and DAPI.

Ceramide Kinase Assay

Two-day old SH-SY5Y cultures (6-well plates, 5×10^6 cells per well) were stimulated with 100 ng/ml TNFα for 30 min after a 60 min pre-incubation with 10 μM GW4869. Cells were washed, scraped into PBS, and sonicated. Samples containing 5 μg total protein (BCA protein assay) were added to ceramide kinase buffer (150 μL final volume) containing 20 mM HEPES (pH 7.2), 50 mM NaCl, 50% glycerol, 1 mM dithiothreitol, 1X PIC and 500 μM ATP. Reactions were commenced by addition of 50 μL lipid solution containing 150 μM NBD-C_{12} ceramide 1% (v/v) Triton X-100, and 2% (w/v) BSA and incubated at 37°C (1 h). After termination with 100 μL dichloromethane Followed by a Bligh-Dyer extraction, lipids were separated by thin layer chromatography (dichloromethane/acetone/methanol/acetic acid/water at 10:4:3:2:1), and NBD-ceramide-1-phosphate was quantified using a GE Healthcare Typhoon Imager (Piscataway, NJ) with ImageQuant software.

Cellular Viability Assay

SH-SY5Y cells were seeded in 96-well tissue culture dishes (5×10^3 cells per well), and grown for 48 hours. Cultures were transfected with siRNA 48 h prior to other treatments. Following TNFα exposure (100 ng/ml, 48 h), XTT reagent prepared according to the manufacturer (Trevigen, Gaithersburg, MD,) was added and allowed to incubate for 4 hours. Viability was determined by absorbance at 490 nm (650 nm reference), using a Beckman Coulter Multimode DTX 880 microplate reader ((Fullerton, CA).

Cyclooxygenase Assay

Two-day old SH-SY5Y cultures (6-well plates, 5×10^6 cells per well) were stimulated with 100 ng/ml TNFα for 30 min after a 60 min pre-incubation with 10 μM GW4869, or alternatively, cultures were exposed to 10 μM of C8-ceramide-1-phosphate for 30 min.

SH-SY5Y cells were harvested in cold PBS and sonicated. Quantitative measurement of COX activity was performed in cell lysates containing equal amounts of total protein (BCA protein assay) using a COX enzyme assay kit according to the manufacture's instruction (Cayman, Ann Arbor, MI).

Arachidonic Acid Release Assay

Two-day old SH-SY5Y cultures (6-well plates, 5×10^6 cells per well) were incubated with 0.5 µCi/mL (5 nM) ^{3}H-arachidonic acid. Following overnight incubation, cells were rinsed two times with PBS, and incubated with media containing 1 mg/mL BSA (bovine serum albumin) for 10 minutes to remove unincorporated radioactivity, followed by PBS rinse. Regular growth media was replaced and cells were stimulated with TNFα (100 ng/ml). Alternatively, cells were pre-incubated with the Mg^{2+}-nSMase inhibitor GW4869 (10 µM, 60 min), the CerK inhibitor K1 (10 µM, 60 min), or pre-transfected with either siRNA targeting CerK, or non-targeting siRNA (200 nM, 48 h). Pre-incubations and transfection spanned the ^{3}H-arachidonic acid labeling time. Aliquots of media were removed at various time points, centrifuged (10,000 x g_{max}, 10 min), and 200 µL of the supernatant was measured in a scintillation counter to determine the relative amount of arachidonic acid metabolites released from the cells. Counts were adjusted based on the total cellular protein determined for each experimental condition (BCA protein assay).

Quantification of Reactive Oxygen Species Production

SH-SY5Y cells were seeded in 96-well tissue culture dishes (5×10^5 cells per well) and grown for 48 hours. Cultures were incubated with 50 µM of the oxidation-sensitive fluorescent indicator 2', 7'-dihydrodichlorofluorescein diacetate (H$_2$DCFDA) for one hour in the presence or absence of pharmacological inhibitors. H$_2$DCFDA is de-acetylated in the cytosol to dihydro-dichlorofluorescein and increases in fluorescence upon oxidation by H$_2$O$_2$ to dichlorofluorescein (DCF). Following exposure to stimuli, cultures were washed with PBS, agitated in lysis buffer (2M Tris-Cl pH 8.0, 2% w/v SDS, 1 mM Na$_3$VO$_4$), and total DCF fluorescence intensity was quantified in 100 µl of

sample cell lysates (equal amount of protein) using a Beckman Coulter Multimode DTX 880 microplate reader (Fullerton, CA) with a 495 nm excitation filter and a 525 emission filter.

Membrane Translocation of p67[phox]

Plasma membrane proteins were prepared by biotinylation and streptavidin-affinity chromatography as described by Li and Shah with minor modifications (Li and Shah 2002). SH-SY5Y neuroblastoma cells were grown in 6-well plates ($5x10^6$ cells per well) for 48 h. Following transfection with either siRNA targeting CerK, or non-targeting siRNA (200 nM, 48 h), cultures were treated with TNFα (100 ng/ml, 15 min). After washing with HBSS-CM (1X HBSS, 0.1 g/l $CaCl_2$, 0.1 g/l $MgCl_2$, pH 7.5), cultures were incubated with 0.5 mg/ml sulfo-NHS-biotin (prepared in 20 mM HEPES, HBSS-CM, pH 8.0) for 40 min on ice, and excess sulfo-NHS-biotin was neutralized with 50 mM glycine (prepared in HBSS-CM) on ice for 15 min. Cells were scraped into HBSS-CM, centrifuged (200 x g_{max}, 2 min), re-suspended in 500 μL loading buffer (20 mM HEPES pH 7.5, HBSS, 1% Triton X-100, 0.2 mg/ml saponin, 1% PIC), and sonicated. Streptavidin-agarose beads (25 μL) were added to the cell lysates (2 h, 4°C). Beads were collected (2,500 x g_{max}, 2 min), re-suspended in 150 μL of loading buffer, and heated (5 min, boiling water bath). Supernatants were obtained by centrifugation (2,500 x g_{max}, 2 min), and total cellular protein content was determined (BCA protein assay).

Western Blotting

Two-day old SH-SY5Y cultures (6-well plates, $5x10^6$ cells per well) were stimulated with 100 ng/ml TNFα for 15 min after a 60 min pre-incubation with 10 μM GW4869, or alternatively, cultures were exposed to 10 μM of C2-ceramide, C2-ceramide-1-phosphate, or C2-dihydroceramide for 15 min. Cells were lysed (2 M Tris-Cl pH 8.0, 2% SDS, 1 mM Na_3VO_4) and following centrifugation (3,000 x g_{max}, 4°C, 20 min), supernatants collected. Alternatively, lysates from siRNA-transfected cells or biotin-labeled cells were collected. Equal amounts of total protein (5-50 μg, BCA protein assay)

were separated by SDS-polyacrylamide (10-15%) gel electrophoresis (125 volts, 50 watts, 75 mA) and proteins transferred onto nitrocellulose or PVDF membranes (2.5 hours, 50 volts, 50 watts, 250 mA) according to Towbin and co-workers (Towbin et al. 1992). Following transfer, membranes were blocked with TBST-BSA (5 mg/ml BSA, 50 mM Tris-Cl pH 7.4, 150 mM NaCl, 0.1% Tween-20), and probed overnight with the appropriate primary antibody (1 µg/µl in TBST). Following incubation with a corresponding horseradish peroxidase-conjugated secondary antibody (0.2 µg/µl in TBST, 45 min), immune-reactivity was detected by chemoluminescence and quantified using a GE Healthcare Typhoon Imager (Piscataway, NJ) running ImageQuant software. Alternatively, immune-reactivity was detected by film exposure, followed by NIH ImageJ analysis (Bethesda, MD).

Statistical Analysis

One-way or two-way analysis of variance (ANOVA) or t-tests were used to determine statistically significant differences between treatments ($p < 0.05$). At least three independent experiments were performed for each condition. *Post hoc* comparisons of specific treatments were performed using a Bonferroni test or a Dunette's test. All error bars represent standard error of the mean (SEM). All statistical analyses were carried out using GraphPad Prism 4 software (La Jolla, CA).

4.4: Results

Neuronal ROS production was stimulated by TNFα.

Oxidative stress is a hallmark of acute, chronic, and psychiatric pathologies of the CNS and accompanies inflammatory processes (Block et al. 2007; Fetler and Amigorena 2005). Numerous studies, including our own (Chapter 2) (Barth et al. 2009), have demonstrated that TNFα causes oxidative stress in many non-neuronal and neuronal cell types both *in vivo* and *in vitro* (Block et al. 2007; Eyster 2007). We assessed in human SH-SY5Y neuroblastoma cells whether TNFα mediated the formation of ROS (oxidative

stress), and whether this was attributable to NOX, COX-2, or 5-LOX, three oxidoreductases commonly associated with inflammatory responses. In order to quantify intracellular ROS production, SH-SY5Y cells were loaded with the redox-sensitive fluorescent indicator 2', 7'-dihydrodichlorofluorescein (DCF). Within 15 min of acute exposure to 100 ng/ml TNFα, DCF-fluorescence intensity significantly increased (1.31 ± 0.04, *p<0.001, n=3), indicative of a generation of intracellular ROS (control: 1.03 ± 0.01, n=3) (Fig. 4.1). Pre-treatment for 60 min with the non-specific NOX inhibitor diphenylene iodonium (DPI, 10 μM), the specific COX-2 inhibitor indomethacin (IDM, 10 μM), the 5-LOX activator-protein inhibitor MK-886 (MK, 10 μM), or the antioxidant N-acetyl-L-cysteine (NAC, 5 mM), completely abrogated TNFα-stimulated intracellular ROS formation (TNFα + DPI: 1.00 ± 0.02, n=3; TNFα + IDM: 1.03 ± 0.01, n=3; TNFα + MK: 0.99 ± 0.04, n=3, TNFα + NAC: 0.92 ± 0.01, n=3) (Fig. 4.1A). These findings revealed that ROS formation in neuronal cells in response to TNFα arose from at least NOX, COX-2, and 5-LOX activity.

We further chose to evaluate a role for ceramide metabolites in response to inflammatory stimuli in neuronal cells. The generation of ceramide in response to various stimuli, including pro-inflammatory cytokines, has been documented and linked to cellular stress (Hannun and Luberto 2000). In our study, we found that blocking the hydrolysis of sphingomyelin to ceramide, by pre-treating with the selective Mg^{2+}-nSMase inhibitor GW4869 (10 μM), negated TNFα-stimulated intracellular ROS formation (1.07 ± 0.01, n=3) (Fig. 4.1B). We also found that exogenously added short-chain ceramide analogs alone (10 μM each, 15 min), caused significant ROS production in SH-SY5Y cells as demonstrated for C2-ceramide (CER; 1.23 ± 0.03, *p<0.001, n=4), C2-ceramide-1-phosphate (C1P; 1.33 ± 0.01, *p<0.001, n=4), or C2-dihydroceramide (DHCER; 1.24 ± 0.02, *p<0.001, n=4). These results implied that ceramide metabolites could play a profound role in the modulation of oxidative stress. Furthermore, while many researchers consider dihydroceramide to be an 'inactive' form of ceramide, these findings supported recent studies demonstrating that dihydroceramides are important bioactive mediators of cellular stress and death pathways (Wang et al. 2008; Zahlten et al. 2007).
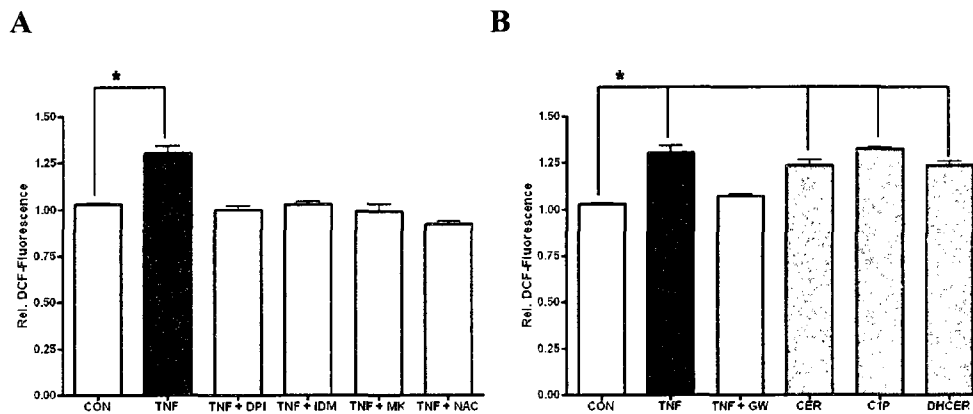
Figure 4.1. TNFα stimulates neuronal ROS production. The production of intracellular ROS was quantified using the oxidation-sensitive fluorescent indicator 2', 7'-dihydrodichlorofluorescein (DCF). Human SH-SY5Y neuroblastoma cells were loaded with 50 µM of the indicator, +/- inhibitors, 60 min prior to treatment. (A) SH-SY5Y cells were treated with TNFα (TNF, 100 ng/ml, 15 min), +/- 10 µM of the NOX inhibitor diphenylene iodonium (DPI), 10 µM of the COX-2 inhibitor indomethacin (IDM), 10 µM of the 5-LOX activator-protein inhibitor MK-886 (MK), or 5 mM of the antioxidant N-acetyl-L-cysteine (NAC). (B) SH-SY5Y cells were treated with TNFα, +/- 10 µM of the Mg^{2+}-nSMase inhibitor GW4869 (GW). Alternatively, cells were treated for 15 min with 10 µM of short-chain ceramide analogs (C2-ceramide, CER; C2-ceramide-1-phosphate, C1P; C2-dihydroceramide, DHCER). Data represent means +/- SEM of at least three independent experiments (1-way ANOVA, *p<0.001, compared to control: CON).

CerK and COX-2 activity were stimulated by TNFα.

To evaluate the link between ceramide metabolism and inflammatory stress, we measured the activities of CerK and COX-2. Our study revealed that TNFα-stimulated intracellular ROS formation was prevented by inhibition of the ceramide-generating Mg^{2+}-nSMase, or COX-2 (Fig. 4.1), and indeed we had found that TNFα stimulated Mg^{2+}-nSMase activity in both SH-SY5Y neuroblastoma cells and primary cortical neurons (data not shown). However other researchers have linked the production of ceramide-1-phosphate, generated by CerK, to the production of prostaglandins by COX enzymes in non-neuronal cells (Subramanian et al. 2005; Subramanian et al. 2007). In this study, we found that TNFα (100 ng/ml, 30 min) stimulated significant CerK activity in SH-SY5Y cells (2.06 ± 0.13, *p<0.001, n=3), compared to the control (1.00 ± 0.08, n=3) (Fig. 4.2A). Intriguingly, TNFα-stimulated CerK activity was completely blocked by 60 min

pre-treatment with 10 μM of the Mg^{2+}-nSMase inhibitor GW4869 (0.34 $\pm$ 0.02, n=3). The efficacy of GW4869 towards CerK was either due to CerK-inhibition, or simply by preventing the generation of the substrate ceramide by Mg^{2+}-nSMase. We also found that TNFα (100 ng/ml, 30 min) stimulated significant COX-2 activity (μU/μg total protein) in SH-SY5Y cells (278 $\pm$ 9, *p<0.001, n=3), compared to the control (33 $\pm$ 1, n=3), that was also blocked by 60 min pre-treatment with 10 μM GW4869 (51 $\pm$ 2, n=3) (Fig. 5.2B). As expected, COX-2 activity was also stimulated by 30 min treatment with 10 μM of the short-chain C8 analog of ceramide-1-phosphate alone (C8-C1P: 151 $\pm$ 5, *p<0.001, n=3). These findings demonstrated that TNFα-stimulated CerK activity, subsequently generating ceramide-1-phosphate, contributed to enhanced COX-2 activity in neuronal cells.

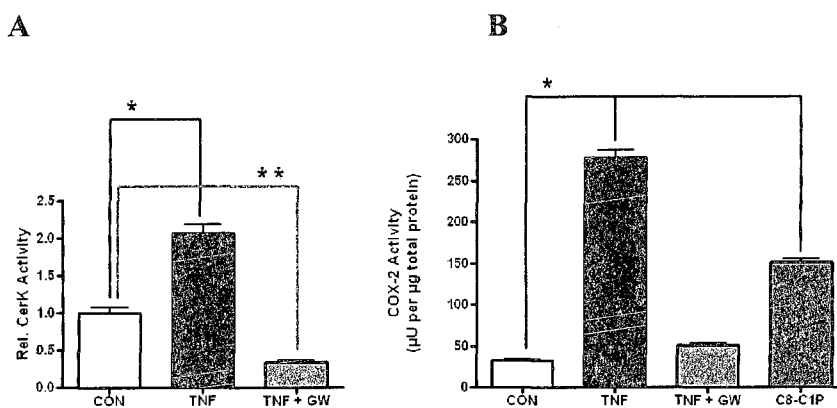A   B

Figure 4.2. TNFα stimulates neuronal CerK and COX-2 activity. CerK and COX-2 activity was evaluated in human SSH-SY5Y neuroblastoma cells. (**A**) CerK activity was quantified by measuring the conversion of the fluorescent NBD-ceramide to NBD-ceramide-1-phosphate. SH-SY5Y cells were exposed to TNFα (TNF, 100 ng/ml, 30 min), +/- 60 min pre-treatment with 10 μM of the Mg^{2+}-nSMase inhibitor GW4869 (GW). (**B**) COX-2 activity was measured by using an enzyme assay kit according to the manufacturer's instructions (Cayman Chemical, Ann Arbor, MI, USA). SH-SY5Y cells were exposed to TNFα (100 ng/ml, 30 min), +/- 60 min pre-treatment with 10 μM GW4869, or alternatively for 30 min with 10 μM of the short-chain C8 analog of ceramide-1-phosphate (C8-C1P). Data represent means +/- SEM of at least three independent experiments (1-way ANOVA, *p<0.001, **p<0.01, compared to control: CON).

Phosphorylation of cPLA$_2$, 5-LOX, and p40^{phox} were stimulated by TNFα.

Phosphorylation of cPLA$_2$, an enzyme responsible for the production of arachidonic acid, causes conformational changes that reveal lipid-binding domains essential towards enzyme activation (Ghosh et al. 2006; Kudo and Murakami 2002). We measured activation of cPLA$_2$ by quantifying phosphorylation of the enzyme. We found in SH-SY5Y cells that phosphorylation of cPLA$_2$ increased significantly following acute (15 min) addition of 100 ng/ml TNFα (2.77 $\pm$ 0.28, *p<0.01, n=3), compared to the control (1.00 $\pm$ 0.24, n=3) (Fig. 4.3A). Notably, phosphorylation was blocked by 60 min pretreatment with 10 μM GW4869 (1.33 $\pm$ 0.27, n=3). However, all three short-chain analogs of ceramides (10 μM each, 15 min) did not significantly increase the phosphorylation of cPLA$_2$ (C2-ceramide: 1.49 $\pm$ 0.27, n=3; C2-ceramide-1-phosphate: 1.73 $\pm$ 0.14, n=3; C2-dihydroceramide: 1.32 $\pm$ 0.25, n=3).

Phosphorylation also plays a prominent role in the activation of NOX enzymes. The assembly of cytosolic subunits with the membrane-bound subunits is regulated in part by phosphorylation. PX (Phox homology) domains play a key role in enabling the interaction of cytosolic subunits p47^{phox} and p40^{phox} with target membranes, bringing these subunits into position to interact with the membrane-bound subunits. These PX domains are revealed only after phosphorylation induces conformational changes that release auto-inhibitory regions (Bedard and Krause 2007; Groemping and Rittinger 2005; Quinn and Gauss 2004). Therefore, we analyzed NOX stimulation by quantifying changes in the phosphorylation of the p40^{phox} subunit. TNFα exposure (100 ng/ml, 15 min) of SH-SY5Y cells substantially increased phosphorylation of p40^{phox} (1.65 $\pm$ 0.12, *p<0.01, n=3), compared to the control (1.02 $\pm$ 0.05, n=3) (Fig. 4.3B), while pre-incubation of SH-SY5Y cultures for 60 min with 10 μM GW4869 completely abolished phosphorylation (1.19 $\pm$ 0.04, n=3) (Fig. 3B). Exposure for 15 min to of exogenous short-chain ceramide or ceramide-1-phosphate did not stimulate significant p40^{phox} phosphorylation (C2-ceramide: 1.30 $\pm$ 0.06, n=3; C2-ceramide-1-phosphate: 1.42 $\pm$ 0.10, n=3), while dihydroceramide did (C2-dihydroceramide: 1.86 $\pm$ 0.10, *p<0.001, n=3).

This later result further substantiates dihydroceramide's ability to stimulate intracellular ROS production.

Next, we evaluated phosphorylation of 5-LOX at Ser[523], an event that has been suggested to regulate the localization of the enzyme (Luo et al. 2005; Radmark and Samuelsson 2007). Acute addition of 100 ng/ml TNFα (15 min) to SH-SY5Y cultures significantly increased phosphorylation of 5-LOX (1.73 ± 0.09, $*p<0.05$, $n=3$), compared to the control (1.02 ± 0.07, $n=3$) (Fig. 4.3C). Phosphorylation was significantly reduced, although only partially, after a 60 min pre-treatment with 10 μM GW4869 (1.37 ± 0.08, $n=3$). As with $cPLA_2$, phosphorylation of 5-LOX was not significantly stimulated by exposure for 15 min with 10 μM of short C2-chain analogs of ceramides (C2-ceramide: 1.43 ± 0.17, $n=3$; C2-ceramide-1-phosphate: 1.36 ± 0.13, $n=3$; C2-dihydroceramide: 1.49 ± 0.15, $n=3$).
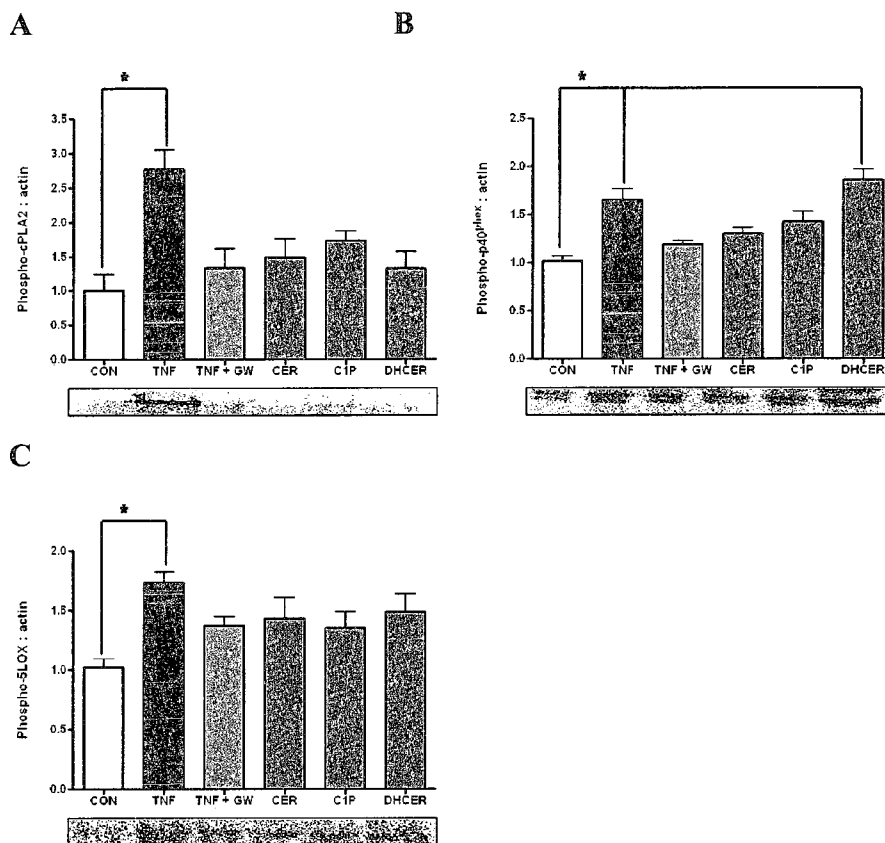
A   B

C

Figure 4.3. TNFα stimulates phosphorylation of cPLA$_2$, 5-LOX, and p40^{phox}. Phosphorylation of cPLA$_2$, p40^{phox}, and 5-LOX was evaluated by western blotting. Human SH-SY5Y neuroblastoma cells were treated with TNFα (TNF, 100 ng/ml, 15 min), +/- 60 min pre-treatment with 10 μM of the Mg^{2+}-nSMase inhibitor GW4869 (GW). Alternatively, cells were treated for 15 min with 10 μM of short-chain ceramide analogs (C2-ceramide, CER; C2-ceramide-1-phosphate, C1P; C2-dihydroceramide, DHCER). Following treatments, cells were lysed and western blotting was used to determine phospho-cPLA$_2$, phospho-p40^{phox}, or phospho-5-LOX levels in samples containing equal total cellular protein. (A) Quantified cPLA$_2$ phosphorylation. (B) Quantified p40^{phox} phosphorylation. (C) Quantified 5-LOX phosphorylation. Data represent means +/- SEM of at least three independent experiments (1-way ANOVA, *p<0.05, compared to control: CON).

Blocking CerK prevented TNFα-stimulated neuronal NOX activity.

Since our study ascribed an important role in neuronal cells for ceramide species as mediators of TNFα-stimulated ROS production, and showed that TNFα could stimulate CerK activity in neuronal cells, it became important to evaluate the role of CerK and ceramide-1-phosphate in regulating NOX in response to inflammatory stimuli. We used

siRNA to knockdown the activity of CerK using a sequence established by the Chalfant group (Lamour et al. 2007). To transfect SH-SY5Y cells with siRNA, we utilized a novel cationic nanoliposome formulation. Compared to other transfection systems, this formulation was specifically designed to be non-toxic and compatible for *in vivo* systemic delivery (Tran et al. 2008). To validate the delivery of siRNA to SH-SY5Y cells, we employed both fluorescently labeled siRNA and fluorescently labeled nanoliposomes (Fig. 4.4A). We observed incorporation of the liposome components into the plasma membranes of cells (red fluorescence), as well as siRNA uptake into perinnuclear and cytoplasmic regions of the cells (green fluorescence). The efficiency of siRNA transfection delivered by cationic nanoliposome (200 nM, 48 h) was determined to be 73%. We utilized Western blotting to evaluate the knockdown of CerK by siRNA (siCK, 200 nM, 48 h) as compared to non-targeted siRNA (siSCR), and found significant knockdown of CerK levels (siCK: 25% $\pm$ 9%, *p<0.01, n=3; siSCR: 100% $\pm$ 13%, n=3) (Fig. 4.4B).
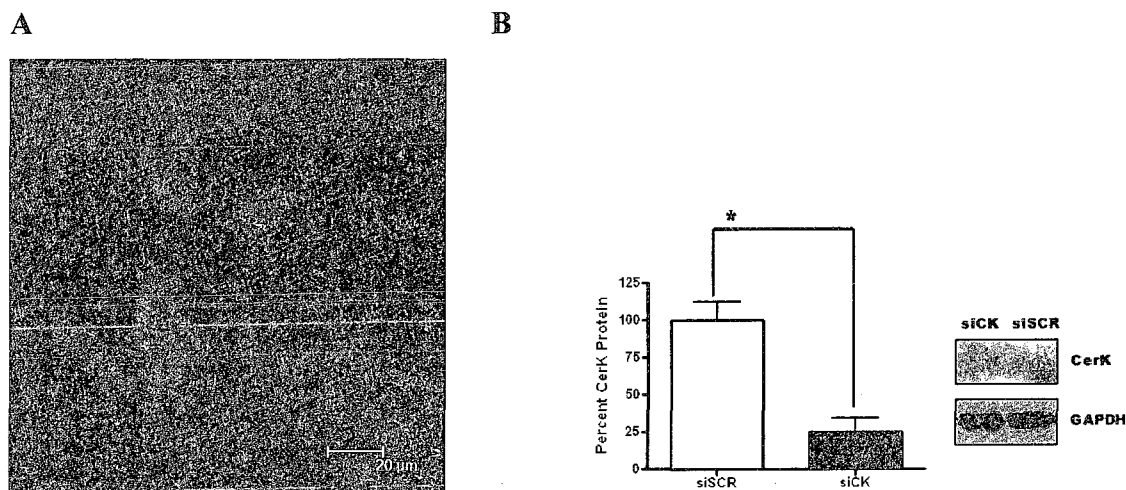
Figure 4.4. Cationic nanoliposomes effectively deliver CerK siRNA. Human SH-SY5Y neuroblastoma cells were transfected with siRNA targeting CerK. Cells were transfected with 200 nM siRNA for 48 hours in the presence of serum using a cationic nanoliposomal formulation. (A) Laser scanning confocal microscopy was used to evaluate uptake of siRNA. 24 hours following transfection, cells were re-plated onto poly-D-lysine-coated glass coverslips and maintained for an additional 24 hours before fixation, mounting, and microscopy. Cellular nuclei were stained with DAPI (blue), the liposome contained a rhodamine-labeled lipid (red), and the RNA was fluorescein-labeled (green) BLOCK-iT Fluorescent Oligo (Invitrogen, Carlsbad, CA). (B) Knockdown of CerK by targeted siRNA (siCK) compared to non-targeted siRNA (siSCR), was validated by Western blotting and quantified by image analysis of band density. Images are representative of three independent experiments, while data represent means +/- SEM of at least three independent experiments (t-test, *p<0.01).

We next began to evaluate the cellular role for CerK in SH-SY5Y cells in response to TNFα. Initially, we evaluated TNFα-stimulated intracellular ROS production, which we earlier showed was due in part to the activation of NOX, COX-2, and 5-LOX. In this study, we observed that TNFα (100 ng/ml, 60 min) stimulated significant ROS production (1.94 ± 0.19, *p<0.01, n=4), compared to the control (1.00 ± 0.13, n=4), which was blocked by 60 min pre-treatment with 10 μM GW4869 (0.98 ± 0.12, n=4). The knockdown of CerK by siRNA (200 nM, 48 h) effectively blocked TNFα-stimulated intracellular ROS production (1.05 ± 0.1, n=4), whereas non-targeted siRNA did not (1.68 ± 0.08, *p<0.05, n=4) (Fig. 4.5A). This finding in neuronal cells is consistent with previous studies showing regulation of cPLA$_2$ by CerK (Balsinde et al.

2000; Pettus et al. 2004; Subramanian et al. 2005; Subramanian et al. 2007), considering cPLA$_2$'s pivotal role in regulating NOX, COX-2, and 5-LOX through its production of arachidonic acid. To more closely evaluate the functionality of NOX, we next evaluated the translocation of the cytosolic subunit p67^{phox} to the plasma membrane in response to TNFα (Fig. 4.5B). As expected, a significant translocation of p67^{phox} to the plasma membrane occurred in response to 15 min treatment with 100 ng/ml TNFα (2.26 $\pm$ 0.16, *p<0.01, n=3), compared to the control (1.00 $\pm$ 0.04, n=3). Furthermore, specifically targeting CerK with siRNA (200 nM, 48 h), but not non-targeted siRNA, blocked TNFα-stimulated p67phox translocation (TNFα + siCK: 1.23 $\pm$ 0.19, n=3; TNFα + siSCR: 2.12 $\pm$ 0.19, *p<0.01, n=3). Altogether, these results demonstrate that CerK plays an essential role as a mediator of TNFα-stimulated neuronal NOX activity.
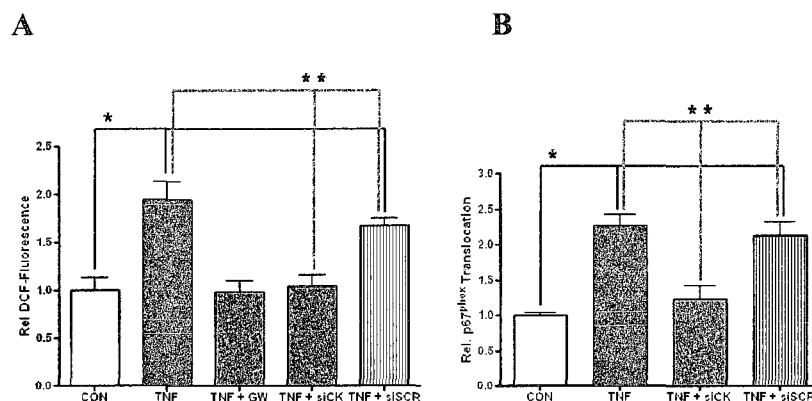

Figure 4.5. Blocking CerK prevents TNFα-stimulated neuronal NOX activity. The role of CerK regulation of NOX was examined in human SH-SY5Y neuroblastoma cells by evaluating intracellular ROS production and translocation of the p67^{phox} cytosolic subunit of NOX to the plasma membrane. Cells were pre-treated siRNA targeting CerK (siCK, 200 nM, 48 h), or non-targeting siRNA (siSCR, 200 nM, 48 h), followed by stimulation with TNFα (TNF, 100 ng/ml, 60 min). Alternatively, cells were pre-treated with the Mg^{2+}-nSMase inhibitor GW4869 (GW, 10 μM, 60 min). **(A)** The production of intracellular ROS was quantified by loading the cells 60 min before TNFα treatment with 50 μM of the oxidation-sensitive fluorescent indicator 2', 7'-dihydrodichlorofluorescein (DCF). **(B)** The translocation of p67^{phox} to the plasma membrane was monitored following TNFα exposure (100 ng/ml, 15 min) by biotinylating membrane proteins, separation by streptavidin-conjugated beads, and Western blot. All data represent means +/- SEM of at least three independent experiments (1-way ANOVA, *p<0.05, compared to control: CON, **p<0.05 compared to TNF + siCK).

Blocking CerK prevented TNFα-stimulated neuronal arachidonic acid release.

Eicosanoid biosynthesis is an important part of many inflammatory processes (Eyster 2007; Farooqui et al. 2007). The COX and LOX oxidoreductases produce ROS and are also responsible for the oxygenation of arachidonic acid, the initial step in the production of eicosanoids. Production of eicosanoids is rapidly followed by their release from the cell, and for this reason, we chose to monitor the release of eicosanoids as an indirect means of measure eicosanoid synthesis. We incubated SH-SY5Y neuroblastoma cells with ^{3}H-labeled arachidonic acid, allowing its overnight incorporation into the cells. Following exposure to 100 ng/ml of TNFα, we collected aliquots of growth media at various time points and quantified arachidonic acid metabolite release by liquid scintillation counting (Fig. 4.6). We found that cells treated with TNFα alone, or cells transfected with non-targeted siRNA prior to TNFα-treatment, released a significantly greater amount of arachidonic acid metabolites over a six hour time course (TNFα-6 h: 482 ± 46, *$p<0.001$, n=3; TNFα + siSCR-6 h: 525 ± 50, *$p<0.001$, n=3) compared to the control (6 h: 223 ± 24, n=3). We further found that siRNA directed against CerK (200 nM, 48 h), 60 min pre-treatment with 10 µM of K1, an inhibitor of CerK, or 60 min pre-treatment with 10 µM of GW4869, a Mg^{2+}-nSMase inhibitor, all prevented TNFα-stimulated arachidonic acid metabolite release (TNFα + siCK-6 h: 176 ± 23, n=3; TNFα + K1-6 h: 274 ± 25, n=3; TNFα + GW4869-6 h: 291 ± 35, n=3).
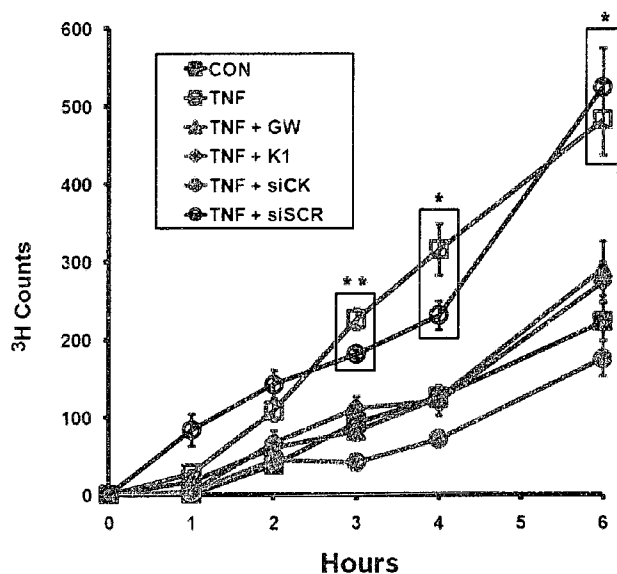
Figure 4.6. Blocking CerK prevents TNFα-stimulated neuronal arachidonic acid release. Human SH-SY5Y neuroblastoma cells were labeled with ^{3}H-arachidonic acid overnight prior to exposure to TNFα (TNF, 100 ng/ml), +/- pre-treatment with the Mg^{2+}-nSMase inhibitor GW4869 (GW, 10 µM, 60 min), the ceramide kinase inhibitor K1 (10 µM, 60 min), siRNA directed specifically against CerK (siCK, 200 nM, 48 h), or non-targeting siRNA (siSCR, 200 nM, 48 h).The release of arachidonic acid or arachidonic acid metabolites was monitored by scintillation counting of the growth media and ^{3}H-counts were adjusted based on total cellular protein (determined by a protein assay). All data represent means +/- SEM of at least three independent experiments. Boxes denote significantly different values between treatments at a time point (2-way ANOVA, *p<0.01), including the control (CON), **p<0.01 compared to all treatments except TNF + K1).

Blocking CerK prevented TNFα-stimulated loss of neuronal viability.

To conclude our study, we evaluated how blocking CerK activity affected the viability of SH-SY5Y neuroblastoma cells exposed to TNFα (Fig. 4.7). As anticipated, we observed a significant decrease in cellular viability when SH-SY5Y cells were treated with 100 ng/ml TNFα for 48 h (67% ± 2%, *p<0.001, n=12), compared to the control (100% ± 4%, n=12). Intriguingly, co-treatment with 10 µM GW4869 did not restore viability (63% ± 2%, *p<0.001, n=10). However, siRNA directed against CerK (200 nM, 48 h) effectively prevented TNFα-induced loss of cellular viability (85% ± 3%, **p<0.001, n=8), whereas non-targeted siRNA did not (68% ± 2%, *p<0.001, n=8). Most

interestingly, the deleterious effects of TNFα on SH-SY5Y cellular viability could be restored, despite CerK inhibition by siRNA, with the addition of exogenous short-chain C8-ceramide-1-phosphate (73% ± 2%, #p<0.01, n=8).
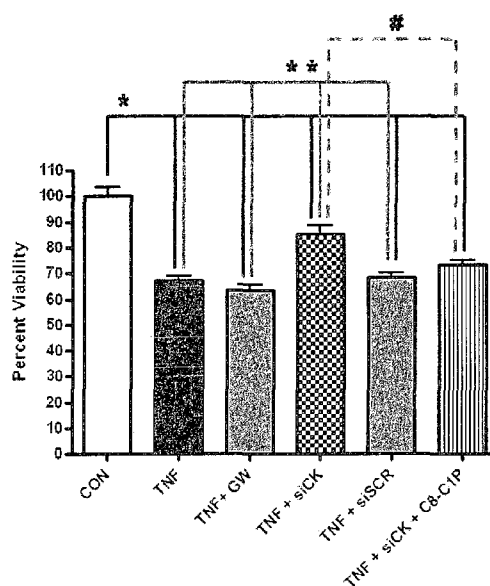

Figure 4.7. Blocking CerK prevents TNFα-stimulated loss of neuronal viability. Viability of human SH-SY5Y neuroblastoma cells was evaluated 48 hours after exposure to TNFα (TNF, 100 ng/ml), +/- co-incubation with the Mg^{2+}-nSMase inhibitor GW4869 (GW, 10 μM), siRNA directed specifically against CerK (siCK, 200 nM), or non-targeting siRNA (siSCR, 200 nM). Cationic nanoliposomes were used to deliver siRNA to cells 48 hours prior to treatment in regular growth media. Alternatively, the short-chain C8 analog of ceramide-1-phosphate (C8-C1P) was used to counter the effects of CerK down-regulation by siRNA. Cellular viability was determined by XTT assay and values were normalized, and expressed as a percentage of the values obtained under control conditions (CON). All data represent means +/- SEM of at least eight independent experiments (1-way ANOVA, *p<0.01, compared to control: CON, **p<0.01 compared to TNF + siCK; t-test, #p<0.01 comparing TNF + siCK to TNF + siCK + C8-C1P).

4.5: Discussion

Bioactive sphingolipids have been shown to regulate a diversity of cellular processes including survival, growth, cellular stress, and inflammation (Eyster 2007; Hannun 1996; Hannun and Luberto 2000). Recently, ceramide-1-phosphate, the product of CerK

activity, was shown to directly interact with $cPLA_2$ and stimulate its activity by enhancing its association with target membranes (Subramanian et al. 2005; Subramanian et al. 2007). This finding implicated ceramide-1-phosphate as a key sphingolipid mediating inflammatory responses, as $cPLA_2$ catalyzes the rate limiting step in eicosanoid biosynthesis (Eyster 2007; Lamour et al. 2007). Importantly, protein kinase activity is required to activate $cPLA_2$ because phosphorylation induces a conformational change exposing lipid-binding domains (Ghosh et al. 2006; Kudo and Murakami 2002). In a similar manner, phosphorylation of 5-LOX, and NOX subunits, other enzymes playing crucial roles in inflammation, results in changes in cellular localization, which regulate their activity (Bedard and Krause 2007; Eyster 2007; Farooqui et al. 2007). Interestingly, ceramide, another bioactive sphingolipid linked primarily to cellular stress, has been shown to regulate protein kinase C ζ (PKCζ) (Bourbon et al. 2000; Bourbon et al. 2002; Fox et al. 2007), $cPLA_2$ (Huwiler et al. 2001), and NOX (Cacicedo et al. 2005; Yi et al. 2007). Ceramide has been shown to activate PKCζ by direct binding, while PKCζ has been shown to strongly activate NOX (Fontayne et al. 2002). We have established ceramide, generated by TNFα-stimulated Mg^{2+}-nSMase activity, as a key mediator of NOX in both primary neurons and the SH-SY5Y neuroblastoma cell line (data not shown). However, in this study we specifically evaluated the role of CerK and its product. ceramide-1-phosphate, as a mediator of TNFα-stimulated neuronal NOX activity (Fig. 4.8). This research is significant because it not only is the first to establish CerK as a regulator of NOX, but it also describes a route, independent of PKCζ activation, by which ceramide, through conversion to ceramide-1-phosphate, can regulate NOX. This study also expanded into neuronal cells, previous research linking CerK to eicosanoid biosynthesis.
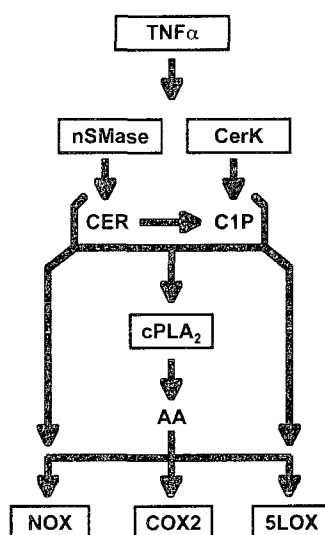
Figure 4.8. CerK mediates TNFα-stimulated neuronal NOX activity and eicosanoid biosynthesis. TNFα evokes an increase in ceramide metabolites through two principal activities: 1) Mg^{2+}-nSMase activity, hydrolyzing sphingomyelin to ceramide (CER), and 2) CerK activity, converting ceramide to ceramide-1-phosphate (C1P). Both ceramide and ceramide-1-phosphate stimulate $cPLA_2$ activity, and thus increase arachidonic acid (AA) production. Ceramide metabolites in conjunction with arachidonic acid, mediate the formation of ROS and eicosanoids in neuronal cells by stimulating the oxidoreductases: NADPH oxidase (NOX), cyclooxygenase-2 (COX-2), and 5-lipoxygenase (5-LOX).

We initially demonstrated that TNFα-stimulated intracellular ROS production in SH-SY5Y neuroblastoma cells was sensitive to pharmacological inhibition of COX, LOX, and NOX. These enzymes are all important oxidoreductases found throughout the body, including in the CNS (Bedard and Krause 2007; Eyster 2007; Farooqui et al. 2007). Arachidonic acid serves as a substrate for both LOXs and COXs, and has been linked to activity of NOXs through interactions with both membrane-bound and cytosolic subunits (Bedard and Krause 2007; Eyster 2007; Farooqui et al. 2007; Groemping and Rittinger 2005; Quinn and Gauss 2004). We further showed that ROS production was sensitive to pharmacological inhibition of Mg^{2+}-nSMase and was mimicked by exogenous short-chain analogs of ceramide, ceramide-1-phosphate, and dihydroceramide. We next investigated COX-2, and found that its activity was stimulated by TNFα in a manner that was sensitive to Mg^{2+}-nSMase inhibition. Since exogenous short-chain ceramide-1-

phosphate also stimulated COX-2 in our model, and ceramide-1-phosphate-dependent cPLA$_2$ generates the substrate for COX-2, we speculated, and found, that TNFα stimulated CerK activity. Interestingly, this CerK activity was blocked by inhibition of Mg^{2+}-nSMase, corroborating our pharmacological findings suggesting Mg^{2+}-nSMase involvement in TNFα-stimulated ROS production.

To more specifically evaluate CerK, and its role in TNFα-stimulated neuronal NOX activity, we employed siRNA directed against CerK. To deliver siRNA, we utilized a novel cationic nanoliposome, which was designed specifically for *in vivo* applications (Tran et al. 2008). It was important to utilize a delivery system suited for *in vivo* applications, and therefore adequate for translational research. We found that knockdown of CerK prevented TNFα-stimulated ROS production, as well as ^{3}H-labeled arachidonic acid-metabolite release, a measure of eicosanoid biosynthesis and release. Both ROS and eicosanoids are neurotoxic, and so it was not surprising that knockdown of CerK prevented TNFα-induced loss of SH-SY5Y cell viability. Since we had earlier shown that ROS are generated by multiple oxidoreductases, it became important to directly evaluate NOX activation. The production of ROS by NOX requires both the phosphorylation and translocation of cytosolic subunits to membrane microdomains (Bedard and Krause 2007; Groemping and Rittinger 2005; Quinn and Gauss 2004). By monitoring the movement of the p67^{phox} subunit to the membrane, we determined that CerK, and therefore ceramide-1-phosphate, was necessary for TNFα-stimulated NOX assembly and activity. The precise role for ceramide-1-phosphate-regulation of NOX may lie in its ability to stimulate cPLA$_2$ activity, and therefore the production of arachidonic acid. However, while arachidonic acid has been suggested to be a component of NOX subunit-targeted membranes, it has also been suggested to activate a proton channel that comprises a portion of the gp91^{phox} membrane-bound subunit (Lowenthal and Levy 1999; Mankelow and Henderson 2001; Mankelow and Henderson 2003; Mankelow et al. 2003; Mankelow et al. 2004). Therefore, while our findings that CerK regulates p67^{phox} membrane translocation are explained through activation of cPLA$_2$ in the former case, the later

would suggest that our findings support a more direct role for CerK in the regulation of NOX. Perhaps ceramide-1-phosphate serves as a key component of membranes targeted by NOX subunits.

Altogether, our study demonstrated that TNFα induced a profound generation of ROS in human SH-SY5Y neuroblastoma cells by activating three oxidoreductase activities, namely COX, LOX, and NOX, all under the regulation of ceramide metabolites. Oxidative stress is an important biological consequence of acute and chronic pathologies of the CNS, as well as psychiatric disorders, and is a primary effect of the associated inflammatory components (Block et al. 2007; Farooqui et al. 2007). In the CNS, the pro-inflammatory cytokine TNFα is released by activated microglia and astrocytes, and its accumulation is highly neurotoxic, inducing oxidative stress and apoptosis. Importantly, for the first time, our study showed that CerK played an essential role in regulating NOX activity, and therefore oxidative stress, in addition to regulating COX- and LOX-mediated eicosanoid biosynthesis in neuronal cells. Targeting CerK could potentially open new therapeutic strategies to alleviate neurodegeneration and improve neuronal survival and connectivity.

4.6: Acknowledgements

4.7: Contributions

Various individuals at both the University of Alaska Fairbanks (UAF) and the Pennsylvania State University College of Medicine (PSU-COM) contributed to this study. Sally Gustafson (UAF) helped to carry out ROS assays and Western blotting. Jody

Hankins (PSU-COM) was especially helpful assisting with ^{3}H-arachidonic acid labeling and scintillation counting. James Kaiser (PSU-COM) assisted with preparation of nanoliposomes and subsequent confocal microscopy to validate siRNA uptake. Mark Kester (PSU-COM) serves as the mentor to both Jody and James, and was essential in allowing portions of this research to be conducted in his laboratory.

4.8: References

Adam-Klages S., Adam D., Wiegmann K., Struve S., Kolanus W., Schneider-Mergener J. and Kronke M. (1996) FAN, a novel WD-repeat protein, couples the p55 TNF-receptor to neutral sphingomyelinase. Cell 86(6):937-947.

Andrieu-Abadie N., Gouaze V., Salvayre R. and Levade T. (2001) Ceramide in apoptosis signaling: relationship with oxidative stress. Free Radic. Biol. Med. 31(6):717-728.

Balsinde J., Balboa M. A., Li W. H., Llopis J. and Dennis E. A. (2000) Cellular regulation of cytosolic group IV phospholipase A2 by phosphatidylinositol bisphosphate levels. J. Immunol. 164(10):5398-5402.

Barth B. M., Stewart-Smeets S. and Kuhn T. B. (2009) Proinflammatory cytokines provoke oxidative damage to actin in neuronal cells mediated by Rac1 and NADPH oxidase. Mol. Cell. Neurosci. .

Bedard K. and Krause K. H. (2007) The NOX family of ROS-generating NADPH oxidases: physiology and pathophysiology. Physiol. Rev. 87(1):245-313.

Block M. L., Zecca L. and Hong J. S. (2007) Microglia-mediated neurotoxicity: uncovering the molecular mechanisms. Nat. Rev. Neurosci. 8(1):57-69.

Bourbon N. A., Sandirasegarane L. and Kester M. (2002) Ceramide-induced inhibition of Akt is mediated through protein kinase C zeta: implications for growth arrest. J. Biol. Chem. 277(5):3286-3292.

Bourbon N. A., Yun J. and Kester M. (2000) Ceramide directly activates protein kinase C zeta to regulate a stress-activated protein kinase signaling complex. J. Biol. Chem. 275(45):35617-35623.

Cacicedo J. M., Benjachareowong S., Chou E., Ruderman N. B. and Ido Y. (2005) Palmitate-induced apoptosis in cultured bovine retinal pericytes: roles of NAD(P)H oxidase, oxidant stress, and ceramide. Diabetes 54(6):1838-1845.

Chalfant C. E. and Spiegel S. (2005) Sphingosine 1-phosphate and ceramide 1-phosphate: expanding roles in cell signaling. J. Cell. Sci. 118(Pt 20):4605-4612.

Channon J. Y. and Leslie C. C. (1990) A calcium-dependent mechanism for associating a soluble arachidonoyl-hydrolyzing phospholipase A2 with membrane in the macrophage cell line RAW 264.7. J. Biol. Chem. 265(10):5409-5413.

Clark J. D., Schievella A. R., Nalefski E. A. and Lin L. L. (1995) Cytosolic phospholipase A2. J. Lipid Mediat. Cell Signal. 12(2-3):83-117.

Eyster K. M. (2007) The membrane and lipids as integral participants in signal transduction: lipid signal transduction for the non-lipid biochemist. Adv. Physiol. Educ. 31(1):5-16.

Farooqui A. A., Horrocks L. A. and Farooqui T. (2007) Modulation of inflammation in brain: a matter of fat. J. Neurochem. 101(3):577-599.

Fetler L. and Amigorena S. (2005) Neuroscience. Brain under surveillance: the microglia patrol. Science 309(5733):392-393.

Fontayne A., Dang P. M., Gougerot-Pocidalo M. A. and El-Benna J. (2002) Phosphorylation of p47phox sites by PKC alpha, beta II, delta, and zeta: effect on binding to p22phox and on NADPH oxidase activation. Biochemistry **41**(24):7743-7750.

Fox T. E., Houck K. L., O'Neill S. M., Nagarajan M., Stover T. C., Pomianowski P. T., Unal O., Yun J. K., Naides S. J. and Kester M. (2007) Ceramide recruits and activates protein kinase C zeta (PKC zeta) within structured membrane microdomains. J. Biol. Chem. **282**(17):12450-12457.

Ghosh M., Tucker D. E., Burchett S. A. and Leslie C. C. (2006) Properties of the Group IV phospholipase A2 family. Prog. Lipid Res. **45**(6):487-510.

Goetzl E. J., An S. and Smith W. L. (1995) Specificity of expression and effects of eicosanoid mediators in normal physiology and human diseases. FASEB J. **9**(11):1051-1058.

Groemping Y. and Rittinger K. (2005) Activation and assembly of the NADPH oxidase: a structural perspective. Biochem. J. **386**(Pt 3):401-416.

Hannun Y. A. (1996) Functions of ceramide in coordinating cellular responses to stress. Science **274**(5294):1855-1859.

Hannun Y. A. and Luberto C. (2000) Ceramide in the eukaryotic stress response. Trends Cell Biol. **10**(2):73-80.

Huwiler A., Johansen B., Skarstad A. and Pfeilschifter J. (2001) Ceramide binds to the CaLB domain of cytosolic phospholipase A2 and facilitates its membrane docking and arachidonic acid release. FASEB J. **15**(1):7-9.

Kudo I. and Murakami M. (2002) Phospholipase A2 enzymes. Prostaglandins Other Lipid Mediat. **68-69**:3-58.

Lamour N. F., Stahelin R. V., Wijesinghe D. S., Maceyka M., Wang E., Allegood J. C., Merrill A. H.,Jr, Cho W. and Chalfant C. E. (2007) Ceramide kinase uses ceramide provided by ceramide transport protein: localization to organelles of eicosanoid synthesis. J. Lipid Res. **48**(6):1293-1304.

Leslie C. C. (1997) Properties and regulation of cytosolic phospholipase A2. J. Biol. Chem. **272**(27):16709-16712.

Li J. M. and Shah A. M. (2002) Intracellular localization and preassembly of the NADPH oxidase complex in cultured endothelial cells. J. Biol. Chem. **277**(22):19952-19960.

Lowenthal A. and Levy R. (1999) Essential requirement of cytosolic phospholipase A(2) for activation of the H(+) channel in phagocyte-like cells. J. Biol. Chem. **274**(31):21603-21608.

Luo M., Jones S. M., Flamand N., Aronoff D. M., Peters-Golden M. and Brock T. G. (2005) Phosphorylation by protein kinase a inhibits nuclear import of 5-lipoxygenase. J. Biol. Chem. **280**(49):40609-40616.

Mankelow T. J. and Henderson L. M. (2003) Proton conduction through full-length gp91phox requires histidine 115. Protoplasma **221**(1-2):101-108.

Mankelow T. J. and Henderson L. M. (2001) Inhibition of the neutrophil NADPH oxidase and associated H+ channel by diethyl pyrocarbonate (DEPC), a histidine-modifying agent: evidence for at least two target sites. Biochem. J. **358**(Pt 2):315-324.

Mankelow T. J., Hu X. W., Adams K. and Henderson L. M. (2004) Investigation of the contribution of histidine 119 to the conduction of protons through human Nox2. Eur. J. Biochem. **271**(20):4026-4033.

Mankelow T. J., Pessach E., Levy R. and Henderson L. M. (2003) The requirement of cytosolic phospholipase A2 for the PMA activation of proton efflux through the N-terminal 230-amino-acid fragment of gp91phox. Biochem. J. 374(Pt 2):315-319.

Marchesini N. and Hannun Y. A. (2004) Acid and neutral sphingomyelinases: roles and mechanisms of regulation. Biochem. Cell Biol. 82(1):27-44.

Murakami M. and Kudo I. (2006) Prostaglandin E synthase: a novel drug target for inflammation and cancer. Curr. Pharm. Des. 12(8):943-954.

Nalefski E. A., Sultzman L. A., Martin D. M., Kriz R. W., Towler P. S., Knopf J. L. and Clark J. D. (1994) Delineation of two functionally distinct domains of cytosolic phospholipase A2, a regulatory Ca(2+)-dependent lipid-binding domain and a Ca(2+)-independent catalytic domain. J. Biol. Chem. 269(27):18239-18249.

Needleman P., Turk J., Jakschik B. A., Morrison A. R. and Lefkowith J. B. (1986) Arachidonic acid metabolism. Annu. Rev. Biochem. 55:69-102.

Nimmerjahn A., Kirchhoff F. and Helmchen F. (2005) Resting microglial cells are highly dynamic surveillants of brain parenchyma in vivo. Science 308(5726):1314-1318.

Pettus B. J., Bielawska A., Subramanian P. et al (2004) Ceramide 1-phosphate is a direct activator of cytosolic phospholipase A2. J. Biol. Chem. 279(12):11320-11326.

Piomelli D. (1993) Arachidonic acid in cell signaling. Curr. Opin. Cell Biol. 5(2):274-280.

Poff C. D. and Balazy M. (2004) Drugs that target lipoxygenases and leukotrienes as emerging therapies for asthma and cancer. Curr. Drug Targets Inflamm. Allergy 3(1):19-33.

Polazzi E. and Contestabile A. (2002) Reciprocal interactions between microglia and neurons: from survival to neuropathology. Rev. Neurosci. 13(3):221-242.

Quinn M. T. and Gauss K. A. (2004) Structure and regulation of the neutrophil respiratory burst oxidase: comparison with nonphagocyte oxidases. J. Leukoc. Biol. 76(4):760-781.

Radmark O. and Samuelsson B. (2007) 5-Lipoxygenase: Regulation and Possible Involvement in Atherosclerosis. Prostaglandins Other Lipid Mediat. 83(3):162-174.

Segui B., Cuvillier O., Adam-Klages S. et al (2001) Involvement of FAN in TNF-induced apoptosis. J. Clin. Invest. 108(1):143-151.

Subramanian P., Stahelin R. V., Szulc Z., Bielawska A., Cho W. and Chalfant C. E. (2005) Ceramide 1-phosphate acts as a positive allosteric activator of group IVA cytosolic phospholipase A2 alpha and enhances the interaction of the enzyme with phosphatidylcholine. J. Biol. Chem. 280(18):17601-17607.

Subramanian P., Vora M., Gentile L. B., Stahelin R. V. and Chalfant C. E. (2007) Anionic lipids activate group IVA cytosolic phospholipase A2 via distinct and separate mechanisms. J. Lipid Res. 48(12):2701-2708.

Towbin H., Staehelin T. and Gordon J. (1992) Electrophoretic transfer of proteins from polyacrylamide gels to nitrocellulose sheets: procedure and some applications. 1979. Biotechnology 24:145-149.

Tran M. A., Gowda R., Sharma A., Park E. J., Adair J., Kester M., Smith N. B. and Robertson G. P. (2008) Targeting V600EB-Raf and Akt3 using nanoliposomal-small interfering RNA inhibits cutaneous melanocytic lesion development. Cancer Res. 68(18):7638-7649.

Wang H., Maurer B. J., Liu Y. Y. et al (2008) N-(4-Hydroxyphenyl)retinamide increases
dihydroceramide and synergizes with dimethylsphingosine to enhance cancer cell
killing. Mol. Cancer. Ther. 7(9):2967-2976.

Yi F., Chen Q. Z., Jin S. and Li P. L. (2007) Mechanism of homocysteine-induced
Rac1/NADPH oxidase activation in mesangial cells: role of guanine nucleotide
exchange factor Vav2. Cell. Physiol. Biochem 20(6):909-918.

Zahlten J., Riep B., Nichols F. C., Walter C., Schmeck B., Bernimoulin J. P. and
Hippenstiel S. (2007) Porphyromonas gingivalis dihydroceramides induce
apoptosis in endothelial cells. J. Dent. Res. 86(7):635-640.

Chapter 5: Inhibition of NADPH oxidase by glucosylceramide confers chemoresistance[4]

5.1: Introductory Paragraph

The bioactive sphingolipid ceramide induces oxidative stress by disrupting mitochondrial function and stimulating NADPH oxidase (NOX) activity, both of which stimulate apoptosis [1-5]. Many anticancer chemotherapeutics (anthracyclines, *Vinca* alkaloids, paclitaxel, and fenretinide), as well as physiological stimuli such as tumor necrosis factor α (TNFα), enhance ceramide accumulation through *de novo* synthesis, degradation of complex sphingolipids, or inhibition of ceramide catabolism, all of which increase oxidative stress in malignant cells [5-7]. Consequently, ceramide metabolism in malignant cells has gained considerable interest as key to combating chemoresistance, in particular the up-regulation of glucosylceramide synthase (GCS) [6,8,9]. We hypothesized that impeding TNFα- or chemotherapy-stimulated NOX activity by GCS could represent an important mechanism of resistance. Utilizing neuroblastoma and glioblastoma cell lines, we determined that GCS activity blocked NOX activity, ultimately contributing to increased malignant cell survival. We also demonstrated a direct resistance mechanism where glucosylceramide, the product of GCS activity, interfered with NOX assembly. Collectively, our findings indicated that pharmacological or molecular inhibition of GCS using non-toxic nanoliposome delivery systems was able to augment NOX activity and improved the efficacy of chemotherapy.

---

[4] Brian M. Barth, Sally J. Gustafson, Megan M. Young, Sriram S. Shanmugavelandy, James M. Kaiser, Todd E. Fox, Myles C. Cabot, Mark Kester, and Thomas B. Kuhn Prepared for submission as a Letter to Nature Cell Biology.

I, Brian Barth, affirm my contributions to the work outlined in this chapter. I contributed to the conceptualization and experimental design of the study, worked directly on all aspects of the study, coordinated collaborations, and prepared the manuscript, all under the supervision, mentorship, and advisement of Dr. Thomas Kuhn. Please see section 5.5 on page 189 for the contributions of the other authors.

5.2: Main Text

The primary goal of chemotherapy is to induce cell death in malignant cells. Most chemotherapeutics target cellular processes associated with survival or growth. Recently, it has become apparent that many chemotherapeutics and endogenous stimuli such as TNFα, stimulate ceramide accumulation which increases oxidative stress and induces apoptosis of tumor cells [1,5,7]. Previously, we had demonstrated that TNFα stimulated NOX activity in SH-SY5Y neuroblastoma cells [10]. Ceramide, a bioactive sphingolipid shown to be generated in response to numerous stimuli including TNFα, has been widely implicated as a modulator of cellular stress and death [4,11,12]. Not surprisingly, many chemotherapeutics have also been shown to induce oxidative stress [13,14]. In our study, we evaluated several chemotherapeutic agents for their ability to stimulate the production of intracellular reactive oxygen species (ROS) in human SH-SY5Y neuroblastoma cells (Fig. 5.1). We utilized diphenylene iodonium (DPI), an inhibitor of NOX enzymes [2], to demonstrate that chemotherapeutic-stimulated intracellular ROS production was due in part, to NOX activity.
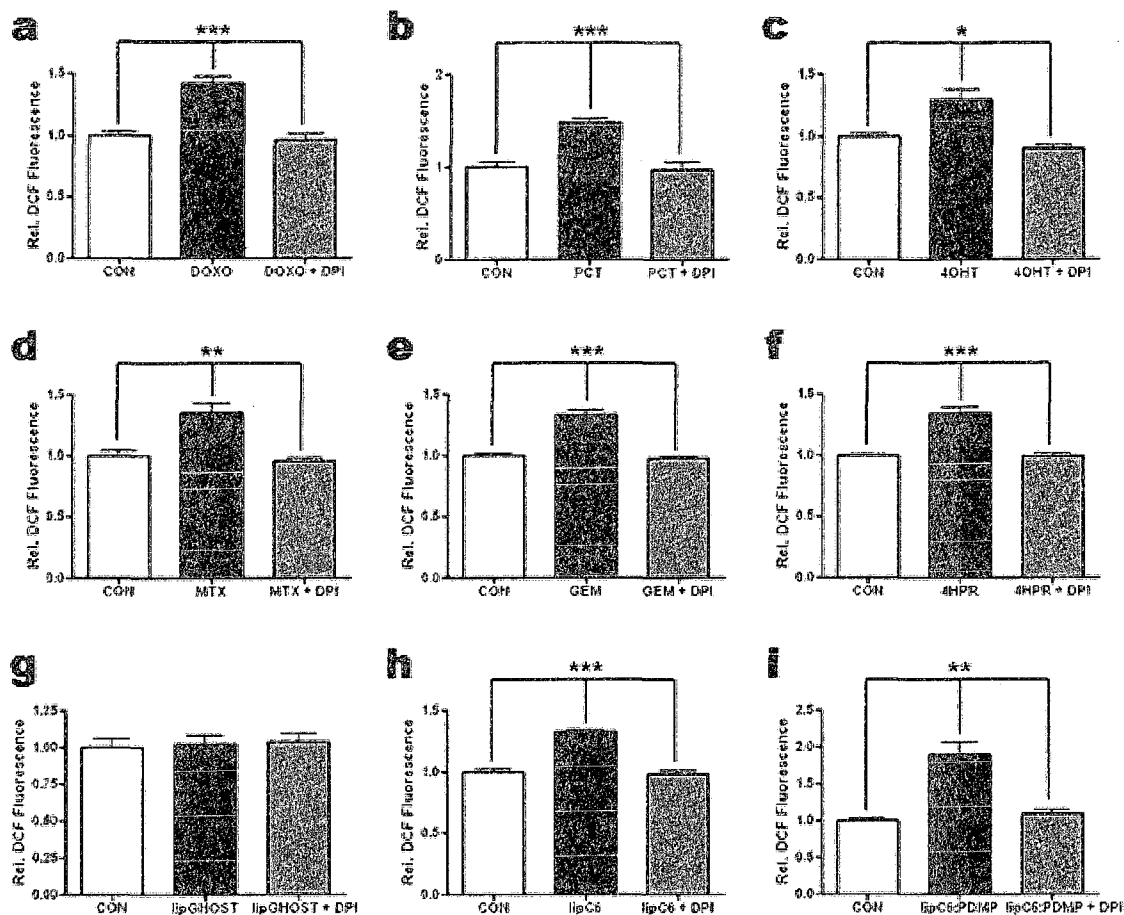
Figure 5.1: Chemotherapeutics stimulate NOX-dependent intracellular ROS production. The production of intracellular ROS was evaluated using the redox-sensitive indicator H₂DCFDA in human SH-SY5Y neuroblastoma cells. Diphenylene iodonium (DPI, 10 μM, 60 min pre-treatment), an inhibitor of NOX, was utilized to demonstrate the NOX-dependence of ROS production in response to various chemotherapeutics. (a) Doxorubicin (DOXO, 8.6 μM, 90 min). (b) Paclitaxel (PCT, 100 nM, 60 min). (c) 4-hydroxy tamoxifen (4OHT, 7.4 μM, 90 min). (d) Methotrexate (MTX, 1 μM, 60 min). (e) Gemcitabine (GEM, 1 μM, 120 min). (f) Fenretinide (4HPR, 1.5 μM, 60 min). (g) Empty (ghost) nanoliposomes (lipGH, 60 min). (h) Nanoliposomes containing 5 μM C6-ceramide (lipC6, 60 min). (i) Nanoliposomes containing both 5 μM C6-ceramide and 5 μM PDMP (lipC6/PDMP, 60 min). Fluorescence, corresponding to ROS, was normalized to the average fluorescence of the control (relative DCF-fluorescence). Data represent the mean +/- SEM of four independent experiments; * p < 0.05, ** p < 0.01, or *** p < 0.001, as determined by 1-way ANOVA.

In our study, we found that significant NOX-dependent intracellular ROS production was stimulated in response to the anthracycline doxorubicin (Fig. 5.1a), the

mitotic inhibitor paclitaxel (Fig. 5.1b), the estrogen receptor antagonist 4-hydroxy tamoxifen (Fig. 5.1c), the anti-metabolite methotrexate (Fig. 5.1d), the nucleoside analog gemcitabine (Fig. 5.1e), and the retinoid derivative fenretinide (Fig. 5.1f). Interestingly, tamoxifen has also been found to inhibit p-glycoprotein, and therefore glucosylceramide synthase by product inhibition, leading to an accumulation of ceramide. Additionally, fenretinide has been shown to stimulate serine palmitoyltransferase and therefore *de* novo synthesis of ceramide, as well as to block dihydroceramide desaturase, leading to accumulations of dihydroceramide [15, 16]. Our results not only tied the generation of intracellular ROS by these compounds to NOX, but also confirmed that known generators of ceramides stimulate NOX-derived intracellular ROS production.

In addition to these more-well known agents, we evaluated three nanoliposomal formulations designed by our laboratory (Supplementary Information, Table 5.S1). One formulation, termed the ghost, is a control formulation that does not contain any ceramide. As expected, the ghost formulation did not stimulate the production of intracellular ROS (Fig. 5.1g). The other nanoliposome formulations contained the C6-, short-chain, analog of ceramide, which has demonstrated *in* vivo efficacy in treating rodent models of breast cancer and melanoma [17, 18]. Furthermore, the C6-ceramide nanoliposomal formulation has been extensively characterized by the Nanotechnology Characterization Laboratory of the National Cancer Institute, and most importantly, was shown to be free of toxic side effects associated with other anti-neoplastic agents [19]. The second nanoliposomal formulation, in addition to C6-ceramide, also contained D-threo-1-phenyl-2-decanoylamino-3-morpholino-1-propanol (PDMP), an inhibitor of GCS, the enzyme that converts ceramide to glucosylceramide [8, 9]. We observed significant NOX-dependent production of intracellular ROS in response to treatment with the C6-ceramide formulation (Fig. 5.1h), and more so with the formulation combining C6-ceramide and PDMP (Fig. 5.1i). This later finding, showing over 40% greater ROS production ($p = 0.0136$, unpaired t-test), demonstrated that blocking GCS significantly improved the efficacy of nanoliposomal C6-ceramide-stimulated NOX-dependent intracellular ROS production in neuroblastoma cells.
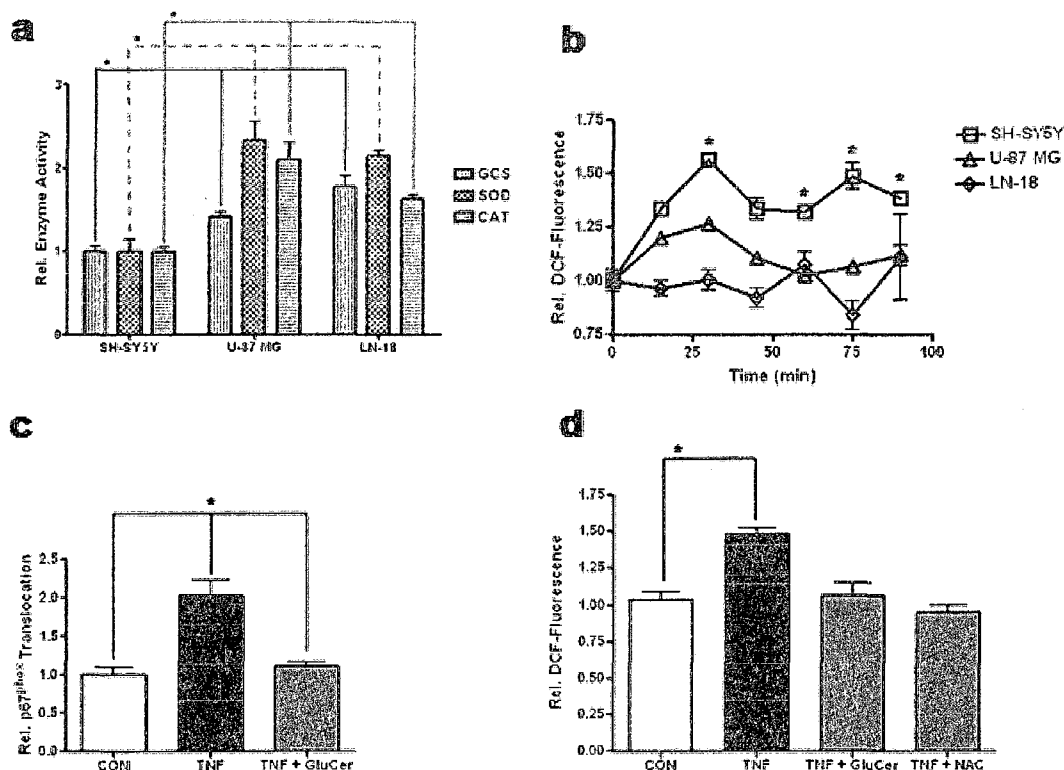
Figure 5.2: Glucosylceramide blocks agonist-stimulated NOX activity. (a) Basal activities of catalase (CAT), superoxide dismutase (SOD), and glucosylceramide synthase (GCS) were compared between human SH-SY5Y neuroblastoma, U-87 MG glioblastoma, and LN-18 glioblastoma cells. Activities were normalized to the average activities of SH-SY5Y cells. Data represent the mean +/- SEM of at least three independent experiments; * p < 0.05, as determined by 1-way ANOVA. (b) The redox-sensitive indicator H_2DCFDA was used to compare production of intracellular ROS between SH-SY5Y, U-87 MG, or LN-18 cells in response to doxorubicin (8.6 μM). Fluorescence, corresponding to ROS, was normalized to the average 0-min fluorescence of the respective cell line (relative DCF-fluorescence). Data represent the mean +/- SEM of three independent experiments; * p < 0.05, as determined by 2-way ANOVA, comparing SH-SY5Y response to both U-87 MG and LN-18 response. (c) Translocation of p67^{phox} to the plasma membrane was evaluated as an indication of NOX assembly. SH-SY5Y cells were exposed to TNFα (TNF, 100 ng/ml, 15 min) +/- 60 min pre-treatment with exogenous C8-glucosylceramide (GluCer, 10 μM). Translocation was normalized to the average translocation of the control. Data represent the mean +/- SEM of three independent experiments; * p < 0.01, as determined by 1-way ANOVA. (d) Intracellular ROS production was evaluated in SH-SY5Y cells exposed to TNFα (TNF, 100 ng/ml, 60 min) +/- 60 min pre-treatment with GluCer (10 μM), or the antioxidant N-acetyl-L-cysteine (NAC, 5 mM). Data represent the mean +/- SEM of three independent experiments; * p < 0.01, as determined by 1-way ANOVA.

A major problem in the treatment of cancer is that of multi-drug chemoresistance. In some circumstances, a diagnosed cancer may already display chemoresistance prior to

chemotherapy, as is the case with some glioblastomas [20,21], while in other cases a cancer may develop resistance, or relapse with resistance, to the chemotherapeutic(s) used during treatment [9]. In addition to research identifying increased ceramide metabolism in chemoresistant cancers, reports have also emerged documenting increased antioxidant defenses in radio- and chemoresistant glioblastomas [21]. In our study, we compared the activities of catalase and superoxide dismutase, primary antioxidant enzymes, and the activity of GCS between human SH-SSY5Y neuroblastoma cells, human U-87 MG glioblastoma cells, and human LN-18 glioblastoma cells (Fig. 5.2a). We found that the activities of these enzymes were all significantly greater in both glioblastomas when compared to those observed in the neuroblastoma cell line. In context with these findings, we also found that SH-SY5Y neuroblastoma cells responded to doxorubicin with a robust increase in intracellular ROS production, whereas U-87 MG and LN-18 glioblastoma cells did not (Fig. 5.2b). We then evaluated a possible link between increased GCS activity and decreased agonist-stimulated intracellular ROS production.

Intriguingly, a genetic deficiency in cerebrosidase termed Gaucher's disease (type I), results in the accumulation of glucosylceramide, that is unable to be degraded [22]. A phenotype of this cerebrosidase deficiency, monocyte dysfunction, is strikingly similar to that of chronic granulomatous disease, a genetic deficiency in one or more of NOX subunits [2,22]. From these similarities, it has been speculated that glucosylceramide could interfere with NOX; an idea initially tested with success in crude cell-free systems [22,23]. In our study, we speculated that agonist-stimulated NOX activity could be impeded directly by GCS's production of glucosylceramide. Indeed, we found that the addition of exogenous glucosylceramide to SH-SY5Y neuroblastoma cells prevented TNFα-stimulated NOX activity. NOX activity is regulated in part by the movement of cytosolic subunits, such as $p67^{phox}$, to the membrane where they complex with membrane-bound subunits to form the active enzyme [2]. We found that glucosylceramide blocked TNFα-stimulated $p67^{phox}$ translocation to the plasma membrane (Fig. 5.2c). This finding was critical because it showed, in a cellular system, that glucosylceramide itself blocked an important step in the assembly of the functional NOX. As expected, we further observed

that TNFα-stimulated intracellular ROS production was abrogated by exogenous glucosylceramide (Fig. 5.2d).

Notably, GCS has been identified as a primary enzyme up-regulated in many cases of chemoresistance [5, 8, 9]. Our findings in this study showing that numerous chemotherapeutics induced NOX-dependent intracellular ROS production, combined with those that showed that glucosylceramide blocks NOX assembly and activity, argue that GCS's role in chemoresistance is more profound than previously thought. GCS was understood to drive chemoresistance by neutralizing ceramide [8, 9], which could also indirectly impede NOX, as ceramide has been shown to be a regulator of NOX-activity [3]. We speculated that blockading of GCS activity would prevent its inhibition of NOX activity, and improve the efficacy of chemotherapy. Indeed we found that the pharmacological agent PDMP augmented doxorubicin-induced intracellular ROS formation in SH-SY5Y neuroblastoma cells, and even restored the effect in U-87 MG and LN-18 glioblastoma cells (Fig. 5.3a-c). We also observed that 3-amino-1,2,4-triazole (3AT), an inhibitor of the antioxidant enzyme catalase, augmented doxorubicin-induced intracellular ROS accumulation in SH-SY5Y neuroblastoma cells, and restored the effect in U-87 MG and LN-18 glioblastoma cells (Fig. 5.3a-c). Furthermore, both PDMP and 3AT improved doxorubicin-induced cell death in the neuroblastoma and glioblastoma cell lines (Fig. 5.3d-f).

The use of pharmacological agents has drawn some criticism due to issues with solubility, specificity, or toxicity, so we employed the more direct approach of molecular targeting utilizing siRNA directed against glucosylceramide synthase [19]. An important aspect of our approach was the use of a non-toxic cationic nanoliposomal delivery method. Typical cationic transfection reagents are impractical for in vivo use due to their severe toxicity. However, our laboratory designed and tested a unique formulation that has shown promise in animal studies, both as an efficacious and non-toxic delivery system [24]. In this study, we demonstrated that siRNA directed against GCS significantly augmented doxorubicin-induced intracellular ROS production in SH-SY5Y neuroblastoma cells, while a non-targeted siRNA did not (Fig. 5.3a). Likewise,

significant doxorubicin-induced intracellular ROS production was restored in both U-87 MG and LN-18 glioblastoma cells when targeted by siRNA directed against GCS, but not a non-targeted siRNA (Fig. 5.3b-c). Furthermore, by targeting GCS with specific siRNA, but not non-targeted siRNA, we demonstrated a significant decrease in cell viability induced by doxorubicin in the neuroblastoma and glioblastoma cell lines (Fig. 5.3d-f). These results showed that targeting GCS, the enzyme responsible for neutralizing ceramide and synthesizing NOX-impeding glucosylceramide, augmented chemotherapy-stimulated intracellular ROS production and cell death.
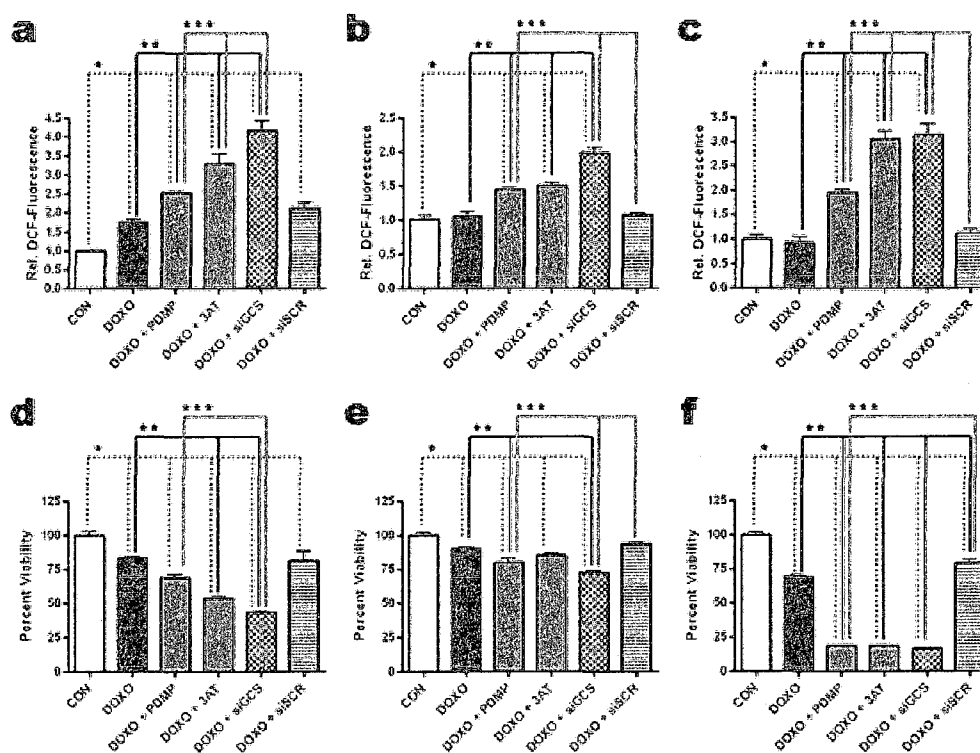
Figure 5.3: Interference with GCS augments intracellular ROS production and improves chemotherapy-induced cell death. Cells were exposed to doxorubicin (DOXO, 8.6 µM) +/- 2 hour pre-treatment with the GCS inhibitor PDMP (10 µM), or the catalase inhibitor 3-amino-1,2,4-triazole (3AT, 1 mM). Alternatively, cells were transfected with 200 nM siRNA directed against GCS (siGCS), or non-targeted siRNA (siSCR), 48 hours prior to treatment. The production of intracellular ROS was examined after 90 min treatment in human SH-SY5Y neuroblastoma, U-87 MG glioblastoma, or LN-18 glioblastoma cells, using the redox-sensitive indicator H_2DCFDA, while cellular viability was determined after 48 hour treatment by XTT assay. Fluorescence, corresponding to ROS, was normalized to the average fluorescence of the control (relative DCF-fluorescence). (a) ROS in SH-SY5Y cells. (b) ROS in U-87 MG cells. (c) ROS in LN-18 cells. (d) Viability of SH-SY5Y cells. (e) Viability of U-87 MG cells. (f) Viability of LN-18 cells. Data represent the mean +/- SEM of four independent experiments; * $p < 0.05$ compared to control (CON), ** $p < 0.05$ compared to DOXO, *** $p < 0.05$ compared to DOXO + PDMP, as determined by 1-way ANOVA.

Overall, our studies revealed that the SH-SY5Y neuroblastoma cell line was relatively more sensitive to agonist-stimulated NOX activity, compared to the U-87 MG and LN-18 glioblastoma cells lines tested. So while inhibiting GCS activity augmented doxorubicin-induced NOX activity and neuroblastoma cell death, we also evaluated how overexpression of GCS affected the cell line. Transfection of SH-SY5Y neuroblastoma cells with a plasmid encoding FLAG-tagged GCS significantly blocked TNFα-

stimulated intracellular ROS production (Fig. 5.4a) and doxorubicin-stimulated intracellular ROS production (Fig. 5.4b). Furthermore, overexpression of GCS completely, and significantly, blocked the TNFα-stimulated decrease in SH-SY5Y cell viability (Fig. 5.4c), and also modestly, yet significantly, blocked doxorubicin-stimulated SH-SY5Y cell viability loss (Fig. 5.4d). GCS overexpression likely does not completely block the doxorubicin-stimulated decrease in SH-SY5Y cell viability due to the concurrent induction of other pathways by doxorubicin that do not involve ceramide or NOX. Lastly, we demonstrated that overexpression of GCS inhibited TNFα-stimulated assembly of NOX in neuroblastoma cells. Overexpression of GCS blocked TNFα-stimulated p67^{phox} translocation to the plasma membrane, while siRNA directed against GCS, but not non-targeted siRNA, augmented TNFα-stimulated p67^{phox} translocation (Fig. 5.4e).
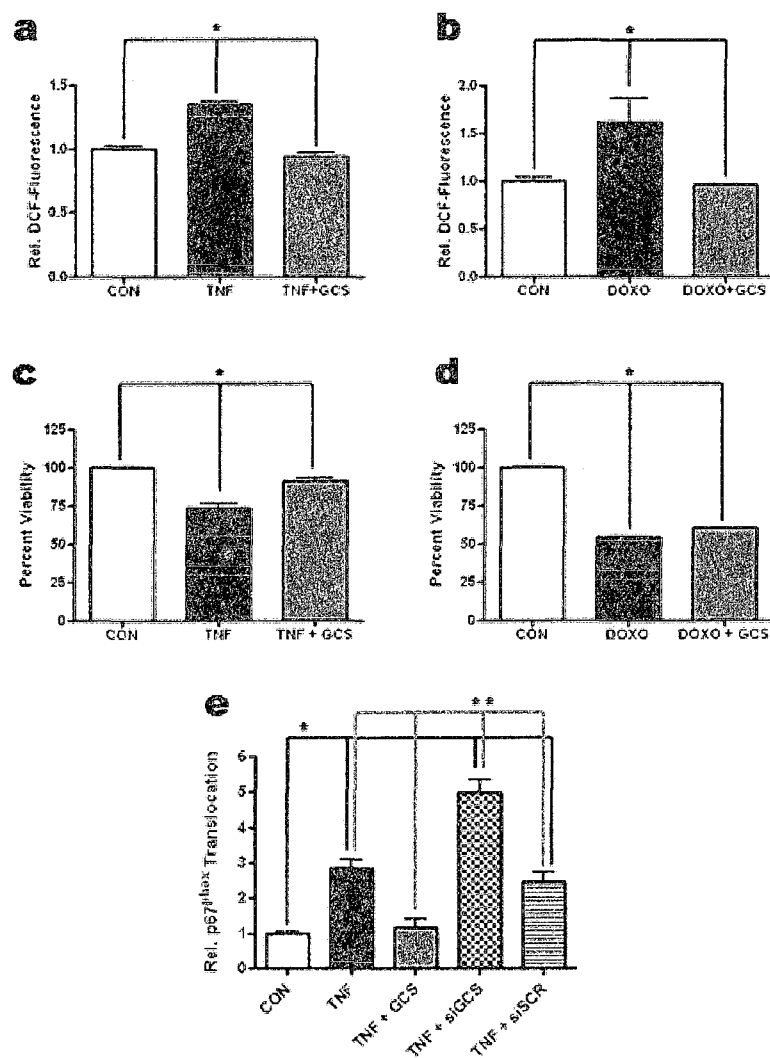
Figure 5.4: Overexpression of GCS blocks NOX and improves survival. Human SH-SY5Y neuroblastoma cells were transfected with 3 µg/ml of a GCS-expressing plasmid, 200 nM siRNA directed against GCS (siGCS), or non-targeted siRNA (siSCR), 48 hours prior to treatment. The production of intracellular ROS was evaluated using the redox-sensitive indicator H_2DCFDA, while cellular viability was determined by XTT assay. Fluorescence, corresponding to ROS, was normalized to the average fluorescence of the control (relative DCF-fluorescence). (a) ROS in cells exposed to TNFα (TNF, 100 ng/ml, 60 min). (b) ROS in cells exposed to doxorubicin (DOXO, 8.6 µM, 90 min). (c) Viability of cells exposed to TNFα (TNF, 100 ng/ml, 48 h). (d) Viability of cells exposed to doxorubicin (DOXO, 8.6 µM, 48 h). Data represent the mean +/- SEM of four (viability), or five (ROS), independent experiments; * $p < 0.05$, as determined by 1-way ANOVA. (e) Translocation of p67[phox] to the plasma membrane was evaluated as an indication of NOX assembly. Translocation was normalized to the average translocation of the control, and represent the mean +/- SEM of three independent experiments; * $p < 0.05$ compared to control (CON), ** $p < 0.01$ compared to TNF + siGCS, as determined by 1-way ANOVA.

Only recently, functional NOX (NOX1-5) activities, similar to the well-documented NOX2 in phagocytes, were identified in many non-phagocytic cell types (microglia, astrocytes, neurons) as a source of ROS production in response to stimuli such as TNFα [2]. Several lipids including arachidonic acid or anionic phospholipids are critical in the activation mechanism of NOX enzymes [2,25]. A recent study also demonstrated that ceramide synthesized *de novo* from the saturated fat palmitate induced the activation of NOX in retinal pericytes [3]. Therefore, it became important to evaluate the role of chemoresistant pathways that metabolize ceramide, such as GCS, in the regulation of NOX activity. Many chemotherapeutics, as well as endogenous stimuli such as TNFα, stimulate ceramide accumulation with a goal to stimulate apoptosis of tumor cells [5,11,12]. Mechanisms of chemoresistance have therefore developed to evade the toxic effects of ceramide, by neutralization, degradation, or conversion to pro-mitogenic and pro-survival metabolites [5]. Moreover, oxidative stress resistance of tumor cells has also recently been described in the form of increased catalase activity in rat glioblastoma cells [21].

While manipulating GCS activity by various methods suggested that ceramide neutralization impeded NOX, exogenous glucosylceramide-driven impediment of NOX activity was not explained. Important to understanding this phenomenon is the fact that while GCS resides on the cytosolic leaflet of the Golgi apparatus, glucosylceramide is promptly re-located to the luminal side [26]. For this reason, natural glucosylceramide is found predominantly on the extracellular leaflet of the plasma membrane, the same location as exogenously added glucosylceramide. Furthermore, glucosylceramide does not laterally diffuse within the plasma membrane due to the hydrophilicty of its head group [26]. Therefore, we speculated that glucosylceramide interfered with NOX assembly via a biophysical mechanism. By studying liposome models of the plasma membranes, we observed that the addition of glucosylceramide significantly decreased the size of these vesicles (Fig. 5.5a). The size of a vesicle is a measure of curvature (equal to the reciprocal of the radius), in that a smaller vesicle is more curved. Therefore, we

postulated that glucosylceramide interferes with NOX by inducing positive curvature, which restricts subunit-subunit and subunit-membrane interactions (Fig. 5.5b).

Many advanced CNS tumors, such as glioblastomas, respond poorly to chemotherapeutic and radiation therapies, while in comparison, resistance in neuroblastomas is less common [20, 27]. Complicating matters, and driving the demand for new and better therapeutics, is the fact that glioblastoma multiform, the most common primary brain tumor, has one of the worst survival rates among all cancers [20]. Accordingly, our research implicating GCS in the depletion of ceramide and glucosylceramide in inhibiting NOX assembly by glucosylceramide, offers important advances to the understanding of glioblastomas, and the design of better therapeutics. On the other hand, it is worth noting that degenerative pathologies, including acute and chronic CNS disorders as well as psychiatric disorders, exhibit oxidative stress as a major component of their pathologies [28, 29]. This is important because in contrast to the goals of cancer therapy, the goals in the treatment of degenerative disorders are to improve the survival and function of normal cells. While ceramide neutralization and degradation are hallmarks of chemoresistance, ceramide accumulation is characteristic of degenerative disorders [4, 11, 12, 29].

a

Basic
BasicGluCer

Number %

25
20
15
10
5
0

25   50   75   100   125

Diameter (nm)

$*$ p = 0.034

BasicCer
BasicCerGluCer

Number %

25
20
15
10
5
0

25   50   75   100   125

Diameter (nm)

$*$ p = 0.025

b

c

Glucosylceramide

GCS

Stimuli
(TNFa or chemotherapeutics)   →   Ceramide   →   NOX   → O_2^- →   Cellular Death

↑GCS, then ↓ Ceramide, & ↑ Glucosylceramide
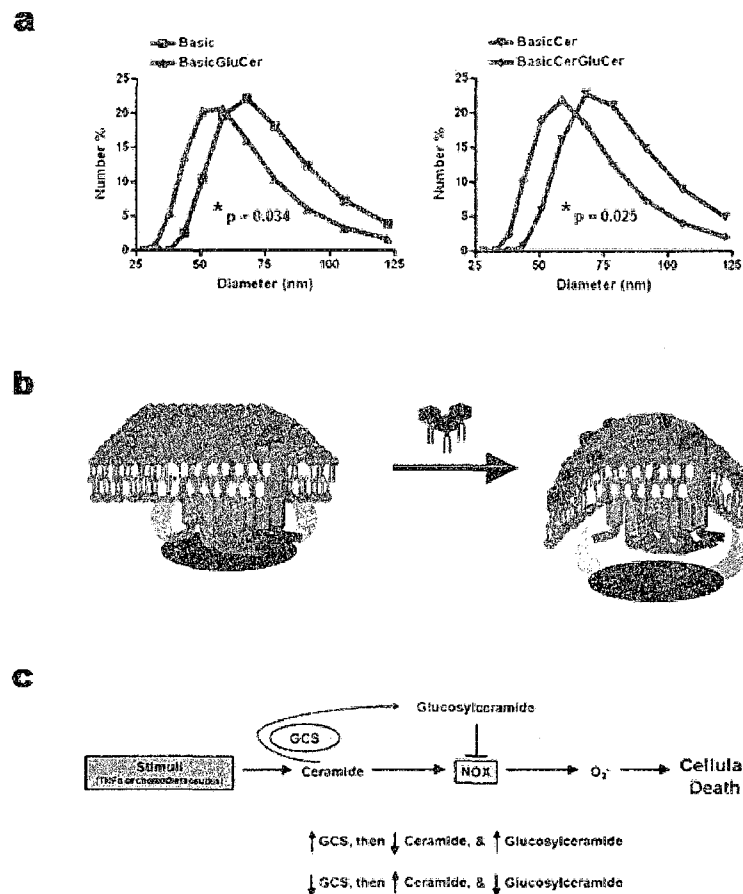
↓GCS, then ↑ Ceramide, & ↓ Glucosylceramide

Figure 5.5: Glucosylceramide prevents NOX activity by altering membrane curvature. Liposomes were prepared as a model of the plasma membrane, and the effect on membrane curvature with glucosylceramide addition was evaluated. (a) Liposomes composed of phospholipids, cholesterol, and sphingomyelin (basic formulation), with or without ceramide, were compared to equivalent counterparts containing glucosylceramide. Size of liposomes, related to curvature (curvature = 1/radius), was determined by light scattering. Data represent the mean of three independent experiments. Significance ($*$ p < 0.05) was determined by unpaired t-test of the mean diameter of respective liposomes. (b) Model depicting the addition of glucosylceramide inducing positive membrane curvature, which restricts the ability of NOX cytosolic components to interact with essential membrane lipids (phospholipids: blue; essential interacting membrane lipids: purple; sphingomyelin: orange; cholesterol: yellow; ceramide: small red circles; glucosylceramide: dark red hexagons; gp91^{phox}: grey trans-membrane domains; p22^{phox}: olive green trans-membrane domains; p40^{phox}: light green crescent; p67^{phox}: dark green oval; p47^{phox}: light blue crescent). (c) Schematic depicting that TNFα, or chemotherapeutics, stimulates NOX through ceramide generation, and that neutralization to glucosylceramide directly blocks NOX while also depleting ceramide.

In summary, ceramide neutralization through the formation of glucosylceramide not only decreases the pro-apoptotic stimulus ceramide, but also abolishes NOX

assembly and activity (Fig. 5.5c), and in conjunction with increased antioxidant enzyme activities, greatly alleviates cell death-inducing oxidative stress associated with chemotherapy or physiological agonists. Consequently, pharmacological inhibition of antioxidant enzymes, such as catalase, or pharmacological or molecular inhibition of GCS restored doxorubicin-toxicity, offering promise as a useful therapeutic avenue for the treatment of advanced cancers of the CNS. While treatment of patients with siRNA is currently not possible due to toxicity associated with delivery systems, our non-toxic cationic nanoliposomal formulation is designed specifically to overcome this hurdle. Additionally, our nanoliposomal formulation combining C6-ceramide and PDMP overcomes the current hurdle to clinical delivery of the GCS inhibitor PDMP associated with its low solubility. Nano-scale delivery systems further offer considerable clinical potential in the delivery of lower, yet more concentrated, therapeutic doses [19, 30]. Altogether, nano-encapsulated pharmacological or molecular agents targeting GCS offer exceptional promise in the treatment of chemoresistant CNS cancers. Specifically so, because interference with GCS overcomes the tumor's ability to neutralize ceramide and block NOX, ultimately restoring the ability to produce ROS and induce tumor cell death.

5.3: Methods

Reagents

DMEM and Penicillin/Streptomycin solution were obtained from Mediatech (Herndon, VA).). Solutions of GlutaMAX-1 and trypsin/EDTA, Hank's Balanced Salt Solution (HBSS), and Amplex Red reagent, as well as fluorescent siRNA, were from Invitrogen (Carlsbad, CA). Fetal bovine serum was received from Atlanta Biologicals (Atlanta, GA). The ON-TARGET plus SMART pool siRNA directed against GCS, and non-targeting siRNA was from Dharmacon (Lafayette, CO). GCS cDNA (Gene: UGCG; Accession: BC038711), was purchased from Thermo Fisher Scientific (Huntsville, AL). Streptavidin-agarose beads, sulfo-NHS-biotin, protease inhibitor cocktail (PIC), a Pico Super Signal chemoluminescent kit, and a BCA protein assay kit were obtained from

Pierce (Rockland, IL). Polyclonal rabbit anti-GCS, rabbit anti-FLAG, rabbit anti-GAPDH, and p67^{phox} antibodies, and corresponding horseradish peroxidase-conjugated secondary antibodies were from Santa Cruz (Santa Cruz, CA). An XTT cell proliferation assay kit was obtained from Trevigen (Gaithersburg, MD). VECTASHIELD hard set mounting medium with 4,6-diamidino-2-phenylindole (DAPI) was purchased from Vector Laboratories (Burlingame, CA). Recombinant human tumor necrosis factor alpha (TNFα) was purchased from Millipore (Temecula, CA). 2', 7'-dihydrodichlorofluorescein diacetate, doxorubicin, paclitaxel, methotrexate, fenretinide, and 4-hydroxy tamoxifen were from EMD Biosciences (San Diego, CA). Gemcitabine was a gift from Dr. Yixing Jiang. D-threo-1-Phenyl-2-decanoylamino-3-morpholino-1-propanol (PDMP) was purchased from Biomol (Plymouth Meeting, PA). All other lipids were from Avanti Polar Lipids (Alabaster, AL). All other reagents were purchased from Sigma (St. Louis, MO).

Cell Culture

Human SH-SY5Y neuroblastoma cells, human U-87 MG glioblastoma cells, and human LN-18 glioblastoma cells were grown in DMEM medium supplemented with 10% fetal bovine serum, 100 U/ml penicillin, and 100 U/ml streptomycin (humidified atmosphere, 5% CO_2, 37°C) in 100 mm tissue culture dishes (Falcon). For amplification, cells were washed off into PBS (phosphate buffer saline) after treatment with 0.5 mg/ml trypsin and 0.2mg/ml EDTA (5-15 min), centrifuged (200 x g_{max}, 2 min) and plated in 100 mm tissue culture dishes (2×10^7 cells per dish), 6-well tissue culture plates (5×10^6 cells per well), or 96-well tissue culture plates (5×10^3 to 5×10^4 cells per well).

Liposome Preparation and Cellular Transfection

Aliquots of lipids were made at appropriate ratios (Supplementary Information, Table 5.S1), and dried to a film under a stream of nitrogen, then hydrated by addition of 0.9% NaCl to a final lipid concentration of 25 mg/ml. Solutions were wrapped in parafilm, heated at 60°C (60 min), and subjected to vortex mixing and sonicated until light no

longer diffracted through the suspension. The lipid vesicle-containing solution was quickly extruded at 60°C by passing the solution 10 times through 100 nm polycarbonate filters in an Avanti Mini-Extruder (Avanti Polar Lipids, Alabaster, AL). Nanoliposome solutions were stored at 4°C until use, protected from light when necessary. To prepare siRNA- or plasmid-loaded cationic nanoliposomes, siRNA, or plasmid DNA, was aliquoted into 0.9% NaCl, and nanoliposomes were added in a 10:1 weight ratio to nucleic acid. The solution was allowed to incubate overnight at room temperature prior to use. The RNA interference sequences utilized (Supplementary Information, Table 5.S2), were from the ON-TARGET plus SMART pool product line of Dharmacon (Lafayette, CO). Confocal microscopy, and Western blotting, was used to validate transfection, knockdown, and overexpression (Supplementary Information, Fig. 5.S1).

Liposome Size Determination

Liposome suspensions were diluted 1:10 in 0.9% NaCl prior to size determination. Light scattering was used to quantify the size of liposomes using a Malvern Instruments Zetasizer Nano (Malvern, Worcestershire, United Kingdom).

Glucosylceramide Synthase Construct Generation

Glucosylceramide synthase cDNA (Gene: UGCG; Accession: BC038711) was transferred by PCR sub-cloning into the mammalian expression vector pcDNA3.1 (Invitrogen, Carlsbad, CA). The construct was sequence-verified by the Molecular Genetics Core Facility at the Pennsylvania State University College of Medicine.

Plasma Membrane Translocation of p67^{phox}

Plasma membrane proteins were prepared by biotinylation and streptavidin affinity purification as previously described [10]. SH-SY5Y cells grown in 6-well plates for transfected with siRNA or plasmid (200 nM, or 3 μg/ml, respectively, 48 h), or C8-glucosylceramide (10 μM, 60 min), prior to TNFα stimulation (100 ng/ml, 15 min). Next, cultures were washed with HBSS pH 7.5 containing 0.1 g/l $CaCl_2$ and 0.1 g/l $MgCl_2$

(HBSS-CM), incubated with 0.5 mg/ml sulfo-NHS-biotin (20 mM HEPES in HBSS-CM pH 8.0, 40 min, on ice), and excess sulfo-NHS-biotin was neutralized with 50 mM glycine (HBSS-CM, on ice, 15 min). Cells were scraped into HBSS-CM, centrifuged (200 x g_{max}, 2 min), lysed in 500 µL loading buffer (20 mM HEPES in HBSS pH 7.5, 1% Triton X-100, 0.2 mg/ml saponin, 1% PIC), and after brief sonication, incubated with streptavidin-agarose beads (25 µl, 2 h, 4°C). Beads were collected by centrifugation (2,500 x g_{max}, 2 min), and re-suspended in 150 µl of loading buffer (5 min, boiling water bath) to release bound protein. Supernatants were obtained by centrifugation (2,500 x g_{max}, 2 min), and analyzed by Western blotting (Supplementary Methods).

Quantification of Reactive Oxygen Species Production

SH-SY5Y, U-87 MG, or LN-18 cells were seeded in 96-well tissue culture dishes (5×10^4 cells per well) and grown for 48 hours. Cultures were incubated with 50 µM of the oxidation-sensitive fluorescent indicator 2', 7'-dihydrodichlorofluorescein diacetate (H_2DCFDA) for one hour in the presence or absence of pharmacological inhibitors, N-acetyl-L-cysteine (5 mM), or C8-glucosylceramide (10 µM). Alternatively, cells were transfected with siRNA (200 nM), or plasmid (3 µg/ml), 48 h prior to exposure, the last hour of which included H_2DCFDA loading. H_2DCFDA is de-acetylated in the cytosol to dihydro-dichlorofluorescein and increases in fluorescence upon oxidation by H_2O_2 to dichlorofluorescein (DCF). Following exposure to stimuli, cultures were washed with PBS, agitated in lysis buffer (2M Tris-Cl pH 8.0, 2% w/v SDS, 1 mM Na_3VO_4), and total DCF fluorescence intensity was quantified in 100 µl of cell lysates using a Beckman Coulter Multimode DTX 880 microplate reader (Fullerton, CA) with a 495 nm excitation filter and a 525 emission filter. All DCF fluorescence data were normalized to the average DCF fluorescence under control conditions (relative DCF-fluorescence values).

Glucosylceramide Synthase Activity

Generation of fluorescent NBD-glucosylceramide was quantified as follows. Samples of whole cell lysates containing 5 µg of total protein (BCA protein assay) were reacted with

100 μM NBD-ceramide in 5 mM MnCl$_2$ pH 7.2, 30 mg/ml BSA, and 1 mM UDP-glucose (100 μl reaction volume, 60 min, 37°C). After termination of the reaction (100 μl dichloromethane), lipids were extracted (Bligh-Dyer), and separated by thin layer chromatography (chloroform/acetone/methanol/acetic acid/water at 10:4:3:2:1). NBD-glucosylceramide was quantified using a GE Healthcare Typhoon Imager (Piscataway, NJ) running ImageQuant software.

Superoxide Dismutase Activity

Interference of ferricytochrome reduction by superoxide was measured as an indication of superoxide dismutase (SOD) activity. Samples of whole cell lysates containing 5 μg of total protein (BCA protein assay) were added to a solution of 50 μM hypoxanthine, 6 nM xanthine oxidase, 100 μM EDTA, and 10 μM ferricytochrome c in a 50 mM potassium phosphate pH 7.8 (100 μl reaction volume, 30 min, 25°C), and ferricytochrome reduction was quantified using a Beckman Coulter Multimode DTX 880 microplate reader (Fullerton, CA), reading absorbance at 550 nm.

Catalase Activity

Interference of horseradish peroxidase-mediated formation of the fluorescent resorufin from Amplex Red was quantified as an indication of catalase activity. Samples of whole cell lysates containing 5 μg of total protein (BCA protein assay) were mixed with 0.1 M Tris-Cl pH 7.4 and 10 mM Mg Cl$_2$ (volume of 75 μl) prior to incubation with 10 μM H$_2$O$_2$ (25 μl) for 30 min at 37°C. Next, an equal volume (100 μl) of horseradish peroxidase (2 U/ml) and Amplex Red (100 μM) was added to the reaction mixture, and resorufin fluorescence was quantified using a Beckman Coulter Multimode DTX 880 microplate reader (Fullerton, CA), with a 530 nm excitation filter and a 590 emission filter.

Cellular Viability Assay

SH-SY5Y, U-87 MG, or LN-18 cells were seeded in 96-well tissue culture dishes (5×10^3 cells per well), and grown for 48 hours. Cultures were co-incubated with pharmacological inhibitors, and either 100 ng/ml TNFα, or 5 μg/ml doxorubicin, for 48 hours. Alternatively, cells were transfected with siRNA (200 nM), or plasmid (3 μg/ml), 48 h prior to TNFα or doxorubicin exposure. XTT reagent prepared according to the manufacturer (Trevigen, Gaithersburg, MD) was added and allowed to incubate for 4 hours. Viability was determined by absorbance at 490 nm (650 nm reference), using a Beckman Coulter Multimode DTX 880 microplate reader ((Fullerton, CA). All values were normalized to the average values under control conditions.

Statistical Analysis

One-way, or two-way, analysis of variance (ANOVA), were used to determine statistically significant differences between treatments ($p < 0.05$). At least three independent experiments were performed for each condition. *Post hoc* comparisons of specific treatments were performed using a Bonferroni test. Unpaired t-tests were used to directly compare mean diameters of respective liposome formulations. All error bars represent standard error of the mean (SEM). All statistical analyses were carried out using GraphPad Prism 4 software (La Jolla, CA).

5.4: Acknowledgements

5.5: Contributions

Various individuals in three separate labs contributed to this study. Sally Gustafson (University of Alaska Fairbanks) helped with viability and ROS assays. Sriram Shanmugavelandy and James Kaiser (Penn State College of Medicine, PSU-COM) assisted with liposome preparation, sizing, and confocal microscopy. Megan Young and Todd Fox (PSU-COM) prepared the plasmid for GCS overexpression. Mark Kester (PSU-COM) serves as the mentor to Sriram, James, Megan, and Todd, and was essential in allowing portions of this research to be conducted in his laboratory. Additionally, Myles Cabot (John Wayne Cancer Institute) assisted in the design and development of the PDMP-containing nanoliposome.

5.6: References

1. Andrieu-Abadie, N., Gouaze, V., Salvayre, R. & Levade, T. Ceramide in apoptosis signaling: relationship with oxidative stress. *Free Radic. Biol. Med.* **31**, 717-728 (2001).

2. Bedard, K. & Krause, K. H. The NOX family of ROS-generating NADPH oxidases: physiology and pathophysiology. *Physiol. Rev.* **87**, 245-313 (2007).

3. Cacicedo, J. M., Benjachareowong, S., Chou, E., Ruderman, N. B. & Ido, Y. Palmitate-induced apoptosis in cultured bovine retinal pericytes: roles of NAD(P)H oxidase, oxidant stress, and ceramide. *Diabetes* **54**, 1838-1845 (2005).

4. Hannun, Y. A. Functions of ceramide in coordinating cellular responses to stress. *Science* **274**, 1855-1859 (1996).

5. Ogretmen, B. & Hannun, Y. A. Biologically active sphingolipids in cancer pathogenesis and treatment. *Nat. Rev. Cancer.* **4**, 604-616 (2004).

6. Senchenkov, A., Litvak, D. A. & Cabot, M. C. Targeting ceramide metabolism--a strategy for overcoming drug resistance. *J. Natl. Cancer Inst.* **93**, 347-357 (2001).

7. Zheng, W. *et al*. Ceramides and other bioactive sphingolipid backbones in health and disease: lipidomic analysis, metabolism and roles in membrane structure, dynamics, signaling and autophagy. *Biochim. Biophys. Acta* **1758**, 1864-1884 (2006).

8. Liu, Y. Y., Han, T. Y., Giuliano, A. E. & Cabot, M. C. Ceramide glycosylation potentiates cellular multidrug resistance. *FASEB J.* **15**, 719-730 (2001).

9. Gouaze-Andersson, V. & Cabot, M. C. Glycosphingolipids and drug resistance. *Biochim. Biophys. Acta* **1758**, 2096-2103 (2006).

10. Barth, B. M., Stewart-Smeets, S. & Kuhn, T. B. Proinflammatory cytokines provoke oxidative damage to actin in neuronal cells mediated by Rac1 and NADPH oxidase. *Mol. Cell. Neurosci.* (2009).

11. Hannun, Y. A. & Luberto, C. Ceramide in the eukaryotic stress response. *Trends Cell Biol.* **10**, 73-80 (2000).

12. Hannun, Y. A. & Obeid, L. M. Principles of bioactive lipid signalling: lessons from sphingolipids. *Nat. Rev. Mol. Cell Biol.* **9**, 139-150 (2008).

13. Ozben, T. Oxidative stress and apoptosis: impact on cancer therapy. *J. Pharm. Sci.* **96**, 2181-2196 (2007).

14. Wang, J. & Yi, J. Cancer cell killing via ROS: to increase or decrease, that is the question. *Cancer. Biol. Ther.* **7**, 1875-1884 (2008).

15. Wang, H., Maurer, B. J., Reynolds, C. P. & Cabot, M. C. N-(4-hydroxyphenyl)retinamide elevates ceramide in neuroblastoma cell lines by coordinate activation of serine palmitoyltransferase and ceramide synthase. *Cancer Res.* **61**, 5102-5105 (2001).

16. Wang, H. *et al.* N-(4-Hydroxyphenyl)retinamide increases dihydroceramide and synergizes with dimethylsphingosine to enhance cancer cell killing. *Mol. Cancer. Ther.* **7**, 2967-2976 (2008).

17. Stover, T. C., Sharma, A., Robertson, G. P. & Kester, M. Systemic delivery of liposomal short-chain ceramide limits solid tumor growth in murine models of breast adenocarcinoma. *Clin. Cancer Res.* **11**, 3465-3474 (2005).

18. Tran, M. A., Smith, C. D., Kester, M. & Robertson, G. P. Combining nanoliposomal ceramide with sorafenib synergistically inhibits melanoma and breast cancer cell survival to decrease tumor development. *Clin. Cancer Res.* **14**, 3571-3581 (2008).

19. Zolnik, B. S. *et al.* Rapid distribution of liposomal short-chain ceramide in vitro and in vivo. *Drug Metab. Dispos.* **36**, 1709-1715 (2008).

20. Belda-Iniesta, C. *et al.* Molecular biology of malignant gliomas. *Clin. Transl. Oncol.* **8**, 635-641 (2006).

21. Smith, P. S., Zhao, W., Spitz, D. R. & Robbins, M. E. Inhibiting catalase activity sensitizes 36B10 rat glioma cells to oxidative stress. *Free Radic. Biol. Med.* **42**, 787-797 (2007).

22. Liel, Y., Rudich, A., Nagauker-Shriker, O., Yermiyahu, T. & Levy, R. Monocyte dysfunction in patients with Gaucher disease: evidence for interference of glucocerebroside with superoxide generation. *Blood* **83**, 2646-2653 (1994).

23. Moskwa, P. *et al.* Glucocerebroside inhibits NADPH oxidase activation in cell-free system. *Biochim. Biophys. Acta* **1688**, 197-203 (2004).

24. Tran, M. A. *et al.* Targeting V600EB-Raf and Akt3 using nanoliposomal-small interfering RNA inhibits cutaneous melanocytic lesion development. *Cancer Res.* **68**, 7638-7649 (2008).

25. Ueyama, T. *et al.* A regulated adaptor function of p40phox: distinct p67phox membrane targeting by p40phox and by p47phox. *Mol. Biol. Cell* **18**, 441-454 (2007).

26. van Meer, G., Voelker, D. R. & Feigenson, G. W. Membrane lipids: where they are and how they behave. *Nat. Rev. Mol. Cell Biol.* **9**, 112-124 (2008).

27. Castel, V., Grau, E., Noguera, R. & Martinez, F. Molecular biology of neuroblastoma. *Clin. Transl. Oncol.* **9**, 478-483 (2007).

28. Block, M. L., Zecca, L. & Hong, J. S. Microglia-mediated neurotoxicity: uncovering the molecular mechanisms. *Nat. Rev. Neurosci.* **8**, 57-69 (2007).

29. Farooqui, A. A., Horrocks, L. A. & Farooqui, T. Modulation of inflammation in brain: a matter of fat. *J. Neurochem.* **101**, 577-599 (2007).

30. Farokhzad, O. C. & Langer, R. Impact of nanotechnology on drug delivery. *ACS Nano* **3**, 16-20 (2009).
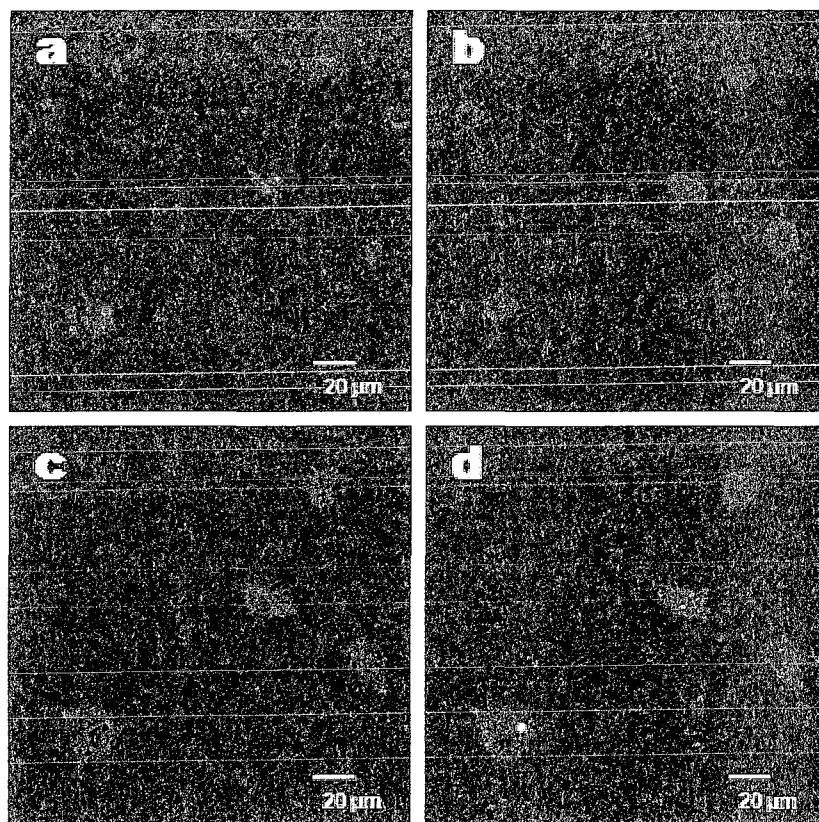
5.7: Supplementary Information

Figure 5.S1: Transfection of cells with siRNA. Human SH-SY5Y neuroblastoma cells were grown in normal growth medium, and transfected with 200 nM siRNA loaded into cationic nanoliposomes. For confocal microscopy, the DOPE of the cationic formulation contained one molar percentage of lissamine rhodamine B-labeled DOPE. 24 hours following transfection, cells were re-plated onto poly-D-lysine-coated glass coverslips, and maintained for an additional 24 hours before fixation, mounting, and microscopy. (a) Green fluorescent non-targeting siRNA (BLOCK-iT Fluorescent Oligo; Invitrogen, Carlsbad, CA). (b) Cellular nuclei stained with DAPI (blue). (c) Liposome component rhodamine-DOPE (red). (d) Merged image.

Formulation	Lipids	Molar Ratio
Cationic	DOTAP: PEG2000-DSPE: DOPE	4.75: 0.5: 4.75
Ghost	DSPC: DOPE: PEG2000-DSPE	5.66: 2.87: 1.47
Ceramide	DSPC: DOPE: PEG2000-DSPE: PEG750-C8CER: C6CER	3.75: 1.75: 0.75: 0.75: 3
Ceramide +PDMP	DSPC: DOPE: PEG2000-DSPE: PEG750-C8CER: C6CER: PDMP	3.75: 1.75: 0.75: 0.75: 1.5: 1.5
Basic	DSPC: DOPC: DOPE: PS: SM: CH	0.8: 0.8: 1: 0.4: 1: 4
BasicCer	DSPC: DOPC: DOPE: PS: SM: CH: C8CER	0.8: 0.8: 1: 0.4: 1: 4: 1
BasicGluCer	DSPC: DOPC: DOPE: PS: SM: CH: GLUCER	0.8: 0.8: 1: 0.4: 1: 4: 1
BasicCerGluCer	DSPC: DOPC: DOPE: PS: SM: CH: C8CER: GLUCER	0.8: 0.8: 1: 0.4: 1: 4: 1: 1

Table 5.S1: Nanoliposome formulations. Liposome formulations were prepared from specific lipids, at particular molar ratios, prior to nano-sizing. 1,2-dioleoyl-*sn*-glycero-3-phosphocholine (DOPC), 1,2-distearoyl-*sn*-glycero-3-phosphocholine (DSPC), 1,2-dioleoyl-*sn*-glycero-3-phosphoethanolamine (DOPE), 1,2-distearoyl-*sn*-glycero-3-phosphoethanolamine-N-[methoxy(polyethylene glycol)-2000] (PEG2000-DSPE), 1,2-dioctanoyl-*sn*-glycero-3-phospho-L-serine (PS), 1,2-dioleoyl-3-trimethylammonium-propane (DOTAP), C6-ceramide (C6CER), C8-ceramide (C8CER), C8-ceramide-1-succinyl[methoxy(polyethylene glycol)-750] (PEG750-C8CER), C8-glucosylceramide (GLUCER), C18-sphingomyelin (SM), cholesterol (CH), and D-threo-1-phenyl-2-decanoylamino-3-morpholino-1-propanol (PDMP).

ID #	Target Sequence
J-006441-05	GCGAAUCCAUGACAAUAUA
J-006441-06	GGACCAAACUACGAAUUAA
J-006441-07	GAUCCUAACUUAAUCAACA
J-006441-08	GGAAUGUCUUGUUUAAUGA

Table 5.S2: Target sequences for siRNA. ON-TARGET plus SMART pool siRNA was obtained from Dharmacon (Lafayette, CO). Four separate sequences within the human glucosylceramide synthase gene (Gene: UGCG; Accession: BC038711) were targeted.

Supplementary Methods

Confocal Microscopy

Two-day old SH-SY5Y cultures (6-well plates, 5×10^6 cells per well) were maintained in regular growth media, and transfected with 200 nM FITC-labeled, non-targeted, siRNA loaded into Rhodamine-labeled cationic nanoliposomes. After 24 h, the cells were detached with trypsin (0.5 mg/ml)/EDTA (0.2mg/ml), and re-plated onto poly-D-lysine (50 μg per cm^2) coated glass cover slips. Following an additional 24 h growth period in regular media, the cells were washed three times in PBS, and fixed for 15 min at room temperature in 2% paraformaldehyde in PBS, pH 7.0. The cover slips were mounted onto glass slides with DAPI-containing mounting medium. Images were acquired using a Leica (TCS SP2 AOBS) scanning confocal microscope (Bannockburn, IL), and filter combinations for FITC, rhodamine, and DAPI.

Western Blotting

Equal amounts of total protein (BCA protein assay) were separated by SDS-polyacrylamide (10%) gel electrophoresis (125 V, 50 Watts, 75 mA). After transfer of proteins onto nitrocellulose membranes (2.5 h, 50 V, 50 Watts, 250 mA), membranes were blocked with TBST-BSA (50 mM Tris-Cl pH 7.4, 150 mM NaCl, 0.1% Tween-20, 5 mg/ml BSA), and probed overnight with a polyclonal rabbit anti-p67^{phox} antibody (1 μg/μl in TBST), a polyclonal rabbit anti-FLAG antibody (1 μg/μl in TBST), a polyclonal rabbit anti-glucosylceramide synthase antibody (1 μg/μl in TBST), or a polyclonal rabbit anti-GAPDH antibody (1 μg/μl in TBST). Following incubation with a horseradish peroxidase-conjugated anti-rabbit secondary antibody (0.2 μg/μl in TBST, 45 min), immune-reactivity was detected by chemoluminescent exposure followed by ImageJ analysis (NIH, Bethesda, MD).

Chapter 6: Wild Alaskan blueberry extracts inhibit a magnesium-dependent neutral sphingomyelinase activity in neurons exposed to TNFα[5]

6.1: Abstract

The proinflammatory cytokine tumor necrosis factors α (TNFα) is key to initiating and orchestrating inflammation, which substantially contributes to the progression of many chronic and acute CNS pathologies. TNFα can stimulate a magnesium (Mg^{2+})-dependent neutral sphingomyelinase (nSMase) resulting in the accumulation of ceramide, a lipid messenger implicated in oxidative stress and apoptosis. Dietary polyphenols were shown to alleviate CNS inflammation largely attributed to their antioxidant properties. We found that preincubation of human SH-SY5Y neuroblastoma cells with organic or aqueous extracts prepared from Alaska wild bog blueberries completely negated Mg^{2+}-nSMase activation upon TNFα exposure. This specific and potent inhibition of Mg^{2+}-nSMase activity was non-antioxidant in nature. This study demonstrated for the first time that Alaska wild bog blueberries harbor the capacity to interfere with a key step in the progression of inflammation in neuronal cells, the activation of Mg^{2+}-nSMase, providing further evidence for the therapeutic potential of blueberries.

I, Brian Barth, affirm my contributions to the work outlined in this chapter. I contributed to the conceptualization and experimental design of the study, worked directly with Sally Gustafson during the course of the study, and helped in the preparation of the manuscript, all under the supervision, mentorship, and advisement of Dr. Thomas Kuhn. Please see section 6.7 on page 207 for the contributions of the other authors.

6.2: Introduction

The pro-inflammatory cytokine tumor necrosis factor alpha (TNFα) exhibits pleiotropic effects in the developing, adult, and injured central nervous system (Allan and Rothwell 2001; Merill 1992; Vitkovic et al. 2000; Viviani et al. 2004). TNFα affects neuronal survival, contributes to the formation, repair and maintenance of synaptic connectivity, modulates outgrowth of neuronal processes, stimulates gene expression, and regulates neuronal redox-state. TNFα plays a key role in the initiation and orchestration of inflammation in many chronic neurodegenerative diseases (Alzheimer's disease, Parkinson's disease, Amyotrophic Lateral Sclerosis), acute CNS injuries (stroke, traumatic injuries), and even psychiatric disorders (autism, schizophrenia) (Fontaine et al. 2002; Keane et al. 2006; Lucas et al. 2006; Vargas et al. 2005). Reactive microglia and astroglia cells, which are both prevalent in most CNS pathologies as well as in the aging CNS, persistently secrete TNFα at high levels (Block et al. 2007). Interactions of TNFα with the TNF receptors type I and II activates numerous cellular signal transduction pathways leading to stress kinase activation, oxidative stress, caspase activation, ceramide production, and ultimately apoptosis of neuronal cells (Locksley et al. 2001).

Sphingolipids are highly prevalent in neuronal plasma membranes and serve as precursors for various lipid second messengers (Futerman and Hannun 2004). For instance, ceramide is cytotoxic for most neuronal cell types and implicated in oxidative stress and apoptosis. Ceramide can be either synthesized *de novo* from the palmitic acid or rapidly formed by hydrolysis of sphingomyelin via a TNFα-sensitive magnesium (Mg^{2+})-dependent neutral sphingomyelinase (nSMase). So far, three mammalian Mg^{2+}-nSMases have been characterized, with Mg^{2+}-nSMase *2* specifically expressed in mammalian brain (Clarke et al. 2006). Inhibiting Mg^{2+}-nSMase *2* activity with GW4869 or via siRNA attenuated TNFα-stimulated apoptosis and generation of reactive oxygen species, demonstrating the vital role of Mg^{2+}-nSMase *2* in apoptosis and inflammatory processes as well as in cell growth and differentiation (Clarke et al. 2006). Diets rich in fruits and vegetables are long known for their benefits to our health (Joseph 2002). In particular, dietary intake of blueberries was shown to alleviate cognitive decline in

animal models and decrease ischemia-induced brain damage (Joseph et al. 2003; Mattson et al. 2002; Sweeney et al. 2002). The active ingredients are largely attributed to the family of polyphenols, which act *in vitro* as highly effective antioxidants and reduce the progression of CNS inflammation (Ramassamy 2006). However, many polyphenols are barely detectable in the CNS after dietary consumption, implying the presence of compounds with non-antioxidant properties serving as potent inhibitors in adverse inflammatory signaling pathways. We investigated whether Wild Alaskan bog blueberries (*Vaccinium uliginosum*) interfere with TNFα-stimulated inflammatory signaling pathways by inhibiting Mg^{2+}-nSMase activity in neuronal cells.

6.3: Materials and Methods

Reagents: Recombinant human TNFα and an MTT (3-(4,5-dimethylthiazol-2-yl)-2,5-diphenyl tetrazolium bromide) Cell Growth assay kit were purchased from Millipore (Temecula, CA). DMEM and Penicillin/Streptomycin solution were obtained from Mediatech (Herndon, VA). GlutaMAX-1, trypsin/EDTA solution, and an Amplex Red Sphingomyelinase assay kit were from Invitrogen (Carlsbad, CA). Fetal bovine serum was received from Atlanta Biologicals (Atlanta, GA). All other reagents were purchased from Sigma (St. Louis, MO).

Cell culture: SH-SY5Y human neuroblastoma cells were grown in DMEM medium supplemented with 10% fetal bovine serum, 100 U/ml Penicillin and 100 U/ml Streptomycin (humidified atmosphere, 5% CO_2, 37°C) in 100 mm dishes (Falcon). Cells were harvested after incubation with trypsin (0.5 mg/ml)/EDTA (0.2mg/ml), briefly triturated, and plated into 6 well or 96 well tissue culture plates (200,000 cells per well or 60,000 cells per well, respectively). Prior to treatments, SH-SY5Y cells in 6 well pates were grown for 72 h whereas SH-SY5Y cells in 96 well plates were grown for 48 h.

Blueberry extract preparation: Wild Alaskan bog blueberries (*Vaccinium uliginosum*) were harvested in the interior of Alaska at three distinct geographical locations (Lake

Minchumina, Fox, and Fairbanks) and stored frozen at -20°C. Blueberries were lyophilized, crushed to a powder, and then extracted without hydrolysis using either an organic solvent or water. To obtain an organic blueberry extract (OBBX), 3.0 g of powdered blueberries were extracted with 20 ml 70% acetone/30% water for 15 minutes with frequent agitation whereas an aqueous blueberry extract (ABBX) was prepared using deionized (18 mΩ) water. Insoluble material was removed by filtration and extracts were roto-vaporized at 40°C prior to lyophilizing. The resulting powder was stored at -20°C. OBBX or ABBX were reconstituted either in 70% acetone/30% water or deionized (18 mΩ) water followed by a 1:20 dilution with 18 mΩ water immediately before addition to SH-SY5Y cells.

Magnesium (Mg^{2+})-dependent neutral sphingomyelinase assay (Mg^{2+}-nSMase):
Subconfluent cultures of SH-SY5Y cells were pretreated with 5 μg/ml OBBX or ABBX for 2 h. Then, SH-SY5Y cells were exposed to TNFα (100 ng/ml) for 15 min, harvested in cold phosphate buffered saline and sonicated. Quantitative measurement of Mg^{2+}-nSMase activity was performed in cell lysates containing equal amounts of total protein (BCA assay, Pierce, Rockland, IL) and using an enzyme coupled Amplex Red fluorescence assay kit (Invitrogen, Carlsbad, CA). Briefly, Mg^{2+}-nSMase activity in samples generates ceramide and phosphocholine. Next, choline is liberated by alkaline phosphatase and converted to betaine and peroxide by choline oxidase. In the last step, in the presence of horseradish peroxidase (HRP), hydrogen peroxide with Amplex Red to form the highly fluorescent product resorufin measured at 590 nm using a Beckman Coulter Multimode DTX 880 microplate reader.

Choline Oxidase Assay: Addition of choline to a mixture of choline oxidase, HRP, and Amplex Red results in the formation of peroxide and subsequently the fluorescent product resorufin. In the absence of choline, the above mixture was preincubated with OBBX (5 μg/ml), ABBX (5 μg/ml and 75 μg/ml), 5 mM N-acetyl-L-cysteine, or 2000 U/ml catalase for 15 min. The reaction was initiated by adding 50 μM choline. After 15

min incubation period (37⁰C), resorufin fluorescence was measured at 590 nm using a Multimode DTX 880 microplate reader.

Cytotoxicity Assay: Briefly, cultures of SH-SY5Y cells were serum deprived overnight and then supplement with blueberry extracts (5 µg/ml or 75 µg/ml) for 48 h. Cytotoxicity was determined using an MTT cell viability assay according to manufacture's instructions (Chemicon). Formazan generation was measured using a Multimode DTX 880 microplate reader.

Statistical Analysis: Analysis of variance (ANOVA) was used to determine statistically significant differences between treatments ($p > 0.05$). *Post hoc* comparisons of specific treatments were performed using a Scheffe test to determine statistical significance based on the calculated ANOVA data. A Dunette's test was used for multiple comparisons between treatments and a single control. All error bars represent standard deviations.

6.4: Results

In various cell types, TNFα stimulates a magnesium (Mg^{2+})-dependent neutral sphingomyelinase (nSMase) activity, which generates ceramide by hydrolyzing sphingomyelin in neuronal plasma membranes, a key step in the progression of inflammation. Dietary consumption of blueberries was shown to alleviate adverse effects of CNS inflammation. Thus, we tested whether organic or aqueous extracts obtained from wild Alaskan bog blueberries (OBBX or ABBX, respectively) interfered with TNFα-stimulated activation of Mg^{2+}-nSMase in SH-SY5Y human neuroblastoma cells. Mg^{2+}-nSMase activity was quantified utilizing an enzyme assay coupling ceramide generation in cell lysates to Amplex Red fluorescence. As show in Figure 6.1, SH-SY5Y cells revealed a dramatic increase in Mg^{2+}-nSMase activity (1.76 ± 0.2, n=7, *$p < 0.05$) upon a 15 min exposure to 100 ng/ml TNFα compared to control cultures (1.00 ± 0.16, n=8). In contrast, the presence of OBBX or ABBX (5 µg/ml each) negated TNFα-stimulated activation of Mg^{2+}-nSMase. The most potent inhibition of Mg^{2+}-nSMase

activity was achieved with OBBX or ABBX from blueberries collected at Lake Minchumina (LM; 1.14 ± 0.09, n=3, p<0.05 and 1.16 ± 0.12, n=3, p<0.05, respectively). In comparison, inhibition of Mg^{2+}-nSMase was less pronounced but still significant using OBBX and ABBX prepared from blueberries collected in Fox (FX; 1.3 ± 0.2, n=3, p<0.05 and 1.37 ± 0.22, n=3, p<0.05, respectively) or Fairbanks (FB; 1.12 ± 0.18, n=3, p<0.05 and 1.31 ± 0.03, n=3, p<0.05, respectively). Taken together our findings suggested that wild Alaskan bog blueberries contain a potent inhibitor against Mg^{2+}-nSMase activity in human neuronal cells.
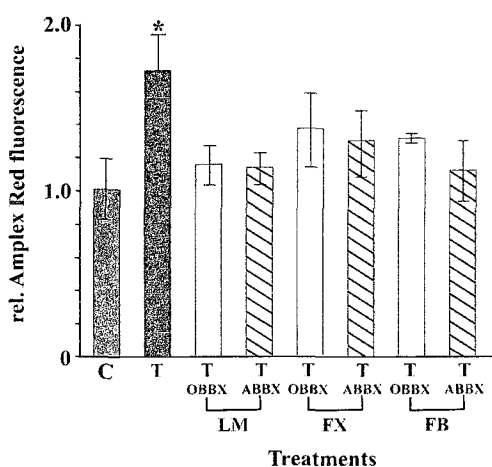

Figure. 6.1: Extracts of wild Alaskan bog blueberries inhibit Mg^{2+}-nSMase activity in neuronal cells. Blueberries were harvested at three different locations in the interior of Alaska: Lake Minchumina (LM), Fox (FX), and Fairbanks (FB). Both organic (70% acetone/30% water) and aqueous extracts were prepared (OBBX and ABBX, respectively) as described in materials and methods. Mg^{2+}-nSMase activity was quantitatively measured in lysates of human SH-SY5Y neuroblastoma cells (equal amount of total soluble protein) using an enzyme assay coupled to Amplex Red fluorescence. All values are normalized to control condition. Exposure of SH-SY5Y cells to 100 ng/ml TNFα for 15 min (T) significantly stimulated Mg^{2+}-nSMase activity (filled bar). In contrast, preincubation of SH-SY5Y cells with 5 μg/ml of OBBX (open bars) or ABBX (hatched bars) for 2 h prior to TNFα stimulation abolished Mg^{2+}-nSMase activity and was indistinguishable from our control (C; gray bar). Error bars represent standard deviations of three independent experiments and statistical significance was determined at *p<0.05 (ANOVA and *post hoc* Scheffe test, Dunette's test for multiple comparison of means).

Since quantitative measurements of Mg^{2+}-nSMase activity in cell lysates relied on the formation of peroxide, inhibition of Mg^{2+}-nSMase in our experimental paradigm could have resulted from simple peroxide scavenging. Blueberries in general and wild Alaskan blueberries in particular exhibit some of the highest antioxidant capacities measured (Prior 1998). We controlled for this alternative taking advantage of a direct choline oxidation assay. Addition of choline to a mixture of choline oxidase, HRP, and Amplex Red results in the formation of fluorescent resorufin. As shown in Figure 6.2, neither addition of ABBX nor OBBX interfered with peroxide production in the direct choline oxidation assay at a concentration (5 μg/ml) shown to completely inhibited Mg^{2+}-nSMase activity. However, increasing concentrations by 15 fold (75 μg/ml ABBX) revealed strong peroxide scavenging activity (FX; $66\pm4\%$, n=8, *p<0.05). As expected, addition of 5 mM N-acetyl-L-cysteine ($51\pm3\%$, n=8, p<0.05) or 2000 U/ml Catalase ($51\pm2\%$, n=8, p<0.05) to the direct choline oxidation assay abolished peroxide generation. These findings suggest the non-antioxidant nature of Mg^{2+}-nSMase inhibition in our blueberry extracts at low concentrations.
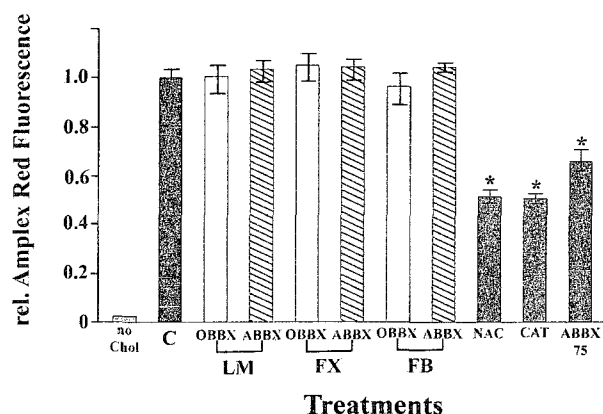
Figure 6.2: Inhibition of Mg^{2+}-nSMase activity results from non-antioxidant compounds in wild Alaskan bog blueberry extracts. In a direct choline oxidation assay, peroxide generation was quantitatively measured via Amplex Red fluorescence through the conversion of choline to betaine and peroxide via choline oxidase. All values were normalized to choline oxidation, our control (C; solid bar). Neither OBBX nor ABBX exhibited peroxide scavenging capacity at a concentration of 5 µg/ml (open bars and hatched bars, respectively), which was shown to potently inhibit Mg^{2+}-nSMase activity. As expected, addition of 5 mM N-acetyl-L-cysteine (NAC) and 2000 U/ml catalase (CAT) significantly interfered with peroxide generation (grey bars). Moreover, addition of 75 µg/ml ABBX to the direct choline oxidation assay also exhibited strong antioxidant capacity (grey bar). Omitting choline in our assay resulted in virtually no fluorescence (no Chol). Error bars represent standard deviations from six independent experiments and statistical significance was determined at *$p<0.05$ (ANOVA and *post hoc* Scheffe test). Extracts were prepared from wild Alaskan bog blueberries harvested at Lake Minchumina (LM), Fox (FX), and Fairbanks (FB).

We further determined viability of human SH-SY5Y neuroblastoma cells upon prolonged exposure to blueberry extracts to verify the specificity of blueberry extracts in inhibiting Mg^{2+}-nSMase activity. Figure 6.3 demonstrates that neither OBBX nor ABBX (5 µg/ml each) compromised SH-SY5Y cell viability over a 48 h time period compared to control, however, when increasing concentrations of extracts 15 fold (75 µg/ml ABBX, FX) cell viability was significantly diminished. As expected, UV irradiation of SH-SY5Y cells for 20 min caused a drastic reduction in cell viability (positive control). This result demonstrates that blueberry extracts (5 µg/ml) did not compromise SH-SY5Y cell viability at concentrations that negated Mg^{2+}-nSMase activation by TNFα.
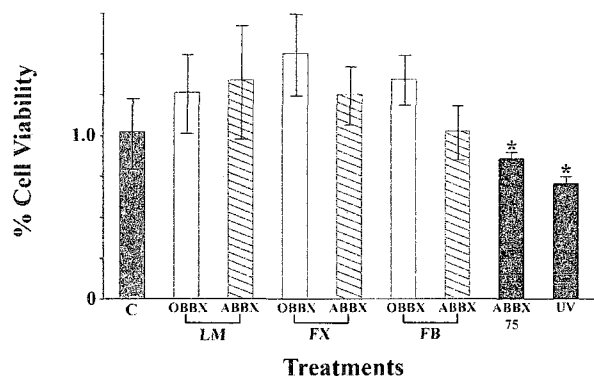
Figure 6.3: Extracts of wild Alaskan bog blueberries are not cytotoxic. Serum free cultures of SH-SY5Y cells were supplemented with OBBX and ABBX (5 μg/ml each) and maintained for 48 h prior to measuring cell viability (MTT assay). All values were normalized to control (C; grey bar). Neither OBBX (open bars) nor ABBX (hatched bars) compromised cell viability at concentrations (5 μg/ml) shown to inhibit Mg^{2+}-nSMase activity. In contrast, cell viability was significantly compromised when increasing ABBX to 75 μg/ml, a 15 fold excess (ABBX-75, FX, solid bar). As a positive control, UV exposure (20 min) of SH-SY5Y cells dramatically reduced cell viability (UV; solid bar). Error bars represent standard deviations of at least four independent experiments and statistical significance was determined at *$p<0.05$ (ANOVA and *post hoc* Scheffe test). We tested blueberries harvested from Lake Minchumina (LM), Fox (FX), and Fairbanks (FB).

6.5: Discussion

We demonstrated for the first time that wild Alaskan bog blueberries have the capacity to inhibit Mg^{2+}-nSMase activity in human neuronal cells upon exposure to the proinflammatory cytokine TNFα (Fig. 6.1). Moreover, our findings strongly suggest that Mg^{2+}-nSMase inhibition was non-antioxidant in nature (Fig. 6.2), extractable in either an organic solvent or water only, and benign to viability of neuronal cells over a sustained time period. So far, three distinct Mg^{2+}-nSMases have been characterized in eukaryotes. Relevant to our study, Mg^{2+}-nSMase *2* is predominantly expressed in the mammalian CNS (Hofmann et al. 2000), and our experimental approach confirmed specificity of the blueberry extract inhibitory affect towards this SMase. First, experiments were performed in the cholinergic and dopaminergic SH-SY5Y neuroblastoma cell line derived from a human CNS tumor. Second, this Mg^{2+}-nSMase was stimulated upon exposure of SH-SY5Y cells to TNFα (Fig. 6.1) as reported for the mammalian CNS Mg^{2+}-nSMase *2*. Third, our assay conditions were specific for Mg^{2+}-nSMase activity.

Fourth, the pharmacological compound GW4869 inhibited TNFα-stimulated activation of Mg^{2+}-nSMase in SH-SY5Y cells (data not shown) in accordance with Luberto et al. (Luberto et al. 2002).

The capacity to inhibit Mg^{2+}-nSMase activity was present in both organic and aqueous extracts of wild Alaskan bog blueberries harvested at three distinct locations (Lake Minchumina, Fox, Fairbanks). Although statistically not significant, organic or aqueous extracts prepared from Lake Minchumina blueberries consistently contained higher potency in inhibiting Mg^{2+}-nSMase compared to either extracts prepared from Fairbanks blueberries or Fox blueberries. These observed differences could arise from extracts not standardized according to a series of phytomarkers or actual distinct compositions of blueberries due to factors such as soil composition, water availability, or sun exposure despite all three blueberry harvest locations lie within 200 miles of each other in the interior of Alaska. Clearly, future studies need to include a standardized comparison among wild Alaskan blueberries as well as blueberries from other US locations to determine whether significant differences in the potency of inhibiting Mg^{2+}-nSMase activity exist. The health benefits of a high dietary consumption of blueberries and many other fruits and vegetables are largely attributed to polyphenolic compounds with antioxidant properties and, in particular, wild Alaskan blueberries exhibit one of the highest antioxidant capacities measured (Wu 2004). Thus, it was crucial to determine whether our blueberry extracts actively suppressed peroxide production since peroxide production was an integral step in our Mg^{2+}-nSMase activity assay. Regardless of the harvest location, we detected no measurable peroxide scavenging capacity in our direct choline oxidation assay supplemented either with organic or aqueous blueberry extracts at 5 µg/ml, a concentration sufficient to abolish Mg^{2+}-nSMase activity. Moreover, this finding is critical since Mg^{2+}-nSMase is redox sensitive and activated by peroxide (Won and Singh 2006). Furthermore, aqueous or organic blueberry extracts inhibited Mg^{2+}-nSMase activity in a direct assay using a fluorescent nSMase substrate (data not shown). Nevertheless, addition of aqueous and organic blueberry extracts at 15 fold higher concentrations significantly suppressed peroxide production indicative of their

antioxidant properties. In conclusion, inhibition of Mg^{2+}-nSMase derives from a non-antioxidant compound present in wild Alaskan bog blueberries.

Finally, inhibition of Mg^{2+}-nSMase activity could also be accounted for by an inherent cytotoxic effect of our blueberry extracts on SH-SY5Y cells. Some residual cell death is expected to occur under serum free conditions for 48 h even in controls. Interestingly, both aqueous and organic blueberry extracts showed a strong tendency to increase cell viability compared to our control. Potentially, the high antioxidant properties of blueberry extracts were beneficial for cell viability analogous to B 29 supplementation of cultured hippocampal neurons.

Activation of Mg^{2+}-nSMase and subsequent generation of ceramide is key to the progression of inflammation and increased oxidative stress in the CNS common to many chronic neurodegenerative pathologies, acute CNS injuries, and even psychiatric disorders. Thus, Mg^{2+}-nSMase represents a pivotal target for therapeutic intervention. The fact that wild Alaskan bog blueberries contain a potent Mg^{2+}-nSMase inhibitor further substantiates the benefits of dietary consumption of blueberries to alleviate inflammation in the CNS (Noyan-Ashraf et al. 2005; Wu et al. 2004).

6.6: Acknowledgements

6.7: Contributions

Two individuals contributed significantly to the research described in this chapter. Colin McGill, a graduate student mentored by Dr. Thomas Clausen, carried out the extraction process on the blueberries. Sally Gustafson also helped by assisting with Mg^{2+}-nSMase and cytotoxicity assays. Colin and Sally both provided important insight during the

evolution of this project, and have continued to work diligently toward the discovery of specific molecular components in the extracts that antagonize Mg^{2+}-nSMase or other components of neuroinflammatory pathways.

6.8: References

Allan S, Rothwell N. 2001. Cytokines and acute neurodegeneration. Nature Reviews Neuroscience 2(10):734-44.

Block ML, Zecca L, Hong JS. 2007. Microglia-mediated neurotoxicity: uncovering the molecular mechanisms. Nat Rev Neurosci 8(1):57-69.

Clarke CJ, Snook CF, Tani M, Matmati N, Marchesini N, Hannun YA. 2006. The extended family of neutral sphingomyelinases. Biochemistry 45(38):11247-56.

Fontaine V, Mohand-Said S, Hanoteau N, Fuchs C, Pfizenmaier K, Eisel U. 2002. Neurodegenerative and neuroprotective effects of tumor Necrosis factor (TNF) in retinal ischemia: opposite roles of TNF receptor 1 and TNF receptor 2. J Neurosci 22(7):RC216.

Futerman AH, Hannun YA. 2004. The complex life of simple sphingolipids. EMBO Rep 5(8):777-82.

Hofmann K, Tomiuk S, Wolff G, Stoffel W. 2000. Cloning and characterization of the mammalian brain-specific, Mg2+-dependent neutral sphingomyelinase. Proc Natl Acad Sci U S A 97(11):5895-900.

Joseph JA, Denisova NA, Arendash G, Gordon M, Diamond D, Shukitt-Hale B, Morgan D. 2003. Blueberry supplementation enhances signaling and prevents behavioral deficits in an Alzheimer disease model. Nutr Neurosci 6(3):153-62.

Joseph JAal, D. 2002. Brain Aging: Identifying the brakes and accelerators. Neurobiol Aging 23:647-977.

Keane RW, Davis AR, Dietrich WD. 2006. Inflammatory and apoptotic signaling after spinal cord injury. J Neurotrauma 23(3-4):335-44.

Locksley RM, Killeen N, Lenardo MJ. 2001. The TNF and TNF receptor superfamilies: integrating mammalian biology. Cell 104(4):487-501.

Luberto C, Hassler DF, Signorelli P, Okamoto Y, Sawai H, Boros E, Hazen-Martin DJ, Obeid LM, Hannun YA, Smith GK. 2002. Inhibition of tumor necrosis factor-induced cell death in MCF7 by a novel inhibitor of neutral sphingomyelinase. J Biol Chem 277(43):41128-39.

Lucas SM, Rothwell NJ, Gibson RM. 2006. The role of inflammation in CNS injury and disease. Br J Pharmacol 147 Suppl 1:S232-40.

Mattson MP, Chan SL, Duan W. 2002. Modification of brain aging and neurodegenerative disorders by genes, diet, and behavior. Physiol Rev 82(3):637-72.

Merill J. 1992. Tumor necrosis factor alpha, interleukin 1 and related cytokines in brain development: normal and phatological. Developmental Neuroscience 14:1-10.

Noyan-Ashraf MH, Sadeghinejad Z, Juurlink BH. 2005. Dietary approach to decrease aging-related CNS inflammation. Nutr Neurosci 8(2):101-10.

Prior R, Cao, C, Martin, A, Sofic, E, McEwen J, O'Brien, C, Liscner, N, Ehlrenfeldt, M, Kalt, W, Krewer, C, Mainland, M. 1998. Antioxidant capacity is influenced by total phenolic and anthocyanin content, maturity and variety of Vaccinium specis. J Agriculture and Food Chemisty 46:2586-93.

Ramassamy C. 2006. Emerging role of polyphenolic compounds in the treatment of neurodegenerative diseases: a review of their intracellular targets. Eur J Pharmacol 545(1):51-64.

Sweeney MI, Kalt W, MacKinnon SL, Ashby J, Gottschall-Pass KT. 2002. Feeding rats diets enriched in lowbush blueberries for six weeks decreases ischemia-induced brain damage. Nutr Neurosci 5(6):427-31.

Vargas DL, Nascimbene C, Krishnan C, Zimmerman AW, Pardo CA. 2005. Neuroglial activation and neuroinflammation in the brain of patients with autism. Ann Neurol 57(1):67-81.

Vitkovic L, Bockart J, Jaque C. 2000. "Inflammatory" cytokines: neuromodulators in normal brain. Journal of Neurochemistry 74:457-71.

Viviani B, Bartesaghi S, Corsini E, Galli CL, Marinovich M. 2004. Cytokines role in neurodegenerative events. Toxicol Lett 149(1-3):85-9.

Won JS, Singh I. 2006. Sphingolipid signaling and redox regulation. Free Radic Biol Med 40(11):1875-88.

Wu L, Noyan Ashraf MH, Facci M, Wang R, Paterson PG, Ferrie A, Juurlink BH. 2004. Dietary approach to attenuate oxidative stress, hypertension, and inflammation in the cardiovascular system. Proc Natl Acad Sci U S A 101(18):7094-9.

Wu X, Beecher, G.R., Holden, J.M., Haytowity, D.B., Gebhardt, S. E., and Prior, R. L. 2004. Lipophilic and hydrophilic antioxidant capacities of common foods in the United States. Journal of Agricultural and Food Chemistry 52:4026-403.

Chapter 7: Conclusions and Future Perspectives

7.1: The mechanism

This thesis research focused on a biochemical pathway central to the progression and potentially initiation of inflammation in the CNS. Neuroinflammation is prevalent following acute CNS trauma, in chronic CNS diseases, and in some psychiatric disorders, and is accompanied by signs of severe oxidative stress (Block et al. 2007; Fetler and Amigorena 2005; Nimmerjahn et al. 2005). The guiding hypothesis of this study attributed a key role to the bioactive lipid ceramide, and to a neuronal NOX, in the underlying molecular mechanism of neuroinflammation. Several important studies provided strong support for this hypothesis.

First, this research identified a neuronal NOX as the principal source of ROS production that was activated by the pro-inflammatory cytokine TNFα, one of the earliest mediators of neuroinflammation. 5-LOX and COX-2 (two oxidoreductases) also contributed to oxidative stress in addition to the action of the neuronal NOX. The NOX is speculated to rely on the omega-6 polyunsaturated fatty acid arachidonic acid by two different hypotheses. One describes arachidonic acid as an indispensable membrane anchor for some cytosolic subunits of the NOX (Groemping and Rittinger 2005; Quinn and Gauss 2004; Ueyama et al. 2007). The other describes arachidonic acid as a regulator of a proton pump contained within the large membrane-bound subunit of the NOX (Lowenthal and Levy 1999; Mankelow and Henderson 2001; Mankelow and Henderson 2003; Mankelow et al. 2003; Mankelow et al. 2004). This research supported both possible hypotheses, showing that TNFα-stimulated neuronal NOX activity was critically dependent on the activity of cPLA$_2$, an enzyme responsible for the production of arachidonic acid.

Second, we demonstrated that TNFα, or the soluble toxic amyloid beta fragment Aβ[1-42], induced a Mg^{2+}-nSMase activity in both human SH-SY5Y neuroblastoma cells and primary cortical neurons obtained from brains of 7-day old chick embryos. Mg^{2+}-nSMase, like other sphingomyelinases generates ceramide from the hydrolysis of sphingomyelin, a complex lipid prevalent in neuronal plasma membranes (Clarke et al. 2006; Farooqui et al. 2007; Marchesini and Hannun 2004). Ceramide is also well known to evoke cellular stress responses and oxidative stress (Hannun 1996; Hannun and Luberto 2000).

Third, we demonstrated that ceramide accumulation resulted in an activation of the neuronal NOX: 1) through the action of Mg^{2+}-nSMase, 2) by exogenous addition of a short-chain ceramide analog, 3) by inhibiting ceramide degradation, and 4) by stimulating *de novo* ceramide biosynthesis. Moreover, the ceramide metabolite ceramide-1-phosphate could also induce NOX activity. This finding is important because ceramide-1-phosphate has recently emerged as a potent regulator of cPLA$_2$ activity through direct interaction with the enzyme itself (Pettus et al. 2004; Subramanian et al. 2005; Subramanian et al. 2007). In our experimental system we determined that TNFα also stimulated CerK activity, phosphorylating ceramide to produce ceramide-1-phosphate. CerK activity was highly sensitive to inhibition of Mg^{2+}-nSMase thereby placing it downstream of Mg^{2+}-nSMase in the neuroinflammatory pathway. Furthermore, inhibition of CerK by RNA interference prevented TNFα-stimulated NOX activity and restored cellular viability.

Fourth, oxidative stress was found to disrupt many cellular functions. We identified actin as one target of neuroinflammatory-stimulated ROS. Irreversible oxidative damage (carbonylation) to actin severely disrupts actin dynamics in neuronal cells. Proper actin cytoskeletal dynamics are essential for fundamental cellular processes such as gene expression, motility, plasticity, vesicular transport and more (Formigli et al. 2007; Gourlay and Ayscough 2005; Lanzetti 2007; Maloney and Bamburg 2007). SphK1 emerged as a second target of ROS damage associated with neuroinflammation.

Sphingosine-1-phosphate, the product of SphK1 activity, is implicated in mechanisms underlying cell survival, cell proliferation, cell motility, and angiogenesis (Alemany et al. 2007). Irreversible oxidative damage to SphK1 and loss of sphingosine-1-phosphate production therefore has severe consequences for cell survival.

Fifth, glucosylceramide was identified as an inhibitor of NOX. Glucosylceramide is the product of glucosylceramide synthase and therefore is a direct product of ceramide neutralization (Gouaze-Andersson and Cabot 2006; Liu et al. 2001). RNA interference directed against glucosylceramide synthase augmented TNFα- or doxorubicin-stimulated NOX activity, while overexpression of glucosylceramide synthase had the opposite effect. Additionally, addition of exogenous glucosylceramide blocked NOX activity. These results suggested that glucosylceramide synthase may inhibit NOX activity either by depleting ceramide, an essential lipid activator, or by direct inference by glucosylceramide, or both.

Altogether, these studies conclusively showed that neuroinflammation could mediate NOX-dependent oxidative stress by modulating ceramide metabolism (Fig. 7.1). It is important to keep in mind that these studies also described a positive, yet detrimental feedback mechanism, involving the oxidation of actin and SphK1, which ultimately impedes neuronal survival and perpetuates the progression of CNS pathologies.
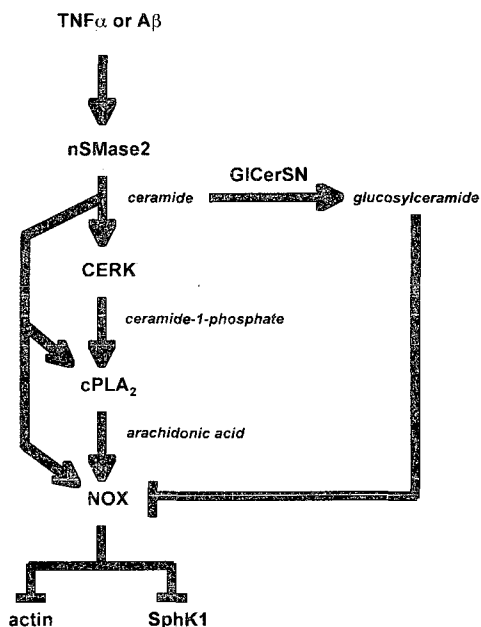
Figure 1: Ceramide metabolism mediates inflammatory-stimulated NADPH oxidase activity in neurons. TNFα (or Aβ$^{1-42}$) stimulated Mg^{2+}-nSMase activity generating ceramide. In addition to ceramide, CerK activity (producing ceramide-1-phosphate) mediated the activity of cPLA$_2$ and a neuronal NADPH oxidase (NOX). Alternatively glucosylceramide, the product of ceramide neutralization by glucosylceramide synthase (GlCerSN), blocked NOX activity. Intriguingly NOX activity impeded actin and SphK1 via oxidation; a positive feedback pathway impeding neuronal survival.

7.2: Neuroprotection and wild Alaskan bog blueberries

Foods rich in antioxidants as well as those with high omega-3 polyunsaturated fat content have been shown to improve CNS health (Galli et al. 2002). Alaskan salmon has one of the highest omega-3 contents of salmon in the entire world; particularly important because these fats impede inflammatory responses including those that occur in the CNS (Farooqui et al. 2007). Likewise, Alaskan blueberries have one of the highest antioxidant capacities of any fruit, which can combat oxidative stress associated with aging as well as with degenerative pathologies (Ramassamy 2006). Unfortunately, antioxidant compounds such as polyphenols rarely accumulate to efficacious levels in the CNS following dietary consumption (Joseph et al. 2003; Noyan-Ashraf et al. 2005;

Ramassamy 2006; Wu et al. 2004). Rather, beneficial effects from consumption of blueberries and other fruits and vegetables may arise from other naturally occurring compounds that antagonize specific biochemical pathways.

This thesis research evaluated crude extracts obtained from wild Alaskan bog blueberries for their potential to interfere with Mg^{2+}-nSMase-mediated neuroinflammation. It was determined that components are present in wild Alaskan bog blueberries, independent of antioxidants, that block TNFα-stimulated Mg^{2+}-nSMase activity in neuronal cells. Preliminary evidence from fractionated extracts (data not shown) suggested that Mg^{2+}-nSMase-inhibitory effects arose from highly lipophilic fractions. These findings may indicate that the inhibitory effect observed might be due to a compound acting in competition with the lipid substrate (sphingomyelin), or by a biophysical effect on the membrane where the Mg^{2+}-nSMase is localized. Additionally, a lipophilic compound could make an ideal therapeutic to treat CNS pathologies due to the probability of crossing the blood-brain-barrier. Altogether, this research showed that wild Alaskan bog blueberries contain components, in addition to antioxidants, with therapeutic potential for the treatment of acute CNS trauma, chronic CNS disease, or psychiatric disorders.

7.3: Implications for neurodegeneration

Neuroinflammation is a response associated with many acute and chronic pathologies of the CNS, as well as with psychiatric disorders (Block et al. 2007; Fetler and Amigorena 2005; Nimmerjahn et al. 2005). The inflammatory response in the CNS is similar to that found outside the CNS in that it targets pathogens, toxins, and other insults in order to eliminate their threat (Block et al. 2007; Sawada et al. 1989; Town et al. 2005). Unfortunately, inflammatory responses can have dramatic and unintended consequences in the CNS; in particular the damage to processes key to neuronal function and survival. Ceramide accumulation and oxidative stress are prevalent in many, if not all neurodegenerative pathologies (Farooqui et al. 2007). Ceramide is a bioactive

sphingolipid that has been implicated as a regulator of a variety of events including cellular stress, oxidative stress, and apoptosis (Hannun 1996; Hannun and Luberto 2000). In this study, activation of Mg^{2+}-nSMase by TNFα (or Aβ^{1-42}) resulted in the generation of ceramide, and further metabolism by CerK produced ceramide-1-phosphate. Both ceramide and ceramide-1-phosphate are potent inducers of ROS accumulation and thus oxidative stress.

The mechanism elucidated in this thesis research described inflammatory-regulation of a neuronal NOX unique from that documented in microglia, the immune cell of the CNS. The NOX, an enzyme responsible for the production of superoxide anion, mediated oxidative damage to key neuronal components in response to inflammatory stimuli. Two specific neuronal targets of oxidative modification were identified as actin and SphK1. Actin and SphK1 are both important for neuronal survival, actin specifically through structure and dynamic cytoskeletal processes (Fiala et al. 2002; Maloney and Bamburg 2007), and SphK1 through production of the pro-survival and pro-growth lipid sphingosine-1-phosphate (Alemany et al. 2007; Mizugishi et al. 2005). Disruption of actin and SphK1 via NOX-dependent oxidation represents a profound finding of this research, namely a pathway of positive feedback where neuronal survival is jeopardized, exacerbating inflammation and leading to neurodegeneration.

Loss of neuron functionality including synaptic plasticity, vesicular trafficking, and neurotransmission, and ultimately neuronal death reflect the cellular correlate of degenerative CNS disorders. The identification of Mg^{2+}-nSMase, CerK, and a neuronal NOX as integral components of a pathway linking neuroinflammation to oxidative stress, and ultimately to neurodegeneration, provides new molecular targets for pharmacotherapy designed to treat acute CNS trauma, chronic CNS disease, and psychiatric disorders and ultimately improve neuronal functionality and survival.

7.4: Implications for cancer

The CNS, like other organs, is susceptible to malignant tumors arising from any of its three cell types (neurons, astrocytes, and microglia). Cancers of the CNS are particularly problematic due to the sensitive nature of the CNS, frequently rendering the tumors inoperable (Belda-Iniesta et al. 2006; Castel et al. 2007). An unfortunate addition to the problem of CNS cancer is the often-unresponsive nature to chemotherapy and radiation therapy. In responsive cancers, both chemotherapy and radiation are shown to induce ceramide accumulation as a mechanism important to the cytotoxic effect of the treatment (Ogretmen and Hannun 2004; Senchenkov et al. 2001; Zheng et al. 2006). Like other ceramide-mediated pathways that stimulate oxidative stress, the ceramide-mediated NOX pathway described in this thesis research is also targeted by chemotherapeutics such as doxorubicin. Although not a specific goal of chemotherapeutics, the onset of oxidative stress is an important mechanism that assists in destroying the targeted cancer while also affecting neighboring cells through a bystander effect (Ozben 2007; Wang and Yi 2008).

Several highly invasive cancers, such as brain and breast cancer, display increased activities of sphingosine kinase-1, acid ceramidase, and glucosylceramide synthase (Gouaze-Andersson and Cabot 2006; Ogretmen and Hannun 2004; Senchenkov et al. 2001). Acid ceramidase and glucosylceramide synthase regulate the clearance of ceramide, and therefore counteract the effects of chemotherapy, as well as radiation. Sphingosine kinase-1, on the other hand, phosphorylates the ceramide-metabolite sphingosine to produce the pro-survival and pro-growth lipid sphingosine-1-phosphate (Alemany et al. 2007; Ogretmen and Hannun 2004). Altogether, these enzymes confer the ability to resist chemotherapy and radiation in cancers where they are upregulated. Recent studies have demonstrated that inhibitors of these enzymes restore the sensitivity of resistant cancers to chemotherapy and radiation (Gouaze-Andersson and Cabot 2006; Ogretmen and Hannun 2004; Senchenkov et al. 2001; Wang et al. 2008).

In addition to increased glucosylceramide synthase activity, this thesis research revealed that glioblastomas, highly invasive and drug-resistant brain cancers, possessed increased superoxide dismutase and catalase activities. These enzymes are important for eliminating ROS and decreasing oxidative damage to cellular components, ultimately protecting the glioblastomas from chemotherapy-stimulated oxidative stress. Intriguingly, it was determined that glucosylceramide also inhibited NOX, demonstrating a feedback effect where ceramide neutralization serves to protect cells from ceramide-stimulated oxidative stress. Since numerous chemotherapeutics have been shown to increase ceramide levels, it is reasonable to speculate that NOX activity may also increase. Drug- and radiation-resistant cancers that up-regulate ceramide clearance pathways may also, via this feedback mechanism, reduce ceramide-stimulated NOX activity and therefore oxidative stress. Combined with an increased capacity to eliminate ROS, these advanced cancer cells posses the ability to evade treatment, survive, and grow despite chemotherapy or radiation.

7.5: Future Perspectives

This thesis research lays the foundation for a variety of further studies. An important advance is the validation, via genetic studies (RNA interference), of pharmacology utilized to evaluate components of the neuroinflammatory pathway studied in this thesis research. In particular, validation of studies performed with the Mg^{2+}-nSMase inhibitor GW4869, and the NOX inhibitor DPI. Studies of NOX are limited by the lack of specific inhibitors. Genetic studies (including real-time PCR) also provide a means to evaluate specific isoforms of NOX that are prevalent in neurons and stimulated by inflammation. Different neuronal isoforms may be localized in differing regions of the cell, which is deserving of study. Localization may regulate the diversity of activities observed with NOX, including responses to inflammatory stimuli, growth factor signaling, as well as ever-changing demands in neuronal plasticity. Additionally, more studies of how neuronal NOX is regulated are needed. Activation of the oxidase requires

phosphorylation and subunit assembly at membranes, events regulated by protein kinases and the Rac GTPase (Groemping and Rittinger 2005; Quinn and Gauss 2004; Ueyama et al. 2007). In light of this study's implication of ceramide as a key stimulator of the NOX, protein kinase C ζ (PKCζ) should be closely evaluated. PKCζ interacts directly with, and is activated by ceramide (Bourbon et al. 2000; Bourbon et al. 2002; Fox et al. 2007). Likewise, ceramide or ceramide-1-phosphate interactions with the NOX deserve future evaluation. The PX domains of the p47^{phox} and p40^{phox} subunits bind to arachidonic acid, phosphoinositides, and anionic phospholipids (Groemping and Rittinger 2005; Quinn and Gauss 2004; Ueyama et al. 2007), a phenomenon also observed with cPLA$_2$ (an enzyme that interacts directly with ceramide-1-phosphate) (Pettus et al. 2004; Subramanian et al. 2005; Subramanian et al. 2007). Future studies should also identify targets of NOX-mediated oxidation. Oxidation of specific amino acids may impact proteins differently by regulating function, localization, or trafficking.

Lastly, complete characterization of the components of wild Alaskan bog blueberries, as well as other natural products, may reveal compounds that protect neurons by antagonizing components of neuroinflammatory pathways. Altogether, future studies should seek to more clearly define the precise links between neuroinflammation, oxidative stress, and neurodegeneration, and ultimately lead to the development of better therapeutic strategies to treat inflammatory-mediated pathologies of the CNS.

7.6: References

Alemany R., van Koppen C. J., Danneberg K., Ter Braak M. and Meyer Zu Heringdorf D. (2007) Regulation and functional roles of sphingosine kinases. Naunyn Schmiedebergs Arch. Pharmacol. 374(5-6):413-428.

Belda-Iniesta C., de Castro Carpeno J., Casado Saenz E., Cejas Guerrero P., Perona R. and Gonzalez Baron M. (2006) Molecular biology of malignant gliomas. Clin. Transl. Oncol. 8(9):635-641.

Block M. L., Zecca L. and Hong J. S. (2007) Microglia-mediated neurotoxicity: uncovering the molecular mechanisms. Nat. Rev. Neurosci. 8(1):57-69.

Bourbon N. A., Sandirasegarane L. and Kester M. (2002) Ceramide-induced inhibition of Akt is mediated through protein kinase Czeta: implications for growth arrest. J. Biol. Chem. 277(5):3286-3292.

Bourbon N. A., Yun J. and Kester M. (2000) Ceramide directly activates protein kinase C zeta to regulate a stress-activated protein kinase signaling complex. J. Biol. Chem. 275(45):35617-35623.

Castel V., Grau E., Noguera R. and Martinez F. (2007) Molecular biology of neuroblastoma. Clin. Transl. Oncol. 9(8):478-483.

Clarke C. J., Snook C. F., Tani M., Matmati N., Marchesini N. and Hannun Y. A. (2006) The extended family of neutral sphingomyelinases. Biochemistry 45(38):11247-11256.

Farooqui A. A., Horrocks L. A. and Farooqui T. (2007) Modulation of inflammation in brain: a matter of fat. J. Neurochem. 101(3):577-599.

Fetler L. and Amigorena S. (2005) Neuroscience. Brain under surveillance: the microglia patrol. Science 309(5733):392-393.

Fiala J. C., Spacek J. and Harris K. M. (2002) Dendritic spine pathology: cause or consequence of neurological disorders? Brain Res. Brain Res. Rev. 39(1):29-54.

Formigli L., Meacci E., Zecchi-Orlandini S. and Orlandini G. E. (2007) Cytoskeletal reorganization in skeletal muscle differentiation: from cell morphology to gene expression. Eur. J. Histochem. 51 Suppl 1:21-28.

Fox T. E., Houck K. L., O'Neill S. M., Nagarajan M., Stover T. C., Pomianowski P. T., Unal O., Yun J. K., Naides S. J. and Kester M. (2007) Ceramide recruits and activates protein kinase C zeta (PKC zeta) within structured membrane microdomains. J. Biol. Chem. 282(17):12450-12457.

Galli R. L., Shukitt-Hale B., Youdim K. A. and Joseph J. A. (2002) Fruit polyphenolics and brain aging: nutritional interventions targeting age-related neuronal and behavioral deficits. Ann. N. Y. Acad. Sci. 959:128-132.

Gouaze-Andersson V. and Cabot M. C. (2006) Glycosphingolipids and drug resistance. Biochim. Biophys. Acta 1758(12):2096-2103.

Gourlay C. W. and Ayscough K. R. (2005) The actin cytoskeleton: a key regulator of apoptosis and ageing? Nat. Rev. Mol. Cell Biol. 6(7):583-589.

Groemping Y. and Rittinger K. (2005) Activation and assembly of the NADPH oxidase: a structural perspective. Biochem. J. 386(Pt 3):401-416.

Hannun Y. A. (1996) Functions of ceramide in coordinating cellular responses to stress. Science 274(5294):1855-1859.

Hannun Y. A. and Luberto C. (2000) Ceramide in the eukaryotic stress response. Trends Cell Biol. 10(2):73-80.

Joseph J. A., Denisova N. A., Arendash G., Gordon M., Diamond D., Shukitt-Hale B. and Morgan D. (2003) Blueberry supplementation enhances signaling and prevents behavioral deficits in an Alzheimer disease model. Nutr. Neurosci. 6(3):153-162.

Lanzetti L. (2007) Actin in membrane trafficking. Curr. Opin. Cell Biol. 19(4):453-458.

Liu Y. Y., Han T. Y., Giuliano A. E. and Cabot M. C. (2001) Ceramide glycosylation potentiates cellular multidrug resistance. FASEB J. 15(3):719-730.

Lowenthal A. and Levy R. (1999) Essential requirement of cytosolic phospholipase A(2) for activation of the H(+) channel in phagocyte-like cells. J. Biol. Chem. 274(31):21603-21608.

Maloney M. T. and Bamburg J. R. (2007) Cofilin-mediated neurodegeneration in Alzheimer's disease and other amyloidopathies. Mol. Neurobiol. 35(1):21-44.

Mankelow T. J. and Henderson L. M. (2003) Proton conduction through full-length gp91phox requires histidine 115. Protoplasma 221(1-2):101-108.

Mankelow T. J. and Henderson L. M. (2001) Inhibition of the neutrophil NADPH oxidase and associated H+ channel by diethyl pyrocarbonate (DEPC), a histidine-modifying agent: evidence for at least two target sites. Biochem. J. 358(Pt 2):315-324.

Mankelow T. J., Hu X. W., Adams K. and Henderson L. M. (2004) Investigation of the contribution of histidine 119 to the conduction of protons through human Nox2. Eur. J. Biochem. 271(20):4026-4033.

Mankelow T. J., Pessach E., Levy R. and Henderson L. M. (2003) The requirement of cytosolic phospholipase A2 for the PMA activation of proton efflux through the N-terminal 230-amino-acid fragment of gp91phox. Biochem. J. 374(Pt 2):315-319.

Marchesini N. and Hannun Y. A. (2004) Acid and neutral sphingomyelinases: roles and mechanisms of regulation. Biochem. Cell Biol. 82(1):27-44.

Mizugishi K., Yamashita T., Olivera A., Miller G. F., Spiegel S. and Proia R. L. (2005) Essential role for sphingosine kinases in neural and vascular development. Mol. Cell. Biol. 25(24):11113-11121.

Nimmerjahn A., Kirchhoff F. and Helmchen F. (2005) Resting microglial cells are highly dynamic surveillants of brain parenchyma in vivo. Science 308(5726):1314-1318.

Noyan-Ashraf M. H., Sadeghinejad Z. and Juurlink B. H. (2005) Dietary approach to decrease aging-related CNS inflammation. Nutr. Neurosci. 8(2):101-110.

Ogretmen B. and Hannun Y. A. (2004) Biologically active sphingolipids in cancer pathogenesis and treatment. Nat. Rev. Cancer. 4(8):604-616.

Ozben T. (2007) Oxidative stress and apoptosis: impact on cancer therapy. J. Pharm. Sci. 96(9):2181-2196.

Pettus B. J., Bielawska A., Subramanian P. et al (2004) Ceramide 1-phosphate is a direct activator of cytosolic phospholipase A2. J. Biol. Chem. 279(12):11320-11326.

Quinn M. T. and Gauss K. A. (2004) Structure and regulation of the neutrophil respiratory burst oxidase: comparison with nonphagocyte oxidases. J. Leukoc. Biol. 76(4):760-781.

Ramassamy C. (2006) Emerging role of polyphenolic compounds in the treatment of neurodegenerative diseases: a review of their intracellular targets. Eur. J. Pharmacol. 545(1):51-64.

Sawada M., Kondo N., Suzumura A. and Marunouchi T. (1989) Production of tumor necrosis factor-alpha by microglia and astrocytes in culture. Brain Res. 491(2):394-397.

Senchenkov A., Litvak D. A. and Cabot M. C. (2001) Targeting ceramide metabolism--a strategy for overcoming drug resistance. J. Natl. Cancer Inst. 93(5):347-357.

Subramanian P., Stahelin R. V., Szulc Z., Bielawska A., Cho W. and Chalfant C. E. (2005) Ceramide 1-phosphate acts as a positive allosteric activator of group IVA cytosolic phospholipase A2 alpha and enhances the interaction of the enzyme with phosphatidylcholine. J. Biol. Chem. 280(18):17601-17607.

Subramanian P., Vora M., Gentile L. B., Stahelin R. V. and Chalfant C. E. (2007) Anionic lipids activate group IVA cytosolic phospholipase A2 via distinct and separate mechanisms. J. Lipid Res. 48(12):2701-2708.

Town T., Nikolic V. and Tan J. (2005) The microglial "activation" continuum: from innate to adaptive responses. J. Neuroinflammation 2:24.

Ueyama T., Tatsuno T., Kawasaki T., Tsujibe S., Shirai Y., Sumimoto H., Leto T. L. and Saito N. (2007) A regulated adaptor function of p40phox: distinct p67phox membrane targeting by p40phox and by p47phox. Mol. Biol. Cell 18(2):441-454.

Wang H., Maurer B. J., Liu Y. Y. et al (2008) N-(4-Hydroxyphenyl)retinamide increases dihydroceramide and synergizes with dimethylsphingosine to enhance cancer cell killing. Mol. Cancer. Ther. 7(9):2967-2976.

Wang J. and Yi J. (2008) Cancer cell killing via ROS: to increase or decrease, that is the question. Cancer. Biol. Ther. 7(12):1875-1884.

Wu L., Noyan Ashraf M. H., Facci M., Wang R., Paterson P. G., Ferrie A. and Juurlink B. H. (2004) Dietary approach to attenuate oxidative stress, hypertension, and inflammation in the cardiovascular system. Proc. Natl. Acad. Sci. U. S. A. 101(18):7094-7099.

Zheng W., Kollmeyer J., Symolon H. et al (2006) Ceramides and other bioactive sphingolipid backbones in health and disease: lipidomic analysis, metabolism and roles in membrane structure, dynamics, signaling and autophagy. Biochim. Biophys. Acta 1758(12):1864-1884.